The Activation of the Glucagon-Like Peptide-1 (GLP-1) Receptor by Peptide and Non-Peptide Ligands

Clare Louise Wishart

Submitted in accordance with the requirements for the degree of

Doctor of Philosophy of Science

University of Leeds

School of Biomedical Sciences

Faculty of Biological Sciences

September 2013

Intellectual Property and Publication Statements

The candidate confirms that the work submitted is her own and that appropriate credit has been given where reference has been made to the work of others.

This copy has been supplied on the understanding that it is copyright material and that no quotation from the thesis may be published without proper acknowledgement.

Acknowledgments

Firstly I would like to offer my sincerest thanks and gratitude to my supervisor, Dr. Dan Donnelly, who has been nothing but encouraging and engaging from day one. I have thoroughly enjoyed every moment of working alongside him and learning from his guidance and wisdom.

My thanks go to my academic assessor Professor Paul Milner whom I have known for several years, and during my time at the University of Leeds he has offered me invaluable advice and inspiration. Additionally I would like to thank my academic project advisor Dr. Michael Harrison for his friendship, help and advice.

I would like to thank Dr. Rosalind Mann and Dr. Elsayed Nasr for welcoming me into the lab as a new PhD student and sharing their experimental techniques with me, these techniques have helped me no end in my time as a research student. Additionally I would like to thank Dr. Natalie Keat for her support whilst I was researching in the LIGHT laboratories.

I am grateful to have collaborated with Dr. Colin Fishwick and Dr. Marco Migliore (University of Leeds, School of Chemistry) who provided me with the 'Pm compounds' and were constantly enthusiastic about their biological consequences.

Special thanks go to Dr. Gareth Rosbrook and Dr. Sue Whittle for their help and support throughout my time at the University of Leeds.

To my future husband Chris, it's been such an experience for us to both do a PhD at the same time. We have shared joy upon each other's success, and felt each other's pain when things have gone wrong in the lab. I feel I wouldn't have done as well as I did if I didn't know you were supporting me throughout the whole process, and you always seem to know the right things to say. You are my rock; I am looking forward to spending the rest of my days with you.

Rachel, I have only known you for a short amount of time but you have brought such light and warmth into my life. It is not often in life that special friendships like ours are forged. I wish you the best of luck to you in the future for your PhD. I hope you enjoy the experience and meeting the variety of interesting characters that academia offers. To you, I gift the PCR staff. May it bring you good luck and success in your future thermal cycling experiments.

Caroline, Benjamin and Dave, it has been brilliant working alongside you in the Garstang laboratories these past two years. Caroline, you are an inspiration and I wish you all the success you deserve. Dave, your wit and quick quips have made me chuckle and I wish you luck in your new postdoc position. Benjamin, I have thoroughly enjoyed your autoclaving

escapades and I hope you manage to publish your ‘will it autoclave?’ paper. Sorry for all the pranks.

I would like to give special thanks to my Mum. You have been so very supportive throughout my entire education, which is now coming to a close. I feel 20 years of learning should tide me over sufficiently. You are the best Mum a girl could wish for, and this thesis is dedicated to you.

I would like to thank my laptop at home for putting up with such high levels of usage.

And finally, I would like to thank the BBSRC for funding this PhD.

Abstract

The glucagon-like peptide-1 receptor (GLP-1R) potentiates glucose-stimulated insulin release from pancreatic β cells and promotes correct β cell function, as such it is a validated target for the treatment of type 2 diabetes (T2D).

GLP-1R is a Family B GPCR, activated by the cognate ligand GLP-1(7-36), a 30 residue peptide hormone secreted after eating, and Exendin4 (Ex4), a 39-residue synthetic peptide. Peptide ligands interact with both the large extracellular domain and core domain of GLP-1R. Core domain interaction is thought to activate the receptor. Whilst the interaction between the receptor extracellular domain and ligand is well characterised, the ligand-core domain interaction and subsequent activation is not fully understood.

Herein, a combination of mutant peptides and non-peptide ligands based on a pyrimidine scaffold (Pm compounds) are used in HTR-FRET cAMP accumulation assays, using recombinant FlpIn-HEK293 cells expressing human GLP-1R, to characterise the activation profiles of these ligands to decipher the underlying activation mechanism at the GLP-1R core domain.

Structure-function studies of Pm compounds showed a trifluoromethyl and sulphur dioxide group are essential for GLP-1R activation, and that they allosterically enhance GLP-1(9-36) and Ex4(9-39) cAMP signalling profiles independently from their own cAMP response. Insulin secretion assays showed Pm compounds potentiate insulin release from INS-1 832/13 cells in combination with truncated GLP-1(9-36), implicating the use of allosteric modulators as treatment for T2D.

Truncated GLP-1(15-36) was capable of binding and activating GLP-1R with low affinity and low potency, yet analogously truncated Ex4(9-39) was an antagonist with high affinity. Previous studies had demonstrated GLP-1(15-36) was an antagonist, and peptide-mediated activity had been attributed to the amino-terminus. Furthermore, the Pm compound-mediated cAMP response at GLP-1R was potentiated by Ex4(9-39). Mutant peptide activation data suggest activating residues D15, V16 and S17 are situated more centrally within the peptide ligand, and an extension to the currently accepted GLP-1R activation model is proposed.

Contents

Abbreviations

AC	adenylyl cyclase
ADCYAP1R1	adenylate cyclase activating polypeptide receptor
ADP	adenosine-5′-diphosphate
AM	adrenomedullin
AP2	adapter protein 2
ATP	adenosine-5′-triphosphate
B	specific binding
B_0	specific binding in the absence of unlabelled competitor
BGL	blood glucose level
B_{MAX}	maximal radioligand binding to a specific membrane prep
Bpa	p-benzoyl-L-phenylalanine
BSA	bovine serum albumin
CALC/ CT	calcitonin
CALCLR	calcitonin-like receptor
CALCR/ CTR	calcitonin receptor
cAMP	3′-5′-cyclic adenosine monophosphate
CASR	calcium sensing receptor
CGRP	calcitonin gene-related peptide
CHO	Chinese hamster ovary
Ci	Curie
CICR	calcium-induced calcium release
CNS	central nervous system
Cpm	counts per minute
CREB	cAMP Response Element Binding factor
CRF	corticotropin-releasing factor
CRF-1R/2R	corticotropin-releasing factor receptor 1 or 2
C-terminus	carboxyl terminus
DMEM	Dulbecco’s modified Eagle’s medium
DMSO	dimethyl sulphoxide

Dpm	disintegrations per minute
DPPIV	Dipeptidyl peptidase-4
EC_{50}	half maximal effective concentration
ECL	extracellular loop
EGF	Epidermal growth factor
E_{MAX}	maximum possible effect for an agonist
Epac	exchange proteins directly activated by cAMP
ER	endoplasmic recticulum
ERK	extracellular signal-related kinase
Ex4	Exendin 4
Ex-interaction	the interaction between the Ex region and GLP-1R NTD
Ex-region	the additional 9 residues following the H-region of Ex4
FBS	foetal bovine serum
FDA	Food and Drug Administration
FZD	frizzled receptors
G protein	guanine nucleotide-binding proteins
GABA	γ-aminobutyric acid
GAIN domain	GPCR autoproteolysis inducing domain
GCG/GCGR	glucagon/ glucagon receptor
GHRH	growth hormone-releasing hormone
GHRHR	growth hormone-releasing hormone receptor
GI tract	gastro-intestinal tract
GIP	Glucose-dependent Insulinotropic Polypeptide
GIPR	Glucose-dependent Insulinotropic Polypeptide receptor
GLP-1/2	Glucagon-Like Peptide-1/2
GLP-1/2R	Glucagon-Like Peptide-1/2 Receptor
GLUT2/4	Glucose transporters 2 or 4
GPCR	G protein-coupled receptor
GPS	GPCR autoproteolyic site
GRK	G-protein receptor kinase
GRM	metabotropic glutamate receptor

GRPP	glicentin-related polypeptide
GTP	Guanosine-5'-triphosphate
GTP-ase	GTP hydrolysing enzyme
HEK293 cells	Human embryonic kidney-293 cells
H-interaction	the interaction between the NTD of GLP-1R and the H-region of GLP-1or Ex4
H-region	the helical segment of GLP-1 and Ex4
HTR-FRET	homogenous time-resolved Förster resonance energy transfer
IBMX	3-isobutyl-5-methylxanthine
IC_{50}	half maximal inhibitory concentration
ICL	intracellular loop
INS-1 cells	rat insulin secreting cells
IP2	intermediate peptide-2
IP3R	inositol 1, 4, 5-triphosphate receptor
J-domain	juxtamembrane domain or NTD
K^+ ATP-channel	ATP-sensitive potassium channel
K_d	affinity constant
K_{off}	off-rate affinity constant
K_{on}	on-rate affinity constant
LANCE	Lanthanide Chelate Excite
MAPK	Mitogen-activated protein (MAP) kinase
MPGF	major proglucagon fragment
NBF-1	nucleotide binding fold-1
N-interaction	the interaction between GLP-1R TMD and the N-region of GLP-1 or Ex4
N-region	the 8 amino most residues of GLP-1 and Ex4
NSF	N-ethylmaleimide-sensitive factor
NTD	The ectodomain of a GPCR
N-terminus	amino terminus
PACAP	Pituitary adenylate cyclase-activating polypeptide
PBS	phosphate buffered saline
PI3K	phosphatidylinositol 3-kinase

PIP2	phosphatidylinositol 4,5-bisphosphate
PKA/C	protein kinase A or C
PKB	protein kinase B (also known as Akt2)
PLC-ε	Phospholipase C-ε
Pm compounds	Pyrimidine scaffold compounds
POMC	palmitoyloleylphosphatidylcholine
PTH	parathyroid hormone
PTH-1R/2R	parathyroid hormone receptor 1/2
PTHrP	parathyroid hormone related peptide
R	inactive receptor conformation
R*	active receptor conformation
RAMP	receptor activity-modifying protein
RINm5F cells	rat insulinoma cells
RRP	ready releasable pool (of insulin containing granules)
SAR	structure-activity relationship
SCTR	secretin receptor
SD	sulphur dioxide
SMO	Smoothened receptors
SUR-1	sulphonylurea receptor-1
T2D	type two diabetes
TAS1-3R	sweet and umami taste receptors
TFM	trifluoromethyl
TIP-39	Tuberoinfundibular peptide of 39 residues
TMD	transmembrane domain
VDCC	voltage dependent calcium channel
VFTM	Venus fly trap motif
VIP	vasoactive intestinal peptide
VIP-1R/2R	vasoactive intestinal peptide receptor 1/ receptor 2
WHO	World Health Organisation
α-SNAP	α-N-ethylmaleimide-sensitive factor attachment protein
β_2AR	β adrenergic receptor 2

List of Figures

List of Tables

Chapter 1

General Introduction

1.0 Preface

This thesis describes the study of the glucagon-like peptide-1 (GLP-1) and its interaction with its cognate receptor, GLP-1R. Peptide and non-peptide ligands are used in this study in order to better understand the modes of ligand binding at the receptor. Since GLP-1R is a member of the Superfamily of G protein-coupled receptors (GPCRs), the introduction will describe the general features of GPCRs including the different classifications of, and structural and functional characteristics of GPCRs, before leading onto GLP-1 specific features.

1.1 G protein-coupled receptors

G protein-coupled receptors (GPCRs) are a manifestation of evolutionary engineering. They convey a physiological stimulus from extracellular sources into an intracellular response such that the cell may respond appropriately toward the signal. This is critical for multicellular organisms which cannot converse directly with the environment and instead have a large complex system of intricately linked tissues, organs and systems to coordinate individual cells to act in favour to sustain the life of the whole organism. Cells have evolved a myriad of ways to sense their environment through analysis of surrounding molecules. Hydrophobic molecules can readily diffuse across the cell membrane due to the inherent hydrophobic nature of the membrane. For influx of molecules which are hydrophilic such as water, ions and sugars present in varying concentrations within an organism, there are transport systems which facilitate passive diffusion or active transport across the membrane. However, for molecules present at a relatively low concentration, GPCRs exist to facilitate signal transduction across the membrane from an external stimulus. GPCRs facilitate signal transduction by initiating a signalling cascade by linking to a secondary effector molecule which promotes the synthesis of many secondary messaging molecules, which go on to affect multiple cellular machinery, thus the signal from a single exogenous molecule is amplified many times over within the cell to initiate an appropriate physiological response.

In order to be classified as a GPCR, the receptor must conform to two requirements: it must have a hepta-helical membrane spanning domain and it must be able to couple to a heterotrimeric guanosine nucleotide-binding protein or G-protein (Fredriksson *et al*., 2003), hence they are named G protein-coupled receptors. Although the receptor classes share little sequence conservation, they share a similar tertiary structure. They are a continuous segment of

protein, monomeric, with the amino-terminus situated extracellularly and the carboxyl terminus situated intracellularly, linked by seven membrane-spanning α-helices which are numbered I-VII and are orientated in an anticlockwise fashion within the membrane when viewed from outside the cell (Hanson & Stevens, 2009; Donnelly, 1997), and these are linked by three extracellular and three intracellular loops. The amino-terminus and extracellular loops are sites prone to glycosylation and have been found to interact with the ligand in many receptors (Göke *et al*., 1994). The intracellular loops and C-terminal region are responsible for the coupling to the G-protein, but are also the sites of further modification for proper receptor function, such as phosphorylation, palmitoylation and ubiquitination, and are also critical for receptor desensitisation and internalisation to terminate signal transduction (Shenoy *et al*., 2001; Goddard & Watts, 2012). Ligands bind on the extracellular face, promoting conformational change for the receptor population to encompass a more active conformation, the adoption of an active conformation is achieved through a conformational change within the TM bundles such that the signal is transduced through the plasma membrane to the opposite intracellular face of the receptors, where the intracellular loops and carboxyl termini are rearranged to adopt a more G protein friendly pose for G protein recruitment (Rasmussen *et al*., 2011). These characteristics the GPCR Superfamily have in common, but the structures of the extracellular domains can vary quite drastically, showing a high degree of sequence variation (Wheatley *et al*., 2011).

GPCRs comprise the largest Superfamily of cell surface receptors with over 1000 members (Gether, 2000). They can bind to a vast plethora of different molecules to transduce cell signalling, including endogenous molecules such as ions, biogenic amines, peptides, glycoproteins, eicosanoids, nucleotides, and proteases, and exogenous molecules which confer senses such as smell by the detection of odorants, taste by binding molecules such as protons or alkali metals, and even sight by the detection of photons (Flower, 1999). The vast diversity of endogenous signals capable of binding and activating GPCRs has led this group of integral membrane proteins to become the most successful group of proteins in terms of drug targets, with an estimated 50% of all available therapeutic drugs targeted at GPCRs. Indeed, 20% of the top best selling drugs belong to the GPCR Family of proteins (Ma & Zemmel, 2002) with such drugs as Claritin (H1 histamine antagonist) and Zyprexa (antagonist or inverse agonist at many dopamine, muscarinic, serotonin and adrenergic receptors) topping the list of sales (Ma & Zemmel, 2002). Despite such a vast array of GPCRs and their cognate ligands, only a relatively small percentage of GPCRs have been exploited as therapeutic targets, as novel drug targets pose a bigger risk to large pharmaceutical companies in terms of returnable profit, but with the advent of high throughput screening processes combined with allosteric ligand screening

processes, the landscape of research and development as we know it may be up for renovation (Conn *et al*., 2009).

1.2 GPCR Classification

1.2.1 The A-F Classification system

Despite a similar tertiary structure shared by all GPCRs, the primary sequences of the GPCRs have little sequence conservation throughout the hundreds of receptors. The first classification attempt to subgroup this diverse group of receptors was performed by the design of a discriminating fingerprint program which could identify the seven hydrophobic regions common to all GPCRs (Attwood & Findlay, 1993). The following year, a classification system was revealed to segregate the GPCR Superfamily into subfamilies A-F based on sequence conservation: Family A represented the rhodopsin-like receptors, further divided into 19 subfamilies; Family B represented those receptors that were related to the secretin receptor; Family C represented glutamate receptors and their close relatives; Family D represented receptors that bind fungal pheromones; Family E represented cAMP receptors and Family F represented frizzled/smoothened receptors (Kolakowski, 1994). The A-F classification system was designed to encompass all GPCRs known to exist at the time, including GPCRs which share little sequence identity nor physiological characteristics with the human GPCRs, such as archaebacterial bacteriorhodopsins. Also, families D and E encompass fungal pheromone and cAMP receptors, which do not exist in humans.

1.2.2 The GRAFS Classification System

The human genome sequencing project permitted the use of phylogenetic analysis on the primary sequences of GPCRs within the human genome by searching for basic fingerprints using the hidden markov model on sequences of known GPCR, and using the fingerprint motifs within the human genome at a nucleotide level to identify novel GPCRs. This screen revealed over 800 GPCRs of which there were 150 orphan receptors with no known ligand at the time, and 342 non-olfactory receptors (Fredriksson *et al.*, 2003). These receptors were grouped according to phylogenetic analysis to derive a new ‘GRAFS’ classification system (Figure 1.1)

where 'GRAFS' is the acronym for the five families identified: 'G' the Glutamate Family with 15 members; 'R' the Rhodopsin Family with 701 members; 'A' the Adhesion Family with 24 members; 'F' the Frizzled/Taste2 Family with 24 members and 'S' the Secretin Family with 15 members. The GRAFS classification system separates out the secretin-like and adhesion-like receptors which were otherwise grouped together in Family B in the previous nomenclature system.

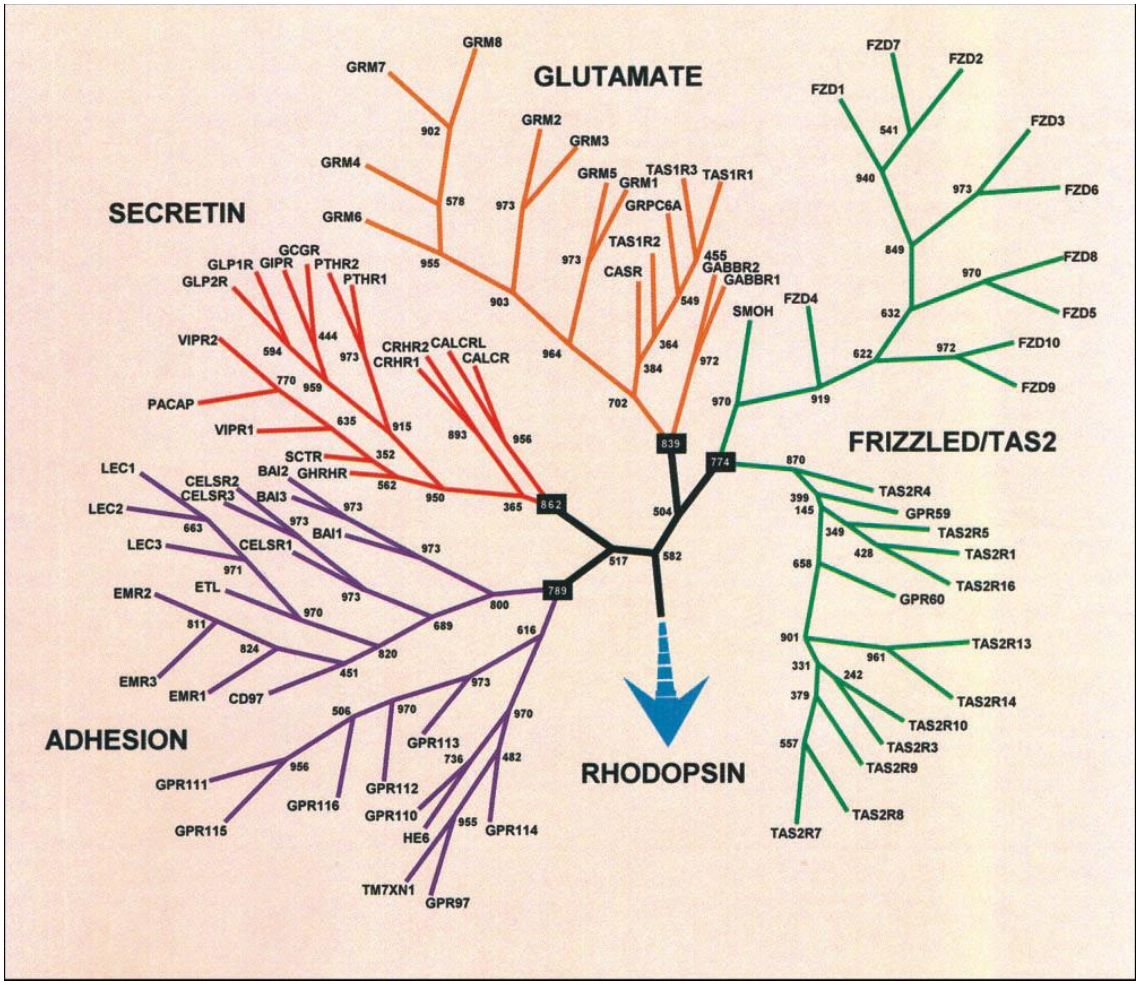

Figure 1.1 The GRAFS classification system of non-olfactory GPCRs as determined by phylogenetic analysis using the maximum parsimony method

The phylogenetic relationship between non-olfactory GPCRs is displayed as a homology tree with five distinct families. The analysis was performed on the predicted transmembrane sequences only, with the amino- and carboxyl- termini omitted. The numerical values shown in Figure 1.1 delineate the sequence difference between one Family and its nearest neighbour. The Rhodopsin Family is not shown in this figure as there are too many to display. Taken from Fredriksson *et al.* 2003 (Figure 2).

1.2.3 Glutamate Family of GPCRs

The **G**lutamate Family of GPCRs comprises 15 members in accordance with the findings of Fredriksson *et al.* 2003; however recent studies have shown the Glutamate Family consists of 22 members (Lagerström & Schiöth, 2008). The Glutamate Family comprises two γ-aminobutyric acid (GABA (neurotransmitter)) receptors, $GABA_BR1$ and $GABA_BR2$, eight metabotropic glutamate receptors (GRM1-GRM8), one calcium sensing receptor (CASR), seven orphan receptors, GPRC6A, and the sweet and umami taste receptors (TAS1R1–3) (Bjarnadóttir *et al*., 2005).

The GABA receptors possess a large bilubular motif at the amino-terminus of the receptor situated extracellularly, which is thought to form a Venus fly-trap motif (VFTM) whereby γ-aminobutyric acid binds between the two folds. In the metabotropic glutamate receptor subcategory the VFTM is connected to the TM domain by a cysteine-rich domain. The GABA receptors act as heterodimers, whereby $GABA_BR1$ and $GABA_BR2$ combine; $GABA_BR1$ acts as the ligand binding partner and $GABA_BR2$ acts as the signalling partner (Galvez *et al*., 2001). The metabotropic glutamate receptors have a large extracellular domain of between 280-500 residues which also folds to form a VFTM like the GABA receptors where a glutamate molecule binds, causing the two lobes to fold inward to engulf the ligand. The binding site of glutamate is fairly well conserved across the other Glutamate Family receptors and the structure of the extracellular motif is structurally similar between the GRM 1-8, CASR, TAS1R1-3 and GPRC6A receptors. The large extracellular domain of these receptors possesses 9 conserved cysteine residues, 6 of which form 3 disulphide bonds within the receptor, critical for maintaining tertiary structure (Liu *et al*., 2004; Hu *et al*., 2000). Calcium ions bind CASR in a similar way to glutamate binding at GRM, yet the CASR has been shown to bind aromatic amino acids phenylalanine and tryptophan, presumably allosterically, which further sensitise the receptor to its agonists: Ca^{2+}, gadolinium and spermine (Conigrave *et al*., 2000), intriguingly some metabotropic glutamate receptors have been shown to bind Ca^{2+} which enhances signalling at these receptors too (Kubo *et al*., 1998). The taste receptors TAS1R(1-3) function as heteromeric complexes. Combination of TAS1R1 and TAS1R3 receptors senses L-glutamine which accounts for the umami flavour, and the TAS1R2 and TAS1R3 heteromer has been shown to detect natural sugars and artificial sweeteners (Nelson *et al*., 2001).

1.2.4 Rhodopsin Family of GPCRs

The **R**hodopsin Family of GPCRs comprises the largest grouping of the GPCR Superfamily, consisting of 460 olfactory and 241 non-olfactory receptors, a total of 701 receptors within this class (Fredriksson *et al*., 2003). There are so many within this group that the Rhodopsin-like receptor class of GPCRs is further divided into four subgroups: α, β, γ and δ. In these subgroups lie further branches of receptors. The α-group of the Rhodopsin Family of GPCR contains at least 18 important drug targets; these drugs include antihistamines, antacid drugs, antipsychotics and cardiovascular drugs.

This Family of GPCRs has been studied extensively and since the millennium more than 18 crystal structures released (Hollenstein *et al*., 2013); both agonist and antagonist bound receptors which detail the conformational changes upon receptor activation. Rhodopsin was the first GPCR to be cloned (Nathans & Hogness, 1984) and crystallised (Palczewski *et al*., 2000), closely followed by β-adrenergic receptor which was cloned in 1986 (Dixon *et al*., 1986) and crystallised in 2007 (Rasmussen *et al*., 2007). The β-adrenergic receptor (β_{AR}) has recently been crystallised in ternary complex with its cognate G-protein ($G_{\alpha s}$) (Rasmussen *et al*., 2011). A comparison between the crystal structures of the ligand binding pockets within the Rhodopsin Family GPCRs showed a common shallow binding pocket for the respective ligands to access the receptor on the extracellular face (Rasmussen *et al*., 2007). The rhodopsin receptor binding pocket is completely obscured from solvent phase by two β hairpin motifs formed by ECL2 and the amino-terminus, which form a plug-like structure folding back into the binding pocket. However, the binding pockets of the β-adrenergic receptors and the A_{2A} adenosine receptor are only partly occluded by the presence of an α-helical motif supplied by the ECL2 regions (Wheatley *et al*., 2011). This difference in levels of occlusion of the binding pocket is presumably because within the rhodopsin receptor the chromophore 11-cis-retinal is already covalently linked to the binding pocket by a Schiff-base, thus the plug is there to protect against Schiff-base hydrolysis and subsequent loss of function of the ligand. Conversely the ligands must diffuse in and out of the binding pocket at the β-adrenergic receptors and A_{2A} adenosine receptors; therefore the binding pocket is best left partial exposed. The structural data showed the extracellular loops and extracellular facing amino-termini play an important role in ligand binding specificity in the Rhodopsin Family.

Common conserved features within the Rhodopsin-like Family of GPCRs include an ionic lock on the extracellular face of the receptor consisting of the highly conserved E/DRY motif located on TM3, and its interaction with the abridging glutamate residues situated on the top of TM6, this interaction is proposed to hold the receptor in the inactive conformation

(Rosenbaum *et al*., 2009) as mutation of these residues results in increased constitutive activity (Rasmussen *et al*., 1999). In dark-state rhodopsin crystal structures, the ionic lock was found to be intact (Li *et al*., 2004), but the analogous ionic lock region in the $\beta2_{AR}$ and $\beta1_{AR}$ structures complexed in the active state was found to be broken (Rasmussen *et al*., 2007). Another highly conserved sequence within the Rhodopsin Family of GPCRs is the NPXXY motif located on the cytoplasmic face of TM7, postulated to act as structural reinforcement of the inactive and active conformation depending on the ligand-binding state, acting almost like a toggle to quickly switch from one conformation to the other. The reinforcement of the state of the receptor is thought to occur via the proline residue which causes a kink in the α-helix of TM 7 (further stabilised by a cluster of water molecules, easily displaced in the presence of agonist in the active conformation), and the tyrosine residue was found to face inward into a crevice formed by TM2, TM3, TM6 and TM7 (Rosenbaum *et al*., 2009).

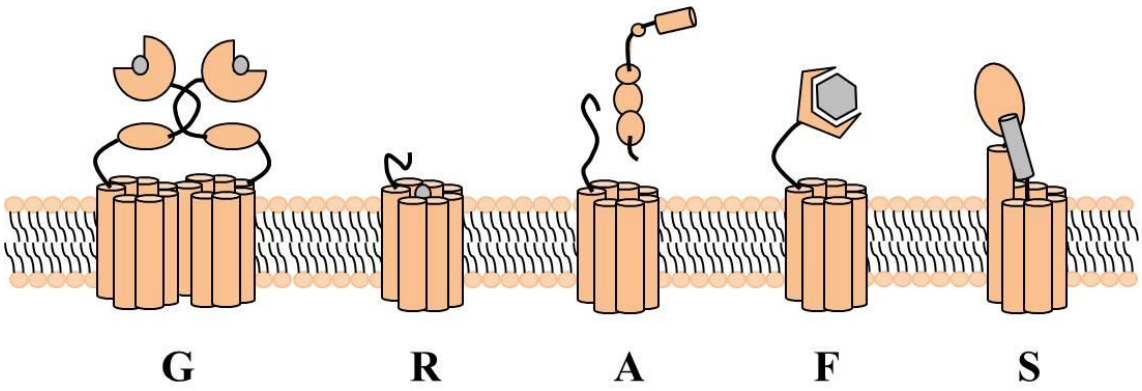

Figure 1.2 Cartoon representation of the different N-terminal architecture of the GPCRs from the GRAFS classification system.

Ligands are shown as grey-filled objects interacting with their cognate receptors (coloured peach). G: Glutamate Family; R: Rhodopsin Family; A: Adhesion Family; F: Frizzled/Tas2 Family; S: Secretin Family.

1.2.5 Adhesion Family of GPCRs

The **A**dhesion Family of GPCRs belong to the Family B class of receptors, along with the secretin receptors, according to the A-F classification system (Kolakowski, 1994), yet phylogenetic analysis determined they were distinct from the Secretin Family on the basis of analysis of the sequences of the TM domains (Fredriksson *et al*., 2003). Indeed, this hypothesis is reiterated when considering the two very different structural features of the extracellular

amino-terminal domains; the Secretin Family possess a rather compact globular fold of between 100-160 residues (Hoare, 2005), yet the Adhesion Family possess a large, extended amino terminal domain of between 200 and 2800 residues in length, which can be composed of one or many adhesion functional domains such as EGF-like repeats and cysteine-rich motifs (Fredriksson *et al*., 2003) likely to contribute to cell-to-cell adhesion (Stacey *et al*., 2000) through contacts with extracellular matrix molecules.

The intensely long and structured extracellular domains of the Adhesion Family are prone to glycosylation, which is hypothesised to make the extracellular domain rigid. The amino terminus of the Adhesion Family is therefore likened to a stalk protruding from the extracellular face (Lagerström & Schiöth, 2008) in contrast to the globular fold of the Secretin-like receptor Family. At the end of the stalk region is a GPCR autoproteolyic site (GPS), which together with the stalk region forms a GAIN domain which catalyses its own proteolysis, separating the TM and amino-terminal domains. Autoproteolysis has been shown to occur in the ER following protein synthesis (Araç *et al*., 2012). This process is thought to be essential for proper tissue development (Tesmer, 2012).

1.2.6 Frizzled Family of GPCRs

The **F**rizzled/Taste2 class of GPCRs as is suggested by the name, is divisible into two major subgroups: the Frizzled receptors, known to be heavily implicated in cancer, embryogenesis and schizophrenia (Schulte & Bryja, 2007), and the Taste2 receptors; the Taste1 receptors belong to the Glutamate Family of GPCRs. There are ten frizzled receptors denoted FZD 1-10, and a smoothened receptor (SMO) (Fredriksson *et al*., 2003).

The frizzled class of GPCRs are so-named after the discovery of a seven transmembrane spanning receptor in *Drosophila* (Vinson *et al*., 1989) with which they share homologous functions in dictating tissue polarity (Wang *et al*., 1996). The extracellular domain of the Frizzled Family has been shown to be between 200 and 320 residues in length (Bhanot *et al*., 1996). The Frizzled class of GPCRs are activated by the WNT Family of lipoglycoproteins during embryogenesis, which bind to the cysteine rich extracellular domain of the FZD receptors. The SMO receptor is likewise involved in embryogenesis and deciding cellular polarity: SMO is inhibited by the PATCH receptor, postulated to act as an oxysterol pump reducing intracellular levels of oxysterols. It is postulated that the PATCH receptor complexes with hedgehog proteins which inhibit the receptor, resulting in increased intracellular concentration of oxysterols, proposed to result in SMO activation (Murone *et al.*, 1999).

The Taste2 receptors were discovered to bind bitter tasting molecules such as cycloheximide and denatonium. The Taste2 Family consists of 25 taste receptors possessing a wide range of sequence diversity with sequence homology between 23-86%, perhaps underpinning how proteins so similar in tertiary structure are able to detect such a wide range of bitter substances (Conte *et al.*, 2002). The Taste2 receptors are short in length, between 290-340 residues, with short amino- and carboxyl-termini and appear to lack the well conserved disulphide bond between two extracellular loops (Adler *et al.*, 2000). The extracellular loops of the taste2 receptors have been implicated in ligand binding, indicating these regions of the receptor may be subject to vast sequence variation in order to accommodate such a large repertoire of binding partners (Pronin *et al.*, 2004).

1.2.7 Secretin Family of GPCRs

The **S**ecretin Family of GPCRs are so-named due to the discovery of the first receptor to belong to this Family which was discovered in rat (Ishihara *et al*., 1991). There are 15 members of this class, including the: secretin receptor (SCTR); glucagon receptor (GCGR); gastric inhibitory peptide receptor (GIPR); glucagon-like peptide-1 and peptide-2 receptors (GLP-1R/ GLP-2R); growth hormone-releasing hormone receptor (GHRHR); calcitonin and calcitonin-like receptor (CALCR/ CALCLR); corticotropin-releasing hormone receptors (CRHR1/ CRHR2); adenylate cyclase activating polypeptide receptor (PAC1/ ADCYAP1R1); parathyroid hormone receptors (PTHR1/ PTHR2) and the vasoactive intestinal peptide receptors (VIPR1/ VIPR2), a brief summary of actions of these receptors can be found in Table 1.1.

The Secretin Family of GPCRs are identifiable by a relatively large, globular amino terminal domain (Figure 1.2, 1.3) that folds into the specific ‘Secretin Family recognition fold’ (Parthier *et al*., 2009), the structure of which is stabilised by six conserved cysteine residues which form three disulphide bonds (Bazarsuren *et al*., 2001).

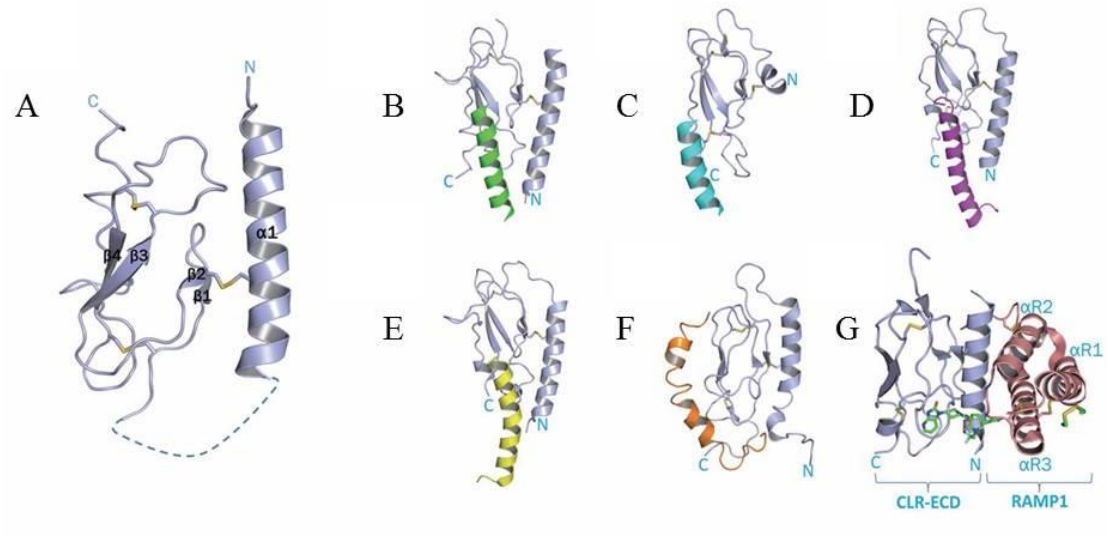

Figure 1.3 The secretin recognition fold of Secretin Family GPCRs with cognate ligands bound.

A. Ribbon diagram depicting the rudimentary structure of the secretin recognition fold at the NTD of the Secretin Family of GPCRs. The amino-terminus delves almost immediately into an α-helical conformation, then to a loop region with high levels of sequence divergence and two pairs of antiparallel β-sheets, with interconnecting disulphide bonds shown as orange sticks. B. human PTH-1R NTD (silver) complexed with PTH(1-34) (green). C. human CRFR-1 NTD (silver) complexed with CRF (pale blue). D. human GIPR NTD (silver) complexed with GIP (magenta). E. human GLP-1R (silver) complexed with GLP-1(7-36) (yellow). F. PAC-1R (silver) complexed with PACAP (orange). G. CALCLR ECD (silver) complexed with telcagepant (green) and RAMP1 (dusty pink). Adapted from Pal *et al.* (2012).

Another conserved feature within the Secretin Family of GPCRs is thought to be a disulphide bond between two conserved cysteine residues situated at ECL1/ TM3 and ECL2 (Mann *et al.*, 2010). Members of the Secretin Family share between 21 and 67% sequence identity; the area most prone to sequence diversity is located within the extracellular N-terminus, which is logical as the amino-terminal domain is responsible for ligand recognition, hence different ligands require different complementary motifs within this region (Lagerström & Schiöth, 2008, Runge *et al.*, 2003). This class of receptors shares no sequence conservation with the Rhodopsin or Glutamate Family of receptors, so do not possess the 'E/DRY' or 'NPXXY' motifs, but do share low sequence identity with the Adhesion Family of receptors (Hoare, 2005), hence the Secretin and Adhesion receptors were classified together as Family B using the A-F GPCR classification system (Kolakowski, 1994).

Some members of the Secretin Family GPCRs are able to bind to receptor activity-modifying proteins or 'RAMPS' which can alter the signalling profile of the receptor. A well noted example of ligand specificity switching in the presence of RAMPS is the calcitonin-like

receptor (CALCLR), where RAMP1 association promotes the selection of calcitonin gene-related peptide (CGRP) as the binding ligand, whereas association with RAMP2 promotes adrenomedullin 1 selectivity, and RAMP3 association promotes adrenomedullin 2 selectivity (Sexton *et al*., 2006).

Secretin Family GPCRs bind to peptide ligands, between 25-50 residues in length (Wheatley *et al*., 2011). The peptide ligands include autocrine factors, hormones and neuropeptides implicated in critical physiological homeostasis and associated pathology. Table 1.1 gives noted examples of the therapeutic relevance of the Secretin Family GPCRs (Archbold *et al*., 2011). The peptide ligands are hypothesised to adopt a mainly α-helical conformation at the carboxyl terminus, although this does seem to depend upon the solvent the ligand is solvated into (Watkins *et al*., 2012). The peptide ligands are hypothesised to bind to both the extracellular amino-terminal domain at the secretin recognition fold (Figure 1.3) and to the transmembrane domain, in a two-domain model (Hoare, 2005). The duality of the binding mechanism has been suggested to act as a brace-like structure holding both the amino and TM domains in place, stabilising the active conformation (Dong *et al*., 2004). The two-domain binding model suggests the globular amino-terminal domain (NTD) of the receptor provides ligand specificity to the ligand C-terminus, and once the ligand is bound acts as an affinity trap for the amino terminus of the peptide ligand which is brought into close proximity to the receptor transmembrane domain (TMD), where the amino terminus binds, causing receptor activation (Hoare, 2005).

As the Secretin Family of GPCRs participate in central homeostatic functions they have attracted the attention of pharmaceutical industries for the development of drugs to treat a plethora of aberrant homeostasis diseases. This Family boasts the highest ratio of drug target to known receptors in a GPCR Family with many receptors already having FDA-approved drugs to target known diseases (Table 1.1) (Tyndall & Sandilya, 2005; Bhavsar *et al*., 2013). The drugs currently available for treating diseases associated with aberrant Secretin Family receptor functions are: exenatide, liraglutide, truncated parathyroid hormone (1-34), calcitonin and glucagon. As peptide therapeutics they require sub-cutaneous administration. There are no non-peptide Secretin Family receptor ligands suitable for commercial therapeutic use, presumably because of the complexity associated with receptor activation requiring use of both the NTD and TMD - it is difficult to design a drug that can span both domains to mimic peptide ligands.

Receptor	Cognate ligand	Principle biological action/s	Clinical relevance	Drugs	RAMP association
CALCR	CT	Calcium homeostasis	Osteoporosis	Miacalcin and Fortical	Yes
CALCR & RAMP1/2/3	Amylin 1-3	Reduces nutrient intake	Obesity and diabetes	Pramlintide	RAMP1,2,3: Amylin receptors
CALCLR & RAMP1	CGRP	Vasodilation	Migraine	No	RAMP1: CGRP-R
CALCLR & RAMP2	Adrenomedullin	Vasodilation/vascular development	Cardiovascular disease and cancer	No	RAMP2: Adrenomedullin receptor
CALCLR & RAMP3	Adrenomedullin	Vasodilation/vascular development	Cardiovascular disease and cancer	No	RAMP3: Adrenomedullin receptor
CRH-R1	CRF-1/UCN-1	ACTH release	Anxiety/depression and IBS	Corticorelin	RAMP2
CRH-R2	CRF-2/UCN 1-3	Central stress response/ cardiac output	Heart disease and cancer	No	Unknown
GHRHR	GHRH	Growth hormone release	Dwarfism	Tesamorelin	No
GIPR	GIP	Insulin secretion	Obesity and diabetes	No	Unknown
GLP-1R	GLP-1	Insulin and glucagon secretion	Diabetes	Exenatide and Liraglutide	No
GLP-2R	GLP-2	Gastro-intestinal endothelial growth	SBS and Crohn's disease	Teduglutide	No
GCGR	Glucagon	Blood glucose homeostasis	Diabetes, hyperglycaemia	Glucagon	RAMP2
ADCYAP1R1	PACAP	Neurotransmission	Neurodegeneration and nociception	No	Unknown
PTH-1R	PTH	Calcium homeostasis	Osteoporosis	Teriparatide	RAMP2
	PTHrP	Developmental regulator	Hypoparathyroidism	No	
PTH-2R	TIP-39	Hypothalmic regulator, pain reception	nociception	No	RAMP3
SCTR	Secretin	Pancreatic exogenous secretion	Duodenal ulcers, Autism, Schizophrenia	No	RAMP3
VIP-1R	VIP/PACAP	Vasodilation and neurotransmission	Inflammation	No	RAMP1,2,3
VIP-2R	VIP/PACAP	Vasodilation and neurotransmission	Inflammation and circadian rhythms	No	RAMP1,2,3

Table 1.1. General overview of the Secretin Family ligands and their cognate receptors, including propensity of RAMP association and clinical relevance. All abbreviations can be found in the abbreviations list, page XI.

1.3 Secretin Family Receptor Crystal Structures-New Data

The crystallisation of GPCRs has largely been hindered by their inherent flexibility, instability in detergents, and low levels of expression. Crystallisation of Family B/ Secretin class receptors has been particularly tricky due to the presence of the large, globular extracellular domain coupled to the conformationally flexible, aliphatic TM bundle via a stalk structure, all of which are mobile as they have evolved to be highly dynamic in nature. Until 2013 there were structures available for the globular extracellular domains of these receptors, but not for the TM bundles. In 2013, two structures of the TM bundle domains were released simultaneously, one documenting the glucagon receptor TM bundle (Siu, 2013) and the other showing the corticotropin-releasing factor receptor type 1 (CRFR-1) TM bundle (Hollenstein *et al*., 2013), both structures lack the NTD.

The CRFR-1 receptor was firstly modified using 12 individual residue substitutions to stabilise the receptor-thus naming the resultant construct 'StaR' for 'stabilised receptor' (Hollenstein *et al*., 2013). Hollenstein and colleagues then proceeded to enter the T4 lysozyme construct into ICL2 and truncated the N-terminus and the C-terminus to remove putative helix 8 to result in a receptor spanning from M104 to A373. This StaR was crystallised in the inactive state using the small molecule antagonist CP-376395 (Figure 1.4). Functional analysis showed that the antagonist bound to the modified receptor with *similar* affinity to wild-type CRFR-1 despite such hefty modifications. The StaR CRFR-1 crystal structure features 7 TM spanning continuous helices orientated in a clockwise fashion connected by interlinking loops, of which only ECL1 showed significant tertiary structure in the form of an α-helix. The conserved cysteine in ECL2 is connected by a disulphide bond to the cysteine atop of TM3, previously speculated to exist at the ECL1/TM3 interface by the Donnelly group (Mann *et al*., 2010). The most pronounced feature of the TM bundle is the 'V' shape (Figure 1.4), with the hollow facing extracellularly and presumed to be the binding cavity for the insertion of the N-terminus of the peptide ligand. The binding pocket is located much further into the heart of the receptor in comparison to the binding pockets in Family A GPCRs. Another prominent feature is the extent of the bend seen in TM7 which is stabilised by the conserved Ser 130 in TM1 coordinating Phe 357 and Ser 353 of TM7.

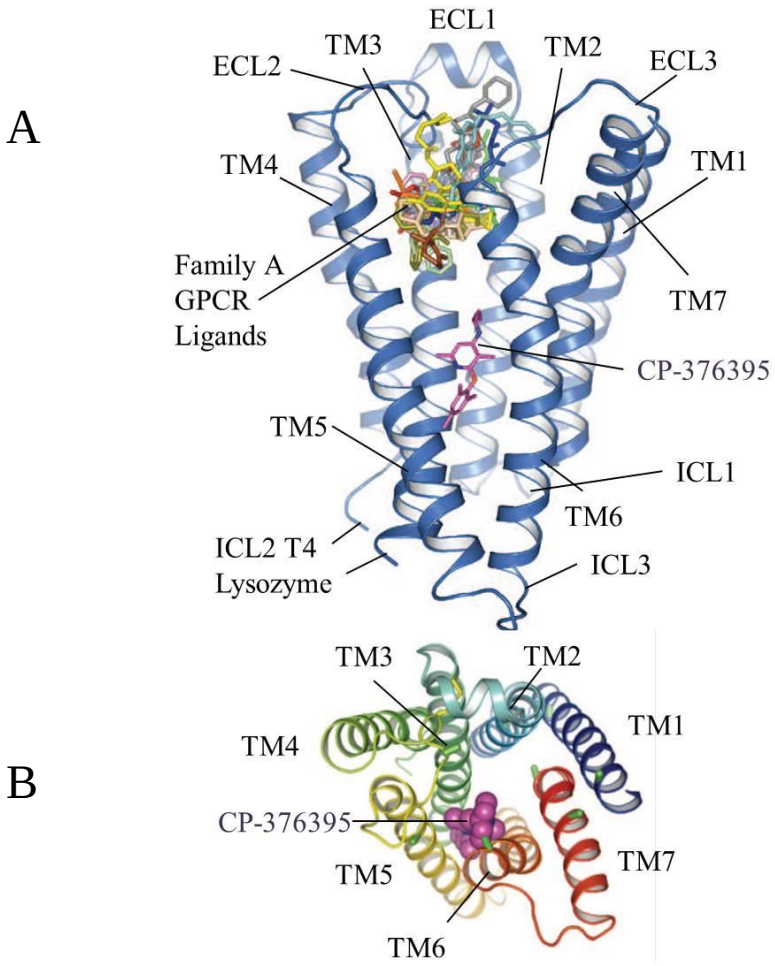

Figure 1.4 Crystal structure of the transmembrane region of the human corticotropin-releasing factor receptor type 1

A. Membrane plane view of the CRFR-1 shown in ribbon representation form complexed with the small molecule antagonist CP-376395 shown in stick format coloured magenta. Structure also superimposes the relative location of select Rhodopsin Family ligand binding sites in comparison to the binding site of CP-376395. ICL2 is left open to indicate the presence of co-crystallised T4 lysozyme for clarity. B. Extracellular plain view into the binding chasm of the human corticotropin-releasing factor receptor with CP-376395 depicted in space fill format. Figure adapted from Hollenstein *et al.* (2013), Figures 5d and 2c as part A and B respectively.

The glucagon receptor was also crystallised in the inactive state using a small molecule antagonist, NNC0640 (Sui *et al.*, 2013). Sui and co-workers synthesised an N-terminally truncated GCGR leaving residue Met 123 as the first native residue. Met 123 was fused to the thermo stabilised E. *coli* apocytochrome b_{562}RIL and the C-terminus truncated to residue 432 to enhance receptor stability, this truncated receptor had identical affinity as the wild-type receptor for the antagonist NNC0640, however the position of NNC0640 could not be determined from the electron density map. Interestingly Sui and co-workers found that the orientation of the TM

helices were conserved between the GCGR and the 15 known Family A GPCR structures, and did not see the pronounced V-shape that Hollenstein and co-workers saw in their structure. Additionally, no tertiary structure was seen in ECL1 like in the CRFR-1 crystal structure. This difference may be due to the difference in receptor stabilisation techniques adopted by the two groups, or it may be that the two TM bundle structures are in fact different in tertiary structure. Sui and co-workers did note that the TM1 helix was extended by an additional 3 α-helical turns above the membrane encompassing residue G125, which is longer than the TM1 helix in any Rhodopsin Family structures. They term this extended TM1 region as the 'stalk' and postulate that its function may be to orientate the NTD in position relative to the TM bundle in order to facilitate ligand binding through correct positioning. Although the crystal structure contained truncated N- and C-terminal regions, Sui and co-workers built a model whereby they coupled the known crystal structure of GLP-1 bound GLP-1R NTD with the solved glucagon TM domain structure in order to analyse potential positioning of the ligand-bound NTD with the TM region. From this model they proposed that the stalk region forms a complete α-helical structure leading to the NTD, reinforced by intra-helical interactions, the extended ECL1 region and interactions with the middle α-helical region of glucagon, suggesting that the stalk region is critical for proper ligand orientation for optimal interaction with the TM domain.

1.4 G Protein Coupling and Signalling Cascades

G protein-coupled receptors derive their name from the fact that they recruit G proteins upon adopting an active conformation. There are two types of G proteins: membrane-associated heterotrimeric and small cytosolic monomeric G proteins. The heterotrimeric G proteins consist of three subunits as the name suggests: α, β and γ. The α subunit is the largest, followed by the β then the γ subunit at approximately 45, 40 and 7 kDa respectively (Kristiansen, 1994). There are at least 28 different α subunits, 5 different β subunits and 12 different γ subunits. The α subunit complexes a guanosine nucleotide, either GDP or GTP, and the β and γ subunits are associated so tightly that they generally do not dissociate from each other, hence there are a vast array of different combinations of α, β and γ subunits possible, although not all combinations are observed in natural physiology. There are four main classes of G-proteins which are so categorised based upon the primary structure of the accompanying α-subunit, these classes are: G_s, G_q, G_i and G_{12}, the main features of which are described in Table 1.2.

Class	Subunit	Prominent Secondary Effector	Effect
G_s	$G\alpha_s$	Adenylyl cyclase 1-9	Stimulation
	$G\alpha_{olf}$	Adenylyl cyclase 3	Stimulation
G_i	$G\alpha_{tr}$	phosphodiesterase 6	Stimulation
	$G\alpha_{tc}$	phosphodiesterase 6	Stimulation
	$G\alpha_g$	phosphodiesterase	Stimulation
	$G\alpha_{i\ (1-3)}$	Adenylyl cyclase 5 and 6	Inhibition
	$G\alpha_o$	Ca^{2+} channels	Inhibition
	$G_{\beta\gamma}$	Phosphatidylinositide 3-kinase β and γ	Stimulation
		Phospholipase C β1-3	Stimulation
G_q	$G\alpha_{q,\ 11,\ 14,\ 15/16}$	Phospholipase C β1-4	Stimulation
G_{12}	$G_{\alpha 12/13}$	Rho-GEF	Stimulation

Table 1.2 Features of the four classes of G-proteins, their accompanying subunits and the effect upon the primary effector substrate. Adapted from Kristiansen, (1994).

In the inactive state the Gα subunit binds GDP, and has high affinity for the βγ subunit, to which it binds. The binding of the βγ subunit greatly enhances the affinity of the Gα subunit for the GPCR, to which it can readily associate and disassociate. Agonist binding at the GPCR promotes the active state conformation which vastly enhances the affinity of the GPCR for the G protein. The GPCR acts as a guanosine nucleotide exchange factor upon G-protein binding; the active receptor encourages dissociation of the GDP molecule bound to the α-subunit by conformational change, where the void is filled by a GTP molecule, present at high intracellular concentrations. GTP-bound Gα subunit has reduced affinity for the βγ subunit, therefore they dissociate. The affinity of the individual subunits for their cognate secondary effectors is markedly increased, which they then bind to and exert either inhibitory or stimulatory effects upon. The secondary effector then catalyses the formation of secondary effector molecules, which in turn cause further signalling cascades throughout the cell. Activated G proteins are capable of stimulating or inhibiting many effector proteins, some of which are shown in table 1.2, but additionally they can interact with tyrosine kinases, GPCR kinases (GRKs) (Pitcher *et al*., 1992), mitogen-activated protein kinases (MAPK) molecules (López-Ilasaca, 1998) and ion channels. The Gα subunit has inherent GTPase activity, therefore over time the GTP molecule is hydrolysed to GDP. Hydrolysis of GTP to GDP reduces the affinity of the Gα subunit for its secondary effector, from which it disassociates and instead recruits a βγ subunit, thereby subduing the signalling cascade process. Indeed, one active GPCR is capable of activating more

than one G protein upon adopting active conformation, and one activated G protein is capable of activating more than one secondary effector, and one secondary effector catalyses the formation of more than one secondary signalling molecule, therefore the signal from the ligand is greatly amplified intracellularly to initiate a great intracellular response from a relatively low concentration of ligand.

Recent crystallographic studies have shown in great detail how G-proteins interact with the β_2 adrenergic receptor (Rasmussen *et al.*, 2011). The G_β and G_γ subunits were found to not interact directly with the receptor, but a large interface was formed between the Gα subunit and ICL2, TM5 and TM6 of the β_2AR. The major structural difference between the active G protein-bound receptor and the inactive carazolol-bound β_2AR (Rasmussen *et al.*, 2007) was a major shift of 14 Å outward of TM6 and an extension of TM5 of 7 residues toward the cytoplasmic face coupled with a small shift outward of the helix. The movement of these helices opened up the core region of the receptor on the cytoplasmic face to permit α-helix 5 docking of the Gα subunit within this crevice. Gα5 helix-receptor interactions were stabilised by a number of mainly hydrophobic interactions within the core domain interface, primarily interacting with hydrophobic residues on the crevice-facing sides on TM3 and TM5. The conserved arginine of the DRY motif at position 131 within TM3 was shown to interact with Y391 of the Gα5 helix within the core domain. R131 of the DRY motif also packed against the Y326 of the conserved NPxxY motif located in TM7. The structure demonstrated extensive hydrophilic interactions between Gα5 and the cytosolic ends of TM3 and the extended TM5 helix. ICL2 was shown to change conformation from an extended loop in the inactive carazolol-bound state to α-helical in the active state. The α5 helix of the Gα subunit was shown to make contact with the ICL2 helix, which was additionally stabilised by intra-protein bonding by interaction of Y141 of ICL2 with T68 and D130 of TM2 and TM3 respectively. Intramolecular and intermolecular interactions caused by the conformational changes within the receptor upon adopting the active conformation are shown to assist docking of the Gα subunit for the receptor; one can see how the affinity of the G protein for the receptor is greatly enhanced upon R* conformation.

GPCRs preferentially couple to one type of G protein, although one GPCR may be capable of associating with different G proteins. A GPCR capable of interacting with more than one ligand can experience *signal bias*, whereby association of a non-native ligand (such as a drug or an allosteric compound) causes a conformational change such that the intracellular face of the GPCR displays an epitope which preferentially binds a different G protein to the one associated with the native ligand binding. One example of this is the GLP-1R, which is capable of interaction with all 4 heterotrimeric G-protein types (Montrose-Rafizadeh *et al.*, 1999) yet preferentially signals through the $G\alpha_s$ pathway, thereby activating AC as its secondary effector,

increasing intracellular levels of cAMP (Koole *et al*., 2010, 2013). Upon small molecule quercetin binding, the signalling profile of GLP-1R was selectively augmented to more prominently activate the $G\alpha_q$ pathway, resulting in enhanced intracellular calcium levels through phospholipase C activation, but only in the presence of high affinity agonists such as GLP-1(7-36) and not low affinity agonists such as oxyntomodulin (Koole *et al*., 2010).

1.5 The Development of Receptor Theory

The simplest model describing receptor-ligand interaction equilibrium was proposed by Clark (1937) as Clark's Law of Mass Action ("when a reversible reaction has attained equilibrium at a given temperature, the reaction quotient remains constant") which demonstrates the binding of ligand to its cognate receptor to become the receptor-ligand complex, assuming only one binding site, and describes the equilibrium rates for such (Figure 1.5).

Figure 1.5 Clark's Law of Mass action.

Equilibrium towards the associated receptor is dictated by the on rate ([A] * [R] * K_{on}) and equilibrium towards the disassociated receptor is governed by the off rate (K_{off} * [AR]). [A] depicts the concentration of agonist, [R] depicts the concentration of receptor and [AR] depicts the concentration of agonist bound receptor.

The two state binding model proposed by Katz and Thesleff was slightly more complex (Katz & Thesleff, 1957). The two state binding model depicts the receptor in an inactive form until the substrate is bound, thereby shifting equilibrium into the substrate-bound active receptor conformation dependent upon the concentration of substrate. According to this model an agonist would shift the equilibrium toward the active (R*) receptor state, whereas an inverse agonist would shift the equilibrium into the inactive (R) state, and an antagonist would not shift equilibrium in either direction (two-state model, Figure 1.6).

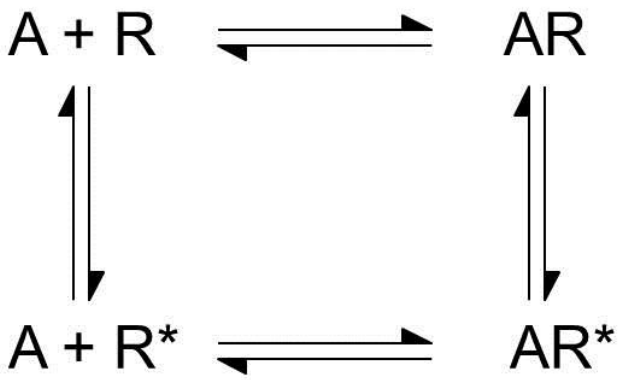

Figure 1.6 Two State Binding Model.

A denotes agonist, R denotes inactive receptor and R* denotes active receptor. Proposed by Katz and Thesleff (1957).

At the time it was not known that the receptors couple to G-proteins, hence low and high affinity receptor states were not taken into consideration, and probably not even thought about at that time (1957). The two state model was accepted as the known model until the discovery that these receptors bind ligands with greater affinity in the presence of guanine nucleotides, paving the way for the ternary complex model (Figure 1.7) involving three counterparts: the receptor, ligand and an 'additional membrane component X' which we now know to be a G protein (Delean *et al*., 1980). It was the following year that Sternweis and co-workers isolated a membrane bound guanine nucleotide-binding protein with GTPase activity that could bind both receptor and secondary effector protein AC (Sternweis *et al*., 1981).

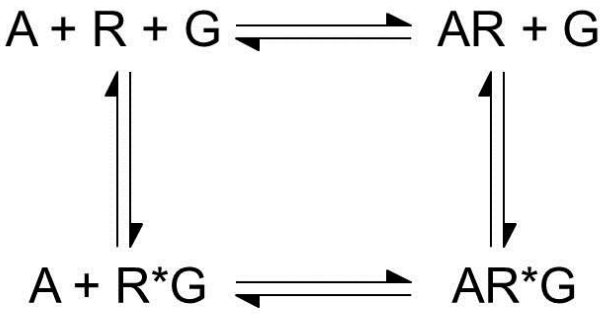

Figure 1.7 The Ternary Complex model

A denotes agonist, R denotes inactive receptor, R* denotes active receptor and G denote G protein. Proposed by DeLean and co-workers (1980).

Mutagenesis studies substituting residues of the C-terminal portion of the β_2AR ICL3 region with the analogous residues found in the α_{1B}AR resulted in a receptor with increased constitutive activity. The mutant receptor also displayed increased affinity for agonists even in the absence of G-proteins (Samama *et al.*, 1993). These two characteristics of the chimeric receptor led to the proposition that receptors are capable of spontaneously adopting an active conformation independently of ligand or G-protein, giving rise to the extended ternary complex model (Figure 1.8) (Samama *et al.*, 1993). The extended ternary model was an extension of the ternary model as suggested by De Lean, with the added spontaneous isomerisation of R to R* occurring independently of ligand or G protein association, whereby the affinities of the receptor for both ligand and G protein are markedly enhanced. In this model, the receptor can be active in the absence of both ligand and G-protein (A + R* + G), the receptor is capable of binding the agonist without undergoing conformational change to the active state (AR + G) and the active receptor can bind a G-protein in the absence of bound agonist (A + R*G) however G-protein cannot bind the receptor unless it is activated in this model.

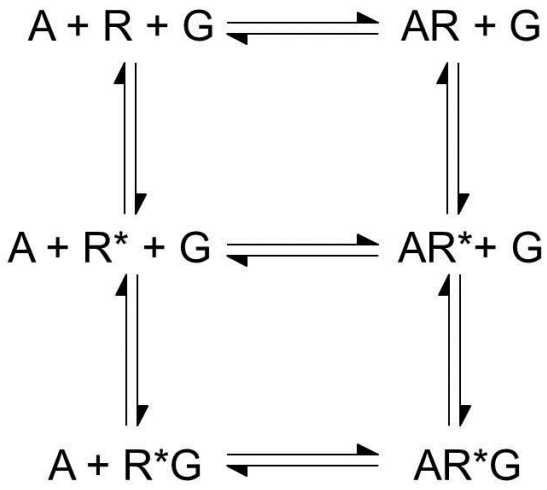

Figure 1.8 The Extended Ternary Complex Model

A denotes agonist, R denotes inactive receptor, R* denotes active receptor and G denote G protein. Proposed by Samama *et al.* (1993).

The extended ternary complex model was further expanded upon until it reached three dimensions, aptly named the cubic ternary complex model (Figure 1.9) (Weiss *et al.*, 1996). In the cubic ternary complex model G-proteins are capable of binding the receptor in the inactive, low affinity state which has lower affinity for both ligand and G-protein, yet has the ability to

bind both, thereby adding another dimension to the extended ternary complex model proposed by Samama and co-workers (Samama *et al*., 1993).

According to the extended ternary model and cubic ternary model, the receptor exists in equilibrium between the inactive (R) state and the active state (R*), mainly in the inactive (R) conformation in the absence of ligand, yet maintains the ability to spontaneously isomerise into the active conformation. This phenomenon gives rise to basal activity where a certain percentage of the receptor population is active at any one time in the absence of ligand; different receptors have different levels of basal activity attributed to differences in primary sequence. Is it generally well accepted that an agonist preferentially binds to the active receptor state (R*), and ligand binding thereby drives the equilibrium to increased proportions of receptors adopting the active conformation. Inverse agonists are proposed to have the opposing effect through their preferential affinity for the receptor inactive state, thereby driving equilibrium towards the R conformation. Antagonists are neutral mediators which have no preference to either R or R* conformations of receptors, therefore they do not affect equilibrium according to the model.

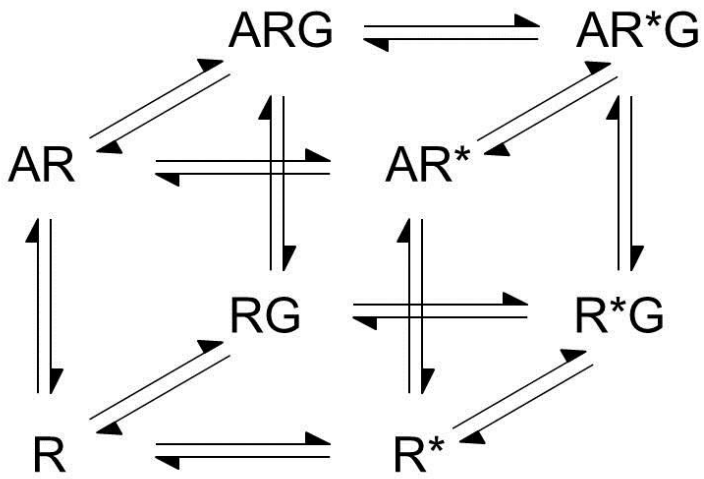

Figure 1.9 The Cubic Ternary Complex

A denotes agonist, R denotes inactive receptor, R* denotes active receptor and G denote G protein. An expansion of the extended ternary complex model proposed by Weiss *et al*. (1996).

It is becoming increasingly clear that these models fall short and do not describe all the conformations that GPCRs and their cognate ligands can adopt (agonists, antagonists, inverse agonists, partial agonists, partial inverse agonists, classes of G protein, allosteric agonists, accessory proteins, receptor oligomerisation, RAMPS and scaffold proteins), nor do the current

models account for the phenomena of signal bias caused by different ligands at the same GPCR which cause preferential coupling to different G proteins through different stimuli. It may well be better to think of GPCRs as inherent dynamic flexible machinery, capable of multiple receptor states along the spectrum of conformational space and time, where one receptor may be capable of hundreds of micro conformations (Kenakin, 2004). This idea is discussed extensively in a review by Kenakin (2003) which overviews many receptors and their ability to exhibit ligand-selective conformations, showing their ability to act as a bipolar recognition unit capable of binding many different molecules which exhibit subtly different receptor conformations. An example of a receptor capable of ligand-selective conformations is the PTH-1R; a receptor capable of activating both AC and PLC, which led to the discovery of a drug capable of stimulating the AC pathway, but not the PLC pathway. Kenakin (2004) proposes the micro conformations induced by drugs are so subtle that they may well overlap in some areas which appear to give similar responses to other ligands, which appear to give a similar response according to the pharmacological tools currently available, but we may see in the future that these conformations can be analysed and exploited in the field of drug research.

1.6 Allosteric Ligands

Another set of ligands which further deepens our knowledge of multiple receptor-state conformations are those ligands which do not bind at the orthosteric binding site where the naturally occurring agonist binds, but rather elsewhere at a structurally dependent locus, these are termed allosteric ligands. In this context, the entire surface of the GPCR and inherent pockets formed in all micro conformations of the dynamic structure of the GPCR may be considered a potential binding site for any bioavailable compound (Christopoulos & Kenakin, 2002). Allosteric ligands may be capable of positive or negative influence to a GPCR, permitting receptor conformation to adopt an active-like state which confers partial or full agonism at the receptor, alternatively they may bind the receptor to promote an inactive conformation, reducing the basal level of activity to full or partial inverse agonism. A classic example of a positive allosteric modulator is the G protein itself, which alters receptor conformation equilibrium into a more active state to promote agonist binding. The quaternary complex model is possibly one of the most complex equilibrium models used to describe the interactions between receptor, orthosteric ligand, allosteric ligand and G protein (Figure 1.10) and describes the relationship and influence they have upon each other. An example of a non-peptide allosteric ligand capable of positive influence on a receptor is compound B; a full

agonist which exhibited μM potency at the GLP-1R, yet the effect could not be antagonised by the orthosteric antagonist Ex4(9-39) at the GLP-1R expressed in HEK293 cells (Sloop *et al*., 2010), demonstrating the site of binding of compound B is distinct from the orthosteric binding pocket.

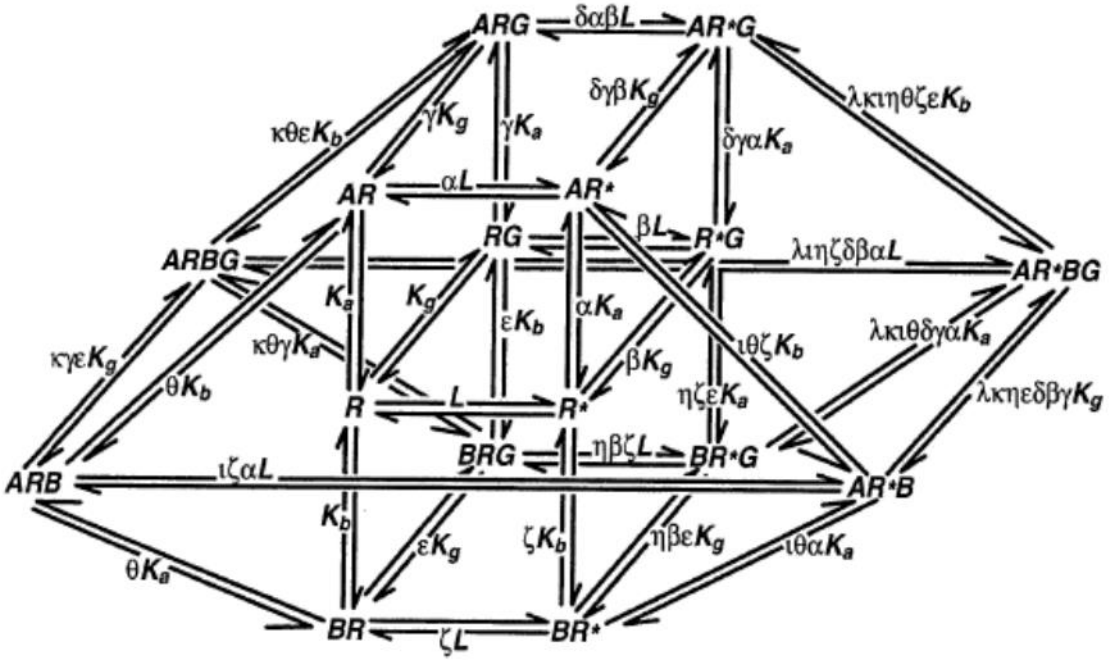

Figure 1.10 The quaternary complex model for allosteric ligand binding.

The quaternary complex model describes the relationship of binding and activation between four entities: the orthosteric ligand, **A**; the allosteric ligand, **B**; the receptor, **R** (in two conformations: inactive (**R**) and active (**R***)); and the G protein, **G**. The parameters used to define the quaternary complex model are as follows: receptor isomerization constant, **L**; equilibrium association constant for orthosteric ligand [A], $\mathbf{K_a}$; equilibrium association constant for allosteric modulator [B], $\mathbf{K_b}$; equilibrium association constant for G protein [G], $\mathbf{K_g}$; activation cooperativity of [A] for the unliganded receptor, **α**; activation cooperativity of [G] for the unliganded receptor, **β**; binding cooperativity between [A] and [G], **γ**; activation cooperativity between [A] and [G], **δ**; binding cooperativity between [B] and [G], **ε**; activation cooperativity of [B] for the unliganded receptor, **ζ**; activation cooperativity between [B] and [G], **η**; binding cooperativity between [A] and [B], **θ**; activation cooperativity between [A] and [B], **ι**; binding cooperativity between [A], [B], and [G], **κ**; activation cooperativity between [A], [B], and [G], **λ**. Figure modified from Christopoulos & Kenakin, Figure 6, page 339 (Christopoulos & Kenakin, 2002).

Allosteric ligands alternatively may just be modulators of the GPCR, altering the conformation without activating a particular pathway. Indeed they may also be capable of signal bias, a theory proposing that certain allosteric modulators display cooperativity with other ligands in a ligand-specific manner for coupling to a certain G protein. An example of an allosteric modulator of this characterisation would be quercetin, a flavonoid non-peptide

compound which has been shown to not have any intrinsic activity at FlpIn-CHO cells constitutively expressing the human GLP-1R, but when administered simultaneously with high affinity agonists such as GLP-1(7-36) or Ex4(1-39) was shown to enhance the intracellular mobilisation of Ca^{2+} in comparison to just agonist alone, yet quercetin did not have any effect on low potency agonists such as GLP-1(1-36) or oxyntomodulin (Koole *et al*., 2010). Quercetin did not augment cAMP responses under the same conditions, showing quercetin selectively modulates intracellular calcium mobilisation by modulating the GLP-1R to selectively couple to the $G\alpha_q$ pathway rather than the $G\alpha_s$ pathway.

A number of other ligands have been shown to possess intrinsic activity at the GLP-1R, but additionally be able to modulate orthosteric agonist responses in a pathway-specific manner; such ligands are termed ago-allosteric modulators. Compound 2 (Koole *et al*., 2010) and compound B (Sloop *et al*., 2010) have both been shown to possess full or partial agonism at the GLP-1R with μM potency, but additionally be able to influence the binding or activation properties of full and partial agonists GLP-1(7-36) and GLP-1(9-36) respectively at the GLP-1R (Li *et al*., 2012). Such characteristics could be exploited in the field of drug discovery and drug screening. Traditionally, small non-peptide molecules have been engineered to mimic the orthosteric agonist properties at the GPCR, for Family A GPCRs with small natural ligands this approach has been successful (Black, 1989) but Family B GPCRs with larger peptidic ligands with receptor-interactions postulated to make multiple contacts at the extracellular domain, extracellular loops 1 and 2 and the core domain (Runge *et al*., 2008), this approach has been less successful.

Allosteric modulators may provide a new avenue of therapeutics; exploiting their pathway specific and signal bias characteristics to augment the signalling profile of endogenous ligands without the need to identify those which bind at the orthosteric site, which largely results in ligand competition for this site, therefore a small non molecular agonist would have to be engineered to have nM potency similar to the endogenous agonist to promote a similar physiological response, again this is difficult due to all possible ligand-receptor interactions required for maximal activation responses. Perhaps drug screening could utilise agonist bound receptor complexes to identify small molecules capable of augmenting many different pathways, rather than the classic technique of identifying small molecules capable of orthosteric binding with only intrinsic agonism for a certain pathway, as this may result in more successful screening trials, as surely many efficacious ligands with different pathway enhancing characteristics have been overlooked using the current commercial drug screening process.

1.7 GPCR Oligomerisation

Further expanding into the vast array of GPCR activation is the notion of GPCR oligomerisation. Originally it was thought that GPCRs acted alone in the membrane (Terrillon & Bouvier, 2004), coupling with one G protein and binding only the one ligand, but as discussed so far, most of these original theories have been challenged by recent discoveries. The members of the Glutamate Family of GPCRs have been proposed to dimerise in order to be able to couple to G proteins to transduce their signal in a finely tuned manner, and have been described as "strict constitutive dimers" (El Moustaine *et al.*, 2012). Dimers can exist as homodimers, consisting of two of the same GPCR, such as the β_2AR which was found to dimerise with itself at the cell surface of HEK-293 cells by use of bioluminescence resonance energy transfer assay (Hebert *et al.*, 1996), or they can exist as heterodimers consisting of two different GPCRs, such as the coupling of GBR1 and GBR2 via a coiled-coil interaction between their respective intracellular carboxyl domains to form the $GABA_B$ receptor (Pin *et al.*, 2005).

With respect to the work in this thesis, it has been discovered that the GLP-1R forms homodimers by using a TM4 interface for both homodimers; this is also true for other Secretin Family receptors (Harikumar *et al.*, 2012). By mutation of the TM4 homodimer interface cAMP production and ERK phosphorylation via the AC and MAPK pathways respectively were attenuated, but intracellular calcium mobilisation was vanquished upon orthosteric peptide ligand mediated stimulation. Furthermore allosteric compound 2-mediated receptor activation of the $G\alpha_s$ pathway was attenuated more than the orthosteric ligand pathway, reducing the levels of cAMP production, whereas the pERK signalling pathway was not significantly altered using the TM4 mutant receptors upon compound 2-mediated stimulation. This suggests that allosteric ligands may require GLP-1R homodimerisation for an optimal signalling profile, and compound 2 displays signalling bias via the cAMP pathway that is significantly attenuated when the GLP-1R is in monomeric form.

GPCR dimerization has been linked to correct translocation from the ER to the cell surface (Milligan *et al.*, 2007), and although not fully necessary for the coupling of G proteins, is required for optimal signalling using the orthosteric signalling pathway in metabotropic glutamate receptors (El Moustaine *et al.*, 2012). Dimerization has also been associated with correct protein folding as seen in the β_2AR, where mutation within the dimerization motif caused ER harbouring of the receptor and was not transported to the cell membrane (Salahpour *et al.*, 2004). Oligomerisation is also required for proper signal transduction (Galvez *et al.*, 2001), G-protein specificity (Fan *et al.*, 2005), signal modulation (Hilairet *et al.*, 2003) and

control of physiological function (AbdAlla *et al*., 2001). Clearly, GPCR oligomerisation is essential for correct receptor function in many aspects.

In addition to forming homodimers or heterodimers with other GPCRs, some Secretin Family GPCRs also possess the ability to interact with receptor activity-modifying proteins or 'RAMPs' which are single transmembrane proteins of around 150 residues in length which complex with GPCRs to act as molecular chaperones, permitting GPCR membrane translocation from the ER and golgi (McLatchie *et al*., 1998). RAMPS also toggle receptor-ligand specificity between different ligand species depending upon which RAMP is associated with the receptor, again, permitting signal bias in a most blatant way (Sexton *et al*., 2006). RAMPS were first discovered in 1998 whereby the elusive receptor of the calcitonin gene related peptide (CGRP) was finally identified to be the calcitonin receptor-like receptor (CRLR) complexed with an accessory protein which McLatchie and co-workers named RAMP1. Co-transfection of HEK293T cells with either CRLR or RAMP1 alone gave no significant rise in CGRP-mediated activity, yet co-transfected gave a much higher response. In the same study they showed that CRLR co-transfected into HEK293T cells with RAMP2 was the selective receptor for adrenomedullin (McLatchie *et al*., 1998), and it is now known that CRLR and RAMP3 also complex together to receive adrenomedullin as the cognate ligand, forming the AM1 and AM2 receptors respectively.

The three RAMPs consist of one TM spanning helix with the amino terminus facing extracellularly and consist of around 90 residues; with a smaller 9 residue carboxyl terminus located intracellularly, yet the three RAMPS show only 30% sequence identity. RAMPS also associate with the calcitonin receptor to toggle ligand selectivity for amylin over calcitonin, where RAMP1 and RAMP3 are most effective at modulating ligand affinity for amylin. RAMPS can associate with other members of the Secretin Family, namely the VIP/ VPAC1 receptor which interacts with all three RAMPS, VPAC2 receptor which interacts with all three RAMPS, CRF1R can interact with RAMP2, PTH-1R which interacts with RAMP2, PTH-2R which interacts with RAMP3 and the GCGR which has been shown to interact with RAMP2 (Wootten *et al*., 2013). The GLP-1R has been shown to not interact with RAMPS.

1.8 Receptor Desensitisation and Internalisation

Ligand binding at GPCRs does not result in a continuous stimulus within the target cell but is rather desensitised to the stimulus (Katz & thesleff, 1957) as a continued stimulus could be detrimental to cell health and potentially hazardous for the health of the organism as a whole. GPCR desensitisation can occur via two mechanisms, via homologous and heterologous desensitisation. Heterologous desensitisation occurs independently of ligand binding to the GPCR and occurs primarily via phosphorylation of tyrosine residues located on the C-terminal tail of GPCRs via secondary protein kinases such as PKA or PKC (Hausdorff *et al*., 1990). Ligand independent phosphorylation of GPCRs targets receptors which have not been activated for internalisation and degradation. In addition to PKA and PKC, other proteins have been shown to be able to phosphorylate GPCRs, namely CK1, CK2 and PKB/Akt which subsequently induce: the ERK signalling pathway, the JUN-kinase signalling pathway and cell migration respectively (Tobin, 2008).

Homologous desensitisation is dependent upon ligand occupancy of the receptor and occurs via the phosphorylation of serine and threonine residues within the C-terminal tail and the intracellular loops via a group of proteins named G protein-coupled receptor serine/ threonine kinases or GRKs, (Kahout & Lefkowitz, 2003). Ligand binding at the extracellular face of the GPCR and concomitant conformational change within the receptor increases the affinity of the receptor for GRKs, thereby increasing the rate of recruitment of these proteins to the receptor. There are seven GRKs and activated GPCRs may recruit one or more GRKs simultaneously. Once the GPCR is phosphorylated it recruits a different class of proteins: the β-arrestins, which when bound cause steric hindrance to the recruitment of G proteins to the activated receptor, thereby uncoupling the GPCRs from G-proteins and hence finely tune signal transduction. There are four types of β-arrestins named 1-4 (Claing *et al*., 2002) which are located within the cytosol in the phosphorylated state until GPCR phosphorylation-mediates sequestration of the de-phosphorylated β-arrestin to the plasma membrane. β-arrestins promote clathrin-dependent GPCR internalisation by firstly interacting with adapter protein 2 (AP2) which then recruits clathrin, thereby acting as an adapter tagging the GPCR to clathrin-coated pits (Hill, 2006). Following clathrin-dependent endocytosis into endosomes, the GPCR is de-phosphorylated and then either recycled back to the cell surface for another round of activation, desensitisation and internalisation (Luttrell & Lefkowitz, 2002), or it can be ubiquitinated, thereby targeting the GPCR for destruction by the proteasome (Shenoy *et al*., 2001).

In addition to clathrin-dependent endosomal internalisation of GPCRs, β-arrestin has also been shown to act as a scaffold protein, mediating tertiary signalling pathways for numerous signalling pathways through being located at the plasma membrane and being associated with a phosphorylated GPCR. β-arrestins have been shown to interact with the mitogen-activated protein kinase (MAPK) family of proteins, such as ERK1 and ERK2, p38 and c-Jun kinases, these are involved in a plethora of cellular functions such as cell cycling regulation, transcriptional control and regulation of apoptosis (DeWire *et al*., 2007). A growing hypothesis is that β-arrestin may also play a part in actin reorganisation to mediate chemotaxis in an agonist-dependent manner via interaction with a plethora of cytoskeletal modifying proteins and enzymes (Min & DeFea, 2011).

1.9 Glucagon-Like Peptide-1

The glucagon-like peptide-1 receptor (GLP-1R) belongs to the Secretin Family of GPCRs (GRAFS classification) or Family B (A-F classification system). The GLP-1R is expressed on the surface of many cell types, including pancreatic α and β cells, hepatocytes, cardiovascular tissues, neurones, renal cells, skeletal muscle, adipocytes and lung tissue (Gautier *et al*., 2005). The cognate ligand of the GLP-1R is a 30 residue peptide hormone, GLP-1. GLP-1 is synthesised from the proglucagon gene expressed in the intestinal L cells as one of many potential products (Figure 1.11), including glucagon, GLP-1, GLP-2 and glicentin; glucagon-like peptides 1 and 2 are so-called because of their high sequence similarity with glucagon (Hansotia. & Drucker, 2005). The proglucagon gene resides on the long arm of chromosome 2 and spans 10kb, constituting 6 exons and 5 introns (Hansotia T. & Drucker, 2005). The glucagon gene was first isolated and cloned in 1983 (Bell *et al*., 1983) and led to the discovery of GLP-1 and GLP-2 situated to the carboxyl terminus of the preproglucagon gene transcript product, and the rat GLP-1R was subsequently cloned in 1992 (Thorens, 1992).

In mammalian cells, the preproglucagon gene is transcribed, translated, and processed alternately depending on the cell type, to give rise to the final active hormones. In the enterochromaffin L cells in the distal ileum and colon, the enzyme proconvertase 1/3 processes the preprohormone transcript to yield GLP-1, as well as some GLP-2. In the α cells of the pancreas located in the Islets of Langerhans, the enzyme proconvertase 2 processes the preprohormone transcript to yield glucagon (Verspohl, 2009). In the L cells, inactive GLP-1 (1-37) undergoes further processing prior to release upon nutrient stimulation, by cleavage of the 6 N-terminal residues from the main peptide to give GLP-1 (7-37). It can then, but not necessarily

does, undergo a final step, to remove the last residue, and amidate the carboxyl group on the 36th residue to give GLP-1 (7-36)amide. GLP-1 (7-36)amide is the most predominant circulating form, although both forms are equipotent, exert the same biological and physiological effects upon receptive cells and have the same half-life. The main physiological function of GLP-1 is the incretin effect.

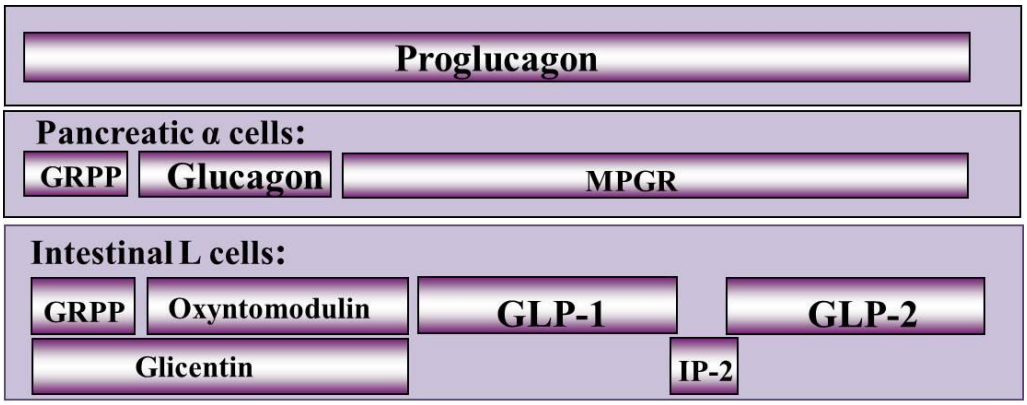

Figure 1.11. Differential processing of the proglucagon gene transcript in different tissues.

Preproglucagon is processed into proglucagon in both the α cells of the pancreas and the intestinal L cells, where it is differentially processed into the fragments shown in the cartoon image. Abbreviations: GLP: glucagon-like peptide; GRPP: glicentin-related polypeptide; IP-2: intermediate peptide-2 and MPGF: major proglucagon fragment.

1.10 The Incretin Effect

The incretin effect describes the phenomenon of oral ingestion and absorption of glucose by the gastro-intestinal tract eliciting a greater insulin response than if isoglycaemic levels of blood glucose were achieved via the parenteral route (Tillil *et al*., 1988). The incretin effect was first exhibited graphically in a 1964 article (Figure 1.12) (McIntyre *et al*., 1964). Within the study an equal dose of glucose was administered intravenously and orally, and blood samples taken periodically to check for levels of circulating glucose and insulin, it was found that each method of glucose administration resulted in a sharp rise in blood glucose levels, but the orally administered glucose resulted in a more profound circulating insulin level (Figure 1.12), indicating the presence of an additional gut-derived factor that potentiated insulin secretion upon ingestion of nutrients. The incretin effect is believed to be mediated by two small peptide hormones secreted by the gastro-intestinal tract; they are glucose dependent

insulinotropic polypeptide (GIP) and glucagon-like peptide 1 (GLP-1); as this thesis is dedicated to GLP-1, only GLP-1-mediated insulinotropic actions will be addressed.

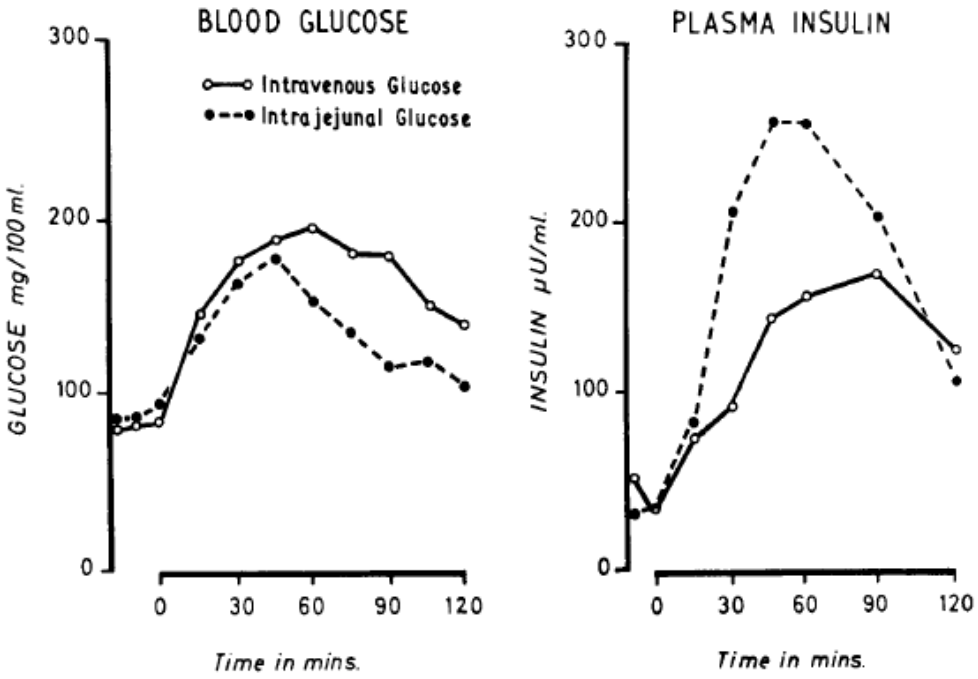

Figure 1.12 The incretin effect in healthy human volunteers.

Graphical representation of blood glucose levels of two healthy male volunteers following intravenous and intrajejunal glucose administration and the concomitant insulin levels derived from each glucose administration technique. Intrajejunal glucose administration resulted in a two-fold increase in circulating insulin levels in comparison to intravenous glucose administration. Taken from McIntyre *et al*. (1964).

As a key peptide hormone in the regulation of circulating insulin levels, the primary trigger for GLP-1 release into circulation is the enteral ingestion of nutrients, namely carbohydrates (Koole *et al*., 2013). Under fasting state conditions circulating levels of GLP-1 are between 5 – 10 pM and following nutrient ingestion rise to between 15 – 50 pM (Kazakos, 2011) in a bi-phasic release mode with an initial peak around 10 – 15 minutes following a meal and then a sustained response, peaking around 60 minutes following ingestion (Herrmann *et al*., 1995).

1.11 Physiological Effectors of GLP-1

The peptide hormone GLP-1 exerts a plethora of homeostatic effects via interaction with the GLP-1R. The first homeostatic effect that was noted was the insulinotropic effect observed following ingestion of food as previously stated. GLP-1 achieves the incretin effect via interaction with the GLP-1R situated at β-cells of the pancreas by a multitude of actions, mainly preparing intracellular machinery for maximal output upon glucose detection (Figure 1.13). GLP-1 action at the β-cell is mainly mediated by two secondary effectors: PKA and Epac2 as discussed below.

Oral consumption of nutrients elevates blood glucose levels (BGL) and circulatory insulin levels. GLUT 2 (Figure 1.13) is a high-capacity, low-affinity facilitative glucose transporter, only transporting glucose from the blood into the β cell when levels are aptly high (Kellett & Brot-Laroche, 2005). Upon entry into the β cell, glucose is quickly metabolised via glycolysis in the cytoplasm, the resultant pyruvate enters the citric acid cycle and oxidative phosphorylation in the mitochondria, resulting in a high ATP:ADP ratio in the cell. The increased ATP:ADP ratio has dual effects upon insulin release (Figure 1.13). Firstly, ATP interacts with the $K_{ir6.2}$ subunit of the K^+_{ATP} channel (Holz *et al.*, 2006) via the nucleotide binding domain of the $K_{ir6.2}$, disabling the efflux of potassium by closing the channel; the concentration of intracellular potassium therefore builds up, causing depolarisation of the plasma membrane. Membrane depolarisation causes opening of the L-type voltage dependent calcium channel (Figure 1.13) resulting in an influx of calcium ions. A raised intracellular calcium level causes primed granules (containing insulin) just below the membrane, to fuse and dock, releasing their contents into circulation (Gloerich & Bos, 2010). This can be amplified by calcium-induced calcium release from the endoplasmic recticulum via the Ryr channel (Figure 1.13) (Gloerich & Bos, 2010), amplifying the net intracellular concentration of calcium, thus potentiating insulin release. GLP-1 poses additive effects to this basic glucose dependent insulin release as described below.

1.11.1 PKA-Mediated Insulin Release

GLP-1 binding at the GLP-1R primarily exerts its effects in a cAMP dependent manner, through two effector proteins, PKA and Epac2. The GLP-1R is primarily coupled to adenylyl cyclase (AC) via $G\alpha_s$. Upon ligand binding and activation of the receptor, the GTP-bound α G-

protein subunit activates AC, which then cyclises ATP molecules to cyclic AMP. Cyclic AMP binds the regulatory domains of PKA, repressing auto-inhibition. PKA accounts for approximately 40-50% of the acute phase release of insulin from readily-releasable pools (RRP) as discovered by Kashima *et al.*, when PKA was inhibited (Kashima *et al.*, 2001). Recently, Song and co-workers showed that phosphorylation of snapin by PKA enhances insulin containing granule interaction with other proteins which mediate insulin exocytosis via membrane fusion, thereby showing that PKA-dependent phosphorylation enhances insulin secretion in a glucose-dependent manner (Song *et al.*, 2011). Furthermore, mouse models expressing constitutively active PKA in pancreatic β cells (by knockout of the PKA regulatory domain) were found to have a significantly increased acute *and* chronic phase insulin response under hyperglycaemic conditions in comparison to control littermates (Kaihara *et al.*, 2013). Indeed, incretin hormones did not potentiate further insulin response in the constitutively active PKA mice models, suggesting incretin hormones act primarily via the cAMP/PKA pathway to augment insulin secretion. PKA also promotes insulin secretion via closure of the K^+_{ATP} channel via phosphorylation of the SUR1 subunit which disrupts ADP binding, therefore the β cell becomes depolarised resulting in Ca^{2+} influx (Light *et al.*, 2002). Finally, it has been shown that GLP-1R cAMP signalling via the PKA pathway inhibits repolarisation of the plasma membrane following the initial depolarisation event, by antagonising voltage-dependent K^+ channels (MacDonald *et al.*, 2003).

PKA also acts indirectly to promote insulin release by enhancing gene transcription of important cellular machinery involved in glucose-sensing and insulin release. Active PKA translocates into the nucleus where it phosphorylates the transcription factor CREB (cAMP Response Element Binding factor) at S133 (Perry & Greig, 2003). Active CREB binds the cAMP Response Element and proceeds in transcription of genes involved in cell survival (Perry & Greig, 2003) and insulin release, such as proinsulinogen, GLUT 2 and glucokinase (Verspohl, 2009). PKA activation leads to long-term genesis of important cellular factors that mediate the insulin response.

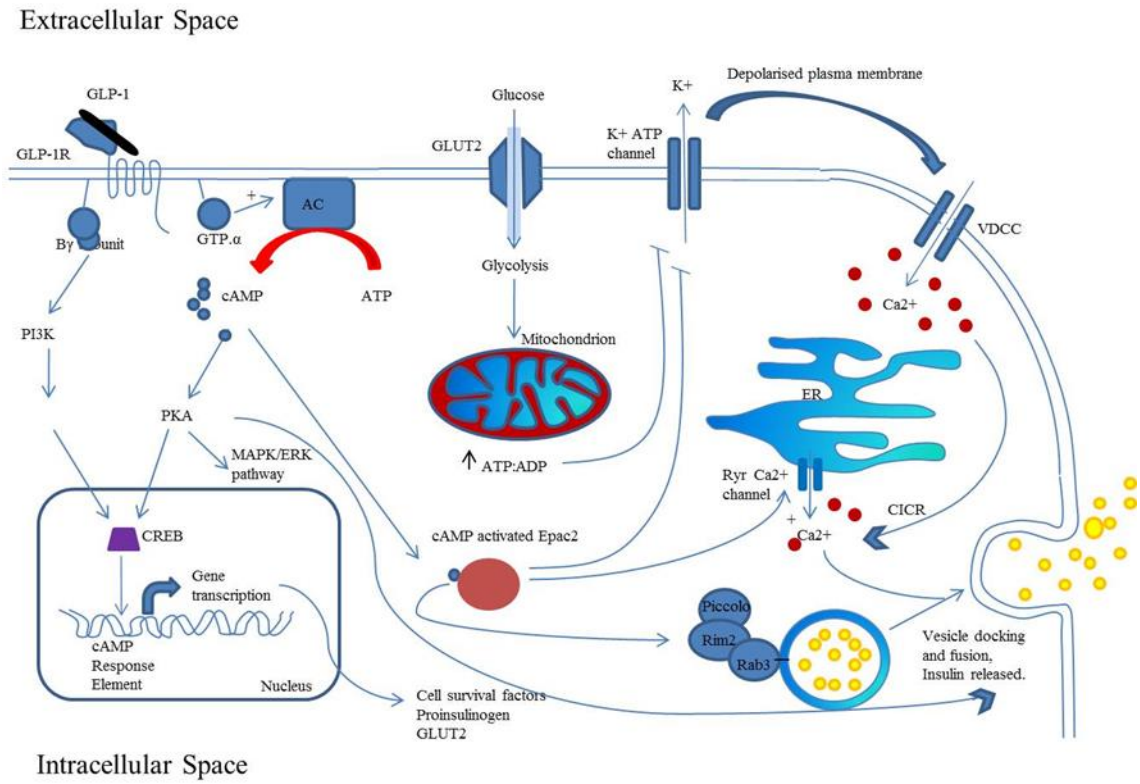

Figure 1.13 Mechanisms of GLP-1 mediated incretin effect at pancreatic β cells.

Lines with arrow heads indicate a positive response/ influence, lines with blunt ends indicate a negative/ inhibitory effect. The abbreviations are as follows: AC, adenylyl cyclase; PI3K, phosphatidylinositol 3-kinase; PKB, protein kinase B/ Akt2; PKA, protein kinase A; MAPK, mitogen-activated protein kinase; ERK, extracellular-signal-regulated kinase; VDCC , voltage dependent calcium channel; CICR, calcium-induced calcium release; ER, endoplasmic recticulum. A change in the intracellular ATP levels is sensed by the Kir-$_{6.2}$ subunit of the $K+_{ATP}$ channel, causing channel closure. Prevention of potassium efflux causes membrane depolarisation and calcium influx through the VDCC, which induces CICR.

1.11.2 Epac2-Mediated Insulin Release

Epac2 is a part of the family of cAMP regulated guanine nucleotide exchange factors. Epac is an acronym for "exchange proteins directly activated by cAMP" (Holz *et al*., 2006). Epac1 is ubiquitously expressed, but Epac2 is less ubiquitous, and amongst other select regions, is expressed in the pancreatic Islets of Langerhans. Epac2 has two binding sites for cAMP in its regulatory region, which relieves autoinhibition upon cAMP association (Holz *et al*., 2006). Epac2 has four proposed modes of enhancing insulin secretion. Firstly, Epac2 binds to the SUR1 regulatory component of the K^+_{ATP} channel at the nucleotide binding fold-1 (NBF-1), this has been hypothesised to quench efflux of potassium ions leading to membrane depolarisation and calcium influx (Gloerich & Bos, 2010). Secondly Epac2 is a GEF for the guanosine

triphosphatase RAP, which then activates phospholipase C-ε in a GTPase dependent manner. PLC-ε is then thought to reduce the concentration of membrane-bound phosphatidylinositol 4,5-bisphosphate (PIP2) in the micro-environment of the K^+_{ATP} channels; as PIP2 stimulates K^+_{ATP} activity, a reduction in localised PIP2 is thought to prevent K^+ efflux, thereby causing membrane depolarisation (Leech *et al.*, 2010). Thirdly, Epac2 mediates calcium-induced calcium release in the presence of raised intracellular calcium levels, most likely by targeting the Ryr channel which resides on the ER membrane (Figure 1.13), which releases intra-endoplasmic calcium stores into the cytosol. The inositol 1,4,5-trisphosphate receptor (IP3R) which also resides on the ER membrane, permits efflux of calcium ions when Ryr is stimulated by Epac2, therefore IP3R and Ryr have an additive effect on calcium induced calcium release (Kang *et al.*, 2005). Lastly, Epac 2 binds to the exocytic machinery Rim2 and Piccolo (Figure 1.13), therefore Epac2 is speculated to regulate vesicle docking and binding; also PKA and Epac2 dependent insulin secretion pathways converge via interaction with snapin, promoting extracellular granular content release (Song *et al.*, 2011).

Both PKA and Epac2 have been shown to assist the refilling of the RRP following the acute phase insulin response (Gromada *et al.*, 2004), and to enhance the relative size of the granules containing insulin for release (Eliasson *et al.*, 2003). These findings correspond to the observation that GLP-1R activation mediates an increase in both acute phase and sustained/chronic phase of insulin release.

1.12 GLP-1-Mediated Glucose Homeostasis

In addition to enhancing the pancreatic output of insulin, GLP-1 also reduces glucagon secretion from the α cells of the pancreas, thereby reducing hepatic glucose output and reducing blood glucose levels further (Orskov *et al.*, 1988). GLP-1 also possesses the ability to promote β-cell proliferation and to decrease the rate of β-cell apoptosis (Li *et al.*, 2003) the overall effect being the relative increase in β cell mass and β cell function. Additionally, GLP-1 mediates differentiation of progenitor cells in the pancreatic duct epithelium (Zhou *et al.*, 1999), thus producing more new β cells. The combination of pancreatic β cell protective effects makes GLP-1 an ideal candidate for therapeutic treatment of T2D.

GLP-1 plays a central role in the ileal brake, to adjust the digestive and absorption capacity of the digestive tract, by slowing the transit of chyme and decreasing secretion of digestive enzymes (Perry & Greig, 2003). The slowing of digestive transit results in chyme

residing in the stomach for longer, thereby elevating satiety and reducing glucose input into circulation. Exogenous GLP-1 administration in experimental studies has been shown to reduce food intake in rodents, likewise, the administration of the GLP-1R antagonist Exendin 4 (9-39) (Ex4(9-39)) eradicates this effect (Van Dijk & Thiele, 1999). Weight loss due to a lessened food intake was observed in the Zucker diabetic rat model, db/db mice, and in rhesus monkeys. In addition a decreased appetite resulted in reduced calorific intake and subsequent weight loss was observed in normal and type 2 diabetics (Meier *et al*., 2002). GLP-1 has been speculated to be able to pass the blood-brain barrier via simple diffusion into the hypothalamic area (Kastin *et al*., 2002), and therein modulate the secretion of hormones which regulate appetite (Larsen *et al*., 1997); this may possibly be the reasoning behind the appetite control seen in these models.

GLP-1 promotes the passage of glucose from the bloodstream into storage cells, such as skeletal muscle, hepatocytes and adipocytes by enhancing insulin sensitivity at these cells (Young *et al*., 1999). GLP-1 is postulated to achieve this by enhancing glycogen synthase activity which converts glucose into glycogen for long term storage (Baggio & Drucker, 2007). The overall effect of these actions is a decrease in circulating BGL. Additionally GLP-1 has been shown to only exert its effects in a glucose dependent manner, therefore if BGL drop below 4.5 mM GLP-1 ceases to promote hypoglycaemic effects, thereby avoiding hypoglycaemia (Verspohl, 2009).

1.13 Extra-Pancreatic Effects of GLP-1

GLP-1 has been shown to exert protective effects on neuronal and pancreatic cells by the activation of cAMP, thus protecting them against apoptosis in various paradigms (Perry & Greig, 2003). GLP-1 and Exendin-4 can protect hippocampal neurones (cultured from embryonic Sprague-Dawley rats) against glutamate-induced apoptosis, suggesting that GLP-1 based therapies not only have insulinotropic properties, but also have the ability to protect β cells against apoptosis, and even have the scope as possible therapies in neurodegenerative diseases (Perry *et al*., 2002). GLP-1 has also been shown to enhance the proliferation and neogenesis of neurones, and to promote learning in rodents (During *et al*., 2003), implicating a definitive role for GLP-1R agonists in the treatment of neurodegenerative diseases such as Alzheimer's and Parkinson's (Duarte *et al*., 2013).

In addition to being neuronally protective and pancreatically protective, GLP-1 has also been shown to have beneficial effects at other organs, such as the heart, lungs and kidneys. Mice

lacking the GLP-1R were shown to have a lower resting heart rate with increased diastolic pressure and abnormal left ventricular wall thickness than in wild type littermates (Gros *et al*., 2003). In addition to improving insulin sensitivity and glucose responses at skeletal muscle and adipose tissues, GLP-1 has also been shown to enhance insulin sensitivity at cardiac endothelial cells, thereby improving function of these cells providing some protection against atherosclerosis (Nyström, 2008). Furthermore, GLP-1 has been shown to reduce the extent of tissue damage and death from ischaemic-reperfusion injury in an *in vitro* perfused rat heart model (Bose *et al*., 2007). GLP-1 has also been associated with reduction of hypertension by relaxing the pulmonary artery, enhancing sodium ion excretion at the kidneys and augmenting mucosal secretion in the endothelia of lung and trachea (Richter *et al*., 1993; Gutzwiller *et al*., 2006).

1.14 GLP-1R Agonists are Therapeutic Agents for Type II Diabetes

Diabetes mellitus is one of the most common examples of metabolic disorder which is most prevalent in developed and developing countries, and is now considered so common it is referred to as an epidemic. In the past 20 years the number of sufferers has increased significantly and the World Health Organisation have estimated that, by 2025, 300 million people worldwide will have developed diabetes (Zimmet *et al*., 2001). Whilst the etiology of type I diabetes is well understood, involving an autoimmune attack on the pancreatic β cells resulting in absolute loss of insulin production, the exact etiology of T2D remains elusive as there are so many contributing factors. In addition to a genetic predisposition, other risk factors for the development of T2D include increased longevity, modern day living: inclusive of hypertension, a sedentary lifestyle and physical inactivity combined with a diet rich in fat and sugar, giving rise to obesity. Hence the term "diabesity" had been coined to describe the obesity-induced onset of T2D (Astrup & Finer, 2000), accounting for over 90% of diabetics, with type I diabetes accounting for about 6% of sufferers (Sicree *et al*., 2006).

T2D is generally characterised by progressive β-cell failure with the associated deficiency in insulin secretion (Lee & Pervaiz, 2007), alongside relative insulin resistance at effector cells such as adipose tissue, hepatocytes and skeletal tissues (Nyström, 2008). The combination of these conditions culminates in loss of proper glycaemic control, resulting in hyperglycaemia which left untreated results in glucotoxicity. Hyperglycaemia cannot be

corrected without the use of physical activity combined with a balanced diet and medical intervention. These conditions are slow to present themselves physically, causing bodily degeneration over time and are potentially lethal if left untreated. The morbid outcomes of T2D include heart attack, stroke, retinopathy, neuropathy, neurodegeneration and renal failure, placing a heavy social and economic burden on healthcare systems (Duarte *et al*., 2012). A number of risk factors contribute towards the worsening of the disease, such as increased blood triacylglycerols, hypertension, hyperglycaemia and obesity (Duarte *et al*., 2013). Interestingly these risk factors have been associated with neuronal dysfunction as seen in some forms of Alzheimer's disease, which has prompted the investigation of the cross-talk between T2D and Alzheimer's disease, with an emerging theory that Alzheimer's disease may actually be a 'type 3 diabetes' caused by relative neuronal insulin resistance (Duarte *et al*., 2013).

Intriguingly, almost all pathological physiological changes which occur as a result of T2D can be addressed using GLP-1, as afore mentioned the effects of GLP-1 are vast. GLP-1 is an incretin; therefore it enhances insulin release from the β-cells, addressing the issue of insufficient insulin release. Additionally it addresses the loss in β-cell mass from T2D associated apoptosis, thereby restoring cell numbers and overall cell function and health to the β cell clusters in the Islets of Langerhans. GLP-1 re-sensitises peripheral tissues to circulating blood insulin levels, which then act to mop up the excess glucose and excess triacylglycerols. Furthermore GLP-1 corrects hypertension by acting on areas of the brain, cardiac epithelia and kidneys. The induced satiety via hypothalamic interaction and participation in the ileal brake results in lowered calorific intake, leading to gradual weight loss which is extremely beneficial in the case of overweight/ obese individuals whom have contracted T2D. Finally, as it is neuroprotective and cardiac protective, GLP-1R stimulation lowers the risk of cardiovascular and neural infarction associated with T2D. Interestingly the levels of GLP-1 secretion in T2D sufferers is markedly reduced, yet GLP-1-mediated insulinotropic effects are retained if normal levels of the peptide are administered as GLP-1R expression remains intact (Toft-Nielsen *et al*., 2001). As such, GLP-1R agonists are currently used in the treatment of T2D.

The plethora of beneficial effects GLP-1 has with respect to the treatment of T2D makes GLP-1 a potential gold-standard therapeutic. Unfortunately, GLP-1 has a short half-life of around 2 minutes, and a majority of GLP-1 is inactive when it reaches the blood from L cells, due to the wide expression of the enzyme di-peptidyl peptidase IV (DPPIV) (Kieffer *et al*., 1995). DPPIV is a ubiquitously expressed aminopeptidase, which readily cleaves GLP-1 at position 2-alanine, resulting in a dipeptide and truncated metabolite GLP-1(9-36) which is orders of magnitude less effective than full-length GLP-1(7-36), and GLP-1(9-36) effects at physiological levels still remain controversial with some groups claiming it has no physical

effect (Vahl *et al*., 2003; Nagell *et al*., 2007) and others claiming it acts as a partial agonist at GLP-1R expressing cells (Elahi *et al*., 2008). GLP-1 is also a substrate for neutral endopeptidase 24.11 which cleaves GLP-1 into a multitude of shorter peptide products which are not efficacious at the GLP-1R (Hupe-Sodmann *et al*., 1995).

There are currently two long-acting DPPIV resistant GLP-1 analogues which are FDA approved to treat T2D, these are Liraglutide (Neumiller & Campbell, 2009) and Exenatide (Bhavsar *et al*., 2013) and they both exert GLP-1R mediated-antidiabetic effects. Liraglutide is a synthetic 31 residue peptide with 97 % sequence identity of GLP-1, with a K34R mutation, and has a palmitoyl motif at K26 which has been speculated to assist binding to serum albumin, thus achieving a lower rate of renal clearance, resulting in an extended half-life of between 10-15 hours. Exenatide was first isolated from the saliva of the Gila monster *H suspectum* (Eng *et al*., 1992) in the form of Ex4; a 39 residue peptide (Ex4(1-39)) which possesses only 53 % sequence identity with GLP-1 (Figure 1.14). Ex4(1-39) exhibits a longer half-life than GLP-1, as the alanine at position 2 of the peptide in GLP-1 is replaced by a glycine residue in Ex4, thereby making it less susceptible to DPPIV mediated cleavage (Al-Sabah & Donnelly, 2003). Regardless of its relatively low sequence identity with GLP-1, Ex4 is a high affinity potent agonist of the GLP-1R (Raufman *et al*., 1992) and has been extremely useful for research into the structure-function relationship of the GLP-1R. Indeed the globular amino-terminus of the GLP-1R was first crystallised using the truncated form of Ex4(9-39), an antagonist (Göke *et al*., 1993; Thorens *et al*., 1993) which assisted in the stabilisation of this domain thereby facilitating crystal formation (Runge *et al*., 2008).

Despite the success of these two peptides in the treatment of T2D, there has been recent concern regarding the possible side-effects of these long lived peptides, mainly these concerns are nausea (Nauck *et al*., 2009), but in some cases they have been associated with pancreatitis (Singh *et al*., 2013) and pancreatic cancer (Cure *et al*., 2008).

1.15 The GLP-1 Receptor

GLP-1 mediates its insulinotropic and antidiabetic effects via interaction with the GLP-1R. The GLP-1R is a Family B1/ Secretin Family GPCR as afore discussed, of 463 residues in length (Thorens, 1992). The first 23 amino acids from the GLP-1R N-terminus serve as a signal peptide and residues 24-145 make up the extracellular N-terminal domain (Figure 1.15) (Thorens, 1992). The extracellular N-terminal domain adopts the secretin receptor fold,

stabilised by the three conserved disulphide bonds between C46/ C71, C62/ C104 and C85/ C126 respectively (Bazarsuren *et al*., 2002), and is glycosylated at specific conserved asparagine residues (Göke *et al*., 2004).

Ligand recognition and receptor activation is thought to occur via the two-domain binding model, whereby the GLP-1 C-terminus recognises the GLP-1R extracellular domain and the GLP-1 N-terminus interacts with the GLP-1R transmembrane domain (Hoare, 2005). Interestingly Runge and co-workers showed that ligand specificity for the GLP-1R is mediated by ligand C-terminus interaction with the receptor extracellular domain using glucagon and GLP-1 chimeric ligands at the GLP-1R (Runge *et al*., 2003). GLP-1 to glucagon peptide ligand chimeric mutations within the C-terminal region of the ligand were not tolerated, whereas GLP-1 to glucagon chimeras within only the N-terminus of the ligand were tolerated at the GLP-1R, suggesting ligand exclusivity and selectivity occurs within the receptor extracellular domain. This is intriguing, as Ex4, a peptide with only 53 % sequence identity to GLP-1, (whereby most sequence identity is found within the N-terminus of both peptides with only 1 residue divergent in the first 9 residues) is able to bind and activate the GLP-1R with high affinity and high potency (Figure 1.14 and Figure 1.15).

As afore mentioned, the crystal structure of the extracellular domain of GLP-1R was crystallised complexed to the antagonist Ex4(9-39) by Runge and co-workers (Runge *et al*., 2008), and was later crystallised complexed with GLP-1 (Underwood *et al*., 2010). The crystal structure of the extracellular N-terminal domain of the GLP-1R is shown below, complexed with Ex4(9-39) (Figure 1.15.A) and GLP-1 (Figure 1.15.B) both show the NTD is formed by an α-helix and two regions of antiparallel β-sheets with interconnecting loops which are held together by a conserved core consisting of residues D67, W72, P86, R102 and W110. These, together with the conserved disulphide bonding residues aid the formation of the binding pocket for ligand C-terminus interaction. Binding of Ex4 at the isolated NTD occurs at the same orthosteric hydrophobic binding pocket that GLP-1 binds to (Figure 1.15). The binding pocket is formed from four discontinuous receptor NTD segments: (L32, T35, V36 and W39 of the α-helix); (Y69); (Y88-W91 of loop 2); and (L123) all combine to form a pocket in the NTD (Runge *et al*., 2008) where water molecules are completely absent in the ligand-complexed structure, thus the hydrophobic effect upon ligand binding is strong.

```
                    7       15     20          30     36
GLP-1(7-36)         HAEGTFTSDVSSYLEGQAAKEFIAWLVKGR
GLP-1(9-36)           EGTFTSDVSSYLEGQAAKEFIAWLVKGR
Exendin4(1-39)      HGEGTFTSDLSKQMEEEVARLFIEWLKNGGPSSGAPPPS
Exendin4(9-39)              DLSKQMEEEVARLFIEWLKNGGPSSGAPPPS
                    1       9           20          30        39
```

Figure 1.14. Sequence alignment of GLP-1 and Ex4 and their N-terminally truncated counterparts GLP-1(9-36) and Exendin 4(9-39).

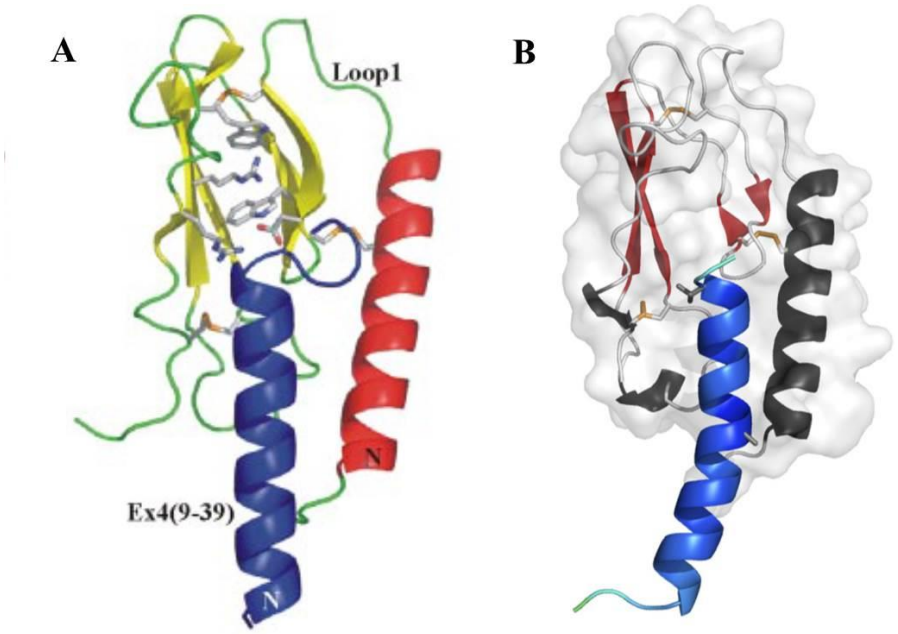

Figure 1.15. Crystal structure of the isolated human GLP-1R NTD-ligand bound complexes.

A. Ex4(9-39) shown as a blue ribbon is complexed with the human GLP-1R NTD with the GLP-1R depicted as α helical ribbons (red) and antiparallel β-sheets (yellow) with interconnecting loops in green and the side chains of conserved residues (D67, W72, P86, R102 and W110) shown as sticks.
B. GLP-1(7-36) shown as a pale blue ribbon is complexed with the human GLP-1R NTD shown in grey space-fill. The N-terminal α-helix is shown as a grey ribbon, the antiparallel β-sheets are shown as red arrows, and the two independent β-sheets are shown as grey arrows. The conserved disulphide bonds are shown as orange coloured sticks. Figure adapted from (Runge *et al.*, 2008) and (Underwood *et al.*, 2010)

1.1.6 GLP-1R Peptide-Ligand Interactions

1.1.6.1 GLP-1R Extracellular Domain Interaction

For ease of explanation and understanding, residues of the protein ligand will be denoted with an asterix (*) following the numerical indictor i.e. GLP-1 aspartic acid at position 15 will be D15*. Although only 30 and 39 residues in length, the GLP-1 and Ex4 peptides respectively can be thought of as having two to three distinct regions; both have a disordered 'N region' and a central α-helical 'H region', while the C-terminal 'Ex region' is unique to Ex4. The peptide-receptor interaction between GLP-1 and Ex4, and the GLP-1R, comprise two analogous components; the 'H-interaction' involving the H region of the peptide ligand binding to the receptor extracellular NTD, providing receptor recognition and a large percentage of the total binding energy, and the 'N-interaction' involving the ligand N-region associating with the receptor TMD and associated loops, contributing both affinity and activity to the receptor. This is known as the two-domain model of activation and is commonly accepted as the model by which Class B/ Secretin Family GPCRs are activated (López de Maturana *et al.*, 2003). The peptide helical region is thought to reside between residues 9-30 in Ex4 and between residues 15-36 in GLP-1 (figure 1 from Al-Sabah & Donnelly, 2003b), and these residues are critical for receptor recognition.

The structure of GLP-1(7-36) in receptor-bound format showed that GLP-1 adopts an α-helical conformation from residues T13*-V33*, with a kink at G22* (E16* equivalent at Ex4) essentially segmenting the helix into 2 smaller helices from T13*-E21*, and Q23*-V33*(Figure 1.16). This kink has been proposed to confer the different properties of the ligands Ex4 and GLP-1, as Ex4 is a rigid α-helix whereas GLP-1 has the propensity to bend and flex around G22* and has even been proposed to lie in an 'L' shape when bound to the full receptor (Lin & Wang, 2009), however the crystal structure solved by Underwood *et al*. (2010) shows GLP-1 adopts a kink rather than an L shape. This difference in opinion of the format of GLP-1R-bound GLP-1(7-36) could be due to the fact that the crystal structure showed binding of the α-helical peptide region to the isolated NTD, thus the non-interacting residues from H7* to Q23* were exposed for contacts with other GLP-1R NTD within the crystal packing formation rather than binding to the TM bundle, which may well be essential for GLP-1 to adopt the proposed 'L' shape. Following crystallisation of the NTD of GLP-1R bound to GLP-1(7-36) and to Ex4(9-39), Underwood *et al*. (2010) superimposed the positioning of the ligands and showed there is indeed a kink present at G22* of GLP-1 but not at E16* of Ex4(9-39) (Figure 1.15). This kink

did indeed show that residues H7-E21 in the amino helix before G22* in GLP-1 are positioned differently to D9*-E15* in Ex4(9-39), suggesting that they approach the TM bundle differently and would have different activation interactions at the core domain of the receptor.

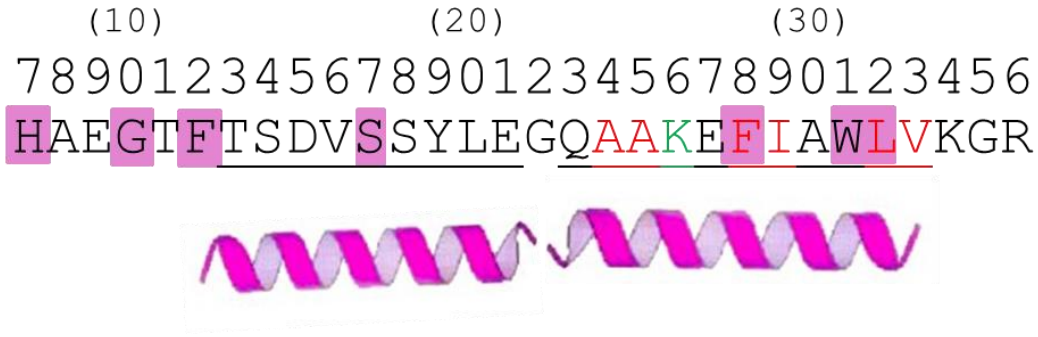

Figure 1.16. The sequence and topology of GLP-1(7-36).

The sequence is denoted in the standard amino-carboxyl terminus fashion. The residues are numbered using 0-9 numbering and are shown above the residue they correspond to, 0 denotes either residues 10, 20 or 30 as shown by the numbers in brackets above the 0. Residues with text coloured red show those amino acids that make hydrophobic contacts with the GLP-1R, green colouring shows the residue responsible for hydrophilic interaction with the receptor. The residues highlighted pink are those residues conserved across secretin peptides GLP-1, GLP-2, Ex4, GIP and glucagon except for H7* which is Y7 in GIP, also S17* is N17* in GLP-2. Underlined residues represent those which adopt an α-helical conformation when bound to the receptor and below those residues is a representation of an α-helix, note G22* is not underlined and the subsequent kink in the α-helix representation below G22*.

An alanine-scan technique was employed by Adelhorst *et al.* (1994) upon residues of the GLP-1 peptide ligand and these were analysed for efficacy and affinity at the GLP-1R. Four residues were identified as critical for affinity which resided within the denoted 'H-region'. These 4 residues: F28*, I29*, L32* and R36* shown in Figure 1.16 were all affected by the alanine mutation to various degrees. The residue which was most affected by the alanine scan was F28* whereby a reduction in potency and affinity was observed. These findings were reinforced by the crystal structure of GLP-1(7-36) complexed with the isolated NTD of GLP-1R (Underwood *et al.*, 2010), where F28* was found to interact with L32 of the receptor by complexing with A24* and A25*. Residues F28* and L32* were found to sandwich W31* within the hydrophobic binding pocket of the receptor, adjacent to W39 of the receptor. W31* is conserved across all secretin peptides: GLP-1, GLP-2, glucagon, Ex4 and GIP, as are the residues F28* and L32*, indicating these residues are essential for maintaining the affinity of peptide ligands via binding at the hydrophobic binding pocket, demonstrating that the exclusion

of water molecules permits efficient binding energy via a strong hydrophobic effect between ligand and receptor.

There are multiple direct contacts between the GLP-1 H-region and GLP-1R via hydrophobic residues interactions, namely V33* which makes side-chain interactions with Y69 and L123 as shown in the crystal structure (Underwood *et al.*, 2010); additionally the backbone carbonyl interacts via H-bonding with the terminal nitrogen of R121. L32* in addition to being essential for stacking within the hydrophobic pocket, was also found to interact with the other terminal nitrogen of R121 via a water molecule, hence alanine mutation of L32* has a two-fold effect, which explains the observation of loss of affinity by Adelhorst *et al.*(1994).

Other non-direct contacts between GLP-1 and the GLP-1R NTD include leucine 32 of the receptor, which complexes A24*, A25* and F28* via the hydrophobic effect and water exclusion, demonstrating the hydrophobicity of GLP-1 is the main governing function that permits receptor-ligand interactions, and mutation of any of the three groupings of hydrophobic residues within the H-region of GLP-1 (Figure 1.16) have deleterious effects on binding at the GLP-1R. Non-hydrophobic contacts are sparse within the H-region; only K26* was shown to have a high probability of making contacts with the side chain of E128 in the crystal structure (highlighted green in Figure 1.16).

The α-helical segment of Ex4 is continuous from residues L10*-N28* and is not kinked due to the placement of glutamic acid at position 16, which is analogous to the glycine residue at position 22 in GLP-1 (Figure 1.17). G22* in the middle of GLP-1 α-helix results in a much more flexible helix than a glutamate residue, due to the absence of a side chain in glycine, therefore the adjacent E15* of Ex4(9-39) (GLP-1 equivalent E21*) is capable of interacting with L32 of the GLP-1R in Ex4, but not in GLP-1, due to the kink in the α-helix. This extra interaction at the extreme N-terminal end of the H-interaction of Ex4 positions the amino-terminus of the helix in a more rigid position toward the TM bundle of the GLP-1R, whereas GLP-1 is more flexible. This inherent rigidness in positioning is further enhanced by intra-molecular bonds within the Ex4 molecule, conferring extra stability to the α-helix. These intra-molecular bonds occur between the positive side chain of R20* and the negative side chains of E16* and E17*, also the positive side chain of K27* interacts with the negative side chain of E24* (Figure 1.17). The H-domain of Ex4 therefore is more static than the H-domain of GLP-1, and these differences in hydrophobic, hydrophilic and intra-chain bonding may account for the observable differences in activity of the truncated peptides GLP-1(15-36) and Ex4(9-39) due to the positioning of the amino-terminal residues and their ability to flex to interact with activating residues within the core domain.

Similarities in structure between GLP-1 and Ex4 as binding partners at the GLP-1R include a hydrophilic and hydrophobic face attributed to the amphipathic nature of the side chains of the α-helix (Donnelly, 2012). Although hydrophobic interaction occurs at the same binding site for the two ligands, there are distinct structural changes to certain residues within the NTD which could translate to alternative signalling patterns between the two ligands. For example K27* of Ex4 (V33* equivalent in GLP-1) complexes with E127 through electrostatic interaction, this is confined to a specific spatial conformation which is not observed in GLP-1-bound receptor. V33* of GLP-1 does not interact with E127, Therefore E127 changes conformation and rotates away from the binding pocket, where it then causes the side chain of L123 to turn toward R121, which in turn causes R121 to flip toward P119 which closes a cavity in the isolated GLP-1 bound NTD, which is water accessible in the Ex4-bound form. The effects of this alternative conformation of ligand bound NTD forms of the GLP-1R are currently not known.

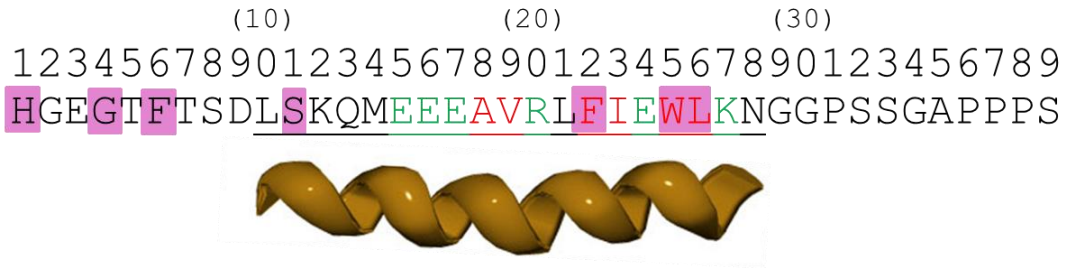

Figure 1.17. The sequence and topology of Ex4(1-39).

The sequence is denoted in the standard amino terminus to carboxyl terminus fashion. The residues are numbered using 0-9 numbering and are shown above the residue they correspond to, 0 denotes either residues 10, 20 or 30 as shown by the numbers in brackets above the 0. Residues with text coloured red show those amino acids that make hydrophobic contacts with the GLP-1R, green colouring shows the residues responsible for hydrophilic interaction with the receptor. The residues highlighted pink are those residues conserved across secretin peptides GLP-1, GLP-2, Ex4, GIP and glucagon except for H7* which is Y7* in GIP, also S17* is N17* in GLP-2. Underlined residues represent those which adopt an α-helical conformation when bound to the receptor and below those residues is a representation of an α-helix, note the helix is continuous and not kinked.

Whereas interactions between GLP-1(7-36) and the receptor rely heavily on the hydrophobic effect, Ex4(9-39) (and by extension Ex4(1-39)) possesses a similar repertoire of hydrophobic interactions in addition to those exclusive to Ex4 which are extensive. For example, F22* interacts with L32, T35, V36 and W39 which all reside on the α-helix of the receptor NTD, this residue is analogous to F28* in GLP-1 which complexes other residues within the ligand into position but does not interact directly with the receptor. Additionally

V19* (A25* equivalent in GLP-1) interacts with numerous residues within the receptor, namely L32, T35 and P90, therefore V19* is critical for Ex4-mediated interaction. The hydrophobic pocket of the GLP-1R is occupied by V19*, F22*, I23* and L26* of Ex4(9-39), therefore each of the three double hydrophobic residues within Ex4(9-39) (Figure 1.17) interacts with the receptor whereas only two of the three double hydrophobic residues within GLP-1(7-36) interact with the receptor, again demonstrating that Ex4 possesses more contacts with the receptor than GLP-1 within the H-region, which may account for the enhanced affinity of the isolated H-region of Ex4 for GLP-1R NTD (Al-Sabah & Donnelly, 2003a). Interestingly W25* (W31* equivalent in GLP-1) has similar roles in both peptides, whereby it is required for stacking with G30* and P31*, so that the residues involved in the hydrophobic interactions at the hydrophobic pocket may be positioned correctly for optimal binding, indeed this particular tryptophan residue is conserved across all secretin ligands suggesting that they all adopt a similar fold, implicating they all bind the NTD of their respective receptors via a hydrophobic cavity presented by the secretin fold (Figure 1.18). In addition to numerous hydrophobic interactions, Ex4(9-39) also makes multiple hydrophilic interactions, namely E15* with L32, R20* with E128 and K27* with E127.

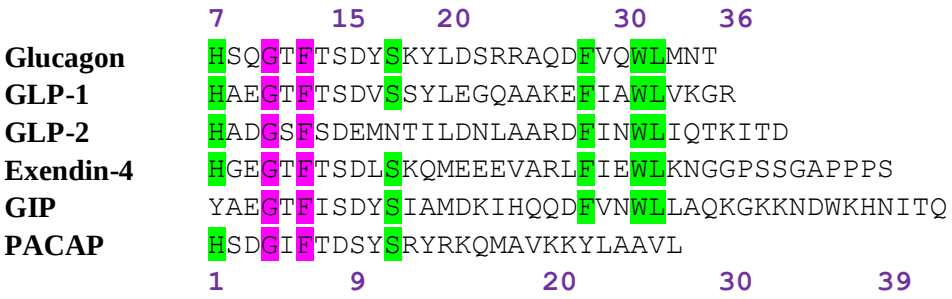

Figure 1.18. Primary sequences of glucagon, GLP-1, GLP-2, Ex4, GIP and PACAP.

The sequences of the secretin-like peptide ligands are shown in the standard amino-to-carboxyl terminus denotation with GLP-1 specific numbering in bold purple text along the top and Ex-4 specific number along the bottom. Those residues fully conserved across the secretin peptides are highlighted magenta and those partially conserved are highlighted green.

1.1.6.2 Exendin-4 Specific Receptor Extracellular Domain Interaction

The residues in the Ex-region were initially believed to form a Trp cage, the smallest protein fold structure known to exist (Neidigh *et al.*, 2001). This theory was partially confirmed by crystallographic studies, showing residues G29*, G30* and P31* partially populate the Trp-

cage form (Runge *et al*., 2008). The crystal structure of Ex4(9-39) bound to the isolated NTD showed a high probability that S32* interacts with E68.

The 'Ex' interaction between Ex4 residues 30-39 account for 16% of the total binding energy at the receptor NTD, through an interaction between S32* and D68* at the rat GLP-1R, but not in the hGLP-1R as the E68* equivalent at the human GLP-1R disallows interaction with S32*, due to its shorter side-chain (Mann *et al*., 2010b) as verified in the crystal structure of the human GLP-1R complexed with Ex4(9-39) (Runge *et al*., 2008).

1.1.6.3 GLP-1 Receptor Core Domain Interaction

The Ex4 and GLP-1 ligands bind orthosterically at the same binding pocket within the GLP-1R NTD (Runge *et al*., 2008; Underwood *et al*., 2010), yet make different interactions with different receptor residues, most likely due to low sequence identity within the H-region between the two ligands (Runge *et al*., 2007). This translates to differences of overall binding energy distribution throughout the system whereby Ex4 bestows approximately 95 % total free binding energy within the H-interaction whereas GLP-1 uses only 82 % total free binding energy (Al-Sabah & Donnelly, 2003b). This suggests a difference in N-interaction between the two ligands despite 89% sequence identity of the two ligands between the first and ninth residue, this theory will be explored within this thesis.

Owing to recent crystallographic work by Runge and colleagues (Runge *et al*., 2008: Underwood *et al*., 2010), a great deal is now known about the structural details of ligand interaction at the NTD of the GLP-1R. However, despite much research, little is known about the structural details of the interaction between the ligand N-terminus and the receptor J domain. Site-directed mutagenesis of residues in the core domain have revealed Asp 198 (López de Maturana & Donnelly, 2002), Lys 288 (Al-Sabah & Donnelly, 2003b), Met 204/Tyr 205 (López de Maturana *et al*., 2004) are critical for full GLP-1(7-36) activity, and the ECL2 double mutants W297A-T298A, L307A-I308A, Y305A-W306A, R299A-N300A, I309A-R310A all showed marked reduction in potency (Mann *et al*., 2010a). Interestingly, some of these mutations within the TMD of the receptor resulted in a decrease in GLP-1 affinity, but not Ex4 affinity (López de Maturana & Donnelly, 2002; Al-Sabah & Donnelly, 2003b), again re-iterating the probability that these two ligands interact differently within the TMD of the GLP-1R.

There have been multiple studies on the amino-terminus of GLP-1 to try to decipher the nature of the interaction of the residues involved in ligand binding, and which ones are critical for activation. For example the ala-scan of GLP-1 residues performed by Adelhorst *et al.* (1994) identified 5 residues that are situated to the extreme N-terminus of the ligand that are affected by Ala-mutation, these were: H7A, G10A, F12A, T13A and D15A. The H7A, G10A and D15A mutations resulted in a loss of affinity of the peptide for the receptor to varying degrees, from a 5-fold decrease in affinity to a 20-fold decrease, yet the potency of these mutated peptides dropped significantly more so, indicating these residues are important in binding but have a more critical role in receptor activation. A similar study by Gallwitz *et al.* (1994) also identified these five residues as being critical for receptor interaction. The F12A and T13A mutations resulted in a decrease in affinity for the receptor with a similar decrease in potency indicating these residues are more important for receptor recognition than activation. This study also identified residues Y19 and E21 as efficacy-providing residues as the potency of alanine mutations at these residues was lowered considerably more than affinity was lowered. Y19 and E21 do not interact with the isolated NTD (Underwood *et al.*, 2010) and protrude outwards suggesting they interact elsewhere within the receptor to enhance activity.

Chimeric receptor/ligand studies have shown that H7* of the GLP-1(7-36) peptide ligand interacts with N302 of the GLP-1R, and T13* docks into a binding pocket at the core domain of GLP-1R composed of I196, L232 and M233 (Moon *et al.*, 2012). Multiple studies utilising photoaffinity labelling probes have proven invaluable in identifying residue-residue interactions at the GLP-1R. By incorporating a photolabile p-benzoyl-L-phenylalanine (Bpa) probe into GLP-1(7-36) ligands at positions V16 and L20, it was found these two residues were capable of interaction with receptor residues L141 (stalk region above TM1) and W297 (ECL 2) respectively (Miller *et al.*, 2011). Using the same technique but observing the immediate amino-terminus of the ligand as the focus of the study, it was shown that H7 of GLP-1(7-36) most likely interacts with the ECL1 residue Y205, and F12 of GLP-1(7-36) interacts with Y145, which is positioned above the first transmembrane helix (Chen, 2010). Another study by Chen *et al.* (2009) focused on the more C-terminally located residues of GLP-1(7-36): G35 and A24, these were found to interact near E125 and E133 of the receptor respectively, both glutamic acid residues reside within the receptor NTD and the findings are consistent with the X-ray crystal structure of bound GLP-1(7-36) (Underwood *et al.*, 2010). These photo-crosslinking studies are consistent with the recently discovered crystal structure of the glucagon receptor TMD, whereby they used homology modelling and mutagenesis studies to forge a model of glucagon binding at the glucagon receptor; Siu *et al.* (2013) show F6 and Y10 (glucagon equivalents of F12 and V16 in GLP-1) most likely interact with Q142 and Y138 respectively at the binding pocket situated by TM1.

The study by Adelhorst *et al.* (1994) was based on alanine scanning of GLP-1 residues, however, if the residue was already an alanine it was mutated to the equivalent residue in glucagon. For Ala8 this resulted in a mutation to a serine residue. This mutation did not affect potency but did affect affinity, suggesting A8 is important for TM bundle recognition. Intriguingly, the truncation of H7 and A8 to give truncated peptide GLP-1(9-36) results in a partial agonist with nM potency, yet over a 20,000-fold reduction in potency in comparison to full length GLP-1(7-36). Indeed, truncation of these two residues resulted in a non-active peptide when used *in vivo*, where GLP-1(9-36) is extensively documented as inactive or even an antagonist at the GLP-1R (Doyle & Egan, 2007; Baggio & Drucker, 2007).

As progression of techniques used in scientific research advance, so too does our knowledge of the GLP-1 receptor-ligand interaction. It was initially thought that in the case of GLP-1 that truncation of the first 2 residues resulted in an antagonist (Vahl *et al.*, 2003); however it is now known that GLP-1(9-36) is not an antagonist but a weak partial agonist (Li *et al.*, 2012). Initially GLP-1(9-36) was thought to be biologically inert as no effect upon insulin release or glucose metabolism was observed (Vahl *et al.*, 2003), yet GLP-1(9-36) was found to possess anti-hyperglycaemic effects upon anaesthetised pigs (Deacon *et al.*, 2002). However, more recently it has been found that GLP-1(9-36) potently inhibits hepatic glucose production from the liver and is a weak insulinotropic agent in healthy human subjects (Elahi *et al.*, 2008). Similarly, it was originally thought that truncation of the first 2 residues of Ex4 to yield truncated Ex4(3-39) resulted in a peptide that could bind, but not activate the GLP-1R (Montrose-Rafizadeh *et al.*, 1997), again we now know this is not the case (Donnelly, 2012; Patterson *et al.*, 2011b).

These updated data are most likely a result of recombinant cell lines overexpressing the GLP-1R to such an extent that ligands that appeared to have no activity in the past may now be viewed as partial agonists. If a ligand does bind and activate a receptor it is more likely to be recognised due to overexpression of the receptors and the amplification of the downstream cAMP signal, such that even a poor agonist may elicit a response through the receptor reserve. Additionally advanced techniques for measuring cAMP production are more robust and high throughput than those methods used even ten years ago. It is now clear that H7 and A8 are important residues for GLP-1R activation, yet they are not the only efficacy-providing residues, as GLP-1(15-36) has recently been shown to retain activity at GLP-1R (Patterson *et al.*, 2011b).

Other studies have identified other residues within the N-terminus of the GLP-1 ligand as crucial for optimal receptor activation and the outcomes are indeed compelling for the notion that the N-interaction is critical for receptor activity. Xiao *et al.* (2001) showed that E9 is important in both binding and activating the GLP-1R as an alanine mutation at this position

resulted in a 81-fold reduction in affinity for the receptor at CHO cells expressing the hGLP-1 receptor, concomitant with a 30-fold decrease in potency in comparison to the wild-type peptide. Siegel *et al.* (1999) found that both S14 and D15 are also critical for receptor affinity and biological activity in RINm5F cells.

More recent studies have identified direct receptor-ligand interactions and pin pointed the locus of the amino-terminus of GLP-1 relative to the receptor. Moon *et al.* (2012) successfully identified H7* as interacting directly with N302 of the receptor situated at the top of TM5 within the ECL2 region of the receptor using chimeric and point-mutated GLP1 and GIP receptors overexpressed in HEK293T cells. Moon *et al.* (2012) identified the relative positioning of T13* as being located within or near a binding pocket formed by I196 (extracellular face of TM 2) L232 and M233 (the top of TM 3). Furthermore, Maturana & Donnelly (2002) located D198 on the extracellular boundary of TM2 as interacting with residues 7-14 of GLP-1 by comparison of GLP-1R D198A binding with GLP-1(7-36) *versus* N-terminally truncated GLP-1(15-36), and found the D198A mutation only affected GLP-1(7-36). Photo-affinity labelling studies performed by Chen *et al*. (2010) have also uncovered the spatial positioning of various GLP-1 residues when complexed to the GLP-1R. For example, the Bpa probe positioned at relative position 6 of GLP-1(7-36), Chen and co-workers found the spatial proximity of this probe to be around the vicinity of T205 of ECL1. These data were re-affirmed by a molecular model proposed by Lin & Wang (2009), whereby they used homology modelling based on the mutagenic data from many Class B GPCRs amongst other complex modelling programmes to devise a model for GLP-1 binding to the GLP-1R; this model was in press at the same time as the molecular structure of the isolate NTD in complex with Ex4(9-39) was released, and both models shared structural features at the NTD which reiterates the reliability of this model. In their model, they show H7* as interacting with D198, whereas the N302 binding site of H7* proposed by Moon *et al.* (2012) at TM5 was more localised to a secondary allosteric site where Cmp1 was proposed to bind in the Lin and Wang model. These data suggest the extreme N terminus of GLP-1 interact with ECL1 and the extracellular facing residues of TM2 at GLP-1R.

Compelling research by Mapelli *et al.* (2009) and During *et al.* (2003) suggest the two-domain model of activation may not be representative of the whole picture in GLP-1R activation, as they both show a very minimalistic sequence of peptide, both of which were capable of GLP-1R activation, shown directly or indirectly. Mapelli *et al.* (2009) created an 11-mer peptide based upon the first 11 residues of GLP-1 (sequence 7*-HAEGTFTSDVS-17*), whereby modified amino acids were placed at positions 8, 12, 16 and 17 (GLP-1 relative numbering) in place of the wild-type residues. These were optimised such that they identified a

mutated peptide segment they named ‘peptide 21’ that was capable of activating the GLP-1R with sub-nM potency: EC_{50} for mutated peptide 21 = 0.087 ± 0.04 nM, where full-length GLP-1 EC_{50} was noted as 0.034 ± 0.01 nM. Another study performed by During *et al.* (2003) showed that only a 9-mer peptide version of GLP-1 with an A8S mutation (sequence 7*-HSEGTFTSD-15*) was capable of enhancing associative and spatial learning in male Sprague Dawley rats when administered peripherally and intracerebroventricularly via interaction with the GLP-1R, and was neuroprotective against kainite-induced apoptosis in hippocampal neurones. These data clearly demonstrated that full GLP-1R activity does not require the full length of the GLP-1 peptide.

1.1.7 Current GLP-1R Activation Models

Members of the Secretin Family are hypothesised to bind their peptide ligands via the ‘two-domain model’ whereby the NTD of the receptor firstly binds the C-terminal region of the peptide ligand; secondly the N-terminus of the peptide ligand interacts with the J domain, thereby activating the receptor (Bergwitz *et al.*, 1996). The first interaction is said to act as an affinity trap, increasing the local concentration of the activity-providing N-terminus of the peptide ligand into close proximity with the J domain to enhance the number of receptors in the active conformation (Hoare, 2005).

Data exemplifying the two-domain model are numerous. The peptide agonist Ex4(1-39) was shown to be capable of rat GLP-1 receptor activation when over-expressed in HEK-293 cells, with nM potency, yet removal of the first 8 amino-terminal residues to give truncated Ex4(9-39) results in a peptide unable to activate the receptor, yet still binds to GLP-1R with nM affinity hence Ex4(9-39) is an antagonist (Göke *et al.*, 1993; Thorens *et al.*, 1993). The endogenous agonist GLP-1(7-36) also activates the GLP-1R with nM potency and has nM affinity for the rat GLP-1 receptor over-expressed in CHO cells, but truncation of the first 8 amino-terminal residues to yield GLP-1(15-36), resulted in abolished GLP-1R activity, yet possessed μM affinity for the receptor (Montrose-Rafizadeh *et al.*, 1997). Considering that truncation of the most amino-terminal residues of Ex4 and GLP-1 resulted in loss of activity, yet retention of affinity, it is easy to see how notion of two separate domains of the peptide ligands confer different properties toward the GLP-1R; whereby the C-terminal region conveys affinity for the receptor, and the N-terminus conveys activity.

Despite elegant work performed by multiple groups on GLP-1 and Secretin Family GPCR activation in general, the consensus for the exact mechanism of activation remains divided. There are multiple theories within the literature of how receptors of this class are activated, all possessing compelling evidence within their own right, and all loosely based around the two-domain model. Firstly there is the two-domain model, discussed extensively within this section, this is probably the most widely accepted mechanism to date as it is quite broad and generalised and does indeed fit all Secretin Family receptors, and all other Family B GPCRs.

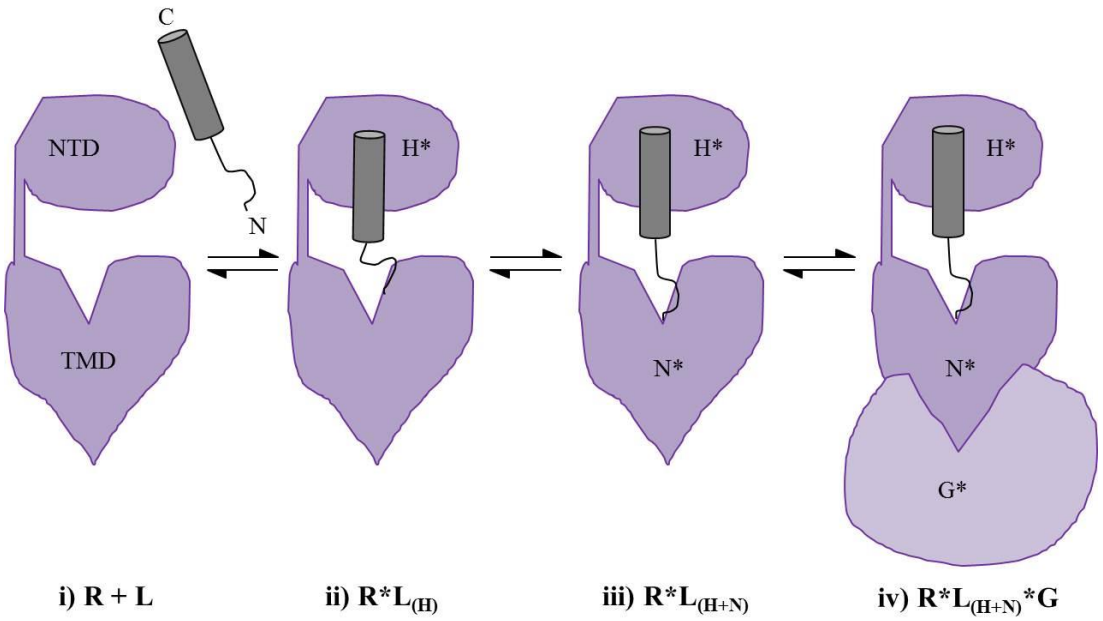

Figure 1.19. Schematic of the sequential steps involved in Class B GPCR activation via the two-domain model.

The GPCR is denoted as the purple body which possesses an extracellular N-terminal domain (NTD) coupled to the transmembrane domain (TMD) with seven transmembrane spanning helices connected via a stalk region. The plasma membrane is not shown for clarity but would reside approximately where the equilibrium arrows are positioned. The ligand is the grey cylindrical body with 'N' and 'C' denoting its orientation, where a cylinder denotes α-helical structure and a line denotes an unstructured peptide chain. Part i. the ligand comes into proximity with the receptor; part ii. The α-helical segment of the ligand binds the receptor NTD, forming the H-interaction as shown by H*; part iii. The unstructured N-terminus of the ligand contacts key residues within the TM bundle thereby forming the N-interaction as shown by N*; part iv. The complete binding of the ligand induces conformational change within the TMD which permits G-protein recruitment (G*).

The first veritable evidence of this two domain model was shown by Bergwitz *et al.* (1996) whereby a peptide ligand comprising the amine-terminus of calcitonin and the carboxyl terminus of PTH bound with high affinity to a chimeric receptor forged with the NTD of the PTH receptor and the TMD of the calcitonin receptor. This model proposes that the α-helical C-

terminus of the ligand (grey cylinder, Figure 1.19.i) recognises the receptor's extracellular NTD and binds, largely governed by the hydrophobic effect, to the putative hydrophobic groove present within the receptor forming the H-interaction (Figure 1.19.ii). This interaction brings the N-terminal region within close proximity to the receptor's TM bundle, increasing the relative local concentration of the N-terminus of GLP-1 which is postulated to possess the critical residues involved in receptor activation. Once the residues bind the complementary residues within the receptor's core domain forming the N-interaction (Figure 1.19.iii) there is a conformational change within the TM bundle and the G-protein is recruited (Figure 1.19.iv).

Secondly there is the endogenous agonist theory presented by Miller and Dong (2007), exemplified in Figure 1.20.

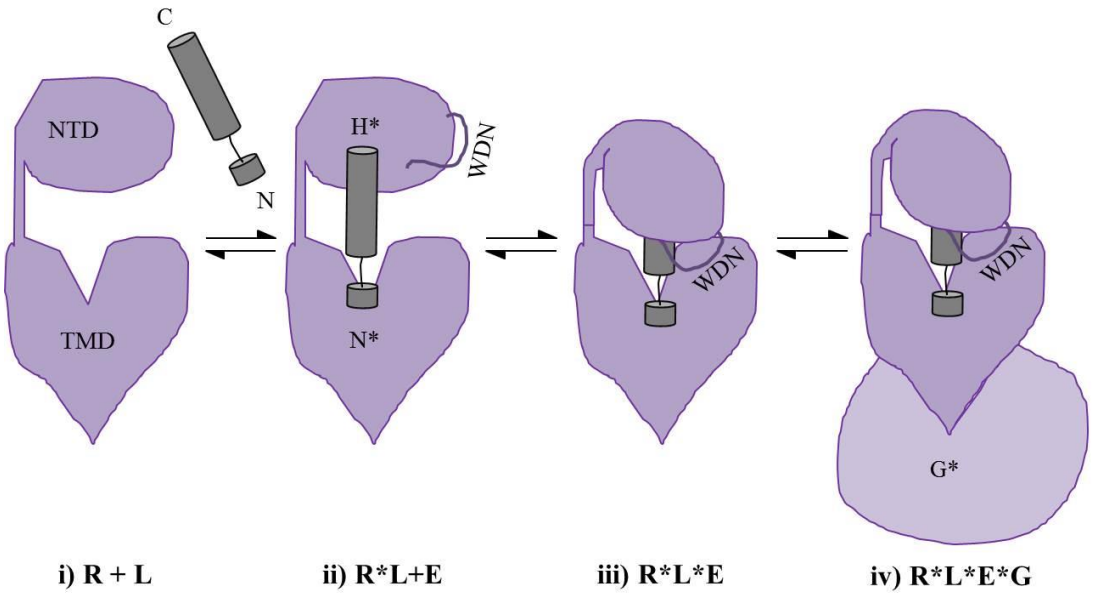

Figure 1.20. Schematic of the sequential stages involved in Class B GPCR activation via the endogenous agonist model.

The GPCR is denoted as the purple body which possesses an extracellular N-terminal domain (NTD) coupled to the transmembrane domain (TMD) with seven transmembrane spanning helices connected via a stalk region. The plasma membrane is not shown for clarity but would reside approximately where the equilibrium arrows are positioned. The ligand is the grey cylindrical body with 'N' and 'C' denoting it's orientation, where a cylinder denotes α-helical structure and a line denotes flexibility within the peptide ligand. Part i, the coiled ligand comes into proximity with the receptor; part ii, the ligand makes interaction with the receptor, with both the H-interaction (H*) and N-interaction (N*) occurring simultaneously, causing a conformational change within the receptor, specifically at the NTD which exposed a previously buried segment containing the WDN motif. Part iii, the receptor then undergoes a second conformational change where the exposed endogenous ligand causes the receptor NTD to move toward the TMD where the WDN motif interacts with residues near TM6; part iv, the combined ligand and endogenous ligand interaction permits G-protein coupling to the TM bundle (G*).

The endogenous ligand theory is based on multiple experiments performed on the secretin receptor, the calcitonin receptor, the VPAC1 receptor and the GLP-1R (Dong *et al.*, 2006) whereby they proposed that there was a segment of peptide hidden within the receptor NTD that is exposed through conformational change upon ligand binding to the receptor. Once the segment is exposed to solvent (purple loop section, Figure 1.20.ii) following ligand binding and subsequent conformational changes within the receptor NTD, this endogenous sequence of peptide is proposed to interact with specific residues that reside at the top of TM6 (Figure 1.20.iii). This key sequence was narrowed down to only three residues within the receptor NTD: a sequence of WDN which is a common motif to all Family B GPCRs. They too found that the peptide ligand secretin interacts with both the NTD and TMD through photocrosslinking studies, therefore this is an extension of the two-domain model, except the receptor activity is derived from the sequence within the receptor NTD and not from the residues situated at the N-terminus of the ligand directly, although receptor-ligand interaction is proposed to act as a tether in this model, promoting correct positioning of the endogenous activating motif with respect to the TMD.

Thirdly, Parthier *et al.* (2009) proposed an interesting theorem whereby the disordered C-terminal segment of the ligand interacts with the extracellular NTD of the receptor, and binding induces α-helical extension throughout the ligand, thus creating a secondary α-helix which is complementary to residues within the receptor core domain, thereby allowing appropriate positioning of the ligand thus promoting interaction with the receptor TM bundle, permitting a more active conformation within the receptor (Figure 1.21). They term this binding-induced ligand conformational change as ‘passing the baton’ whereby the baton in this metaphor is a receptor-complementary α-helical motif. This theory is based upon the NMR structures of secretin-type and Family B GPCR ligands, where they have no apparent secondary structure in aqueous solution (Thornton & Gorenstein, 1994), and the observation that these structures are not the same as the structures observed in recent crystallographic data, thus they propose that correct ligand poses for optimal receptor activation are only realised secondary to receptor recognition. They suggest that the primary interaction between the C-terminus of the ligand and the receptor NTD is not driven by the amphipathic helical structure and residue interaction within the α-helical conformation, but rather governed entirely by the hydrophobic effect, which then promotes correct protein folding within the peptide ligand, extending down throughout the disordered peptide chain until the active ligand peptide structure is adopted (Figure 1.21).

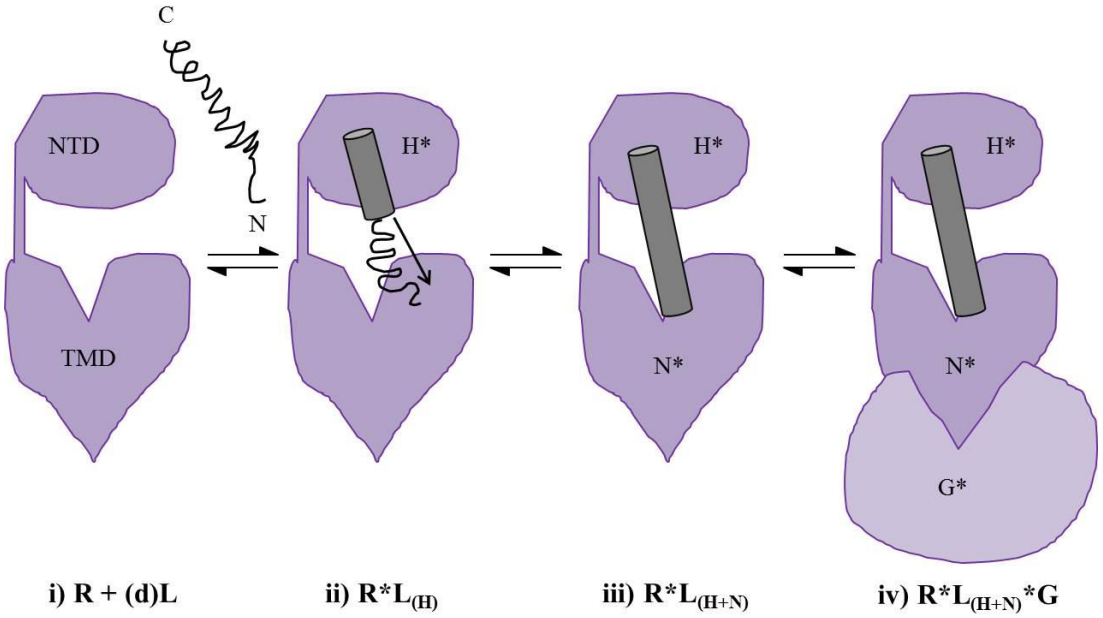

Figure 1.21. Schematic of the sequential stages involved in Class B GPCR activation via the α-helical extension/ 'passing the baton' model.

The GPCR is denoted as the purple body which possesses an extracellular N-terminal domain (NTD) coupled to the transmembrane domain (TMD) with seven transmembrane spanning helices connected via a stalk region. The plasma membrane is not shown for clarity but would reside approximately where the equilibrium arrows are positioned. The ligand is the grey cylindrical body with 'N' and 'C' denoting it's orientation, where a cylinder denotes α-helical structure and a line denotes an unstructured peptide chain. Part i, the disordered ligand comes into proximity with the receptor; part ii, binding of the C-terminus of the ligand to the NTD of the receptor induces the ligand to acquire an α-helical structure, which then extends down through to the N-terminus of the ligand as shown by the arrow. Part iii, after completing α-helical transformation the dual-amphipathic nature of the ligand promotes binding of the now structured N-terminus to the receptor TMD, forming the N-interaction (N*); part iv, the formation of N* promotes rigidity within the TMD of the receptor, locking it into active conformation, which then attracts G-protein coupling (G*).

Finally, a mode of GLP-1R receptor activation has been proposed by Lin & Wang (2009) via molecular modelling of the GLP-1R in a fully hydrated palmitoyl-oleyl-phosphatidyl-choline (POMC) membrane based on mutagenic, structural, TM locus prediction, molecular dynamic simulation and homology modelling. In the model presented by Lin & Wang the ligand locks into the receptor in an 'L' shape and this promotes receptor NTD rotation in regards to the positioning of the transmembrane bundle (Figure 1.22.A). In this model there are two structurally distinct isoforms of the GLP-1R, one in the *apo*-form (Figure 1.22.A left) where the α-helix within the receptor NTD (coloured lime green) partially blocks the binding site of GLP-1, this is postulated to be the inactive conformation. Upon GLP-1 binding (the purple ribbon in Figure 1.22), the lime green α-helix has changed conformation, no longer obscuring the orthosteric binding site at the NTD. This change in the NTD also translates

through to the core domain as seen in Figure 1.22.A, right, where molecular dynamic simulation predicts that the NTD bends downward toward the TMD, or rotates on top of the TMD, they propose that this movement is concomitant with recruitment of the G-protein for downstream signalling.

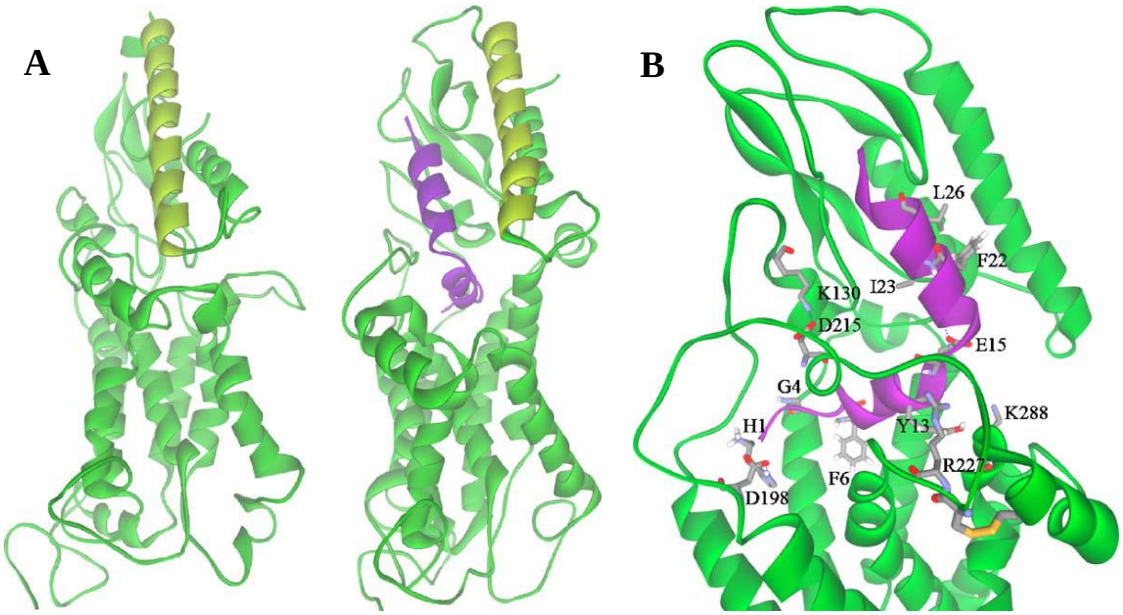

Figure 1.22. Ribbon diagram of the GLP-1R complexed with GLP-1 and alone as predicted by molecular modelling (taken from Lin & Wang, 2008).

Figure A, the inactive conformation of GLP-1R (left) and the active GLP-1 bound GLP-1R complex (right) following a 20 ns molecular dynamics simulation. The lime green helix spanning residues T27- L50 obscures the orthosteric site of the GLP-1R in the inactive conformation, yet upon binding of GLP-1 (purple helix) it undergoes a conformational change no longer obscuring the binding site. A conformational change is also observed in the TMD by movement of some helices; the POPC bilayer is omitted for better visualisation of helical movement. Figure B, the molecular interactions between GLP-1 (purple) and the GLP-1R (green) as deciphered by homology modelling and molecular docking. The authors assert that H7* hydrogen bonds with D198 of the receptor, F12* interacts with the hydrophobic cavity formed by the tops of several TM helices, Y19* forms electrostatic interactions with R227 and K288, and F28*, I29* and L32* make hydrophobic contacts with W39 of the receptor. They also propose G10*, D15*, E21*, Q23* and A24* are responsible for holding the ligand in the correct binding pose and do not directly interact with the receptor. In their figures they used the Ex4 denotation of residue positioning within the GLP-1 ligand i.e. residues 1-30. Permission to use the figures was granted by the authors Fu Lin and Renxiao Wang.

Lin & Wang suggest that the two isoforms of the receptor shown in Figure 1.22.A are both present in the cell due to low frequency conformational movements-giving rise to basal activity, yet in the absence of ligand the equilibrium favours the inactive state where the orthosteric site is partially blocked by the NTD α-helix. The presence of orthosteric agonist then encourages the receptor to adopt the active conformation by locking it in place, forcing equilibrium to the right. They also postulate that the allosteric agonist, compound 1, is capable

of locking the receptor into the active conformation, causing the NTD to expose the orthosteric binding site by α-helix movement, permitting easier access to the binding pocket for the orthosteric ligand, thereby explaining the cooperativity observed between orthosteric and allosteric ligand.

The work in this thesis aims to examine the specifics of ligand interaction at the transmembrane region by analysis of N-terminally truncated ligands at the human GLP-1R.

1.1.8 Non-Peptide Ligand Agonists of GLP-1R

There has been increased interest for the discovery of non-peptide GLP-1R agonists as therapeutics for T2D treatment recently. As non-peptide therapeutics they would potentially be taken orally as they would be resistant to peptidase-mediated cleavage, as oppose to administration via self-injection which many would view as beneficial. Despite the prerequisite that the non-peptide ligand would have to encompass the binding region as occupied by orthosteric ligands to achieve maximal efficacy (Hoare, 2005), which has largely hampered the discovery of non-peptide ligands; there has been success recently in finding numerous classes of non-peptide ligands for the GLP-1R. GLP-1R agonist classes include: quinoxalines such as 'compound 1' and 'compound 2' (Knudsen *et al*., 2007), pyrimidines such as BETP otherwise known as 'compound B' (4-(3-benzyloxyphenyl)-2-ethylsulfinyl-6-(trifluoromethyl)pyrimidine (Sloop *et al*., 2010), and cyclobutane derivatives such as Boc5 (1,3-bis [[4-(tert-butoxycarbonylamino) benzoyl]amino]-2,4-bis[3-methoxy-4-(thiophene-2-carbonyloxy)-phenyl] cyclobutane-1, 3-dicarboxylic acid) and Sp4 (Chen *et al*., 2007). Although none of the non-peptide agonists of the GLP-1R are suitable for therapeutic use, they are useful tools in understanding GLP-1R activation (Willard *et al*., 2012). The work in this thesis aims to identify functional characteristics of a small group of pyrimidine derivatives that prove optimal to GLP-1R activity.

The first non-peptide antagonist of the GLP-1R was identified in 2001 by Tibaduiza *et al.* (Tibaduiza *et al*., 2001), a small molecule named T-0632, which was found to display 100-fold affinity for the human GLP-1R *versus* rat GLP-1R expressed in COS-7 cells. T-0632 was originally identified as a cholecystokinin receptor 1 antagonist; it was shown to bind, via Trp^{33}, to the human GLP-1R with an IC_{50} of 1.2 μM. T-0632 binds to the cholecystokinin receptor 1 with an IC_{50} of 31 nM (Taniguchi *et al*., 1996), thus is much more selective for the cholecystokinin receptor 1, and thus is not suitable for studies with GLP-1R.

Non peptide agonists of GLP-1R may also display allosteric modulation, capable of enhancing the signalling profile of an orthosteric ligand agonist, an example being "compound 2" (Naichang *et al*., 2012). At GLP-1R compound 2 exhibited μM potency and 72% E_{MAX} of native peptide GLP-1(7-36), yet when administered concomitantly with the truncated metabolite GLP-1(9-36), the non-peptide enhanced the potency and the efficacy of the cAMP response of GLP-1(9-36) to nM potency and full agonism. Conversely, allosteric modulators may shift the receptor into a more preferable conformation for endogenous peptide binding but do not actually activate the receptor themselves, one such example is quercetin at the GLP-1R (Koole *et al*., 2010). Koole *et al.* demonstrated quercetin was unable to compete for binding at the orthosteric site using I^{125}-Ex4(9-39) as the competitor using affinity binding studies, however they did show that compound 2 was able to displace binding of radiolabelled I^{125}-Ex4(9-39) at the GLP-1R, suggesting compound 2 does not bind at a site distinct from the orthosteric site. Quercetin was found not to possess intrinsic activity for stimulating the $G\alpha_q$ pathway, yet did augment mobilisation of Ca^{2+} in a positive manner in the presence of GLP-1(7-36) in a dose-dependent manner.

Compound 2 was also found to alter stimulus bias at the GLP-1 receptor (Koole *et al*., 2010), increase affinity of GLP-1(7-36) for the receptor (Knudsen *et al*., 2007) and to enhance GLP-1(9-36)amide activity at the receptor (Naichang *et al*., 2012). Although compound 2 has been shown to be cytotoxic to HEK-293 cells (Coopman *et al*., 2010), it nonetheless demonstrates the ability of small non peptide ligands to alter the receptor conformation to enhance cell signalling in the presence of the truncated metabolite GLP-1(9-36). This exciting new avenue proposes a novel type of therapeutics whereby bioavailable, orally administered compounds could be taken alongside a meal, and these would be able to allosterically influence the GLP-1R to manipulate circulating endogenous peptides GLP-1(7-36) and the more abundant truncated metabolite GLP-1(9-36) to enhance insulin secretion and regulate beta cell signalling to a more physiological pattern.

1.19 Aims of This Study

Small molecule ligands may bind anywhere within the receptor, many bind allosterically at a site distinct from the natural ligand binding site. Currently there is not much information on the structure-function relationship of these small molecules and a better understanding is required for the further development of drug design (Willard *et al*., 2012). As such, one of the primary aims of this thesis is to determine the structure-activity relationship of the various functional groups of a small library of low molecular weight pyrimidine-scaffold

compounds at hGLP-1R-expressing FLP-IN HEK cells by assaying their ability to activate the $G\alpha_s$ pathway. A secondary aim of this thesis is to analyse the allosteric effects of pyrimidine-scaffold compounds to modulate the cAMP responses of truncated GLP-1 and Ex4 peptides at hGLP-1R-expressing FLP-IN HEK cells, focusing on the effects of functional group positioning upon resultant cAMP response.

The GLP-1R is a valid target for the treatment of T2D with two synthetic GLP-1 peptide analogous available for the treatment of this disease, exenatide and liraglutide. However, as peptides these must be administered by self-injection by the patient, which results in lowered compliance. Additionally there has been recent evidence that liraglutide and exenatide have minor to major side effects (Cure *et al.*, 2008; Nauck *et al.*, 2009; Singh *et al.*, 2013). There has been interest recently in the search for small orally available non-peptide ligands of the GLP-1R for the treatment of T2D which would circumvent the need for intravenous administration. This thesis aims to determine the ability of the most efficacious pyrimidine-scaffold compound (based on the results from a preliminary cAMP screening assay) to enhance insulin secretion from a rat insulinoma cell line. As the metabolite GLP-1(9-36) is present in higher circulating concentrations than the full length secretagogue GLP-1(7-36) due to DDP-IV cleavage, the ability of GLP-1(9-36) to enhance insulin secretion will also be studied.

As a Family B GPCR, GLP-1R is hypothesised to be activated by a two-domain binding mechanism. The interaction of the ligand C-terminus with the receptor extracellular domain has been well documented owing to the crystal structure of the GLP-1R NTD in complex with both Ex4(9-39) and GLP-1(7-36), however there is no determined structural data of the interaction between the ligand N-terminus and the receptor core domain. Knowledge of the peptide-core domain interaction has come from more indirect approaches such as peptide mutagenesis studies and homology modelling. This study focuses on the mechanism of activation of the two peptides GLP-1 and Ex4 at the human GLP-1R to determine if the activation profiles are different; this will be achieved by analysis of analagously truncated versions of these peptides in order to glean information of ligand-receptor interaction at the core domain.

Additionally this thesis studies the two-domain binding model of GLP-1 at GLP-1R: whereby the first 8 residues are hypothesised to be the activating residues and residues situated more C-terminally are responsible for receptor binding. Work within this thesis analyses the ability of truncated GLP-1 peptides lacking either the affinity-providing helical region, or the activity-providing amine-region in order to locate the residues responsible for GLP-1R activation by analysing the efficacy and affinity of peptides using modern FRET techniques and radioligand displacement assays.

Chapter 2

Methods & Materials

2.1 MATERIALS

2.1.1 General Materials

All general dry materials were purchased from Sigma-Aldrich unless otherwise specified, the addresses of all providers can be found at the end of this document. The reagents were dissolved using distilled and filtered water provided by a Millipore Milli-Q filtration system, the water herein referred to as 'MQ'. Syringes, needles and disposable filtration units were purchased from Terumo. Centrifuge tubes, microfuge tubes and absolute ethanol were purchased from Scientific Laboratory Supplies (SLS). Protective nitrile gloves were purchased from Fisher Scientific Ltd. Serological pipettes with graduation markings were purchased from Sarstedt.

2.1.2 Cell Culture Reagents

2.1.2.1 HEK-293 Cell Culture Reagents

Dulbecco's modified Eagle's medium (DMEM, Sigma-Aldrich, D5796), foetal bovine serum (FBS(i), Sigma-Aldrich, F7524), penicillin-streptomycin (P/S, Sigma-Aldrich, P4458), ciprofloxacin HCl (SLS, 17850), Dulbecco's phosphate buffered saline (PBS, Sigma-Aldrich, D8537), dimethyl sulphoxide (DMSO, Sigma-Aldrich, D2650), poly-D-lysine (Sigma-Aldrich, P7405), Hygromycin B (Invitrogen, 10687010), TrypLE™ express (Invitrogen, 12604013), versene (Invitrogen, 15040033), Lipofectamine™ 2000 transfection reagent (Invitrogen, 11668027), culture flasks (Fisher Scientific Ltd., TKT-130), cryogenic vials (Fisher Scientific Ltd., CRY-960-010T), Propan-2-ol (Fisher Scientific Ltd., P/7490/17). Leica EC3 light microscope (Leica Microsystems).

2.1.2.2 INS-1 832/13 Cell Culture Reagents

Roswell Park Memorial Institute (RPMI) 1640 medium (Sigma-Aldrich, R0883), L-glutamine-penicillin-streptomycin solution (Sigma-Aldrich, G1146), sodium pyruvate (Sigma-Aldrich, S8636), foetal bovine serum (FBS(ii), Invitrogen, 10082139), 2-mercaptoethanol

(Sigma-Aldrich, M3148), HEPES (Sigma-Aldrich, H3375), Dulbecco's phosphate buffered saline (PBS, Sigma-Aldrich, D8537), ciprofloxacin HCl (SLS, 17850), TrypLE™ express (Invitrogen, 12604013), dimethyl sulphoxide (DMSO, Sigma-Aldrich, D2650), cryogenic vials (Fisher Scientific Ltd., CRY-960-010T), culture flasks (Sarstedt, 83.1813.002). Leica EC3 light microscope (Leica Microsystems). 24-well plates (Sarstedt).

2.1.3 Molecular Cloning Reagents

All restriction endonucleases were purchased from New England Biolabs. GeneRuler™ ladder mix was used as a DNA ladder (Fermentas, SM0333). Ethidium bromide was purchased from MP Biomedicals Europe (11ETBC1001) and made to 10 mg/mL stock solution using MQ. XL1-Blue competent cells were purchased from Stratagene (200249) as was PfuUltra™ High-Fidelity DNA Polymerase (600382). QuikChange™ site directed mutagenesis primers were custom designed in house and purchased from Sigma-Aldrich. Pre-mixed 10mM dideoxynucleotide triphosphates were purchased from Clontech (639125). Thin-walled 0.2 mL PCR tubes were used for thermal cycling (Starlab UK Ltd., I1402-4308) which were compatible for use with the PCR Sprint thermal cycler (Hybaid). XL-1 Blue *E.coli* cells were used for DNA amplification (Stratagene, 200249). Plasmids were isolated and purified using the HiSpeed® midi kit (Qiagen, 12643). Transformations were performed using 14 mL polypropylene tubes (Greiner Bio-One Ltd., 187262).

2.1.4 LANCE® Reagents

The LANCE® cAMP kit was purchased from Perkin Elmer (500 point (AD0262), 1000 point (AD0262E) or 10000 point (AD0263)), as was the VICTOR™ X4 multilabel plate reader. Hank's balanced salt solution (HBSS) was purchased from Invitrogen (14025100). 3-isobutyl-1-methylxanthine (IBMX, Insight Biotechnology, sc-201188A) was made to a 50mM stock concentration using DMSO and stored in the freezer. Sodium hydroxide pellets (Sigma-Aldrich, 221465) dissolved using MQ to 1.5 Mwas used to alter the pH of HBSS to pH 7.4 after addition of 5 mM HEPES (Sigma-Aldrich, H3375) to give prepared HBSS. BSA was purchased from Sigma-Aldrich (A7906), and added to prepared HBSS to a working concentration of 0.1% (*w*/*v*) and shall hereby be referred to as 'stimulation buffer'. Stimulation buffer was stored in a

polystyrene 150mL container (SLS, SLS7570) at 4°C, for up to three days usage. Universal polystyrene 30 mL containers (SLS, SLS7502) and 7 mL bijou tubes (Sigma-Aldrich, Z376795) were used to dilute solutions for use. Ligands were diluted into 96 well plates (Greiner Bio-One Ltd., (651201)) and the cAMP accumulation assay was carried out in 384-well white opaque OptiPlates (Greiner Bio-One Ltd., (781075)). TopSeal-A sheets with adhesive backing were used to cover the OptiPlates to prevent evaporation (Perkin Elmer, 6005250).

2.1.5 Radioligand Assay Reagents

^{125}I-GLP-1 (7-36) NH_2 was a kind gift from Novo Nordisk with a specific activity of 2200 Ci/mmol. Membrane-associated hot GLP-1 was collected via attachment of a filter plate with hydrophilic membrane 0.45μM pore (Millipore, MSHVN4550) to a multiScreen$_{HTS}$ vacuum manifold (Millipore, MSVMHTS00). Receptor-expressing cells destined for membrane harvesting were grown on 160 cm^2 vented tissue culture dishes (SLS, 168381), and harvested using a 32 cm cell scraper (Nunc, 179707). Nunc plates were laced with L-poly-D lysine (Sigma-Aldrich, P7405-5MG) prior to cell seeding. 23G needles (Terumo, SZR-275-510P) were used with 1, 5, 10 and 50 mL syringes (Terumo) to homogenise the membranes. Filter plates were blocked using 0.1 % (v/v) polyethyleneimine (MP Biomedicals, 219544450) in 1 x PBS (Invitrogen, 18912014). Filter disks were inserted into 5 mL culture tubes (Sigma-Aldrich, Z376795-1PAK) and read in a Riastar C5410 gamma counter (Canberra-Packard). The Insulin ^{125}I RIA kit 500T (MP Biomedicals, 07-260105) was used to assess insulin secretion. Pre racked p200 filter tips were used when transferring radioligand to avoid unnecessary accidental contamination of pipettes (Greiner Bio-One, 739288). Membrane protein concentration was quantified using the bicinchoninic acid assay; bicinchonic acid (Sigma-Aldrich, B-9643) and copper II sulphate (Sigma-Aldrich, C-2284), flat-bottomed 96 well polystyrene plate (Greiner Bio-One, 655101), absorbances were read using the FLUOstar Omega plate reader (BMG Labtech)

2.1.6 GLP-1R Ligands

Custom designed truncated analogues of GLP-1(7-36) and Exendin-4(1-39) were designed in house and synthesised by Genosphere Biotechnologies. Commercially available

peptides (such as full length GLP-1 (H-6795) and Exendin-4 (H-8730)) were purchased from Bachem. Peptides were diluted to a stock concentration of either 1 x 10^{-3} M or 1 x 10^{-2} M (depending upon M_w) using MQ. The pyrimidine substituted compound library was designed and synthesised by Dr. Migliore (School of Chemistry, University of Leeds) following an initial hit at AstraZeneca for Pm1 as a partial GLP-1R agonist. The lyophilised compounds were diluted to 1 x 10^{-2} M using DMSO (Sigma, D8418)

2.1.7 Plasmids and DNA

pcDNA5/ FRT (Invitrogen, V6010-20) harbouring the wild type human GLP-1R cDNA was a kind gift from AstraZeneca. pOG44 (Invitrogen, V6005-20) was used in combination with pcDNA5/ FRT containing cys/ala human GLP-1R cDNA with Flp-In™ -293 cells (Invitrogen, R750-07) to engineer mutant human GLP-1R expressing cell lines.

2.1.8 Bacterial Media Components

Agar, tryptone and yeast extract were all purchased from Oxoid Ltd. (LP0011B, LP0042B and LP0021B respectively). Sodium chloride (Fisher Scientific, S271500), glucose (Sigma-Aldrich, G-8270), casein hydrolysate (Sigma-Aldrich, 22090-100G), magnesium chloride (Sigma-Aldrich, M9272) and magnesium sulphate (Sigma-Aldrich, 13143) were all used in super optimal broth. The antibiotics used for selection were: ampicillin and tetracycline. Ampicillin sodium salt was purchased from Sigma-Aldrich (A9518-5G) and made to a stock solution of 50 mg/mL using MQ. This was filter sterilised, aliquotted into 0.5 mL microcentrifuge tubes and stored at -20°C. Tetracycline hydrate was purchased from (Sigma-Aldrich, 268054-25G). This was made to 12.5 mg/mL using ethanol (Sigma-Aldrich, 32221) and stored at -20°C. Bacterial strain XL1-Blue Supercompetent *E.coli* (Stratagene, 200236).

2.1.9 Bacterial Growth Medium

Lysogeny broth (LB): 10 g/L NaCl, 10 g/L tryptone and 5 g/L yeast extract using distilled H_2O. Heat sterilised at 126 °C for 11 minutes using a 2100 Classic autoclave (Prestige Medical).

2 x TY broth: 5 g/L NaCl, 16 g/L tryptone and 10 g/L yeast extract using distilled H_2O. Heat sterilised at 126 °C for 11 minutes using a 2100 Classic autoclave (Prestige Medical).

Super optimal broth (SOB): 0.5 g/L NaCl, 20 g/L tryptone, 5 g/L yeast extract, 2.5 mM KCl, the volume was made up to 98 % complete using distilled H_2O and the pH adjusted to 7.0. This was heat sterilised at 126 °C for 11 minutes using a 2100 Classic autoclave (Prestige Medical).Using aseptic techniques, filter sterilised $MgCl_2$ and $MgSO_4$ were added to a final concentration of 10 mM each.

Super optimal broth with catabolite repression (SOC): Made as for SOB, except filter sterilised glucose was added using aseptic technique following autoclaving.

LB agar plates: lysogeny broth was supplemented with 1.5 % (*w*/*v*) bacterial agar, a magnetic flea was added to the bottle before heat sterilising at 126 °C for 11 minutes using a 2100 Classic autoclave (Prestige Medical). Once sterilised, the bottle was placed on an Ikamag® Reo magnetic stirrer (Drehzahl Electronics) to allow the medium to cool evenly. Once the temperature had reached approximately 55 to 60°C, selective antibiotic was added to the appropriate concentration and the bottle returned back to the magnetic stirrer for a further one minute to mix. Under aseptic conditions, the bases of 9 cm diameter Petri dishes were evenly covered with 20 mL LB agar and allowed to polymerise beneath a flame for 30 minutes at room temperature. The plates were stored inverted at 4°C for up to two weeks.

2.1.10 Antibiotic Supplement Concentrations

Ampicillin: 100 μg/mL diluted in filter sterilised water

Hygromycin B high stringency: 200 μg/mL diluted in filter sterilised PBS

Hygromycin B low stringency: 100 μg/mL diluted in filter sterilised PBS

Tetracycline: 25 μg/mL diluted in 70 % ethanol

2.2 METHODS

2.2.1 Mammalian Cell Culture Methodology

2.2.1.1 HEK-293 Cell Growth Media

HEK-293 cells were grown in complete medium (CM10) which consisted of DMEM supplemented with 10 % FBS(i) and 100 U/mL penicillin and 100 µg/mL streptomycin. Cells were grown as monolayers in 25 cm^2, 75 cm^2 or 175 cm^2 ventilated Nunc flasks; housed in a Biohit incubator (Wolf) set at 37°C, 5% CO_2 and 100 % humidity. All solutions used in the propagation of HEK-293 cells were sterile and pre warmed to 37°C prior to use. All procedures following were performed in a sterile Aura B4 BioAir® tissue culture hood (Wolf) using aseptic technique.

2.2.1.2 INS-1 832/13 Cell Growth Media

INS-1 832/13 cells were grown in RPMI 1640 media supplemented with 10 % FBS(ii), 100 U/mL penicillin, 100 µg/mL streptomycin, 2 mM L-glutamine, 1 mM sodium pyruvate, 10 mM HEPES and 50 µM β-mercaptoethanol. Cells were grown as monolayers in 75 cm^2 ventilated Sarstedt flasks housed in a Biohit incubator (Wolf) set at 37°C, 5% CO_2 and 100 % humidity. All solutions used in the propagation of HEK-293 cells were sterile and pre warmed to 37°C prior to use. All procedures following were performed in a sterile Aura B4 BioAir® tissue culture hood (Wolf) using aseptic technique.

2.2.1.3 General Propagation and Passage of HEK-293 and INS-1 832/13 Cells

Cell growth media was removed by decanting and the cells gently washed with 2 mL of PBS for 25 cm^2 flasks or 3 mL for 75 cm^2 flasks. Cells were detached using 1 or 2 mL TrypLE™ Express for 25 or 75 cm^2 flasks respectively. The detached cells were washed to a corner using PBS to a final volume of 10 mL, whereby the cells were collected and transferred to a sterile 15 mL falcon tube and centrifuged for 3 minutes at 1288 *g* (Eppendorf centrifuge

5702, Eppendorf) The cell pellet was resuspended in 1 mL CM10 or supplemented RPMI media and seeded into new flasks. Confluent HEK-293 cells were typically split 1 in 20 (50 µL resuspended cell pellet) for routine maintenance, or were seeded to a density appropriate to required usage. HEK-293 cells were split once every 4 days to avoid over growth and excessive cell number mediated de-adherence. Flasks were supplemented with 8 mL or 15 mL CM10 respectively for 25 and 75 cm^2 flasks. INS-1 832/13 cells were detached, centrifuged and re seeded as stated above, however the flasks were supplemented with 22 mL RPMI media.

2.2.1.4 Long Term Storage of Cells

HEK-293 cells were cultured until approximately 70% of the 75 cm^2 vessel was covered with a monolayer of cells. Cells were washed with 3 mL PBS, detached using 2 mL TrypLE™ express and centrifuged at 1288 *g* using an eppendorf 5702 tabletop centrifuge. Cells were resuspended in 4 mL 4°C freeze medium (70 % DMEM, 20 % FBS (i) and 10 % DMSO) and placed in 4 cryovials. The cryovials were placed in a freezing container (Mr. Frosty, Sigma-Aldrich, C1562) which seats cryovials in a rack suspended in isopropanol; the isopropanol achieves a change in temperature of 1 degree Celsius per minute to allow slow freezing and reduces the chance of water crystal formation. The freezing container was incubated at -80°C for 48 hours in a Panasonic ultra-low temperature VIP freezer (Sanyo, MDF-U55V) before the cryovials were transferred to a liquid nitrogen vessel (Taylor-Wharton, 35VHC). INS-1 832/13 cells were treated in the same way as HEK-293 cells, except the freeze medium consisted of 90% FBS (ii) and 10% DMSO.

The recovery of cells from long term storage was implemented by incubating the cryovial in a 37°C water bath for 4 minutes until no longer frozen and transferred to a 25 cm^2 culture vessel containing 8 mL growth media. The cells were incubated for 4 hours to allow the healthy cells to adhere to the flask surface, after which they were washed with 2 mL PBS to remove dead and dying cells, and the media replaced.

2.2.1.5 Transient Transfection of FlpIn-HEK293 Cells

FlpIn-HEK293 cells were transiently transfected using pcDNA5/FRT encoding the cysteine to alanine mutant human GLP-1R cDNA. FlpIn-HEK293 cells were cultured in 25 cm^2

vessels until 90 % of the surface was covered with adherent cells on the day of transfection. The day prior to transfection the cells were washed with 2 mL PBS and the media replaced with 8 mL 90 % DMEM and 10 % FBS (antibiotic-free media). On the day of transfection the cells were washed with 2 mL PBS and the media again replaced with 5 mL antibiotic free media. 20 µL Lipofectamine™ 2000 transfection reagent was added to 480 µL DMEM and incubated at room temperature for 5 minutes. Meanwhile 8 µg DNA was diluted into a total volume of 500 µL DMEM. Following the 5 minute incubation the DNA/ DMEM mix and Lipofectamine™ 2000/ DMEM mix were combined and incubated at room temperature for 20 minutes to allow the Lipofectamine™ 2000-DNA complexes to form. The 1 mL Lipofectamine™ 2000/ DNA complex was added to the 5 mL antibiotic free media and the cells were incubated at 37°C for 4-6 hours to allow the complexes to be internalised into the cells; the cells were then washed with 2 mL PBS and 8 mL of antibiotic free media added. Transgene expression was tested 48 hours after transfection by cAMP accumulation assay (**2.2.3.1**).

2.2.1.6 Stable Transfection of FlpIn-HEK293 Cells

Stable transfection of FlpIn-HEK293 cells was achieved using the same methodology as the transient transfection protocol, except that 8 µg DNA contained the two plasmids: pOG44 and pcDNA5/FRT (Cys-Ala) human GLP-1R in a 9:1 ratio. The 500 µL DNA/ DMEM mix therefore contained 7200 ng pOG44 and 800 ng pcDNA5/FRT (Cys-Ala) human GLP-1R.

The protocol was identical to the transient transfection protocol until 48 hours following transfection, whereby instead of testing for transgene expression using a cAMP accumulation assay, the cells which had successfully incorporated the transgene into their transcriptionally active locus were selected for by hygromycin B selection.

At 48 hours following transfection, the cells were washed using 2 mL PBS, and detached using 1 mL TrypLE™ express. The cells were collected into a sterile 15 mL polypropylene tube and centrifuged at 1288 *g* for 3 minutes at room temperature. The supernatant was discarded and cell pellet resuspended in 1 mL CM10. For each mutant, two new flasks were initiated by performing a 1 in 5 (200 µL pellet) and a 1 in 10 (100 µL pellet) split into new 25 cm^2 flasks. CM10 was supplemented with 200 µg/mL of hygromycin B, and 5 mL was added to each 25 cm^2 flask. The cells were washed with 2 mL PBS to remove dead and dying cells and the media replaced with fresh CM10 supplemented with hygromycin B every 48 hours until lone cells with hygromycin B resistance had replicated sufficiently to create a colony of clonal cells (this took approximately 3 weeks). When distinct colonies were visible both

under the microscope (Leica Microsystems, EC3) and to the naked eye, cells were washed with 2 mL PBS and detached using 1 mL TrypLE™ express. The cells were collected into a 15 mL polypropylene tube and centrifuged at 1288 *g* for 3 minutes at room temperature. The pellet was resuspended in 1 mL CM10 and the whole pellet re-seeded into the same flask and made up to 10 mL using CM10 supplemented with 100 μg/mL hygromycin B; this separated the cells from population-dense colonies where growth was hindered, to a more amiable monolayer growth arrangement. This mixed population cell line was then cultured as described (**2.2.1.3**) and at least 2 cryovials of each mutant strain frozen for long term storage (**2.2.1.4**).

2.2.1.7 Crude Membrane Preparations

Five 160 cm^2 ventilated petri dishes were laced with 5 mL L-poly-*D*-lysine (100 μg/mL) and left to polymerise aerobically for 30 minutes. After the monolayer of L-poly-*D*-lysine had set, excess reagent was removed by thoroughly washing each plate with 10 mL PBS. Plates were seeded evenly using the cells from one 175 cm^2 culture vessel, consisting of Flp-In HEK-293 cells constitutively expressing the wild type human GLP-1R. The plates were made up to 40 mL total volume using CM10 and grown to confluence at 37°C, 5 % CO_2 and 100 % humidity. The rest of the protocol was not performed in a tissue culture hood. The five petri dishes were removed of media before the addition of 15 mL of ice cold MQ. The petri dishes were incubated at 4°C for 5 minutes to allow osmotic cell lysis to occur. The plate surface was then washed five times using 10 mL ice cold PBS to remove intracellular organelles and other non-membrane associated items. The adhered membranes were then removed from the plate surface using a 32 cm cell scraper and distributed into microcentrifuge tubes. The membranes were pelleted using a bench top centrifuge set in the cold room (Biofuge 13, Jencons) for 30 minutes. The supernatant was removed, and the pellet obtained from combining all five dishes was resuspended in 1 mL of HEPES binding buffer (HBB: 25 mM HEPES, 2.5 mM $CaCl_2$, 1 mM $MgCl_2$, 50 g/L bacitracin, pH of 7.4). The crude membrane preparation was then passed through a 23 G needle to homogenise the membranes, aliquotted into 100 μL samples, snap frozen in dry ice and stored at -80°C.

2.2.1.8 Bicinchoninic Acid Assay

The crude membrane preparation (**2.2.1.7**) was subject to a bicinchoninic acid (BCA) assay to determine total protein content. A 1 mg/mL BSA standard was made using 10 mg BSA and 10 mL MQ; this was then diluted using MQ to a final volume of 50 µL to give 0.2, 0.4, 0.6 and 0.8 mg/mL of BSA to construct a calibration curve. Crude membrane preparations were defrosted on ice for 1 hour prior to being passed through a 23 G needle. Membranes were solubilised in an equal volume of MQ, and diluted to different factors using MQ, such as a: 1 in 5, 1 in 10, 1 in 50 and 1 in 100 dilution. To a flat-bottomed 96 well polypropylene plate, 10 µL of the BSA standards were added in triplicate, as were the crude membrane dilutions. To each of the wells, an additional 200 µL of BCA reagent (a 1:50 ratio of 4 % $CuSO_4$ and BCA) was added; 22 mL of BCA reagent is sufficient for one complete 96 well plate. The plate was sealed to prevent evaporation, and was incubated at 37°C for 30 minutes to allow colour development. The absorbance of the BSA standards and the membrane samples were read at 562 nm using a FLUOstar Omega plate reader. The protein content of the crude membrane sample was then calculated according to the BSA standards.

2.2.2 Molecular Biology and Cloning Methodology

2.2.2.1 Preparation of Chemically Competent *E.coli*

A sterile inoculation loop was used to transfer the remnants of a vial of XL1-Blue super competent *E.coli* cells to an LB agar plate supplemented with 25 µg/mL tetracycline using the streaking out technique under aseptic conditions. The plate was incubated, inverted, at 37°C for 16 hours. A single colony was picked using a sterile p200 yellow tip and used to inoculate 20 mL SOC encased in a 250 mL concial flask, supplemented with 25 µg/mL tetracycline; this was incubated at 37°C in an Orbi-Safe shaking incubator set at 220 rpm for 16 hours and was the primary inoculate. Two 2 L conical flasks containing 250 mL 2 x TY media supplemented with 25 µg/mL tetracycline were inoculated with 2.5 mL of the primary inoculate; these were grown at 37°C with shaking until the OD_{600} reached 0.5. The cell culture was transferred to pre-chilled centrifuge tubes and the cells pelleted by centrifugal force using the Sorvall RC-5B centrifuge with the F14S rotor, set to 2500 *g* for 15 minutes at 4°C. The rest of the protocol was performed in the cold room. The supernatant was discarded and the centrifuge tube left inverted on tissue for 2 minutes to minimise media contamination. Each pellet was resuspended in 83 mL sterile

RF1 (100 mM rubidium chloride, 50 mM manganese chloride, 30 mM potassium acetate, 10 mM calcium chloride, 15% (*v*/*v*) glycerol, pH 5.8) until no clumps remained, this was incubated on ice for 1 hour prior to centrifugation at 2500 *g* for 15 minutes at 4°C. The supernatant was discarded and the centrifuge tubes were left inverted on tissue for 2 minutes to allow minimal RF1 contamination. Each pellet was thoroughly resuspended in 20 mL sterile RF2 (10 mM MOPS, 10 mM rubidium chloride, 75 mM calcium chloride, 15% (*v*/*v*) glycerol) and incubated on ice for 15 minutes. The cell suspension was then aliquotted into pre-cooled 500 µL microcentrifuge tubes; 100 µL of cell suspension was placed into each microfuge tube and was snap frozen in dry ice in ethanol and stored at -80°C. Following this procedure the *E.coli* cells were chemically competent and were capable of a transformation efficacy of approximately 5.0 x 10^6 cfu/µg cDNA.

2.2.2.2 Transformation of Chemically Competent *E.coli*

Commercially available XL1-Blue Supercompetent *E.coli* were used for transformation of low quality DNA such as following a ligation or QuikChange reaction, as the transformation efficiency is 1 x 10^9 cfu/µg DNA. DNA transformation using high quality plasmids isolated by alkaline lysis was performed using in-house made chemically competent *E.coli* (**2.2.2.1**).

An aliquot of chemically competent *E.coli* was incubated on ice for 15 to 30 minutes to thaw. Per reaction, 1-2 µL of variable concentration DNA was transferred to the bottom of a pre-chilled thin-walled 14 mL polypropylene tube, 50 µL of chemically competent cells were transferred on top of the DNA and gently tapped to mix. The cell/DNA mix was incubated on ice for 30 minutes to allow mixing. Cells were heat shocked for 45 seconds in a 42°C water bath and returned to ice for a further 2 minutes. 500 µL pre warmed SOB media was added to the cells and incubated at 37°C in an Orbi-Safe incubator (Sanyo) set to 220 rpm for one hour to allow gene expression.

If high quality DNA was used initially, 50 µL and 100 µL were plated out on pre warmed agar plates with selective antibiotic. If low quality DNA was used initially, the cells were pelleted at 1620 *g* (Eppendorf 5804R centrifuge) for 5 minutes, the supernatant discarded, the pellet resuspended in 100 µL SOB, and all the cells were plated out onto a pre warmed LB agar plate. In each case, the plates were incubated inverted in a 37°C incubator for 16 hours to allow colony formation.

2.2.2.3 Small Scale Alkaline Lysis (Miniprep)

Small scale alkaline lysis was used to isolate the particular vector in question. A single colony resulting from transformation (**2.2.2.2**) was used to inoculate 5 mL LB medium supplemented with the selective antibiotic. The cells were grown for 16 hours in an Orbi-Safe incubator (Sanyo) at 37°C with 220 rpm shaking. 1.5 mL of the cell suspension was pelleted by centrifugation at 3,300 *g* (Eppendorf 5415R centrifuge) at 4°C for 5 minutes. The supernatant was discarded and microfuge tube left inverted on tissue for 1 minute to minimise LB medium contamination. The pellet was resuspended in 200 µL suspension buffer (25 mM tris-HCl pH 8.0, 50 mM glucose, 10 mM EDTA), and lysed at room temperature for 5 minutes using 400 µL lysis buffer (200 mM NaOH, 1 % SDS). Lysis was terminated by the addition of 300 µL neutralisation buffer (7.5 M ammonium acetate pH 7.8, 10 mg/mL RNaseA). The sample was incubated on ice for 10 minutes to allow precipitate to form. Precipitate was pelleted by centrifugation at 16,100 *g* (Eppendorf 5415R centrifuge) at 4°C for 15 minutes. The supernatant was transferred to a second microfuge tube that contained 600 µL isopropanol and was incubated on ice for ten minutes to allow DNA precipitation. The DNA was pelleted by centrifugation at 16,000 *g* at 4°C for 15 minutes. The supernatant was discarded and the pellet washed with 200 µL 70 % ethanol before being centrifuged at 16,000 *g* at 4°C for 5 minutes. The supernatant was discarded and the DNA pellet was air dried in a 37°C incubator for 30 minutes, then resuspended in 50 µL MQ. The DNA was stored at -20°C and the concentration was quantified by spectrophotometry **2.2.2.6**.

2.2.2.4 Endonuclease Digest of DNA

Approximately 200 µg DNA was subject to cleavage using restriction endonucleases supplied by NEB; due to the varying concentration of DNA stocks, the volume digested in the reaction varied, the volume was always made to a total of 20 µL using MQ. To the reaction mix, 2 µL of 10 x concentrated NEB buffer was used to correspond to 100 % endonuclease activity according to the manufacturer's instructions, alongside 10 U of restriction enzyme and 1 µL of 100 x concentrated BSA. The reagents were mixed thoroughly and incubated at 37°C for 2 hours. If two enzymes were used simultaneously, the units of enzyme used were halved to maintain 10 U of enzyme per reaction, and the buffer was selected so that enzyme activity was equal and maximal for both enzymes. If the DNA endonuclease digest was for analytical purposes, the resulting reaction was terminated by heating to 80°C for 5 minutes and cooled to

4°C on ice for 5 minutes to prevent loss of sample by evaporation. The contents were collected at the bottom of the microfuge tube by centrifugation, and visualised using agarose gel electrophoresis (**2.2.2.5**).

2.2.2.5 Agarose Gel Electrophoresis

Separation of DNA molecules on the basis of molecular weight was achieved by electrophoresis using a 1 % agarose gel. A gel cast was assembled by wrapping autoclave tape on the top and bottom of a casting tray and a comb inserted 1 cm below the top of the tray. The agarose gel was made by the addition of 1.5 g agarose into 150 mL of TAE buffer (40 mM Tris pH 8.0, 20 mM acetic acid, 1 mM EDTA) and dissolved by boiling using a microwave. The gel mix was cooled to 50°C prior to the addition of 1 µg/mL ethidium bromide, the two were mixed and poured into the gel cast and allowed to polymerise in the cold room. When fully polymerised, the autoclave tape was removed and the gel lowered into an electrophoresis tank (Bio-Rad wide mini sub™ cell), the comb was gently removed and the tank filled 1 mm above the surface of the gel with TAE buffer. Samples to be analysed were mixed with 5 times concentrated loading buffer (0.25 % (*w*/*v*) bromophenol blue, 0.35 % (*w*/*v*) glycerol pH 8.0) and 20 µL of the sample was loaded into each well. The samples were loaded alongside 5 µL of GeneRuler™ DNA ladder mix as a size reference. The tank was connected to a Bio-Rad power pack (Bio-Rad PowerPac 200) and the samples were electrophoresed at 2.0 mA, 100 volts for 40 to 60 minutes to allow optimal separation of fragments. The electrophoresed DNA fragments were visualised using a UV illuminator box and images were captured using a Bio-Rad camera system (Bio-Rad Gel Doc™ XR, 170-8170). Images were processed using Quantity-One-4.6.1 software.

2.2.2.6 DNA Quantification

The concentration and relative purity of DNA preparations were quantified using UV light spectroscopy (Eppendorf Biophotometer). Plasmid samples were diluted 3 µL into 97 µL MQ and mixed in a microfuge tube. The spectrophotometer was set to calculate dsDNA concentrations, which automatically calculated levels of protein contaminants and background contamination by measuring absorbance at 260, 280 and 340 nm respectively. The spectrophotometer was standardised using 100 µL of MQ in a UV spectrum cuvette (Eppendorf

UVette®, EPP-952010069). The samples were transferred from the microfuge tube to a UV spectrum cuvette and the readings noted. The readings were corrected for the dilution factor and concentration estimated by using the following formula.

$$DNA\ concentration\ (ng/\mu L) = 50\ ng/\mu L \times A_{260} \times dilution\ factor$$

2.2.2.7 Sequencing of Plasmid DNA

Cysteine mutant human GLP-1R DNA in the pcDNA5/FRT vector was sequenced using the Sanger sequencing service provided by Beckman Coulter Genomics. Samples were diluted to a concentration of 100 ng/µL using MQ. To a 1.5 mL microfuge tube, 15 µL of the sample to be sequenced was transferred, and a 'capmarker' (provided by Beckman Coulter) was placed on the lid of the tube. The capmarker corresponded to the online ordering system of Beckman Coulter which registers the contents of the microfuge tube based on the number denoted on the capmarker. The sample order was registered online and the T7 forward or BGH reverse primer to be used for sequencing was chosen depending on the location of the mutation to be analysed within the sequence. Upon online order completion, the samples were placed in a snap seal plastic bag, which was placed in a shipping box, which was then placed inside a pre-paid envelope (all of which were provided by Beckman coulter) and sent for sequencing using TNT courier services. Once sequencing was completed, the results were downloaded from the online site in FASTA format and analysed by ClustalW2 sequencing software (EBI).

2.2.2.8 Medium Scale Alkaline Lysis (Midiprep)

Up to 1 mL of high quality DNA of transfection grade was prepared using the Qiagen HiSpeed™ midiprep kit (Qiagen, 12643). The protocol was followed according to manufacturer's specifications using the high copy number vector culture volume of 50 mL. The resultant purified DNA was checked for concentration and purity (**2.2.2.6**).

2.2.3 Pharmacological Characterisation Methodology

2.2.3.1 LANCE® cAMP Accumulation Assay

A myriad of peptidic ligands, non peptidic ligands and combinations thereof were assessed for their ability to cause cAMP production in Flp-In HEK 293 cells, which transiently or stably expressed the receptor of interest. Full length (28-39 residue) peptides and compounds were incubated with the cells for 10 minutes; truncated (10-27 residues total length) peptides were incubated with the cells for 30 minutes unless stated otherwise. Non-peptide ligands were incubated with the cells for 10 minutes.

The ligands to be assayed were diluted into stimulation buffer (Hank's Balanced Salt Solution (HBSS), 5 mM HEPES, 0.1 % (*w*/*v*) BSA pH 7.4) supplemented with 1 mM IBMX, and diluted to the appropriate concentration range to be assayed. The ligands were diluted into a v-bottomed 96-well plate; usually 8 different ligand concentrations were used, diluted several orders of magnitude using a $\log_{10}$ scale.

The cells expressing the receptor of interest were washed using 3 mL PBS twice and detached by incubating the cells with 2 mL PBS at 37°C for 5 minutes. The cells were harvested using 8 mL of PBS, transferred to a sterile 15 mL and pelleted at 1,288 *g* for 3 minutes at room temperature (Eppendorf 5804R centrifuge). The supernatant was discarded and the cell pellet resuspended in a volume of PBS to give the optimal density for haemocytometry, this volume varied depending on flask size and density of the cells. Total cell number was estimated by dispensing 25 µL of cell suspension onto the upper and lower chambers of a counting chamber (Hawksley, AS1000) and counted to estimate how many cells were present in total. The cells were pelleted again by centrifugation at 1,288 *g* for 3 minutes at room temperature (Eppendorf 5804R centrifuge). The supernatant was discarded and the pellet resuspended in 1 mL of stimulation buffer which was pre-warmed to 37°C, and diluted into stimulation buffer to give 1.6 x 10^6 cells/mL. To a volume appropriate for assay requirements, 0.005 % (*v*/*v*) of Alexa Fluor® 647-labelled anti-cAMP antibody was added.

To a white 384-well OptiPlate, 6 µL of the ligand was combined with 6 µL of the cell suspension, each concentration of ligand was assayed in triplicate, so an average 8-concentration ligand assay encompassed 24 wells. The OptiPlate was covered with a TopSeal-A adhesive sheet and incubated at 37°C for the length of time specified.

The detection mix contents were provided in the LANCE kit and contained the elements required to form a competitive tracer complex containing Eu-W8044 labelled streptavidin,

biotinylated cAMP and detection buffer containing SDS for cell lysis. Eu-W8044 labelled streptavidin was diluted 0.00044 % (*v*/*v*) and biotinylated cAMP was diluted 0.00133 % (*v*/*v*) into an appropriate volume of detection buffer to provide sufficient detection mix for assay requirements. The detection mix was incubated at room temperature for 15 minutes to allow complex formation to occur. Cellular stimulation was terminated by the addition of 12 µL detection mix to each well. The OptiPlate was incubated at room temperature for one hour to allow equilibrium to be established between the tracer complex and endogenous/ biotinylated cAMP.

The OptiPlate was measured for fluorescence emission at 615 and 665 nm using a VICTOR™ X5 multilabel plate reader (Perkin Elmer). Data were collected using Microsoft Excel software (2007) and was analysed using GraphPad Prism 6.0 software (**2.2.4.1**).

2.2.3.2 Radioligand Binding Assays

All procedures involving the radioligand were implemented in the designated work area. When handling the radioligand there was a protective lead-lined Perspex sheet to minimise exposure to radioactivity to vital organs. Contact with radioligand was kept to a minimum and disposal of radioligand was carried out according to health and safety regulations on the RSID.

2.2.3.2.a Specific Binding Assay

A lysed-cell vacuum filtration approach was taken to assess ligand affinities at the human GLP-1R (adapted from Hoare *et al*., 1999). The specific binding of ^{125}I-GLP-1(7-36)NH_2 radioligand to isolated membranes containing the human GLP-1R was performed to obtain the appropriate membrane dilution that would give optimal specific binding. Typically this membrane dilution gave 3-5 µg of total protein during the assay, and gave less than 10 % of the total counts added to each well to conform to the Cheng-Prusoff equation (Cheng and Prusoff 1973) in order to determine the affinity constant K_a and B_{MAX} from the IC_{50}.

Crude membrane preparations obtained as described (**2.2.1.7**) were thawed on ice for 1 hour prior to experimentation. The membranes were passed through a 23G needle several times and diluted to 2 %, 1%, 0.66% and 0.5% (*v*/*v*) into HEPES binding buffer (HBB) supplemented with 0.2 % *w*/*v* BSA to a final volume of 1 mL. Hot ligand (^{125}I-GLP-1(7-36)NH_2) was diluted

into an appropriate volume of HBB to have a specific radioactivity of 50 pM in the assay (approximately 50,000 cpm of activity per well). Unlabelled or 'cold' GLP-1(7-36)NH_2 was diluted into an appropriate volume of HBB to a final concentration of 4 x 10^{-5} M; such a high concentration of cold GLP-1(7-36)NH_2 was used to ensure 100% of the GLP-1 receptors were occupied with cold ligand, so any counts remaining were non-specifically bound hot ligand.

Into a v-bottomed polypropylene 96 well plate, 50 µL of HBB was added in triplicate for each membrane dilution for total binding analysis, and 50 µL of cold GLP-1(7-36)NH_2 was added in triplicate for each membrane dilution for non-specific binding analysis. 50 µL of hot GLP-1(7-36)NH_2 was added to each well containing either ligand or buffer to give 100 uL of ligand mix. To each well, 100 µL of the specified dilution of membrane was added. The plate was covered and incubated at room temperature for 1 hour to allow equilibrium to occur.

During the 1 hour incubation, one or two MultiScreen™ 96-well filtration plates were pre-soaked for at least 30 minutes using 200 µL blocking buffer (PBS containing 0.1 % (*v*/*v*) PEI) per well. The filter plate was then housed in a vacuum manifold and the blocking buffer sucked through the filter disk. The radioligand-associated membranes and contents of the 96 well plate were transferred to the filter plate and subsequently washed three times with 200 µL 4°C wash buffer (PBS, 0.1 % BSA). Excess liquid insufficiently aspirated off the bottom of the plate was blotted on tissue for one minute, the backing of the plate was removed and the filter disks excised. The filter disks were placed in individual 5 mL culture tubes and counted for gamma radiation (RiaStar 5405 counter, Packard). Specific binding of ^{125}I-GLP-1(7-36)NH_2 to hGLP-1R expressing membrane was calculated as the difference between total and non-specific binding.

2.2.3.2.b Competitive Radioligand Binding Assay

Crude membrane preparations obtained as described (**2.2.1.7**) were thawed on ice for 1 hour prior to experimentation. The membranes were passed through a 23G needle several times and diluted using HBB supplemented with 0.2 % w/v BSA to the concentration determined by the specific binding assay (**2.2.3.2.a**) in to a volume appropriate for the assay. Peptide and non-peptide ligands were diluted using HBB. Several orders of magnitude of cold ligand were used, using a range of 8 concentrations. 50 µL of each ligand concentration was dispensed into a v-bottomed polypropylene 96 well plate in triplicate. To this, 50 µL of hot ligand was dispensed, and then 100 µL of membrane solution was added to each well. The plate was covered and incubated at room temperature for 1 hour to allow equilibrium to occur.

During the 1 hour incubation, one or two MultiScreen™ 96-well filtration plates were pre-soaked for at least 30 minutes using 200 μL blocking buffer. The filter plate was then housed in a vacuum manifold and the blocking buffer sucked through the filter disk. The radioligand-associated membranes and contents of the 96 well plate were transferred to the filter plate and subsequently washed three times with 200 μL 4°C wash buffer. Excess liquid insufficiently aspirated from the bottom of the plate was blotted on tissue for one minute, the backing of the plate was removed and the filter disks excised. The filter disks were placed in individual 5 mL culture tubes and counted for gamma radiation (RiaStar 5405 counter, Packard).

2.2.3.3 Insulin Secretion Assay

INS-1 832/13 cells (gift from Prof. C Newgard, Duke University, Durham, NC) were washed and detached from the base of the flask using 3 mL PBS and 2 mL TrypLE express respectively. INS-1 832/13 cells were harvested and pelleted at room temperature, 1,400 *g* for 5 minutes (Eppendorf 5703 centrifuge). The pellet was resuspended into supplemented RPMI-1640 medium, counted using a haemocytometer (Hawksley), and sewn into pre poly-D-lysine hydrobromide treated 24-well plates (Sarstedt) at a density of 5 x 10^5 cells/ well. Cells were cultured in supplemented RPMI-1640 medium for 72 hours until 95 % confluency was achieved. Cells were washed with 2 mL secretion buffer (114 mM NaCl, 4.7 mM KCl, 1.2 mM KH_2PO_4, 1.16 mM $MgSO_4$, 20 mM HEPES, 2.5 mM $CaCl_2$, 25.5 mM $NaHCO_3$, 0.2 % (*w/v*) BSA, pH 7.2) and treated with 1 mL of secretion buffer supplemented with 3 mM glucose for 3 hours at 37°C to deplete the available concentration of glucose. Following the low glucose incubation, the 3 mM glucose solution was removed and replaced with 1 mL per well of 16.7 mM glucose solution containing the concentrations of the secretagogues being assayed, all diluted into secretion buffer. INS-1 832/13 cells were incubated at 37 °C for 2 hours with 16.7 mM glucose and the secretagogues. The incubant was harvested into microfuge tubes and centrifuged at 1,288 *g*, 4°C for 5 minutes (eppendorf 5415R centrifuge) to remove any residual cells, the supernatant was used for analysis using the ImmuChem™ insulin ^{125}I RIA kit (MP Biomedicals). The kit was prepared, performed and data analysed following manufacturer's instructions.

2.2.4 Data Analysis

2.2.4.1 Dose-Response Curve Analysis

The curves in the figures are an example of a single experiment, representative of at least three independent experiments. Each point on the curve was the average value for triplicate readings; the error bars displayed represent the S.E.M. The reciprocal values in the cAMP accumulation assay curves were taken and then normalised to the maximum cAMP response within that data set. The counts obtained in each binding assay were normalised to the highest specific binding count within that specific data set. The binding curves were fitted to a one-site model and cAMP accumulation curves were constructed using the non-linear regression function to give a sigmoidal dose-response curve using GraphPad PRISM 6.0 software (San Diego, CA).

pEC_{50} and *p*IC_{50} values in the tables are the $-\log_{10}$ mean plus S.E.M values from three independent experiments. Statistical significance of assay replicates was calculated using the Student's t-test.

2.2.4.2 Pm Compound Structure Diagrams

The Pm compounds were drawn using ACD/ChemSketch freeware software.

2.2.4.3 B_{MAX} Calculations

Maximal binding values for the radioligand binding assays (B_{MAX}) were calculated using a modified version of the Cheng-Prusoff equation as given below (Akera & Cheng, 1977).

$$B_{max} = B_o \bullet \frac{IC_{50}}{[L]}$$

Where B_{MAX} is the maximal binding and an estimation of the number of receptors per mg of protein in the crude membrane sample, B_0 is the binding detected in the absence of

unlabelled ligand, IC_{50} is the half inhibitory concentration of the ligand during a homologous competition assay, and [L] is the free concentration of hot ligand (which is assumed to be the total concentration applied to the sample if the cpm obtained on the filter disk is < 10 % of the total cpm input into the reaction). The Riastar C5410 gamma counter was estimated to have approximately 80% counting efficiency; this was taken into account when calculating dpm from cpm.

Protein content estimate from BCA assay

The BCA assay determined there was 7.6 mg/mL of protein in the total membrane preparation.

A membrane dilution of 1/200 was used :

$7.6\ mg \cdot mL^{-1} / 200 = 0.038\ mg/mL$

100 µL of membrane preparation was used in each well, therefore the mass of protein used per well was:

$(0.038\ mg \cdot mL^{-1} / 1000\mu L) * 100\ \mu L = 3.8 \times 10^{-3}$ mg protein

B_{MAX} Calculation from homologous binding experiments

An example of B_{MAX} analysis from one homologous competition binding experiment is as follows:

From curve parameters provided by GraphPad Prism 6.0:

Top = 6964 cpm

Bottom = 476.9 cpm

$IC_{50} = 8.25 \times 10^{-10}$ M

Total counts added = 54668.4 cpm

Specific Binding

Specific binding in cpm= top-bottom = 8214 – 439.5 = 7774.5 cpm

= 6964 – 476.9

=6487.1 cpm

The RiaStar 5405 gamma counter was 80% efficient therefore:

(6487.1/80%)*100 % = 8108.875 dpm

$1Ci = 2.22 \times 10^{12}$ dpm

2.22×10^{12} dpm / 8108.875 dpm = 273774105.5

1Ci / 273774105.5= 3.65×10^{-9} Ci

3.65×10^{-6} mCi

3.65×10^{-3} μCi

Therefore there are 3.65×10^{-3} μCi of specific binding in the sample.

The specific radioactivity of I^{125}-GLP-1(7-36) is 2.2 μCi/pmol.

GLP-1 binding at the GLP-1R has a 1:1 stoichiometry; therefore the number of moles present in the sample specifically bound to the receptor represents the number of moles of iodinated GLP-1(7-36), therefore:

3.65×10^{-3} μCi / 2.2 μCi/pmol = 1.66×10^{-3} pmol GLP-1(7-36) capable of binding in the sample, equivalent to 1.66 fmol bound.

The modified Cheng-Prusoff (1973) equation (Akera & Cheng, 1977) has the following parametres: B_0, [L], IC_{50} and B_{MAX}, of which the following have been calculated:

B_0 = 1.66 fmol (calculated above)

IC_{50} = 8.248 x 10^{-10} M (calculated from nonlinear regression)

[L] = the free concentration of hot ligand

[L] = total moles of hot ligand added to the assay – moles of hot ligand bound

Total radioactivity added to the assay was 54668.4 cpm

(54668.4 cpm / 80%) * 100% = 68335.5 dpm

2.2 x 10^{12} dpm / 68335.5 dpm = 32194101.16

1 Ci / 32194101.16 = 3.106 x 10^{-2} μCi

3.106 x 10^{-2} μCi /2.2 μCi/pmol = 0.0141 pmol or 14.118 fmol radiolabelled GLP-1(7-36) added in total.

% bound radioligand = (fmol ^{125}I-GLP-1(7-36) bound specifically / fmol ^{125}I-GLP-1(7-36) added in total)*100

(1.66/14.118)*100 = 11.76 % ^{125}I-GLP-1(7-36) bound

Therefore 88.24 % ^{125}I-GLP-1(7-36) free.

The concentration of radioligand added to each well was 75 pM

(75 pM / 100)*88.24 = 66.18 pM

[L] = 66.18 pM

[L] = 6.62 x 10^{-11} M

$$B_{max} = B_o \bullet \frac{IC_{50}}{[L]}$$

B_0 = 1.66 fmol

IC_{50} = 8.248 x 10^{-10} M

[L] = 6.62 x 10^{-11} M

B_{MAX} = (1.66 fmol * (8.248 x 10^{-10} M / 6.62 x 10^{-11} M))/ mg protein

B_{MAX} = 20.68 fmol / 3.8 x 10^{-3} mg

B_{MAX} = 5.44 pmol/mg protein

Only hGLP-1R over-expressing FLP-IN HEK 293 cells were used in this study. These were obtained from one batch of crude membrane preparations, and the average B_{MAX} from n=5 individual homologous binding assays presented within this study was 8.37 pmol/mg membrane protein.

Chapter 3

Small Molecule-Mediated Modulation of the Human Glucagon-Like Peptide-1 Receptor

3.1 Introduction

3.1.1. Small molecule ligands of the GLP-1R

The Glucagon-Like Peptide-1 receptor has been a pharmacological target for the development of small molecular agonists for at least the past decade (Teng *et al*., 2000), in order to provide orally available medicines for the treatment of T2D. This has proven problematic as GLP-1R is a Class B GPCR of the Secretin Subfamily, requiring large receptor-ligand interaction interfaces, alongside contacts with the extracellular loops and the transmembrane domain for optimal signal transduction (Wheatley *et al*., 2011). The difficulty of developing small molecule GLP-1R agonists has been attributed to this mechanism of activation; non-peptide ligands are too small to be able to interact with both the extracellular NTD and the transmembrane domain.

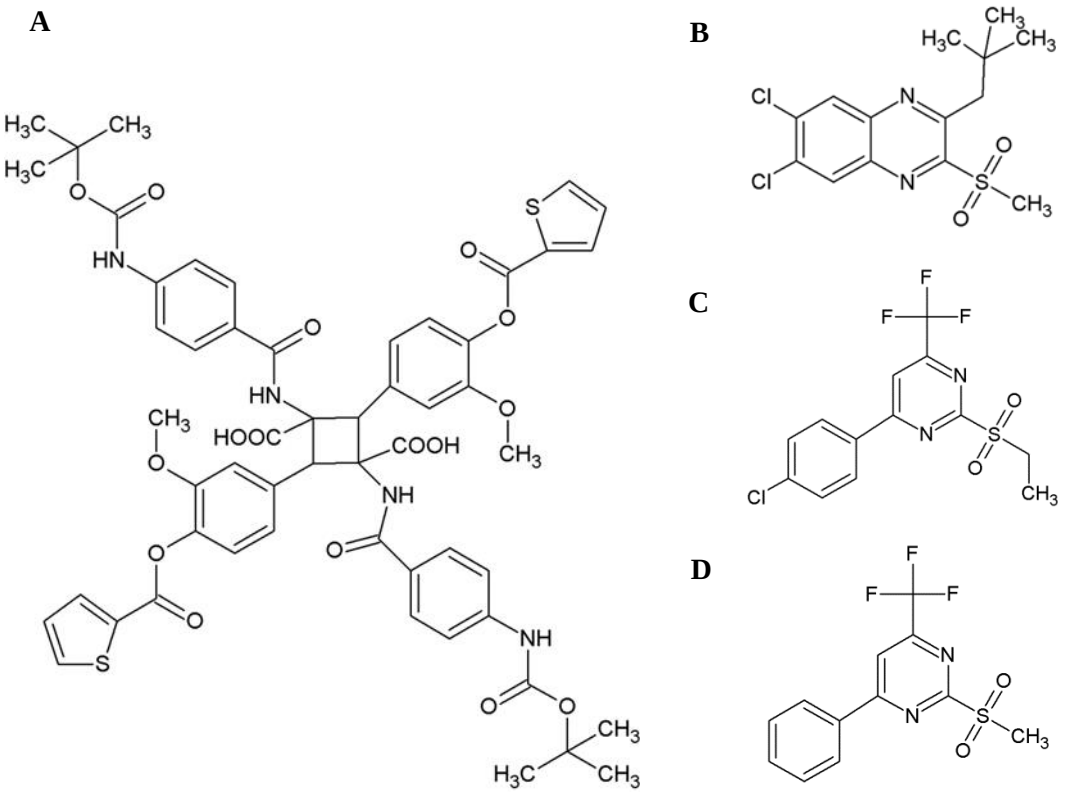

Figure 3.1.
Structures of examples of some non-peptide agonists of the hGLP-1R. A. Boc5. B. Compound 2. C. Compound A. D. Pm 1.

Little is known about the intricate details of non-peptide ligand interaction with the GLP-1R, it is not known where the orthosteric binding pocket resides, nor how many allosteric binding pockets there are. Ideally, a high-resolution crystal structure of the GLP-1R would be disclosed to the public domain to push back the boundaries of knowledge in this field for those who eagerly await the knowledge of how and where small molecules or the native ligand bind the receptor. Knowledge of this would surely facilitate rational drug design for these notoriously difficult drug targets.

Nevertheless, many small molecule ligands for the GLP-1R (and indeed other Class B GPCRs) have been discovered (Chen *et al*., 2007; Knudsen *et al*., 2007; Koole *et al*., 2010; Sloop *et al*., 2010) with the first non-peptide agonist fully disclosed named "Compound 2" with the chemical name N-*tert*-butyl-6,7-dichloro-3-methylsulphonyl-quinoxalin-2-amine (Teng *et al*., 2000), and the first non-peptide antagonist to be described and the structure disclosed to the public domain named "T-0632" (Tibaduiza *et al*., 2001). Other examples of non-peptide agonists of GLP-1R include Boc5, compound 2 and compound A, the structures of these ligands are shown in Figure 3.1.

3.1.2. Non-peptide allosteric modulation

A relatively new concept of small non-peptide ligand based GPCR receptor modulation has recently driven the field of drug discovery toward the investigation of non-peptide allosteric modulation in Class B GPCRs (Hoare, 2007). Despite the Secretin Family of receptors being relatively small in comparison to class A Rhodopsin-like receptors, many class B GPCRs are attractive therapeutic targets, such as the glucagon receptor to treat hepatic glucose output in type 2 diabetics, the CRF1 receptor for treatment of stress disorders and the CGRP receptor for treating migraine. Some Class B GPCRs already have peptide therapeutics derived from the native peptide themselves, such as Miacalcin (calcitonin) targeting the Calcitonin receptor to treat osteoporosis, Teriparatide (PTH(1-34)) targeting the PTH1 receptor, again to treat osteoporosis (Berg *et al*., 2003), and Exenatide (exendin-4(1-39)) targeting the GLP-1R to treat type 2 diabetes (Bhavsar *et al*., 2013).

Present peptide therapeutics only bind to the orthosteric site, thus there can be no form of interaction between endogenous peptide and therapeutic peptide, only competition and steric hindrance. This is advantageous to *reduce* signalling at the receptor target, yet if *enhanced* receptor stimulus is the therapeutic goal, it would surely be beneficial for the endogenous peptide and therapeutic to work in positive cooperativity with one another at the target receptor.

Non-peptide allosteric modulators take advantage of the intricate and complex two-domain mechanism of Class B GPCR receptor activation as they bind at the receptor to a topographically distinct site from the orthosteric site, causing a conformational change within the receptor. This conformational change may be transmitted toward the orthosteric site essentially creating a new state of GPCR structure, changing with it the receptor's binding and functional capabilities. The exact binding sites of many non-peptide ligands are generally unknown, with the currently accepted consensus being that there is no one specific exosite where all allosteric modulators bind, but multiple within one receptor. For example, the first documented antagonist for the GLP-1R, T-0632, is a non-competitive antagonist that binds to the extracellular amino-terminus of the GLP-1R and specifically makes interactions with tryptophan 33 (Tibidzua *et al.*, 2001). Boc 5, a substituted cyclobutane derivative is a full agonist at the GLP-1R, its cAMP accumulation profile can be hampered by Ex4(9-39) and Boc 5 can compete for binding at the orthosteric site with Ex4(9-39), suggesting orthosteric binding (Chen *et al.*, 2007). Partial agonist compound 3, structurally similar to compound 2, was found to bind to the transmembrane region of the GLP-1R, specifically, phenylalanine 195 in TM 2 and threonine 391 in TM 7 (Underwood *et al.*, 2011). As allosteric modulators have the ability to bind the amino (N) or the TM domain, they have the ability to modify affinity as well as efficacy, but one is not necessarily concomitant with the other.

3.1.3. The 'Pm' compounds

As part of a project to discover leads for non-peptidic agonists of GLP-1R, our collaborators: Prof. Fishwick, Prof. Johnson and Dr. Migliore (School of Chemistry, University of Leeds) synthesised 48 compounds (named as the Pm series, Figure 3.2) based around the structure of Pm1 (Figure 3.1.D), which had first been identified via a high-throughput screen by AstraZeneca. As part of this project, Dr. Migliore made chemical modifications to three areas of the compound such that our group could study the effect of functional group modification upon GLP-1R activation. Specifically, the modifications were made to: the trifluoromethyl (TFM) group situated at position 1 on the pyrimidine ring; to the sulphur dioxide (SD) group situated at position 3 on the pyrimidine ring; and to the benzene ring (BR) situated at position 5 on the pyrimidine ring. Unfortunately in 2010 a publication by Eli Lilly showed a small non-peptide agonist based upon the same scaffold (Compound A; Sloop *et al.*, 2010). Nevertheless, exploration of the pharmacological properties of example agonists from the series continued and some interesting characteristics were discovered. The data in this chapter aim to extricate the structure-activity relationship of this ligand library with the GLP-1R.

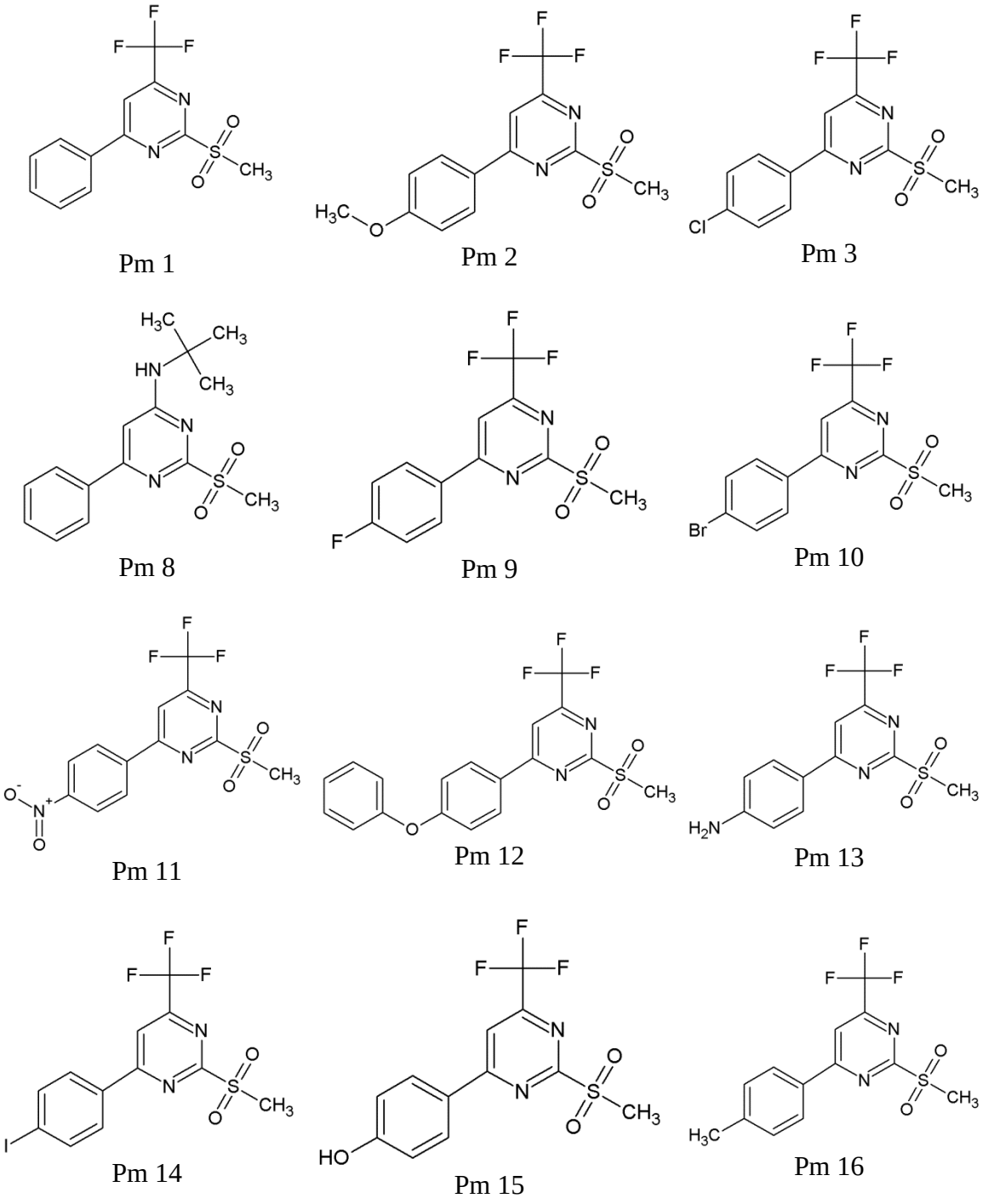

Figure 3.2.A. Library of Pm compounds in numerical order, structures 1 to 16.

Chemical structure and name are given for each modified compound. Pm 2 to Pm 62 have chemical modifications based upon the original Pm compound hit from AstraZeneca termed 'Pm 1' at the trifluoromethyl, sulphur dioxide and benzene ring functional groups that reside at positions 1, 3 and 5 of the pyrimidine ring respectively.

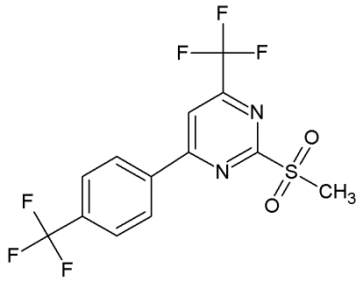

Pm 17

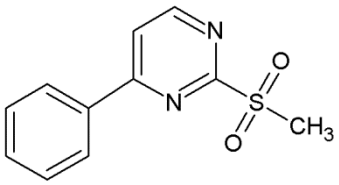

Pm 27

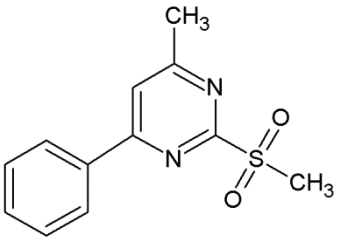

Pm 28

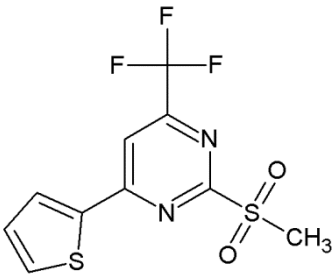

Pm 31

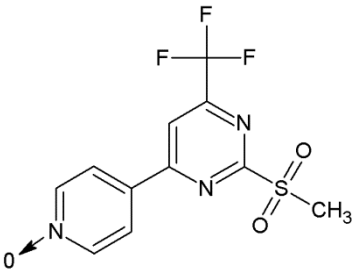

Pm 32

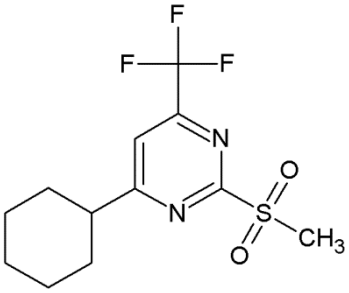

Pm 33

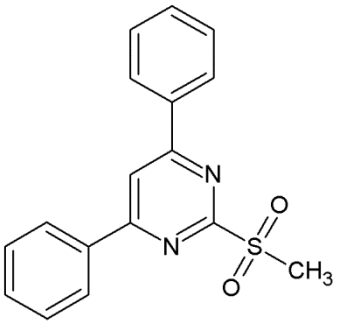

Pm 34

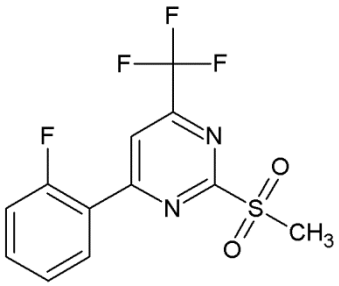

Pm 35

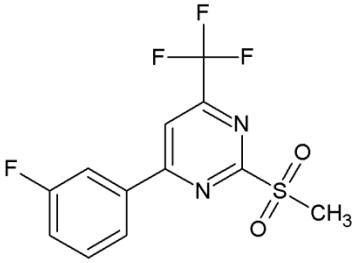

Pm 36

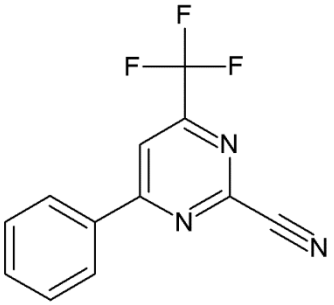

Pm 37

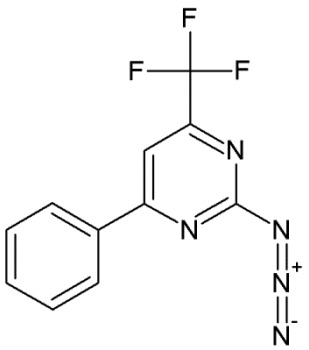

Pm 38

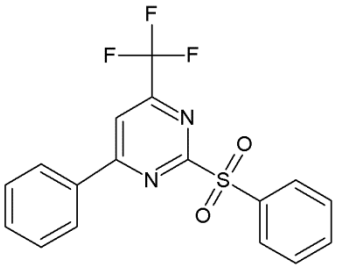

Pm 39

Figure 3.2.B. Library of Pm compounds in numerical order, structures 17 to 39.

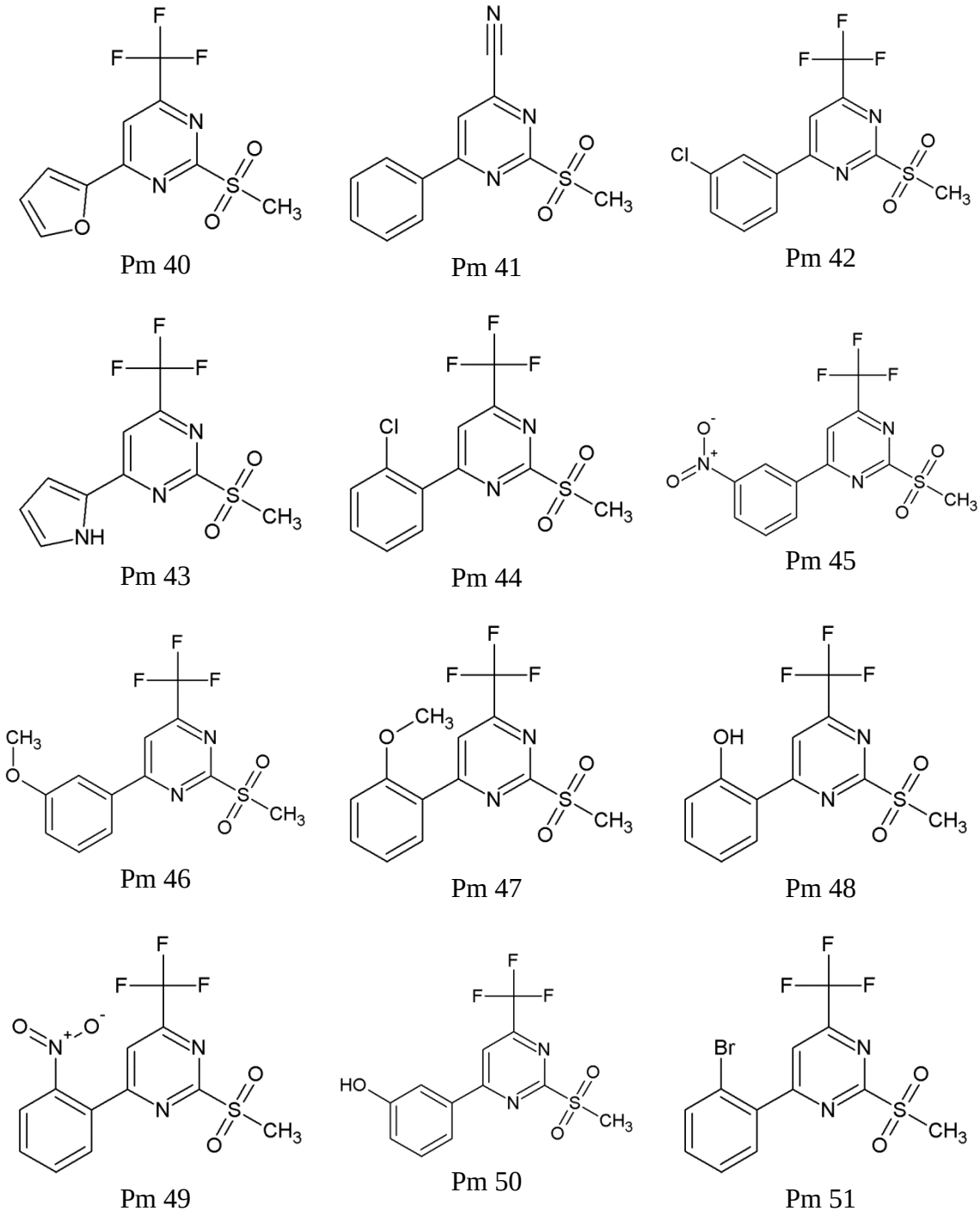

Figure 3.2.C. Library of Pm compounds in numerical order, structures 40 to 51.

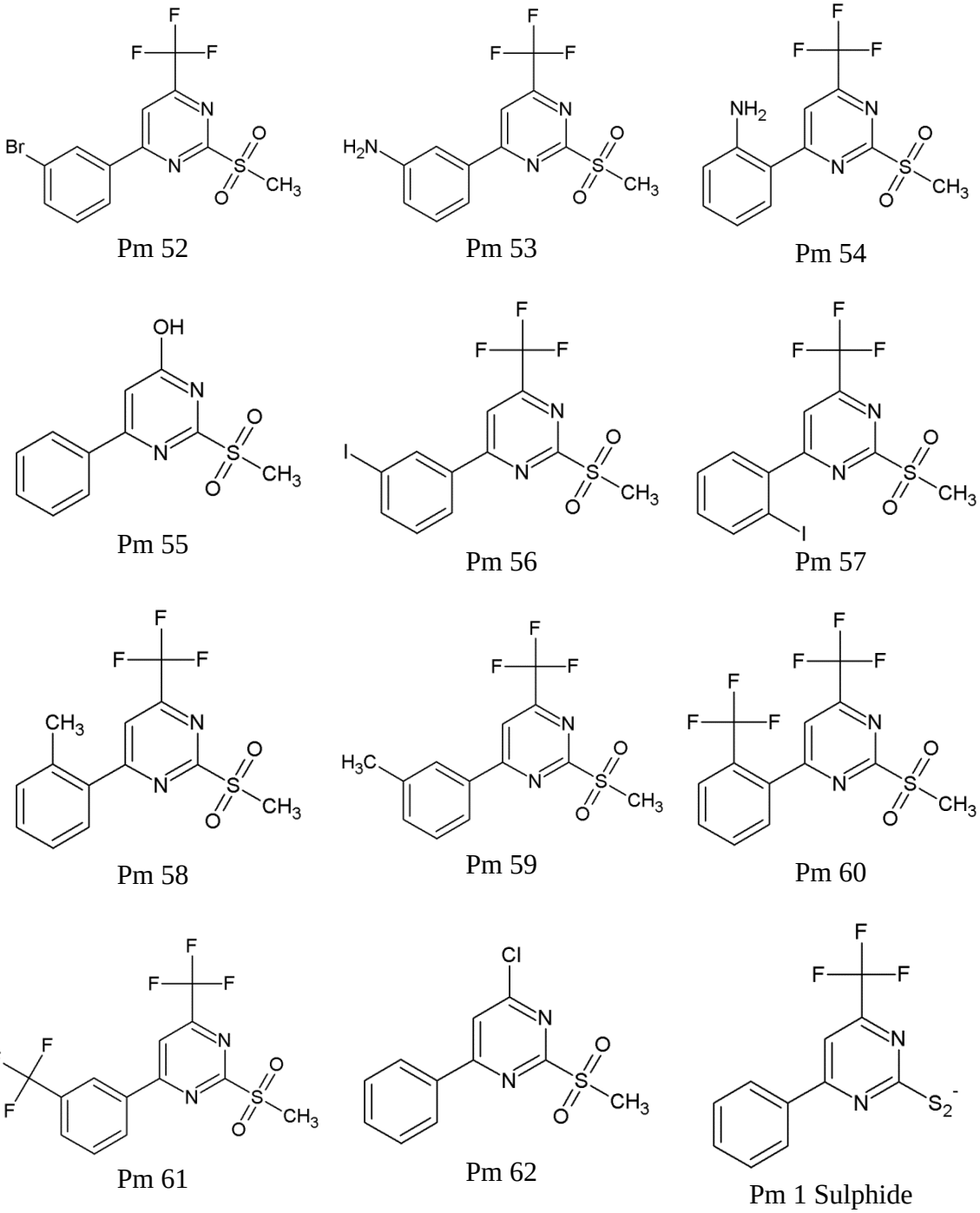

Figure 3.2.D. Library of Pm compounds in numerical order, structures 52 to 62, including Pm 1 sulphide.

3.2 Aims and Strategy

Small molecule non-peptide activators of GLP-1R are being sought to better understand the mechanism with which this large extracellular domain-containing Family B GPCR is activated (Willard *et al*., 2012). Much interest has been placed into engineering high affinity small molecules with high potency, yet relatively few studies have gone into the investigation of the structure-activity relationship of these small molecules, which could be key to the future of designing novel therapeutic agents for the treatment of type two diabetes. This chapter aims to address the structure-activity relationship of small molecules at the human GLP-1R, and to assess their role as possible therapeutics for the treatment of T2D. Specifically this chapter aims to:

- Identify the most active Pm compound at the hGLP-1R by examining the cAMP response in human (h) GLP-1R-expressing HEK cells.

- Elucidate the generic site of binding of the Pm compound (orthosteric or allosteric) by affinity binding studies at isolated membranes containing the hGLP-1R, and by antagonist competition assays.

- Investigate the activation characteristics of the Pm compound by performing dual activation assays with other peptide ligands at hGLP-1R expressing cells.

- Examine the structure-activity relationship of the Pm compounds to isolate important functional groups required for activation of the receptor.

- Implicate the use of the Pm compounds as possible therapeutics for the treatment of T2D by analysis of their actions as secretagogues in insulin-secreting INS-1 832/13 cells.

3.3 Methodology

3.3.1 Cell-Free cAMP Standard Curve

A standard curve was performed according to manufacturer's instructions. Specifically, a cell-free assay was performed to gage the responsive region of the LANCE kit by utilising the standard cAMP solution supplied in the kit to mimic the cAMP produced by cells upon ligand-mediated stimulation. Standard cAMP was diluted to the range shown in Figure 3.3.A using stimulation buffer and 1 mM IBMX into 96-well v-bottomed plates. Alexa Fluor® 647-labelled anti-cAMP antibody was diluted into stimulation buffer to a final concentration of 0.005 % (*v*/*v*). Standard cAMP dilutions and diluted Alexa Fluor® 647-labelled anti-cAMP antibody were combined into wells of a 384-well Optiplate and incubated for 30 minutes at room temperature. The rest of the procedure was followed as per the 'LANCE' methodology located in section 2.2.3.1.

3.3.2. FlpIn-HEK293 cAMP Forskolin curve

Forskolin was incubated with a range of FLP-IN HEK cell numbers as defined in Figure 3.3.B for 30 minutes at 37 °C as per the recommendations in the LANCE guide.

3.3.3 Antagonist Competition Assay

Human GLP-1R-expressing HEK cells were harvested and collected as per section 2.2.3.1. They were resuspended to a final concentration of 3.3 x 10^6 cells/ mL which is twice as concentrated as usual. This was to ensure a concentration of 10,000 cells/ well in the final assay. Alexa Fluor® 647-labelled anti-cAMP antibody was diluted into the cell suspension to a final concentration of 0.01 % (*v*/*v*). 3 µL of the double concentrated cell-antibody mix was combined with 3 µL of 2 x concentration antagonist Ex4 (9-39) into a 384-well Optiplate for 10 minutes at 37°C to allow equilibrium binding of antagonist at the GLP-1R. The peptide or non-peptide ligand to be assayed was diluted in stimulation buffer with 1 mM IBMX, supplemented with 1 x concentration of antagonist Ex4 (9-39) to ensure constant concentration of antagonist within the assay. 6 µL of agonist-antagonist mix was combined with the cell-antagonist mix in the 384-

well optiplate and incubated for a further 10 minutes at 37°C. The rest of the procedure was followed as per the 'LANCE' methodology located in section 2.2.3.1.

3.3.4. Dual-Activation Assay

Pm 42 was diluted to the concentrations depicted in Figure 3.9 using stimulation buffer supplemented with 1 mM IBMX. The peptide ligand to be investigated was then diluted into this instead of stimulation buffer. Both peptide and Pm 42 were diluted to 2 x concentration to ensure 1 x concentration when added to an equal volume of cell suspension. Cells were stimulated for 10 minutes at 37°C and the rest of the procedure was followed as per the 'LANCE' methodology in section 2.2.3.1.

3.4 Results

3.4.1. Cell Number Optimisation

LANCE™ cyclic AMP accumulation assays were performed in order the gage the optimal experimental range of the assay, thereby enhancing the reliability of the data. The LANCE™ cAMP kit can accurately measure cAMP levels within the approximate range of 10 nM to 0.1 nM (Figure 3.3.A). Cyclic AMP concentrations outside this range are not as accurate and replicate values may vary significantly because of this. It is therefore crucial to determine the correct cell number to be used in an assay, so that the EC_{50} of an assayed ligand will fall within this window. The assay window was determined by plotting a known concentration of standard cAMP that came as provided, against the emission signal at 665 nm (LANCE signal 665 nm) as shown in Figure 3.3.A, this is a standard curve. The standard curve showed that within the assay, the desired linear region depicting the sensitive range that lies between 10 and 0.32 nM cAMP (Log_{10} -8 to -9.5), and that this range of cAMP is relative to a LANCE signal of about 20,000-40,000 at 665 nm as shown by the markers (Figure 3.3.A).

Using the sensitive assay window of LANCE emission (665 nm) of between 20,000-40,000 relative units, a forskolin curve was performed to determine the number of cells per well to use in an assay. Forskolin is a small compound with a molecular weight of 410.5 Da, capable of activating adenylyl cyclase directly without the need for GPCR participation; therefore giving a guide of the maximum and minimum cAMP production of a specific cell line. Four concentrations of FLP-IN HEK 293 cells were employed: 1,000; 2,500; 5,000 and 10,000 cells per well, and these were stimulated with a range of forskolin from 100 µM to 1 nM, the resultant dose-response curve is shown in Figure 3.3.B. The results indicated that a higher cell number resulted in a higher basal cAMP level, thus the emission signal at 665 nm decreased in the absence of ligand. This is to be expected as the presence of IBMX prevents phosphodiesterase from cleaving the phosphodiester bond in cAMP to produce AMP, therefore background levels of cAMP will accumulate over time, and the more cells present, the higher the level of endogenous cAMP. The forskolin curve that best fits the standard curve sensitive assay window (emission of 20,000-40,000 at 665 nm) is the curve using 10,000 cells per well as the majority of points on the curve reside within the sensitive assay window-more so than any other cell concentration. Subsequently for the rest of this study, 10,000 cells per well were used.

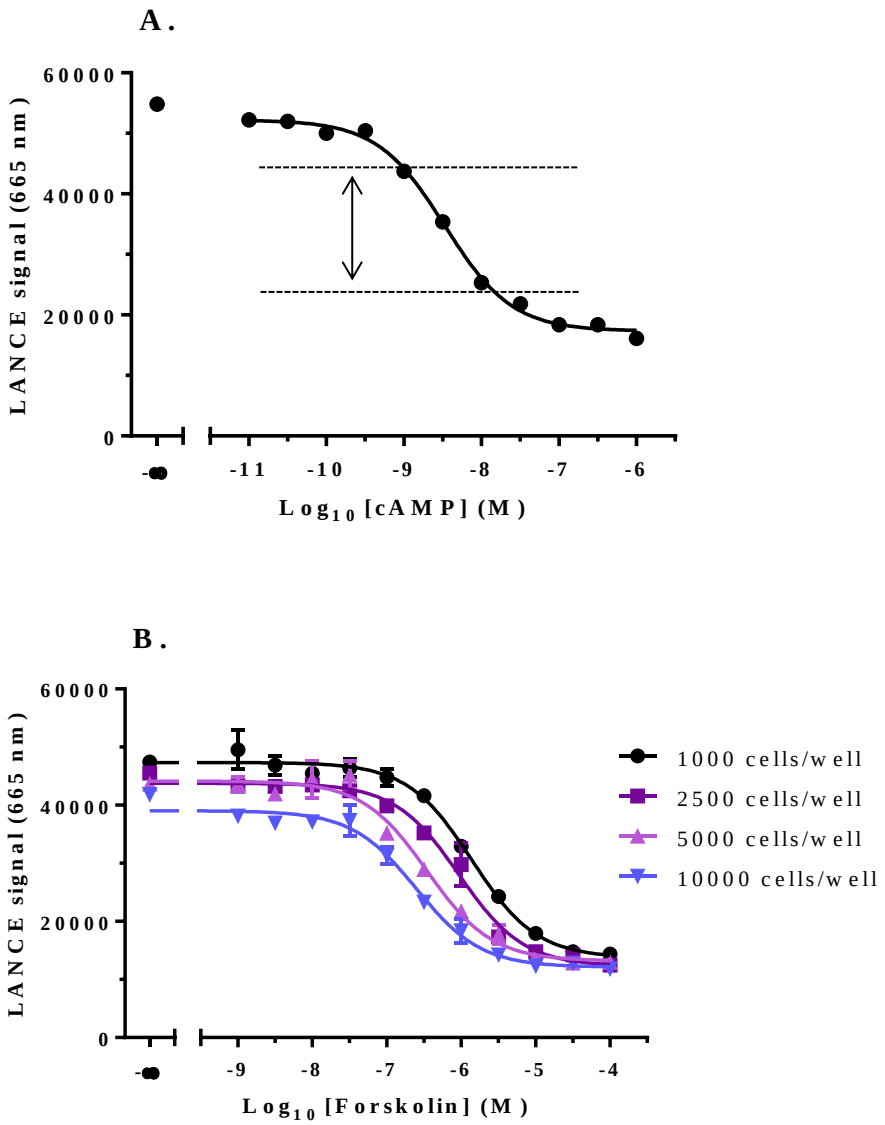

Figure 3.3 Optimisation of cell numbers for subsequent experimentation.

A: Standard curve using a standard known concentration of cAMP in place of cells to gage the ideal assay window as indicated by the arrow. **B**: Forskolin dose-response curve using 1,000 (●), 2,500 (■), 5,000 (▲) and 10,000 (▼) cells per well of FLP-IN HEK-293 cells, stably transfected with a vector (pcDNA5/FRT) containing the hGLP-1R cDNA. The cell number that best fits the standard curve optimal assay window is 10,000 cells per well.

3.4.2. Optimisation of concentration of Pm compounds

Non-transfected FLP-IN HEK cells were stimulated with GLP-1(7-36), Pm 1, Boc 5 and compound A. Conditions were applied to the stable FLP-IN HEK293 cell line as shown in Figure 3.4.B. The non-transfected FLP-IN HEK293 cells did not respond to the ligands as shown in Figure 3.4.A, whereas the cell line expressing hGLP-1R responded as expected

(Figure 3.4.B). These data show the ligands do not activate FLP-IN HEK293 cells unless they have been transfected with pcDNA5/FRT harbouring hGLP-1R cDNA.

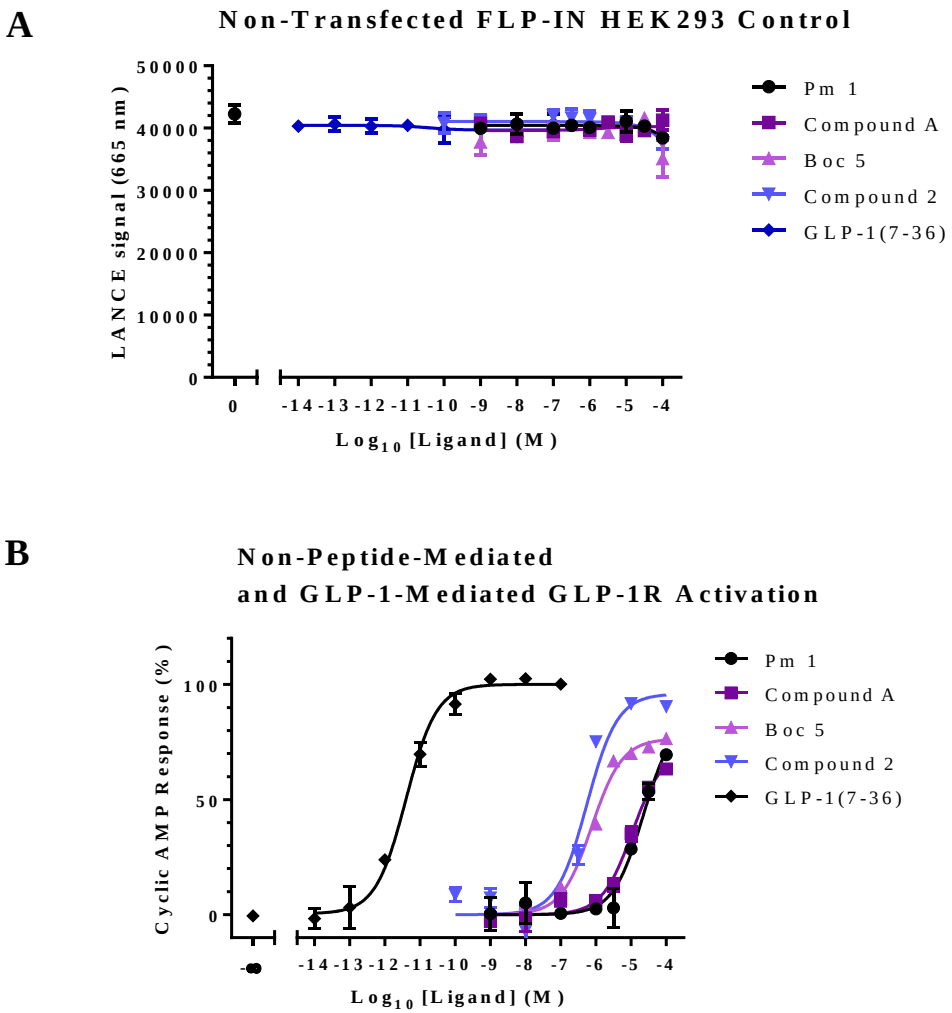

Figure 3.4. The cAMP response of peptide and non-peptide ligands at untransfected and transfected FLP-IN HEK 293 cells constitutively expressing hGLP-1R.

Untransfected **(A)** and transfected **(B)** FLP-IN HEK293 cells constitutively expressing hGLP-1R were stimulated with peptide and non-peptide ligands for 10 minutes. **A.** shows the raw data obtained from stimulation which could not be normalised. Graphs show data from one experiment which is representative of n=3 individual experiments. Data for activity and potency of graph 3.4.B are shown below in Table 3.1.

The initial aim of this study was to assess the ability of the Pm compounds to activate the human GLP-1R, thus their efficacy was studied to assess the most active compound. Primary activity data were collected by using a single concentration of ligand at the most efficacious concentration. To analyse the optimum single concentration of small non-peptide to

be used, hGLP-1R-expressing cells were subjected to cAMP stimulation using a range of non-peptides known to stimulate GLP-1R (compound 2, compound A and Boc5). These compounds were used alongside GLP-1(7-36) to show the difference in potency between peptide and non-peptide ligands. Pm 1 was used to indicate the approximate dose-response range of all Pm compounds by extension, as they are very similar in structure. Figure 3.4 shows the dose-response curve of these compounds at the hGLP-1R, the accompanying pEC_{50} and $\%E_{MAX}$ data are shown in Table 3.1.

	Pm 1	Compound A	Boc 5	Compound 2	GLP-1(7-36)
pEC_{50}	4.7 ± 0.1	4.9 ± 0.04	6.2 ± 0.1	6.2 ± 0.1	10.7 ± 0.6
$\%E_{MAX}$	84.9 ± 2.5	72.2 ± 4.3	80.1 ± 3.7	94.2 ± 1.8	100.0 ± 0.0

Table 3.1. pEC_{50} and $\%E_{MAX}$ of commercially available compounds at hGLP-1R expressing cells.

Values shown represent the average potencies and activities ± S.E.M across n=3 individual experiments. Note that the $\%E_{MAX}$ values obtained from Figure 3.4.B for Pm 1 and compound A are not precise as their dose-response curves do not plateau, therefore the GraphPad Prism 6.0 software extrapolated the $\%E_{MAX}$ values according to the parameters used for non-linear regression calculation.

3.4.3. Pm compound-mediated GLP-1R stimulation

Figure 3.4 showed the most efficacious dose of non-peptide ligand at hGLP-1R expressing cells was 100 μM. This single concentration was applied to a small-scale screening process of the Pm compounds (Figure 3.5) to investigate which Pm compound was most effective at hGLP-1 receptor activation. Figure 3.5.A and B show the activities of those Pm compounds with a benzyl ring modification. Each graph is grouped into compounds with the same functional group in different positions on the benzyl ring. Almost all Pm compounds with a modification to the benzene ring gave a cAMP response comparable with Pm 1, the only exception being Pm 47 which gave a weak response (E_{MAX} = 9.2 %, n=4) with a large S.E.M.

Figure 3.5.C shows the cAMP responses of 100 μM Pm compounds with a TMF group modification (1) or a SD group modification (2). All cAMP responses are shown next to a Pm 1 response to give a reference as to the cAMP response of the starting compound, and to demonstrate how changing the TFM or SD group effects receptor stimulation.

TFM and SD modifications mainly showed a reduced a cAMP response in comparison to those Pm compounds without a modification. The exceptions were: Pm 34 (benzene ring substitution of the TFM group), Pm 62 (chlorine substitution of the TFM group) and Pm 39 (benzene ring addition to the SD group). Pm 34 negatively affected the cAMP production (E_{MAX} = -17.1 % ± 12.5, n=4), Pm 62 however positively affected cAMP production (E_{MAX} = 27.3 % ± 1.1, n=3), and Pm 39 also positively affected cAMP production (E_{MAX} = 68.4 % ± 2.6, n=3). Pm 37 (cyanide replacement of SD) and Pm 38 (azide replacement of SD) were non-responsive at the hGLP-1R expressing cells.

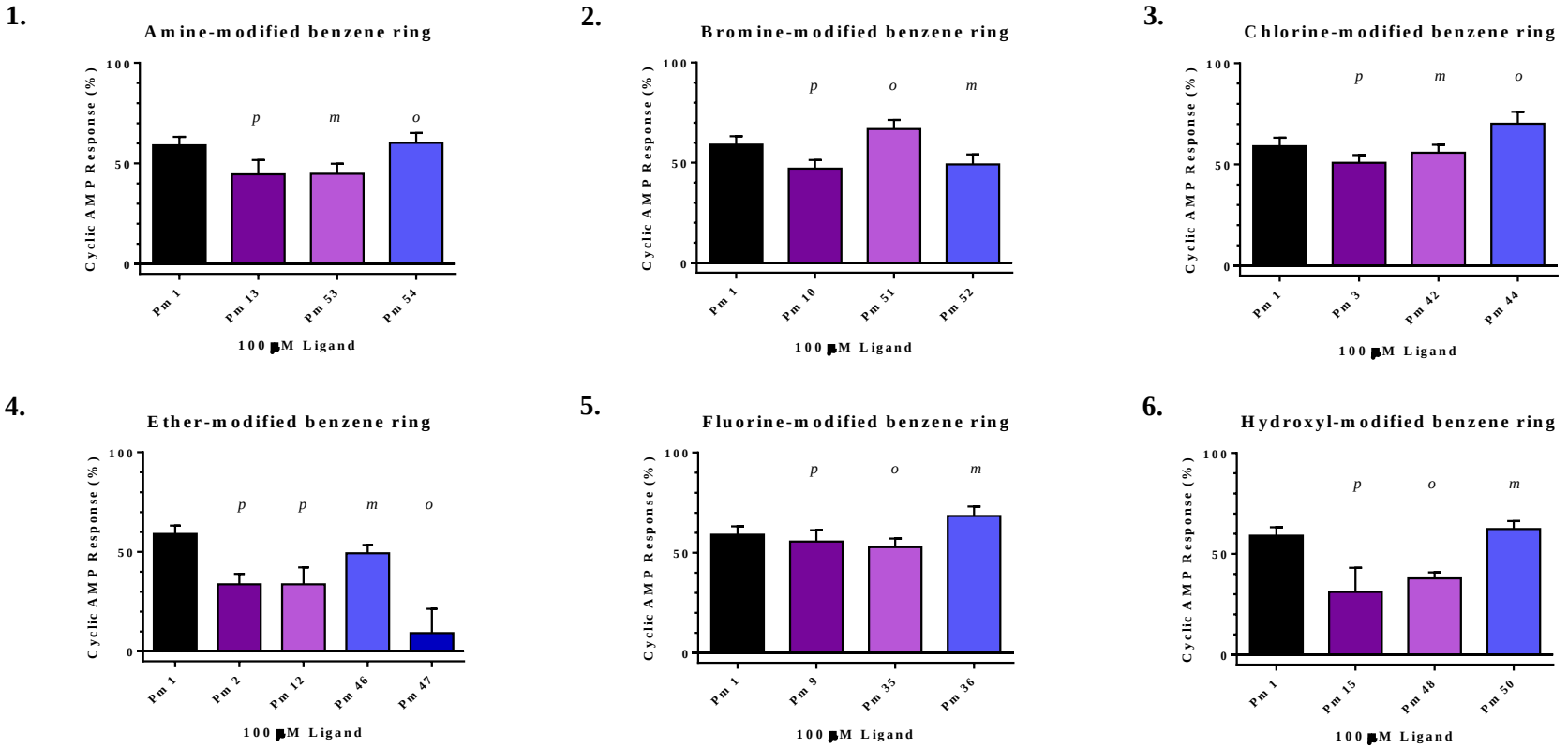

Figure 3.5.A cAMP response of Pm compounds with benzene ring modifications at hGLP-1R-expressing HEK cells.

Compounds are grouped into functional group modification and compared to the response given by Pm1. Each graph shows a particular typeof benzyl ring modification in either the *para* (*p*), *meta* (*m*) or *ortho* (*o*) position. Pm 12 has a benzene ring linked by an ether bond in place of a methyl group linked by an ether bond at the *para* position, hence has been grouped with the ether-modified Pm compounds. Human GLP-1R-expressing HEK 293 cells were sown at a density of 10,000 cells/well and stimulated with 100 μM of compound for 10 minutes. The results are expressed as a percentage of cAMP response of 1 μM GLP-1(7-36)NH_2. The graphs shown are amalgamations of n=3 individual experiments.

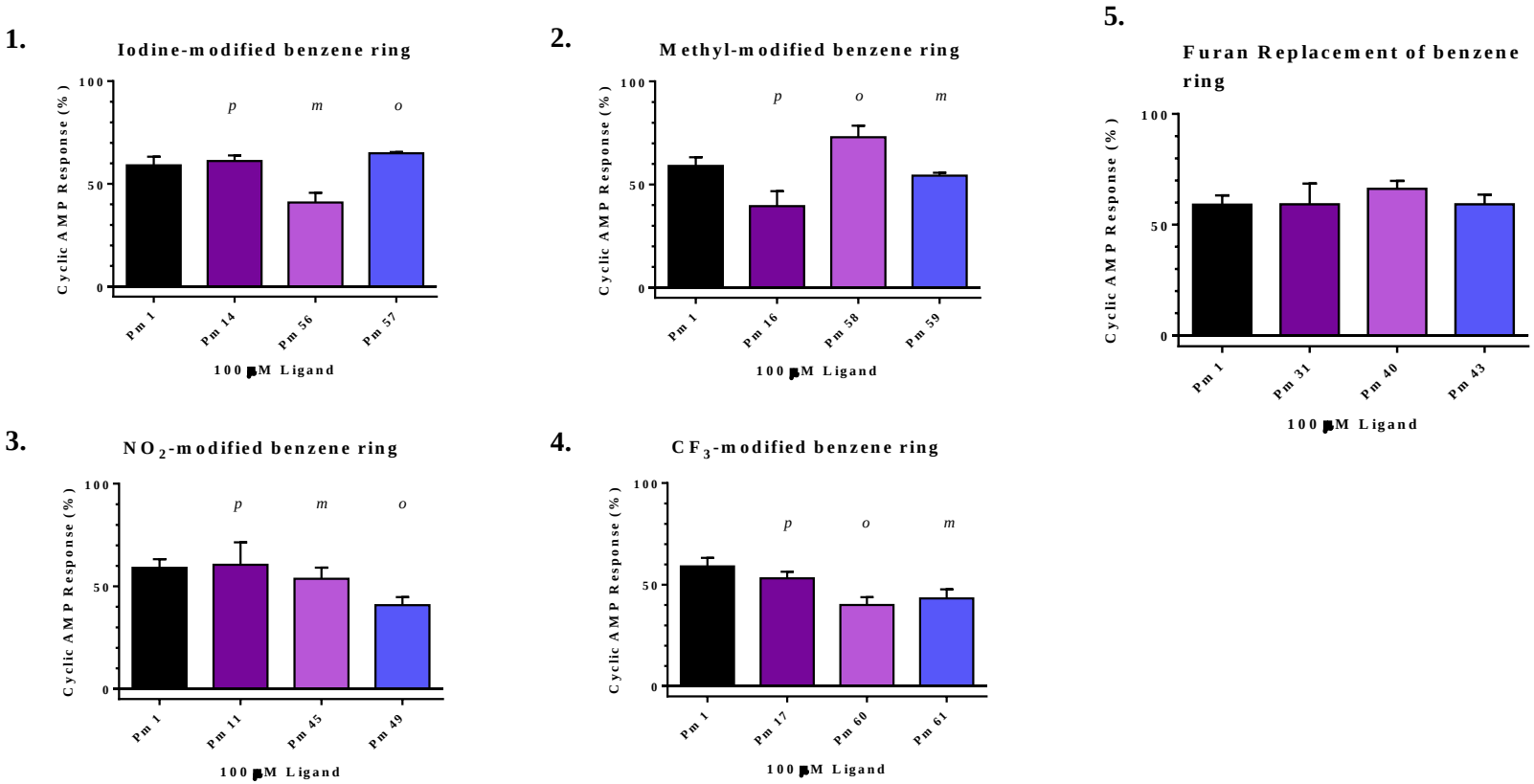

Figure 3.5.B Cyclic AMP response of Pm compounds with benzene ring modifications using 100 μM doses at the human GLP-1R.

Compounds are grouped into functional group modification and compared to the response given by Pm1. Each graph shows a particular typeof benzyl ring modification in either the *para* (*p*), *meta* (*m*) or *ortho* (*o*) position. Human GLP-1R-expressing HEK 293 cells were sown at a density of 10,000 cells/well and stimulated with 100 μM of compound for 10 minutes. The results are expressed as a percentage of cAMP response of 1 μM GLP-1(7-36)NH_2. The graphs shown are amalgamations of n=3 individual experiments.

1.

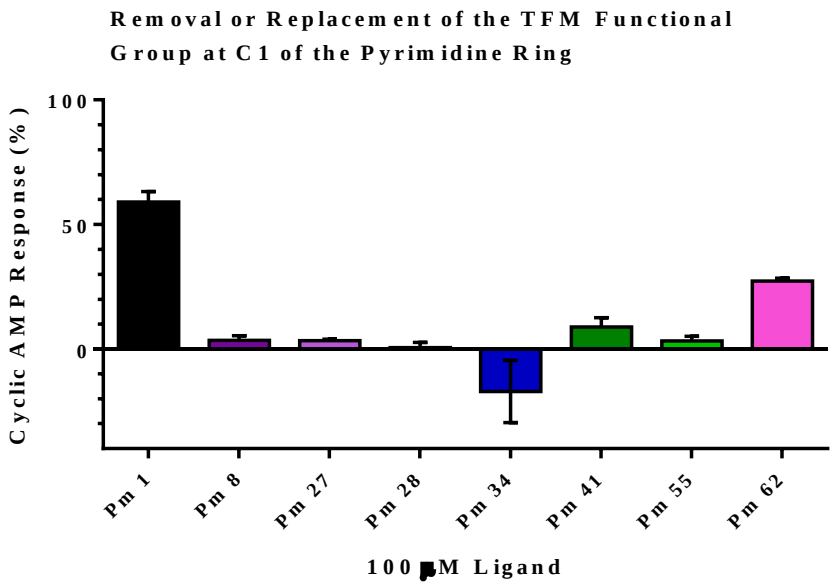

2.

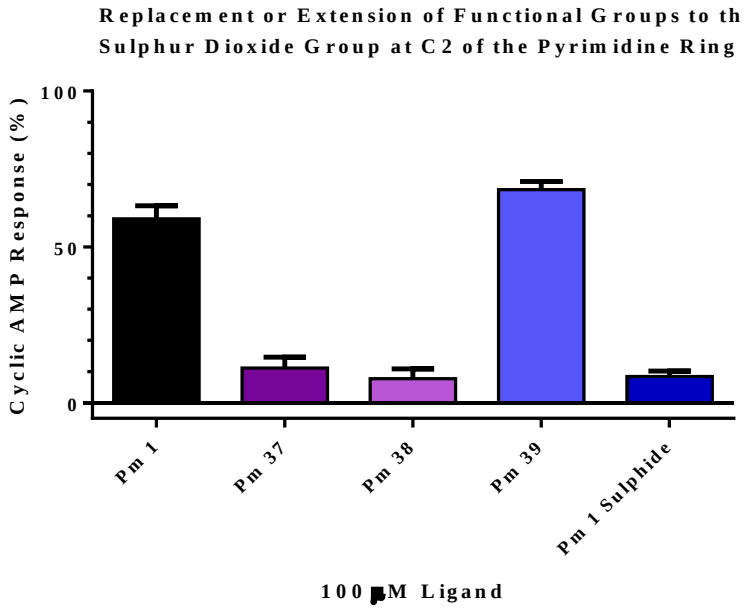

Figure 3.5.C Cyclic AMP response of Pm compounds with trifluoromethyl or sulphur dioxide group modifications using 100 µM doses at hGLP-1R-expressing HEK cells.

Compounds are grouped into functional group modification and compared to the response given by Pm1.**1.** cAMP response of TFM group modified Pm compounds. **2.** cAMP response of SD group modified Pm compounds. Human GLP-1R-expressing HEK 293 cells were sown at a density of 10,000 cells/well and stimulated with 100 µM of compound for 10 minutes. The results are expressed as a percentage of cAMP response of 1 µM GLP-1(7-36)NH_2.The graphs shown are amalgamations of n=3 individual experiments.

Compound	Average ± S.E.M (%)	Compound	Average ± S.E.M (%)
Pm 1	59.0 ± 4.2	**Pm 40**	66.2 ± 3.6
Pm 2	33.7 ± 5.3	Pm 41	8.8 ± 3.8
Pm 3	50.8 ± 3.8	**Pm 42**	55.8 ± 3.9
Pm 8	3.5 ± 1.8	**Pm 43**	59.1 ± 4.4
Pm 9	55.6 ± 5.7	**Pm 44**	70.1 ± 5.9
Pm 10	47.0 ± 4.3	Pm 45	53.7 ± 3.4
Pm 11	60.5 ± 10.9	Pm 46	49.3 ± 4.2
Pm 12	33.7 ± 8.5	Pm 47	9.2 ± 12.2
Pm 13	44.6 ± 7.1	Pm 48	37.8 ± 3.0
Pm 14	61.1 ± 2.7	Pm 49	40.8 ± 3.0
Pm 15	31.1 ± 12.0	**Pm 50**	62.3 ± 4.0
Pm 16	39.5 ± 7.3	**Pm 51**	66.8 ± 4.5
Pm 17	53.1 ± 3.3	Pm 52	49.1 ± 5.0
Pm 27	3.3 ± 0.6	Pm 53	44.8 ± 5.0
Pm 28	0.6 ± 2.0	**Pm 54**	60.2 ± 4.9
Pm 31	59.2 ± 9.3	Pm 55	3.2 ± 1.9
Pm 32	45.1 ± 2.7	Pm 56	40.9 ± 4.7
Pm 33	51.7 ± 7.0	**Pm 57**	64.9 ± 0.6
Pm 34	-17.1 ± 12.5	**Pm 58**	72.9 ± 5.6
Pm 35	52.8 ± 4.3	Pm 59	54.3 ± 1.4
Pm 36	68.4 ± 4.7	Pm 60	40.0 ± 3.9
Pm 37	11.1 ± 3.5	Pm 62	27.3 ± 1.1
Pm 38	7.7 ± 3.2	Pm 1 Sulphide	8.4 ± 1.8
Pm 39	68.4 ± 2.6	Boc 5	74.1 ± 1.6

Table 3.2 Average % E_{MAX} cAMP response of 100 µM compound at human GLP-1R-expressing FLP-IN HEK 293 cells.

Values shown are representative of at least n=3 separate experiments performed in triplicate. Values are expressed as a percentage of the response elicited by 1 µM GLP-1(7-36)NH_2 which was performed alongside each individual experiment (data not shown). The cAMP responses correspond to Figures 3.5.A, B and C. Red highlighting indicates those 15 Pm compounds with the highest cAMP response.

The cAMP responses in Figures 3.5.A, B and C were quantified as a percentage response of 1 µM GLP-1(7-36). Table 3.2 lists the average responses +/- S.E.M elicited by 100 µM of each Pm compound at the human GLP-1R. The 15 most active of the Pm compounds are highlighted in red in Table 3.2. In descending order of efficacy the most active compounds were: Pm 58 (72.9 %), Pm 44 (70.1 %), Pm 39 (68.4 %), Pm 36 (68.4 %), Pm 51 (66.8 %), Pm 40 (66.2%), Pm 57 (64.9 %), Pm 50 (62.3%), Pm 14 (61.1 %), Pm 11 (60.5 %), Pm 54 (60.2 %), Pm 31 (59.2 %), Pm 43 (59.1%), Pm 42 (55.8 %) and Pm 9 (55.6 %). These were then tested in a cell free control for signal quenching. Pm 31, Pm 40 and Pm 43 (furan replacement of the benzene ring at C3 of the pyrimidine ring) all depleted the signal at 665 nm (Figure 3.6) and were not used further since their activity may be artefactual.

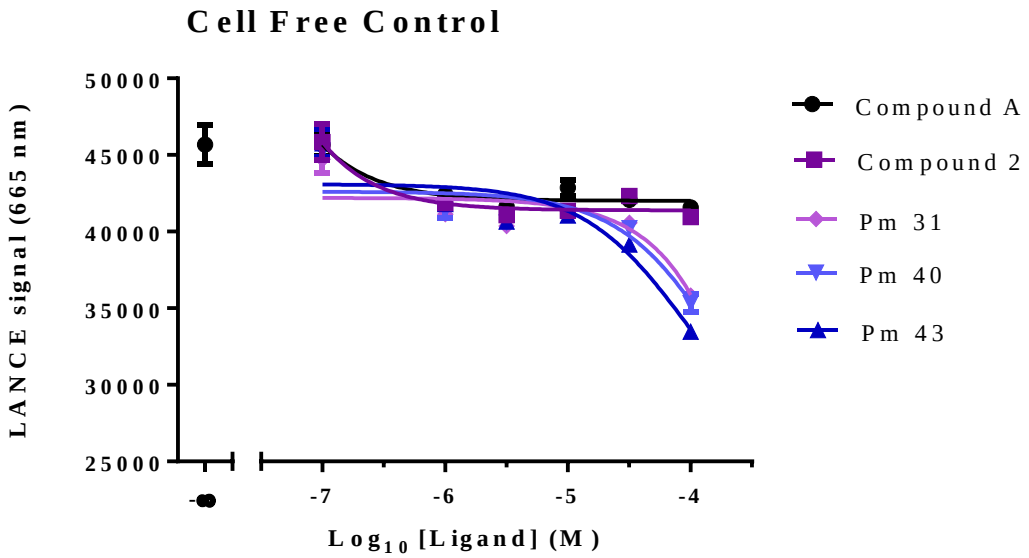

Figure 3.6. Cell free control of emission signal (665nm) depleting Pm compounds 31, 40 and 43 with non-depleting compound 2 and compound A.

Furan replacement of the benzene ring of Pm compounds results in signal depletion at 665 nm in a cell free environment when used in a LANCE™ assay, mimicking cAMP accumulation.

The most active Pm compounds were further analysed for potency by performing a full dose-response curve using a range of concentrations from 100 µM to 1 nM at human GLP-1R expressing cells as shown in Figure 3.7.A and B with the corresponding potency and activity data displayed in Table 3.3.

3.4.4. Analysis of the most efficacious Pm compounds

The dose-response curves of the most efficacious Pm compounds were very similar; hence they are shown in two separate graphs (Figure 3.7.A and B) for ease of analysis. The results were plotted alongside the dose response curve of the full receptor agonist GLP-1(7-36) to demonstrate the fold-change in activities of a peptide agonist *versus* a small non-peptide ligand. The fold change is several orders of magnitude, from an EC_{50} of 16.2 pM for GLP-1(7-36), approximately 15.1 mM for Pm 39, over 9 x 10^6-fold less potent.

Table 3.3 lists the average pEC_{50} and % E_{MAX} +/- S.E.M values of the 13 most active Pm compounds from n=3 separate experiments. The most potent and most efficacious Pm compounds are highlighted in red in Table 3.3. Pm 11 is the most active, achieving almost full activity of the receptor, with an E_{MAX} of 94.5 % it is almost a full ligand, yet it has poor potency. Pm 42 is the most potent ligand with an EC_{50} of 6.5 μM. Pm 42 is almost 4 x 10^5-fold less potent than the full receptor agonist GLP-1(7-36), and with a maximal activity of 55.9 % it is only a partial agonist. However, μM potency is around the values of potency given for small molecule ligands at the GLP-1R in the literature, and in contrast to the other Pm compounds, Pm 42 is the only compound that clearly plateaus to maximal activity as shown in Figure 3.7.B.

The other compounds did not achieve maximal activity using a dose up to 100 μM. A concentration higher than 100 μM cannot be exceeded within a cell-based assay due to the relative concentration of DMSO that would accompany concentrations higher than 100 μM. At a Pm compound concentration of 1 mM, the volume of DMSO would reach 10 % in the assay; DMSO perturbs the cell membranes and dehydrates the cells leading to cytotoxicity (Westh, 2004) therefore accurate cAMP stimulation at 1 mM would be difficult to obtain. The % E_{MAX} values given in Table 3.3 are a result of extrapolation of the curve by GraphPad Prism; therefore they may be unreliable despite strict adherence to equations and algorithms within the software. Due to curve extrapolation for the Pm compounds that did not plateau to obtain %E_{MAX} values, the EC_{50} values are also non-precise as they are by definition reliant on a precise %E_{MAX} value to be calculated with confidence: As Pm 42 was the only compound to produce a dose-response curve with a clear plateau at hGLP-1R expressing cells, Pm 42 was chosen for further experimentation as the dose-response curves are reliable and can be analysed confidently.

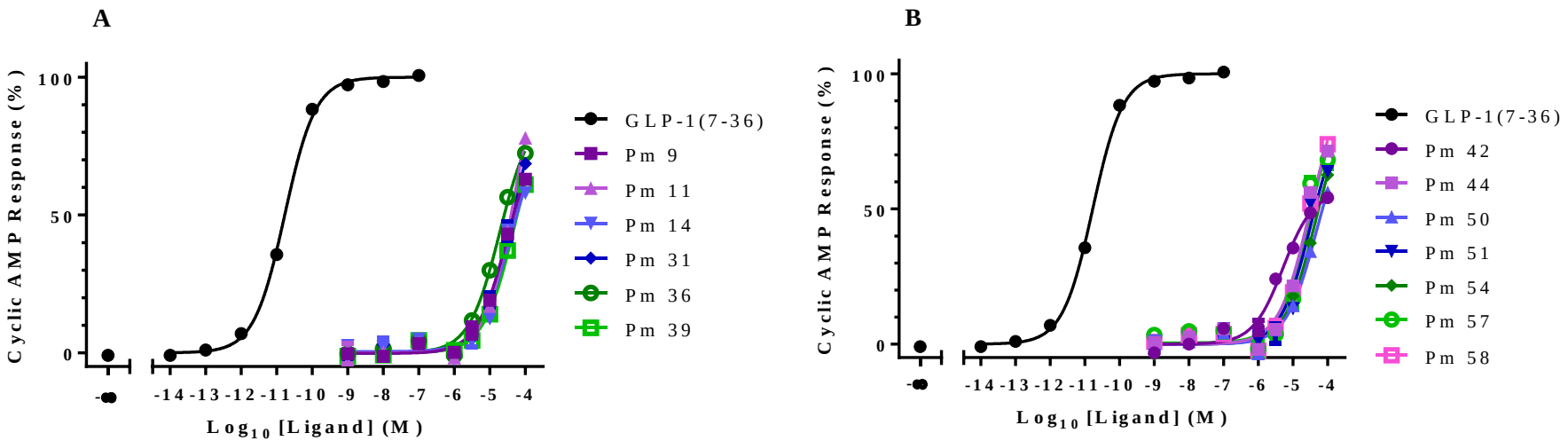

Figure 3.7 Dose-response cAMP accumulation curves of the most efficacious compounds shown alongside full agonist GLP-1(7-36)amide at the human GLP-1 receptor expressed in FLP-IN HEK-293 cells.

A: Pm 9, 11, 14, 31, 36 and 39. **B**: Pm 42, 44, 50, 51, 54, 57 and 58. The compounds selected were based upon the values obtained in Table 3.3. The curves shown are from one individual experiment and are representative of n=3 independent experiments. .

Compound	Average pEC_{50} ± S.E.M	Average % E_{MAX} ± S.E.M
Pm 9	4.42 ± 0.11	76.73 ± 4.91
Pm 11	4.23 ± 0.16	94.48 ± 3.11
Pm 14	4.38 ± 0.09	73.30 ± 3.22
Pm 31	4.38 ± 0.05	84.35 ± 6.52
Pm 36	4.18 ± 0.59	86.34 ± 8.27
Pm 39	3.82 ± 0.47	81.04 ± 5.58
Pm 42	5.19 ± 0.11	55.87 ± 3.08
Pm 44	4.81 ± 0.17	80.09 ± 10.15
Pm 50	4.10 ± 0.17	83.15 ± 6.30
Pm 51	4.56 ± 0.05	71.58 ± 11.25
Pm 54	4.06 ± 0.22	84.01 ± 5.47
Pm 57	4.56 ± 0.13	65.22 ± 6.74
Pm 58	4.60 ± 0.19	88.59 ± 6.16
GLP-1(7-36)	10.79 ± 0.15	100.00 ± 0.00

Table 3.3 Average pEC_{50} and % E_{MAX} values obtained for the most active compounds at the human GLP-1R.

Compound concentrations were assayed from 1 x 10^{-4} to 1 x 10^{-9} M in three separate experiments. Average pEC_{50} and E_{MAX} ± S.E.M are as shown. Pm compound E_{MAX} is expressed as a percentage of the cAMP response elicited by 1 µM GLP-1(7-36)amide which was performed alongside each individual experiment. The most potent compound is Pm 42 and the most active compound is Pm 11 as highlighted in red. The $\%E_{MAX}$ of Pm compounds other than Pm 42 were obtained as a result of extrapolation of the non-plateaued dose-response curves, therefore are not reliable, hence Pm 42 was used for further analysis.

3.4.5. Further analysis of Pm 42

Pm 42 was analysed alongside full agonist GLP-1(7-36)amide, partial agonist GLP-1(9-36)amide and antagonist Ex4(9-39)amide to compare and contrast maximal activity and potency of these ligands. Figure 3.8.A shows the cAMP accumulation profiles of these four ligands at the human GLP-1R, and Table 3.4 shows the relative potencies and activities of those ligands. GLP-1(7-36) gives a full and potent response with an EC_{50} of 16.2 pM. GLP-1(9-36) is much less potent with an EC_{50} of 107 nM and partial agonism (84.2 % activity). Pm 42 is less potent and less active still, with an EC_{50} of 6.5 μM and an E_{MAX} of 55.9 %. Exendin 4(9-39) in incapable of activating the human GLP-1R therefore there are no values available. These data correspond to the activities and potencies listed in the literature (Mann *et al*., 2010a; Li *et al*., 2012) for the human GLP-1R, reinforcing previously published data.

The same ligands were also used in a heterologous competitive binding assay as shown in Figure 3.8.B against the radioligand ^{125}I-GLP-1(7-36)NH_2 to investigate the affinity of Pm 42 for the human GLP-1R. This was performed to analyse the relationship of affinity to activity in the context of the non-peptide ligand, and to further characterise the receptor as GLP-1R. The pIC$_{50}$ values for the ligands are displayed alongside the pEC$_{50}$ and %E$_{MAX}$ data in Table 3.4. The peptide ligands all competed for binding at the GLP-1R at the orthosteric site, as exemplified by the decrease of specific binding of ^{125}I-GLP-1(7-36)NH_2 as competing ligand concentration was increased. Table 3.4 showed GLP-1(7-36) had a pIC$_{50}$ of 9.2, GLP-1(9-36) had a pIC$_{50}$ of 7.1 and Ex4(9-39) had a pIC$_{50}$ of 8.2, these values correspond to previously published data (Mann *et al*., 2010a). Pm 42 however cannot compete against ^{125}I-GLP-1(7-36)NH_2 for binding at the receptor, therefore no data were obtained for Pm 42 affinity. These data suggest that Pm 42 does not bind at the orthosteric binding site and binds elsewhere to activate the receptor, at a so-called allosteric or exosite.

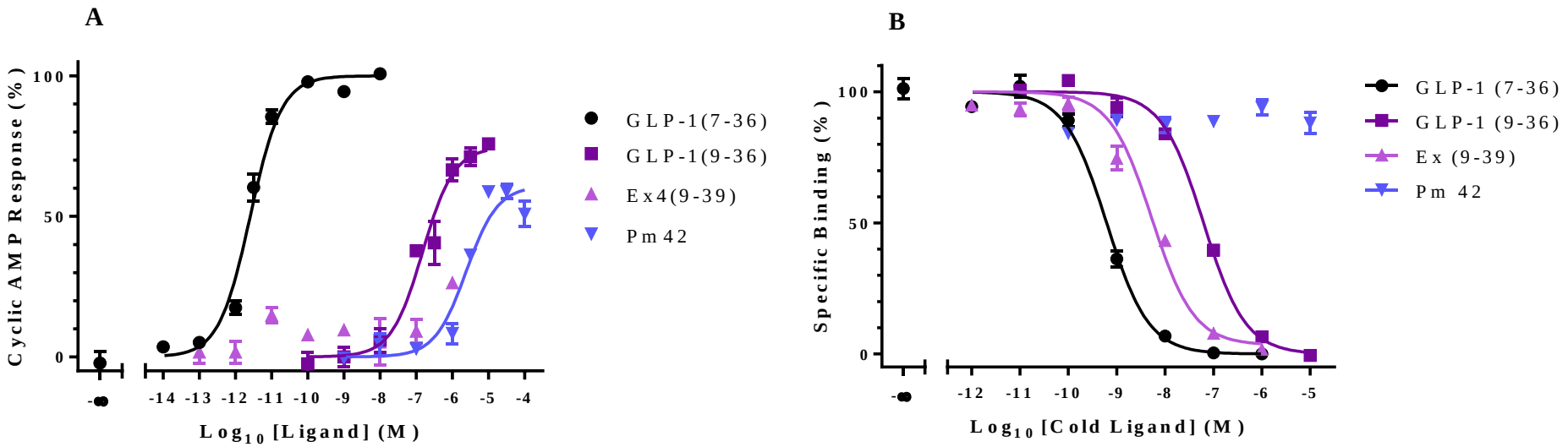

Figure 3.8. Intracellular cAMP accumulation and affinity profile of ligands at human GLP-1R-expressing FlpIn-HEK 293 cells.

A: cAMP activation profile of hGLP-1R. [pEC_{50} and % E_{MAX} +/- S.E.M] values from n=3 experiments are as follows: (●) GLP-1(7-36) [10.79 ± 0.15, 100.0 % ± 0.0]; (■) GLP-1(9-36) [6.97 ± 0.09, 84.17 % ± 2.2]; (▲) exendin-4(9-39) [N/A, N/A]; (▼) Pm 42[5.19 ± 0.11, 55.87 % ± 3.08]. **B** Affinity profile of hGLP-1R, [pIC_{50}] values from n=3 experiments are as follows: (●) GLP-1(7-36) [9.24 ± 0.12]; (■) GLP-1(9-36) [7.08 ± 0.04]; (▲) exendin-4(9-39) [8.15 ± 0.01]; (▼) Pm 42 N/A.

	pIC_{50}	pEC_{50}	% E_{MAX}
GLP-1(7-36)	9.24 ± 0.12	10.79 ± 0.15	100
GLP-1(9-36)	7.08 ± 0.04	6.97 ± 0.09	84.17 ± 2.20
Ex4(9-39)	8.15 ± 0.01	ND	ND
Pm42	ND	5.19 ± 0.11	55.87 ± 3.08

Table 3.4 Binding and activation properties of the ligands depicted in Figure 3.8, at the human GLP-1 receptor expressed in FLP-IN HEK-293 cells.

Values represent mean pIC_{50}, pEC_{50} and $\%E_{MAX}$ values ± S.E.M. for three independent experiments performed in triplicate. % E_{MAX} is relative to the maximal signal produced by GLP-1(7-36). ND means that no value could be determined.

The hypothesis that Pm 42 binds allosterically to the GLP-1R was explored further in the next section by using dual-activity and antagonist-competition assays in the following section.

3.4.6. Pm 42 acts allosterically at the hGLP-1R

To strengthen the hypothesis that Pm 42 is unable to bind at the orthosteric site an antagonist competition curve was performed using the antagonist Ex4(9-39) in a cAMP accumulation assay. Ex4(9-39) is capable of binding at the orthosteric site (Figure 3.8.B) with nM affinity (Table 3.4) but is unable to activate the receptor (Figure 3.8.A). Figure 3.9.A shows an antagonist competition curve between GLP-1(7-36) and Ex4(9-39). GLP-1(7-36) can clearly overcome the antagonistic effects of Ex4(9-39) as the agonist dose-response curve is capable of reaching maximal stimulation in the presence of antagonist (Table 3.5). In the presence of higher Ex4(9-39) concentration the GLP-1(7-36) dose-response curve shifts to the right, lowering GLP-1(7-36) potency (Table 3.5) yet maximal stimulation is always achieved. This reinforces previous claims that Ex4(9-39) is a competitive antagonist as the non-stimulatory effects are reversible by adding more agonist.

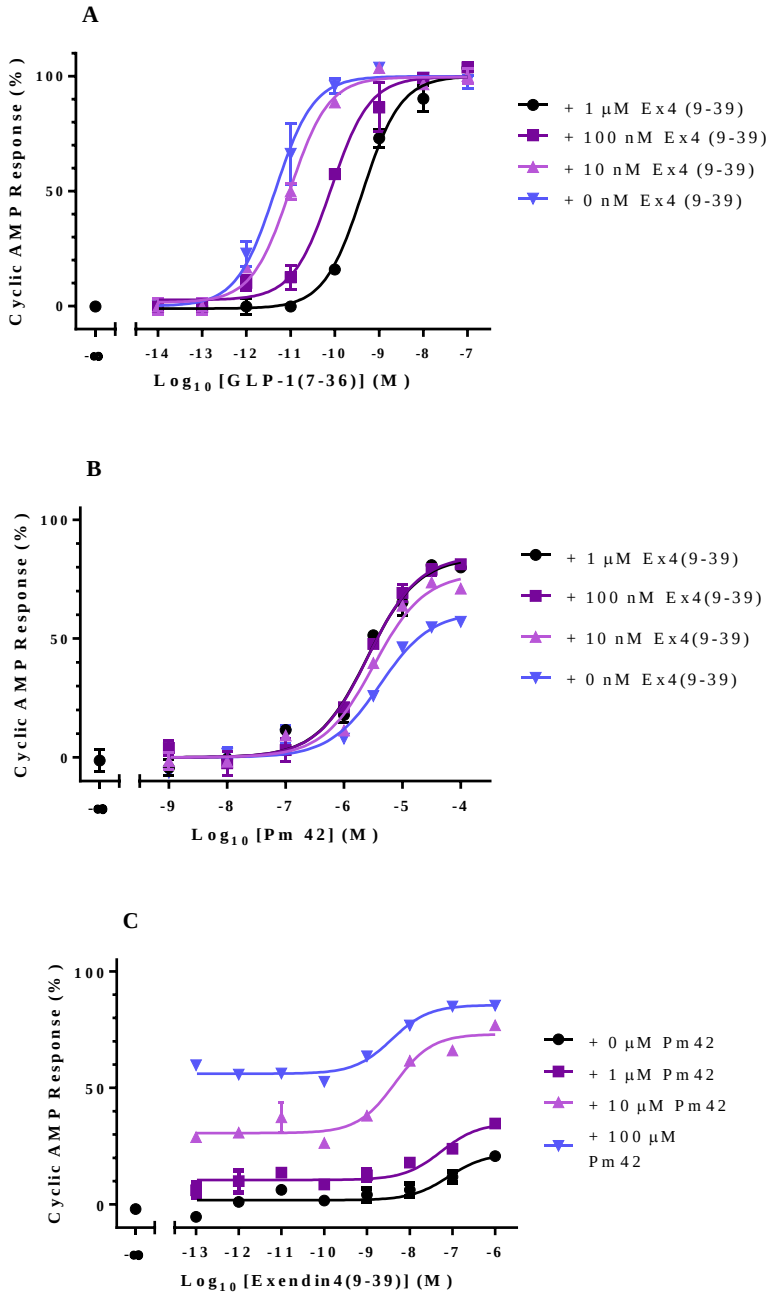

Figure 3.9 Exendin 4(9-39) antagonist competition assays at hGLP-1R-expressing FLP-IN HEK 293 cells.

A. GLP-1(7-36) dose-response curves in the presence of increasing concentrations of antagonist exendin 4(9-39). **B**. Pm 42 dose-response curves in the presence of increasing concentrations of exendin 4(9-39). **C**. Exendin 4(9-39) dose response curves in the presence of increasing concentrations of the non-peptide partial agonist Pm 42. Graphs are representative of n=3 individual experiments performed in triplicate.

Corresponding potency and efficacy values are shown in Table 3.5 for A, Table 3.6 for B, and Table 3.7 for graph C.

[Ex4(9-39)]	0 nM	10 nM	100 nM	1 μM
***p*EC$_{50}$ GLP-1(7-36)**	10.79 ± 0.15	10.38 ± 0.74	9.76 ± 0.70	8.88 ± 0.72

Table 3.5 *p*EC$_{50}$ +/- S.E.M of GLP-1(7-36) at the hGLP-1R in the presence of Ex4(9-39) at 4 concentrations as shown.

Human GLP-1R expressing FLP-IN HEK 293 cells were pre-stimulated with the concentration of Ex4(9-39) denoted in the grey boxes of the table before being stimulated for 10 mintues with GLP-1(7-36) to give agonist dose response curves in the presence of four antagonist concentrations. Increased antagonist concentrations decreases the *p*EC$_{50}$, shifting the dose-response curve to the right. E$_{MAX}$ always achieved 100 %.

The antagonist competition curve from Figure 3.9.A was replicated using Pm 42 in place of GLP-1(7-36); the results are shown in Figure 3.9.B. The Pm 42 dose-response curve shifted upwards when exposed to increasing concentrations of Ex4(9-39) (Figure 3.9.B) from approximately 61 % maximal activity to 85 % in the presence of 1 μM Ex4(9-39). Additionally the potency of the Pm 42 dose-response curve increases in a dose-dependent manner upon addition of antagonist, from an EC$_{50}$ of 4.2 μM alone, to 2.5 μM in the presence of 1 μM antagonist (Table 3.6).

[Ex-4(9-39)]	0 nM	10 nM	100 nM	1 μM
***p*EC$_{50}$**	5.38 ± 0.10	5.49 ± 0.08	5.59 ± 0.13	5.60 ± 0.12
%E$_{MAX}$	61.28 ± 5.55	77.47 ± 3.72	84.20 ± 2.49	85.02 ± 2.31

Table 3.6. *p*EC$_{50}$ and % E$_{MAX}$ +/- S.E.M of Pm 42 at the hGLP-1R in the presence of 4 concentrations of Ex4(9-39).

Human GLP-1R expressing FLP-IN HEK 293 cells were pre-stimulated with the concentration of Ex4(9-39) denoted in the grey boxes of the table before being stimulated for 10 minutes with Pm 42 to give agonist dose response curves (Figure 3.9.B) in the presence of four antagonist concentrations. An increased antagonist concentration increases both the *p*EC$_{50}$ and % E$_{MAX}$ of the Pm 42 dose-response curve. Data derived from n=3 independent experiments.

To further elucidate the unexpected observation of an antagonist seemingly making the receptor more active, the antagonist competition assay was duplicated again using Pm 42 and Ex4(9-39), but with a dose-response curve of Ex4(9-39) performed in the presence of increasing concentrations of Pm 42; the resultant dose-response curve is shown in Figure 3.9.C, and Table 3.7 shows the *p*EC$_{50}$, % E$_{MAX}$ and % Span of the curves. The % Span gives an indication of the

effect of Ex4(9-39) in the presence of Pm 42. Under increasing concentrations of Pm 42, the basal level of cAMP production increases. As the concentration of Pm 42 remains constant, the EC_{50} shown in the graph and the pEC_{50} given in the table is the resultant effect of increased Ex4(9-39) concentrations, indicating Ex4(9-39) has the propensity to act as an agonist in the presence of non-peptide ligand Pm 42. The pEC_{50} values elicited by Ex4(9-39) in the presence of Pm 42 (Table 3.7) closely resemble the pIC_{50} values of Ex4(9-39) (pIC_{50} = 8.15 ± 0.01) (Table 3.4) further suggesting the antagonist acts as an agonist with nM potency in the presence of Pm 42. More intriguing is that as the concentration of Pm 42 is increased, the apparent extra response invoked by the antagonist becomes more potent. An example of this is evident in Table 3.7, the EC_{50} of exendin 4(9-39) in the presence of 1 μM Pm 42 is 29.5 nM, whereas in the presence of 100 μM Pm 42, the EC_{50} of exendin-4(9-39) is 2.7 nM; over a ten-fold increase in potency.

	0 μM Pm 42	**1 μM Pm 42**	**10 μM Pm 42**	**100 μM Pm 42**
***p*EC$_{50}$**	5.28 ± 1.71	7.53 ± 0.38	8.49 ± 0.16	8.57 ± 0.12
%E$_{MAX}$	19.88 ± 1.03	30.74 ± 2.41	76.97 ± 2.11	86.36 ± 0.47
% Span	17.73 ± 1.81	22.21 ± 1.11	37.65 ± 2.41	29.44 ± 1.49

Table 3.7. *p*EC$_{50}$, % E$_{MAX}$ and % Span +/- S.E.M of Ex4(9-39) at the hGLP-1R in the presence of 4 concentrations of Pm 42.

Human GLP-1R expressing FLP-IN HEK 293 cells were pre-stimulated with Ex4(9-39) for 10 minutes, and then stimulated for a further 10 minutes with Pm 42 to give an antagonist dose response curves (Figure 3.9 C). % Span takes into consideration the basal cAMP level in the presence of active concentrations of Pm 42, giving a true estimation to the influence of the antagonist in human GLP-1R stimulation in the presence of Pm 42.

3.4.7 Pm 42 Allosterically modulates GLP-1(9-36) activity

The allosteric interaction between Pm 42 and Ex4(9-39), which is the N-terminally truncated analogue of Ex4(1-39), prompted the investigation of the potential for this non-peptidic compound to allosterically modulate the N-terminally truncated metabolite GLP-1(9-36)amide. In addition, GLP-1(15-36)amide which possesses the equivalent level of N-terminal truncation of GLP-1(7-36) relative to Ex4(9-39) with a 9 amino acid depletion from the amino terminus, was studied, in addition to the full length peptide GLP-1(7-36) amide. Graphical

representation from n=3 experiments for each peptide are shown in Figure 3.10 and corresponding pEC_{50}, %Span and $\%E_{MAX}$ values are listed in Table 3.8.

The average pEC_{50} for GLP-1(7-36) alone was 10.88 ± 0.09, whilst in the presence of 100 μM Pm 42 it was 10.78 ± 0.14 (Figure 3.10.A, Table 3.8.i.), therefore Pm 42 had no additional effect on GLP-1(7-36) potency. Mean pEC_{50} values for GLP-1(15-36) alone was 6.51 ± 0.10, whilst co-administered with 100 μM Pm 42 it was 6.69 ± 0.18 (Table 3.8.iii.), again Pm 42 had no additional effect upon GLP-1(15-36) potency. GLP-1(15-36)-induced activity was increased in a dose-dependent manner; % E_{MAX} for GLP-1(15-36) alone was 81.02 ± 3.03, whilst in the presence of 100 μM Pm 42 this increased to 91.78 ± 2.87 %. The %Span explains this phenomenon however, as the starting cAMP levels (under non-responsive GLP-1(15-36) concentrations of between 1-10 nM (Figure 3.10.C)) with increasing Pm 42 concentration increase respectively, thus the %Span achieved actually decreases with increased Pm 42 administration, resulting in %Span values of 44.65 ± 10.05, 52.36 ± 2.70, 69.30 ± 5.13, and 78.41 ± 2.28 in the presence of 100 μM, 10 μM, 1 μM and 0 μM Pm 42 respectively. However, GLP-1(9-36) displayed allosteric modulation by Pm42. Mean pEC_{50} values from three independent experiments represented by Figure 3.10.B were: GLP-1(9-36) alone, 6.67 ± 0.06; with 1 μM Pm42, 7.18 ± 0.12; with 10 μM Pm42, 8.05 ± 0.08; with 100 μM Pm42, 8.35 ± 0.05. Therefore, while Pm42 had no effect on the potency of GLP-1(7-36)NH_2 or GLP-1(15-36)NH_2 (Figures 3.10.A and 3.10.C), at concentrations of Pm42 above 1 μM, GLP-1(9-36)NH_2 displayed a left-shifted concentration-response curve and an increased $\%E_{MAX}$ (Table 3.8.ii), from a partial agonist 83.33 ± 2.88 % activity, to fully active in the presence of 10 μM Pm 42.

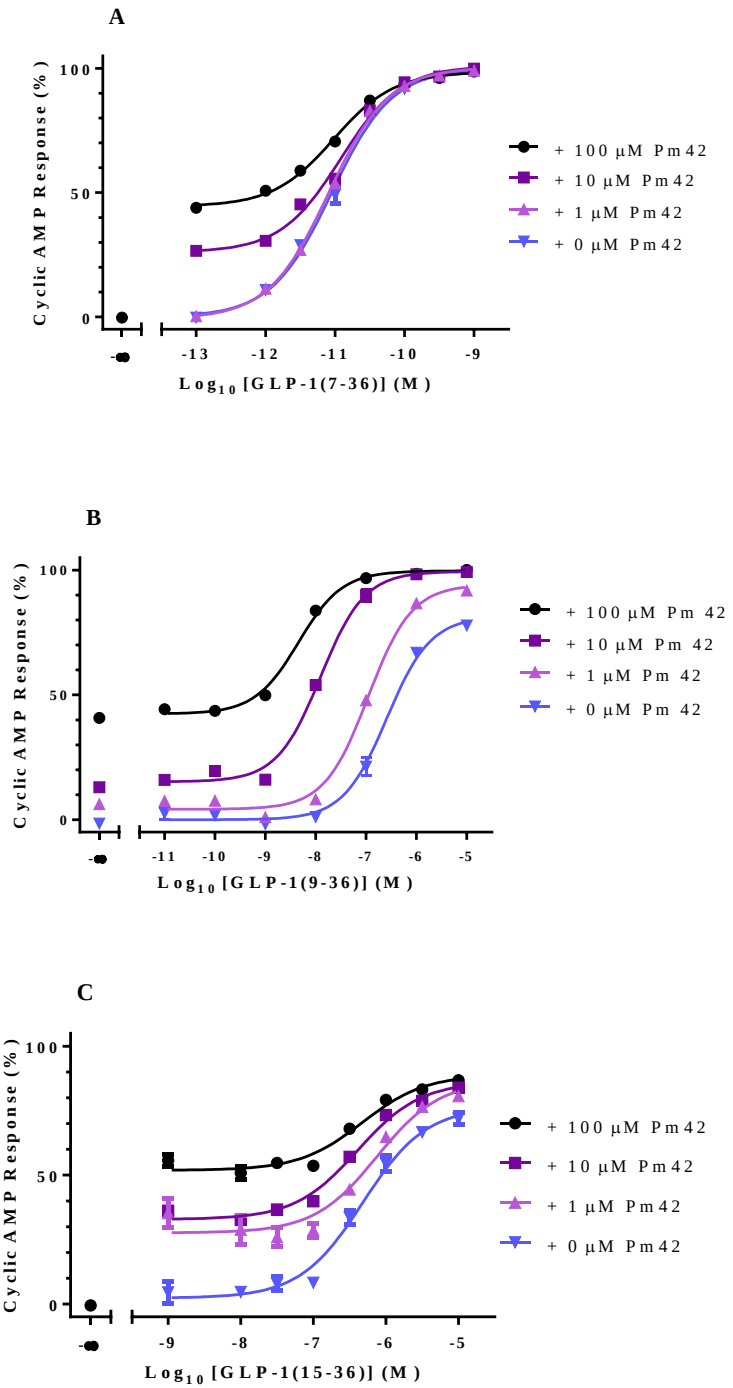

Figure 3.10 Dual activation assays at the hGLP-1R.

Dose-response curves of (**A**) GLP-1(7-36), (**B**) GLP-1(9-36), (**C**) GLP-1(15-36) in the presence of 0 µM (▼), 1 µM (▲), 10 µM (■) and 100 µM (●) Pm 42 at human GLP-1R expressing FLP-IN HEK 293 cells. Cells were co-stimulated for 10 minutes using peptide and non-peptide ligands. % E_{MAX} values are expressed as a percentage of the response elicited by 1 µM GLP-1(7-36)NH_2 which was performed alongside each individual experiment.

Table 3.8.i.

GLP-1(7-36)	0 μM Pm42	100 μM Pm42	10 μM Pm42	1 μM Pm42
***p*EC$_{50}$**	10.88 ± 0.09	10.78 ± 0.14	10.79 ± 0.07	10.89 ± 0.11
%E$_{MAX}$	100.0 ± 0.0	98.89 ± 0.18	101.17 ± 0.29	100.62 ± 0.48
%Span	100.0 ± 0.0	57.19 ± 3.07	82.45 ± 4.04	101.07 ± 0.30

Table 3.8.ii.

GLP-1(9-36)	0 μM Pm 42	100 μM Pm 42	10 μM Pm 42	1 μM Pm 42
***p*EC$_{50}$**	6.67 ± 0.06	8.35 ± 0.05	8.05 ± 0.08	7.18 ± 0.12
%E$_{MAX}$	83.33 ± 2.88	100.08 ± 0.27	100.32 ± 0.54	98.10 ± 2.19
%Span	84.71 ± 1.48	57.23 ± 2.02	76.41 ± 6.27	96.74 ± 1.63

Table 3.8.iii.

GLP-1(15-36)	0 μM Pm 42	100 μM Pm 42	10 μM Pm 42	1 μM Pm 42
***p*EC$_{50}$**	6.51 ± 0.10	6.69 ± 0.18	6.53 ± 0.24	6.30 ± 0.13
%E$_{MAX}$	81.02 ± 3.03	91.78 ± 2.87	88.48 ± 2.91	88.35 ± 1.10
%Span	78.41 ± 2.28	44.65 ± 10.05	52.36 ± 2.70	69.30 ± 5.13

Table 3.8 *p*EC$_{50}$, % E$_{MAX}$ and % Span +/- S.E.M of GLP-1(7-36)NH$_2$ (i), GLP-1(9-36)NH$_2$ (ii) and GLP-1(15-36)NH$_2$ (iii) at hGLP-1R expressing FLP-1IN HEK 293 cells alone and co-administered with 1 μM, 10 μM and 100 μM of Pm 42.

% Span takes into consideration the base line cAMP level in the presence of active concentrations of Pm 42, giving a true estimation to the influence of the peptide agonist in human GLP-1R stimulation in the presence of a non-peptidic compound

3.4.8. Pm 42 allosterically enhances insulin secretion in INS-1 832/13 cells

The allosteric effects of Pm 42 upon the truncated metabolite GLP-1(9-36) were further examined by monitoring the insulin-releasing effects of these two ligands used alone or in concert at INS-1 832/13 cells. The allosteric effects of Pm 42-mediated cAMP release in the presence of GLP-1(9-36) prompted investigation of the level of cooperativity at more

physiological levels of GLP-1R expression, the hypothesis being Pm 42 may be able to potentiate insulin secretion. This hypothesis is based on literature claiming GLP-1R activation potentiates the titre of insulin release via activation of the cAMP pathway, and Pm 42 enhances cAMP production at recombinant cells over expressing the human GLP-1R when in the presence of GLP-1(9-36).

Following a low glucose episode (3 mM) lasting 3 hours at 37°C, INS-1 832/13 cells were stimulated for 2 hours under high glucose conditions (16.7 mM glucose) in the presence of the secretagogue GLP-1(7-36), and a combination of concentrations of GLP-1R agonists GLP-1(9-36) and Pm 42. Graphical representation from n=3 independent experiments is shown in Figure 3.11 with complementary mean +/- S.E.M data of insulin release in Table 3.9.

In the presence of 16.7 mM glucose, 1 μM GLP-1(7-36)NH_2 resulted in a significant ($P < 0.01$, n=3) potentiation of insulin secretion in keeping with the known properties of this incretin hormone. However, whilst 10 μM Pm 42 alone did not result in any significant increase in insulin secretion, when applied in conjunction with GLP-1(9-36)amide it was able to enhance the activity of this natural metabolite to levels comparable with GLP-1(7-36)amide ($p < 0.05$ at 0.1 μM and 5 μM GLP-1(9-36) and $p < 0.01$ for 1 μM GLP-1(9-36)) (Figure 3.11).

Pm 42 was incapable of further significant insulin secretion over 16.7 mM glucose alone (10 μM Pm 42: 53.95 ± 4.74 *versus* glucose alone: 43.40 ± 11.35 μLU/0.5mL). Similarly, concentrations of 0.1 μM and 1 μM GLP-1(9-36) were incapable of stimulating insulin secretion to a significant level above glucose alone (39.99 ± 3.13 and 48.04 ± 2.20 μLU/0.5mL insulin secretion respectively). However, when 10 μM Pm 42 was administered simultaneously with 1 μM GLP-1(9-36) the two ligands interacted to enhance insulin secretion to levels comparable with the natural intact secretagogue GLP-1(7-36) (78.96 ± 6.04 (1 μM GLP-1(9-36) + 10 μM Pm 42) *versus* 86.15 ± 11.34 (GLP-1(7-36)) μLU/0.5mL insulin respectively). When 10 μM Pm 42 was administered alongside 5 μM GLP-1(9-36) the level of insulin secretion exceeded that given by 1 μM GLP-1(7-36) as shown in Table 3.9 (109.25 ± 11.45 μLU/0.5mL c.f. 86.15 ± 11.34 μLU/0.5mL insulin respectively).

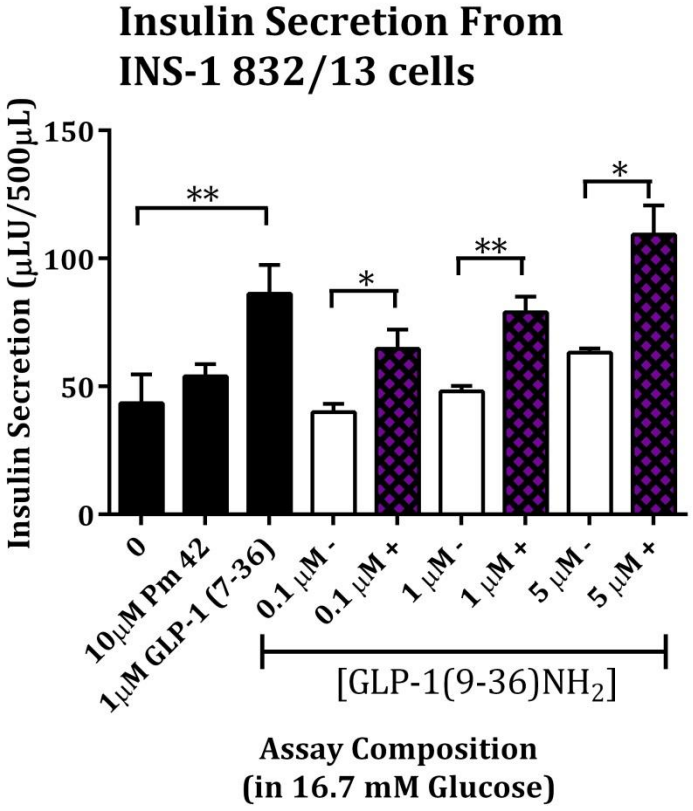

Figure 3.11 Insulin secretion at INS-1 832/13 cells under high glucose conditions in the presence of secretagogues.

INS-1 832/13 cells were stimulated for 2 hours in the presence of 16.7 mM glucose and the secretagogues denoted along the x axis. White bars represent GLP-1(9-36) in the absence (-) of 10 μM Pm 42, purple bars with black hatching represent GLP-1(9-36) in the presence (+) of 10 μM Pm 42. Bar chart shows the average data collected from n=3 independent experiments, error bars denote the standard error of the mean. Student's t-test results confirm statistical significance: *$p<0.05$, **$p<0.01$.

A

[GLP-1(9-36)]	Insulin response (µLU/0.5mL)	
	Peptide Only	Peptide + 10 µM Pm 42
0.1 µM	39.99 ± 3.13	64.63 ± 7.55
1.0 µM	48.04 ± 2.20	78.96 ± 6.04
5.0 µM	63.24 ± 1.62	109.25 ± 11.45

B

Ligand	Insulin response (µLU/ 0.5mL)
None	43.40 ± 11.35
10 µM Pm 42	53.95 ± 4.74
1 µM GLP-1(7-36)	86.15 ± 11.34

Table 3.9. Mean insulin secretion responses of GLP-1R agonists: GLP-1(7-36), GLP-1(9-36), Pm 42, and a combination thereof at INS-1 832/13 cells performed in the presence of 16.7 mM glucose.

A. The insulin response of INS-1 832/13 cells when stimulated using various GLP-1(9-36) in the presence and absence of 10 µM Pm 42. **B.** Insulin secretion responses of the controls.

Data are complementary to Figure 3.11. Data show the mean insulin secretion responses +/- S.E.M for n=3 independent experiments. The pEC_{50} of Pm 42 in a cAMP dose-response curve is approximately 5.2, therefore 10 µM was chosen as the dosage to use. Similarly, a 1 µM dose of GLP-1(7-36) achieves 100 % maximal stimulation of the GLP-1R in cyclic AMP assays.

3.4.9. GLP-1R modulation of the Pm compound library by cAMP analysis

As Pm 42 showed cooperativity in the presence of truncated peptides Ex4(9-39) and GLP-1(9-36) at GLP-1R, it was hypothesised that there may be a correlation in the Pm library of compounds between functional group modification and cooperativity with Ex4(9-39) and GLP-1(9-36) at GLP-1R. In order to efficiently screen the other Pm compounds for their ability to enhance the activity of truncated peptide ligands at the human GLP-1R, a miniature screen was devised, herein referred to as the 'miniscreen'.

The miniscreen was designed to monitor the most informative points of a cAMP dose-response curve (as circled in Figure 3.12.A) by incubating recombinant human GLP-1R-expressing FlpIn-HEK 293 cells in the presence of only those concentrations and combinations of ligand/s that would yield those most informative points. For example, the truncated metabolite GLP-1(9-36) alone at a concentration of 10 nM in a cAMP dose-response curve at the human GLP-1R resides at the cusp of the curve, just before this partial agonist begins to take

effect, essentially giving a cAMP response of approximately 0 %. However, in the presence of 100 μM Pm 42, the same GLP-1(9-36) concentration (10 nM) gave a cAMP response of approximately 85 % (Figure 3.12.A). Of course, 100 μM Pm 42 gave a cAMP response when administered alone of approximately 56 % (Table 3.3) of that of 1 μM GLP-1(7-36) (100 % cAMP response), however, if there were no allosteric cooperative modulation of the receptor, then it would be expected that the co-stimulation of a peptide ligand concentration that gave a 0 % cAMP response alongside a ligand that gave a 56 % cAMP response would give 56 % cAMP production-simple addition. However if there were a positive cooperative allosteric relationship between the non-peptidic ligand and the truncated peptide ligand at the GLP-1R, then the cAMP response would increase. Therefore by comparing the expected null hypothesis of no cooperativity between the ligands with the observable experimental evidence upon co-stimulation of the receptor, it is possible to characterise a small molecular ligand as having allosteric properties, or not, by observing just these three basic points derived from a dose-response curve: 100 μM Pm compound alone, 10 nM GLP-1(9-36) alone, and finally 100 μM Pm compound co-administered with 10 nM GLP-1(9-36). This principle would be replicated for monitoring allosteric modulation between the Pm compounds and the antagonist Ex4(9-39).

The three main values of interest were analysed for all the remaining Pm compounds in the library using FLP-IN HEK 293 cells over expressing recombinant human GLP-1R for n=3 independent experiments. This experiment yielded many bar charts as exemplified by the chart in Figure 3.12.B and a vast data set spread sheet which is located in the appendices. Figure 3.12.B is a representative bar chart of the highlighted, circled regions of the dose-response curve shown in part A of Figure 3.12. The x axis of Figure 3.12.B represents the assay composition where numbers 1-7 denote a specific combination of ligands at specific concentrations for efficient screening.

The assay compositions for efficient miniscreen as denoted in Figure 3.12.B were:

1. cAMP response of 100 μM of the compound alone

2. cAMP response of 10 nM GLP-1(9-36) alone

3. numerical addition of cAMP responses of 10 nM GLP-1(9-36) and 100 μM Pm compound (the expected response assuming no cooperativity between ligands)

4. cAMP response following co-stimulation of GLP-1R with 100 μM Pm compound with 10 nM GLP-1(9-36)

5. cAMP response of 10 nM exendin 4(9-39)

6. added cAMP responses of 10 nM exendin 4(9-39) and 100 μM Pm compound (the expected response assuming no cooperativity between ligands)

7. cAMP response following co-stimulation of 100 μM Pm compound with 10 nM exendin 4(9-39)

A paired, two-tailed Student's t-test was performed between the cAMP responses given in assay compositions 3 and 4 for the observable effect of GLP-1(9-36) with the non-peptide, and compositions 6 and 7 to compare effect of Ex4(9-39) with the non-peptide ligand, where *$p<0.05$, **$p<0.01$, ***$p<0.001$ for n=3 experiments.

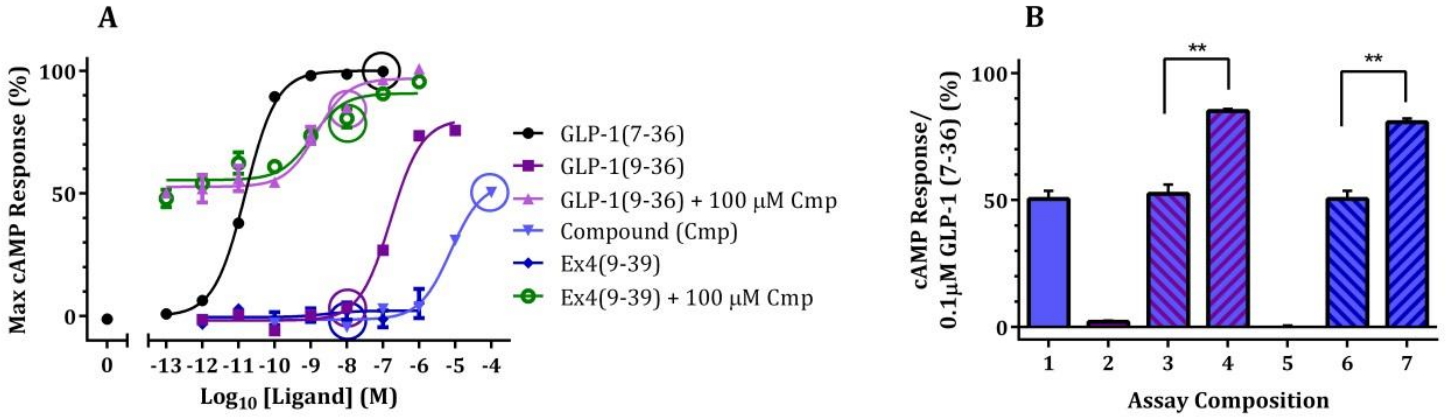

Figure 3.12. Visual representation of how the mini-screen was devised to interpret the extent of Pm compound-mediated allostery at the hGLP-1R .

A: Dose-response curve of ligands in the presence and absence of Pm compound. The points of interest are circled to indicate their importance with regard to the mini screen. **B** Bars are colour-coordinated with part A to indicate the presence of peptide. Assay compositions are as follows: **[1]** 100 μM compound; **[2]** 10 nM GLP-1(9-36); **[3]** The addition of cAMP response of bars 1 and 2 (no cooperativity between ligands); **[4]** The observed effect by simultaneous stimulation of hGLP-1R by GLP-1(9-36) and Pm compound; **[5]** 10 nM Ex4(9-39); **[6]** The addition of cAMP response of bars 1 and 5 (expected if no allostery); **[7]** The observed effect by simultaneous stimulation of hGLP-1R by Ex4(9-39) and Pm compound. Error bars represent the mean ± SEM of n=3 replicates performed in triplicate. * indicates $p<0.05$, ** $p<0.01$ (Student's t-test) representing statistical significance of observed versus expected effects of addition of Pm compound and peptide. Values are expressed as a percentage of the response elicited by 0.1 μM GLP-1(7-36).

3.4.10 Miniscreen results of all Pm compounds at the hGLP-1R

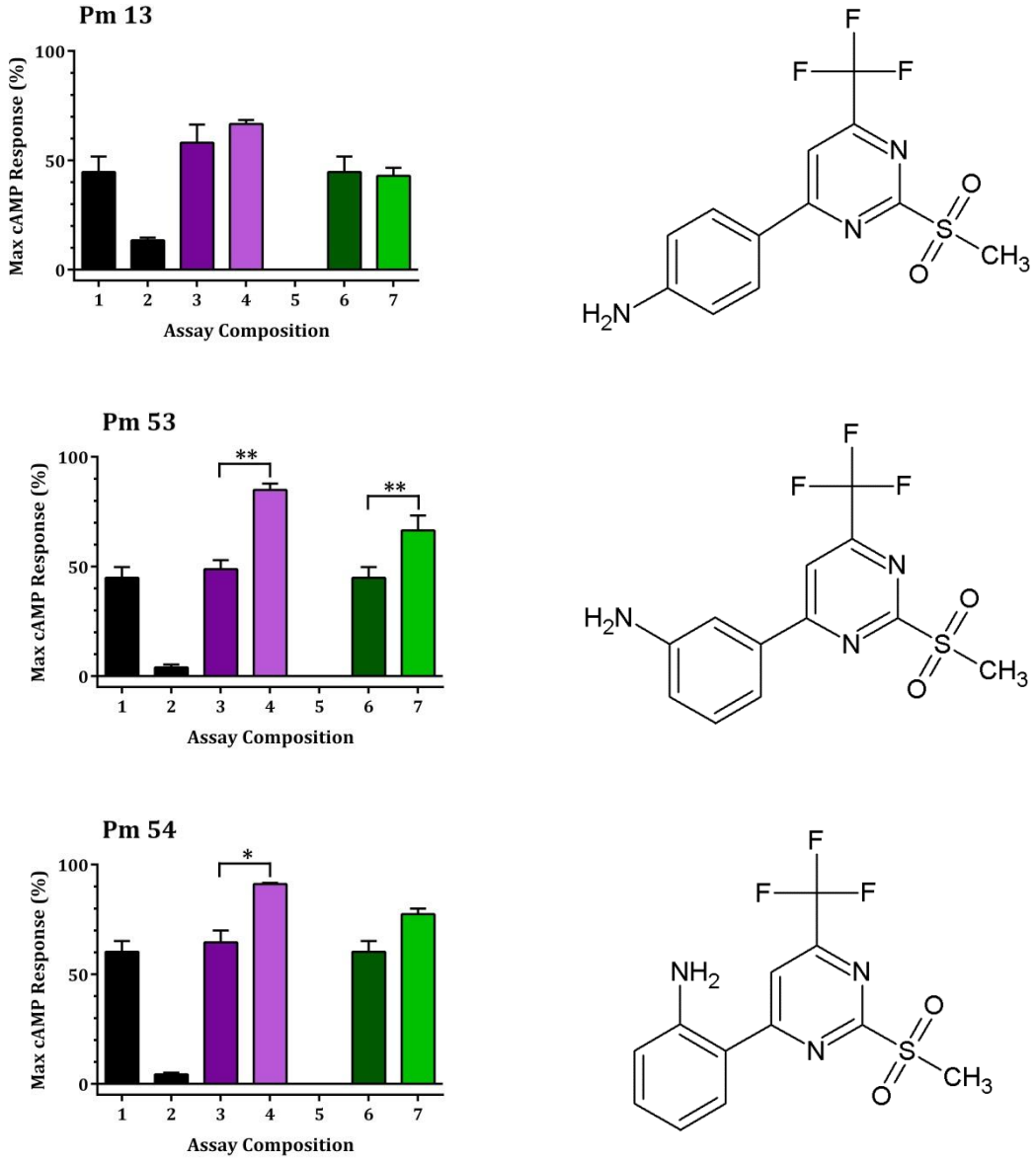

Figure 3.13 cAMP accumulation profiles of Pm compounds with an amine-modified benzene ring.

When administered alone, the amine-modified Pm compounds had a similar cAMP response of around 50%, with the *ortho* positioning of the amine achieving slightly higher than the *para* and *meta* positions (Figure 3.13). Pm 13 (*para*-modifed amine) is not capable of enhancing the cAMP responses of either GLP-1(9-36) or Ex4(9-39), suggesting Pm 13 is purely an agonist and not ago-allosteric in nature. Pm 53 (*meta*-modified amine) enhanced cAMP production of both peptide ligands (**P<0.01, n=3).

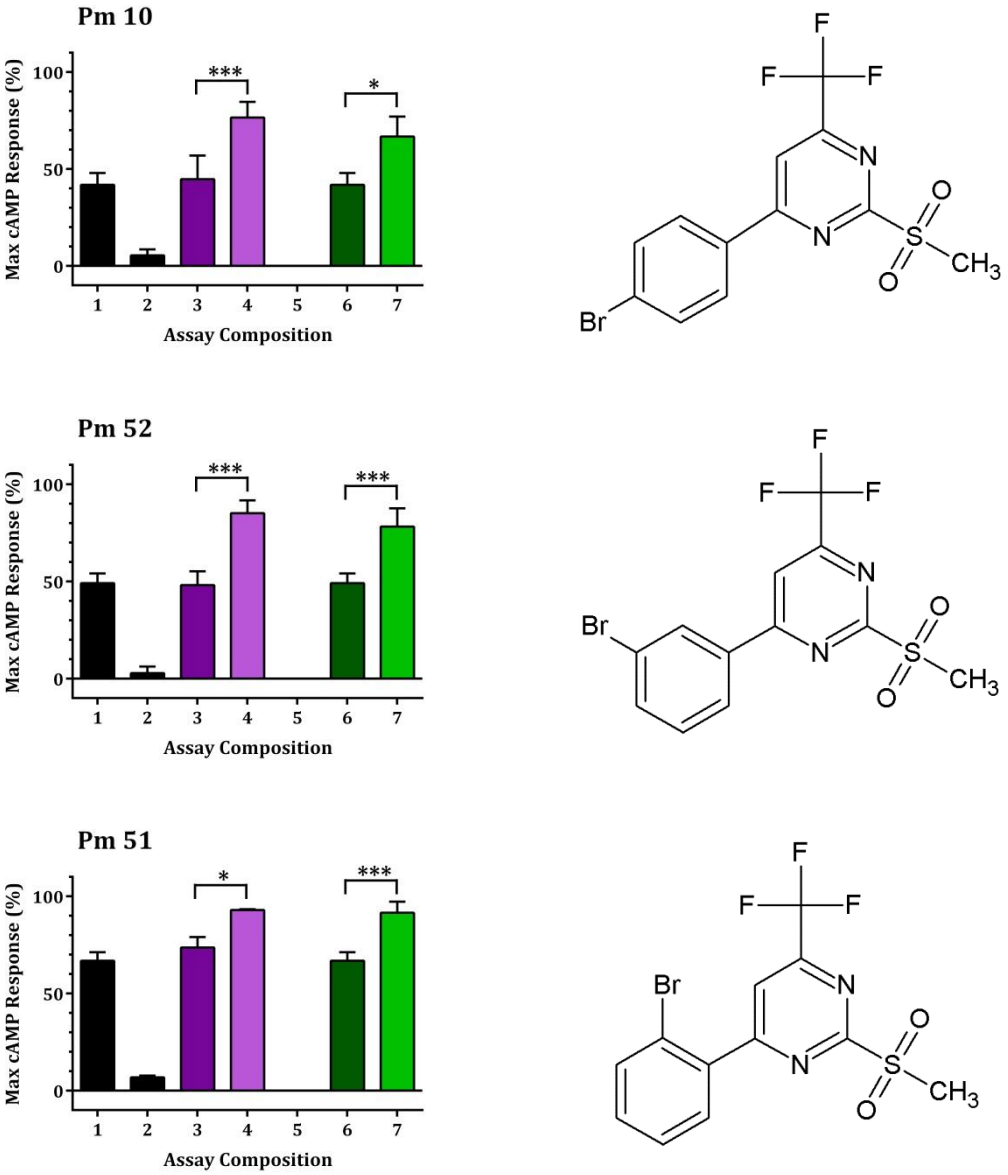

Figure 3.14 cAMP accumulation profiles of Pm compounds with a bromine-modified benzene ring.

Upon GLP-1R stimulation with bromine-modified Pm compounds, Figure 3.14 shows the *ortho*-positioned modification were most efficacious, similar to the amine modified group. Each bromine-modified Pm compound was capable of modulating the receptor to be more active in the presence of both GLP-1(9-36) and Ex4(9-39). In the presence of Pm 52, the cAMP responses of both GLP-1(9-36) and Ex4(9-39) significantly increased (***$p<0.001$, n=3). Pm 10 and 51 modulated the truncated peptides to a lesser extent than Pm 52.

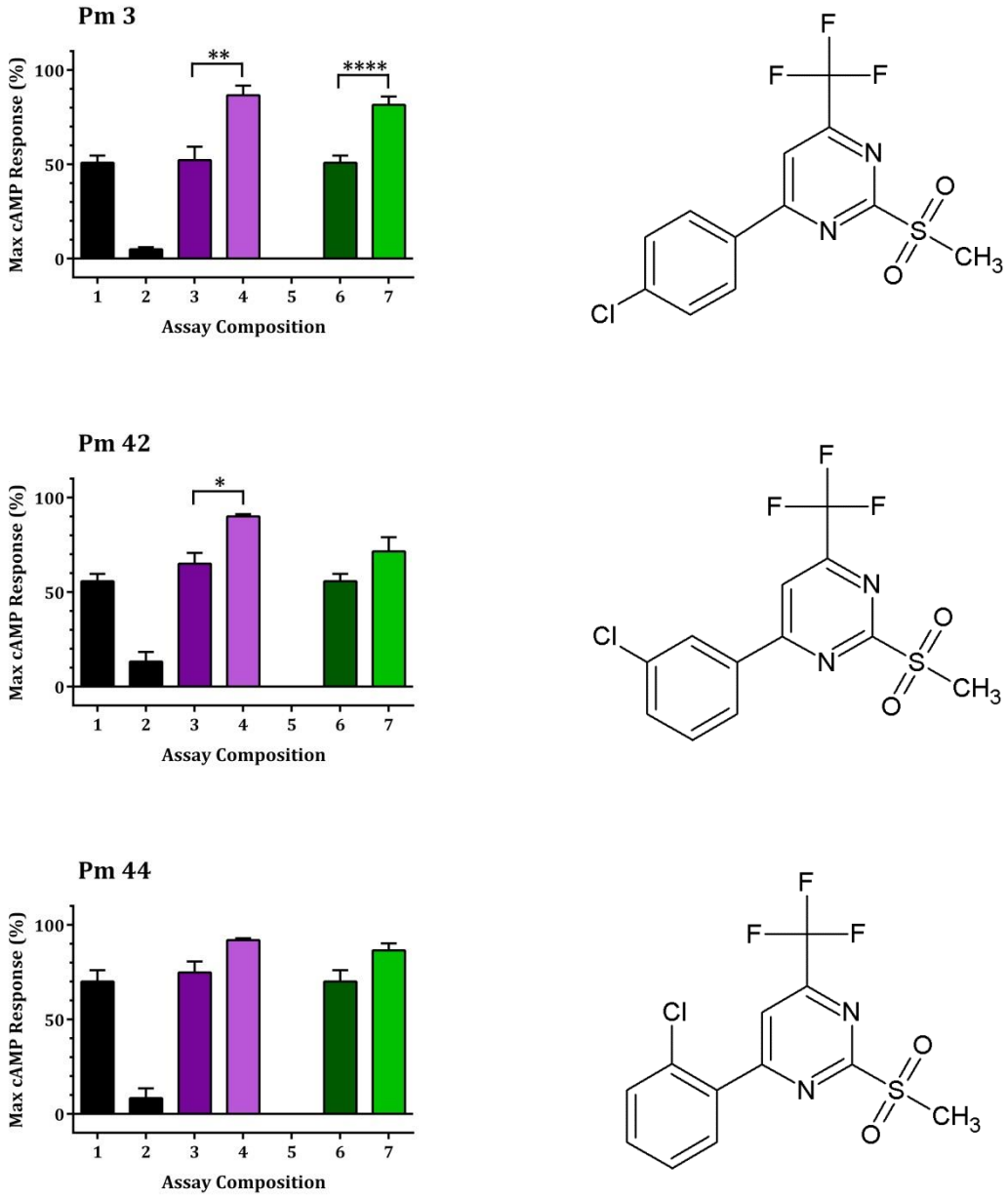

Figure 3.15 cAMP accumulation profiles of Pm compounds with a chlorine-modified benzene ring.

Upon GLP-1R stimulation with chlorine-modified Pm compounds, Figure 3.15 shows the *ortho*-positioned modification were most efficacious, with an E_{MAX} of around 70 %, whereas the *para* and *meta* positions reach around 50% of maximal activity. Despite an increased cAMP response in the presence of both GLP-1(9-36) and Ex4(9-39) for all chlorine modified Pm compounds, only *para*-modified Pm 3 achieved significant (**P<0.01 and ****P<0.0005) increase in cAMP production in the presence of both peptides. Pm 42 modulated GLP-1(9-36) significantly (*P<0.05). Pm 44 modulated neither peptide significantly, suggesting it was not ago-allosteric.

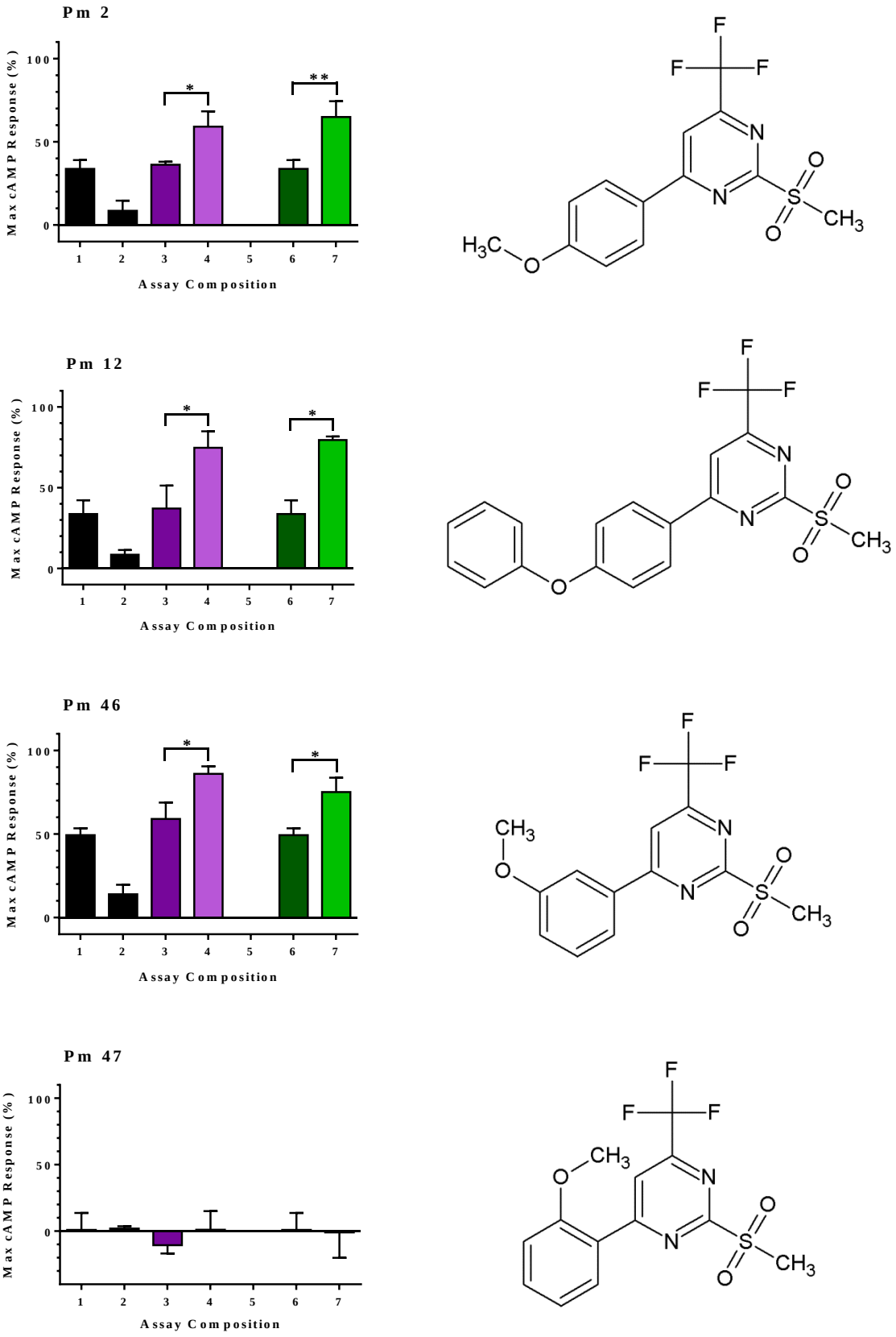

Figure 3.16 cAMP accumulation profiles of Pm compounds with an ether-modified benzene ring.

Figure 3.16 showed *ortho*-modified methyl-ester group Pm 47 was not capable of a cAMP response, nor capable of cooperativity with GLP-1(9-36) or Ex4(9-39). The other ether-modified Pm compounds 2, 12 and 46 all gave a similar cAMP response, ranging from approximately 30-50% maximal production of cAMP when administered alone. Indeed, Pm 2, 12 and 46 were all capable of peptide-ligand cooperativity with both GLP-1(9-36) and Ex4(9-39) to a significant level (of at least *$P<0.05$, $n=3$) therefore all displayed levels of allosteric modulation.

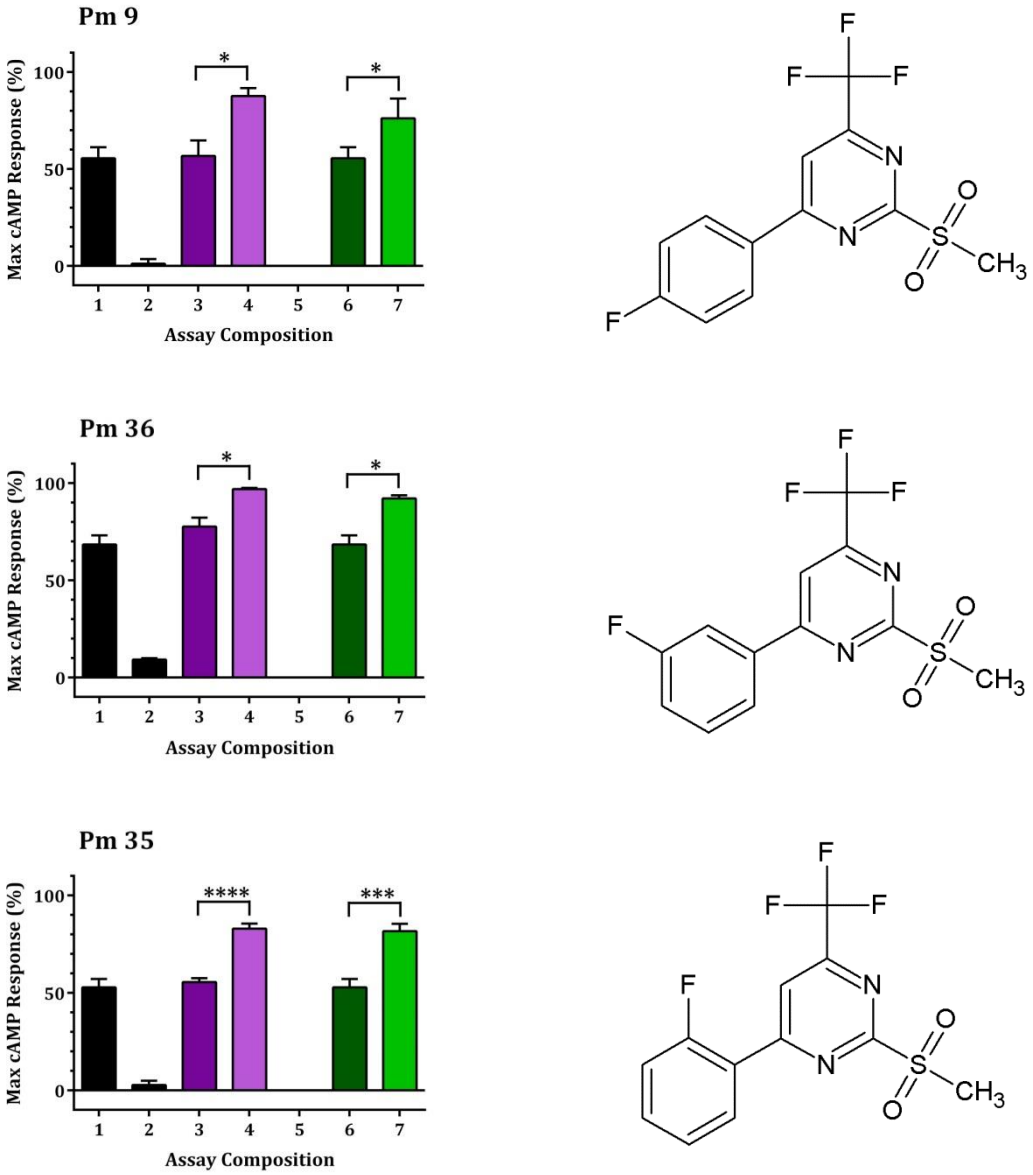

Figure 3.17 cAMP accumulation profiles of Pm compounds with a fluorine-modified benzene ring.

The fluorine-modified Pm compounds showed the ability to activate the hGLP-1R to approximately 50-70 % maximal cAMP response when administered alone at 100 μM. The most efficacious compound was Pm 36, the *meta*-modification. Pm 9 and Pm 36 both modulated activity of the truncated peptides to the same level of statistical significance (*P<0.05), yet *ortho*-modified Pm 35 modulated the peptide responses at GLP-1R to much higher levels of significance in the presence of GLP-1(9-36) (****P<0.0005, n=3) and Ex4(9-39) (***P<0.001) respectively.

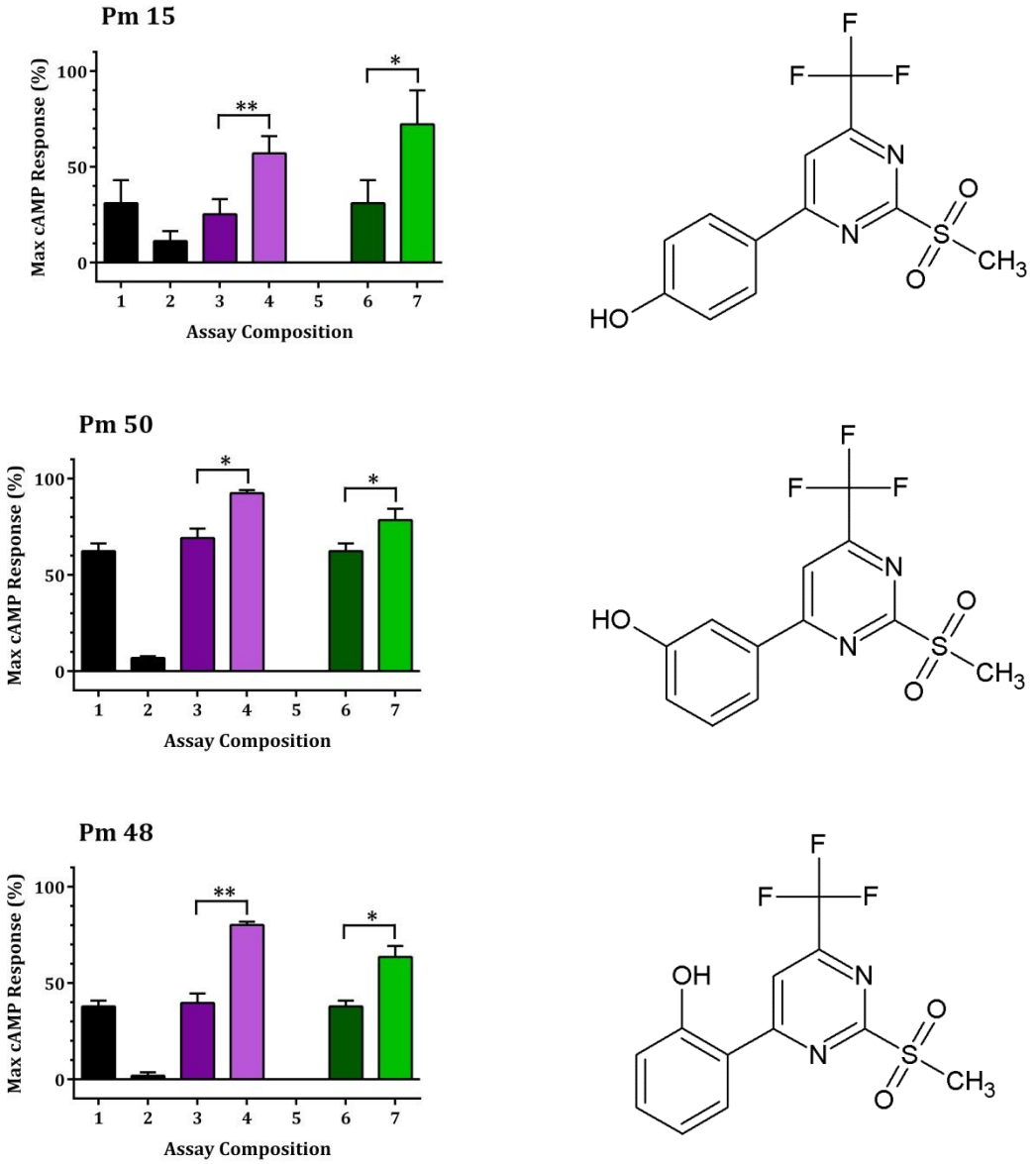

Figure 3.18 cAMP accumulation profiles of Pm compounds with a hydroxyl-modified benzene ring.

Pm 15 (*para*-modified hydroxyl) was a poor agonist when administered alone, (~30% E_{MAX}, S.E.M>10%, n=3). Pm 15 modified the response of the truncated peptides to levels of statistical significance, and appeared more effective with Ex4(9-39) than GLP-1(9-36). Pm 48 (*ortho*-modified hydroxyl) was a better ligand alone (~40% E_{MAX}) and modulated the receptor to give a more active response in the presence of the truncated peptides. Pm 50 (*meta*-hydroxyl modification) was the most active compound out of the three (~60% E_{MAX} at 100 μM, n=3), yet the increase in cAMP production was not as pronounced as the other two compounds in the presence of GLP-1(9-36) nor Ex4(9-39).

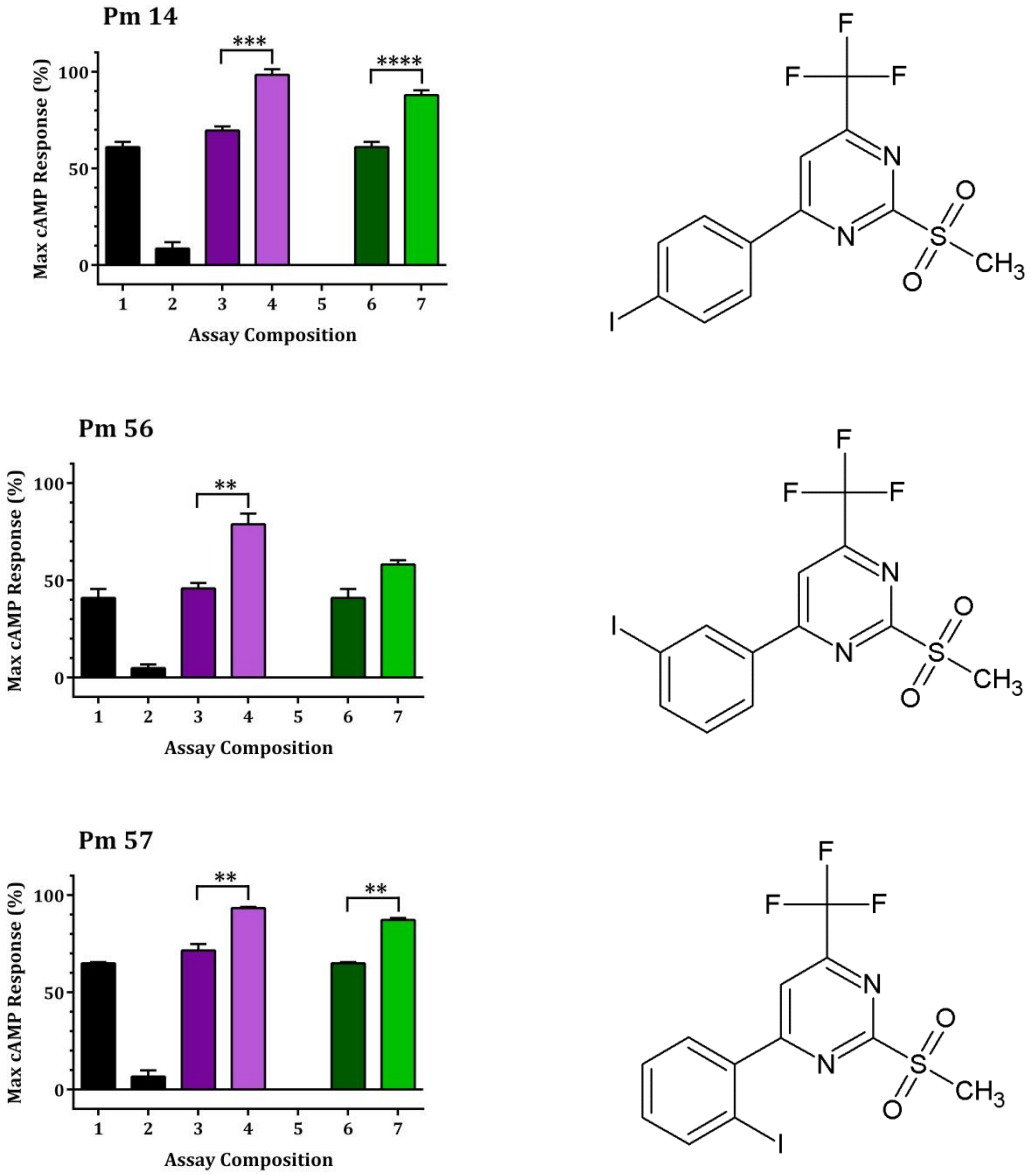

Figure 3.19 cAMP accumulation profiles of Pm compounds with an iodine-modified benzene ring.

Para and *ortho*-iodine modified compounds Pm 14 and 57 showed similar cAMP responses when administered alone at the GLP-1R (~60% E_{MAX}, n=3), but *meta*-iodine modified Pm 56 was less responsive (~40% EMAX, n=3). Pm 14 was capable of receptor modulation such that in the presence of 10 nM GLP-1(9-36) it achieved almost full receptor activity (***P<0.001), and with Ex4(9-39) Pm 14 achieved ~85% cAMP production (****P<0.0005). Both Pm 56 and 57 were capable of increased cAMP production when administered alongside GLP-1(9-36), and to a lesser extent Ex4(9-39). Pm 56 did not modulate receptor activity when administered with Ex4(9-39) to a statistical significant level.

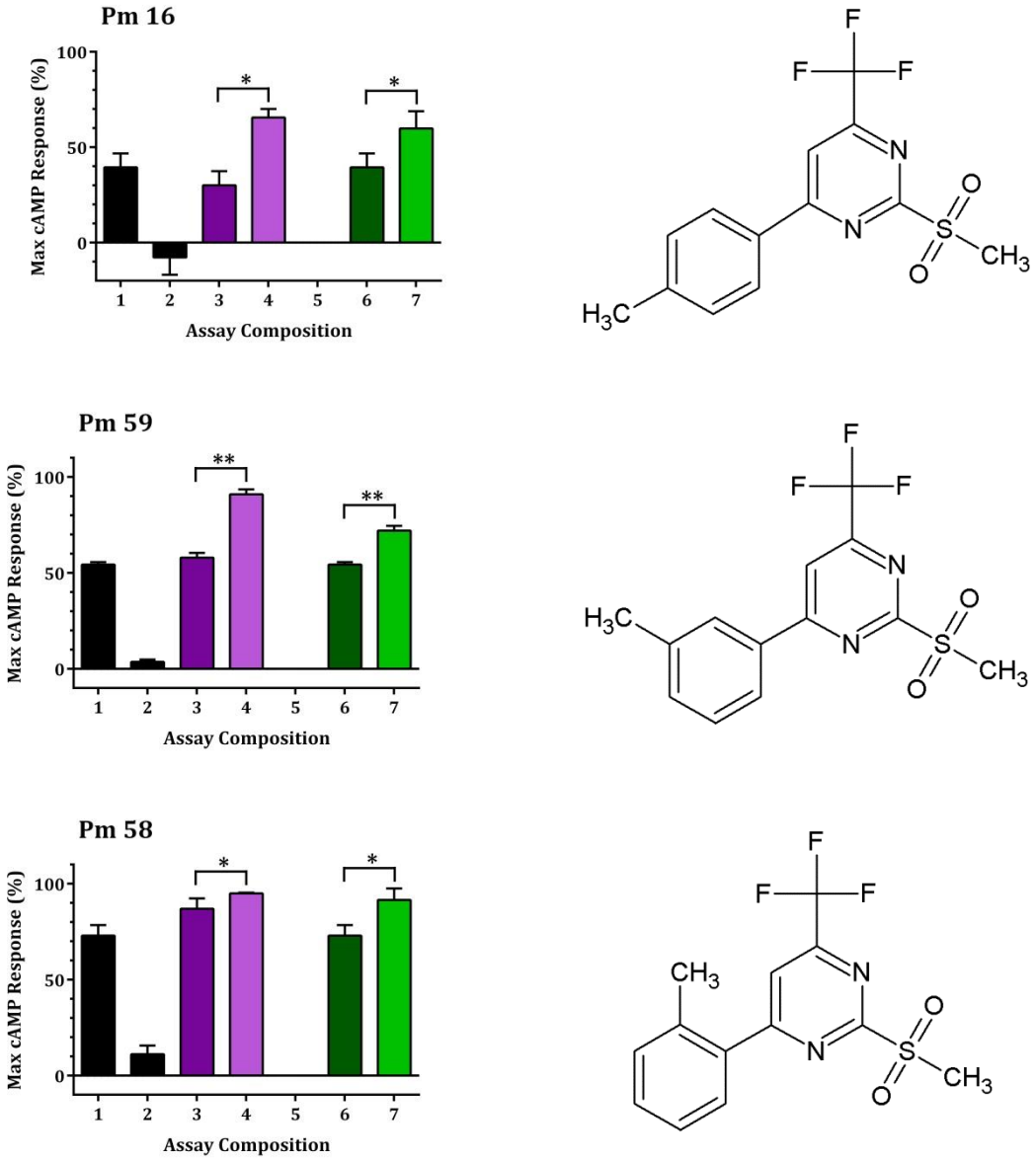

Figure 3.20 cAMP accumulation profiles of Pm compounds with a methyl-modified benzene ring.

Ortho-methyl modified Pm compound 58 showed a strong cAMP response at the GLP-1R when administered alone (~70% E_{MAX}, n=3). *Para* and *meta*-methyl modified compounds Pm 16 and 59 were less effective alone (%E_{MAX} of about 40 and 55% respectively, n=3). Despite being less effective alone, Pm 59 activated GLP-1R to a level comparable to Pm 58 when in the presence of GLP-1(9-36). Pm 16, 59 and 58 all positively modulated Ex4(9-39) responses (10 nM) to statistically significant levels (*P<0.05, **P<0.01 and *P<0.05 respectively).

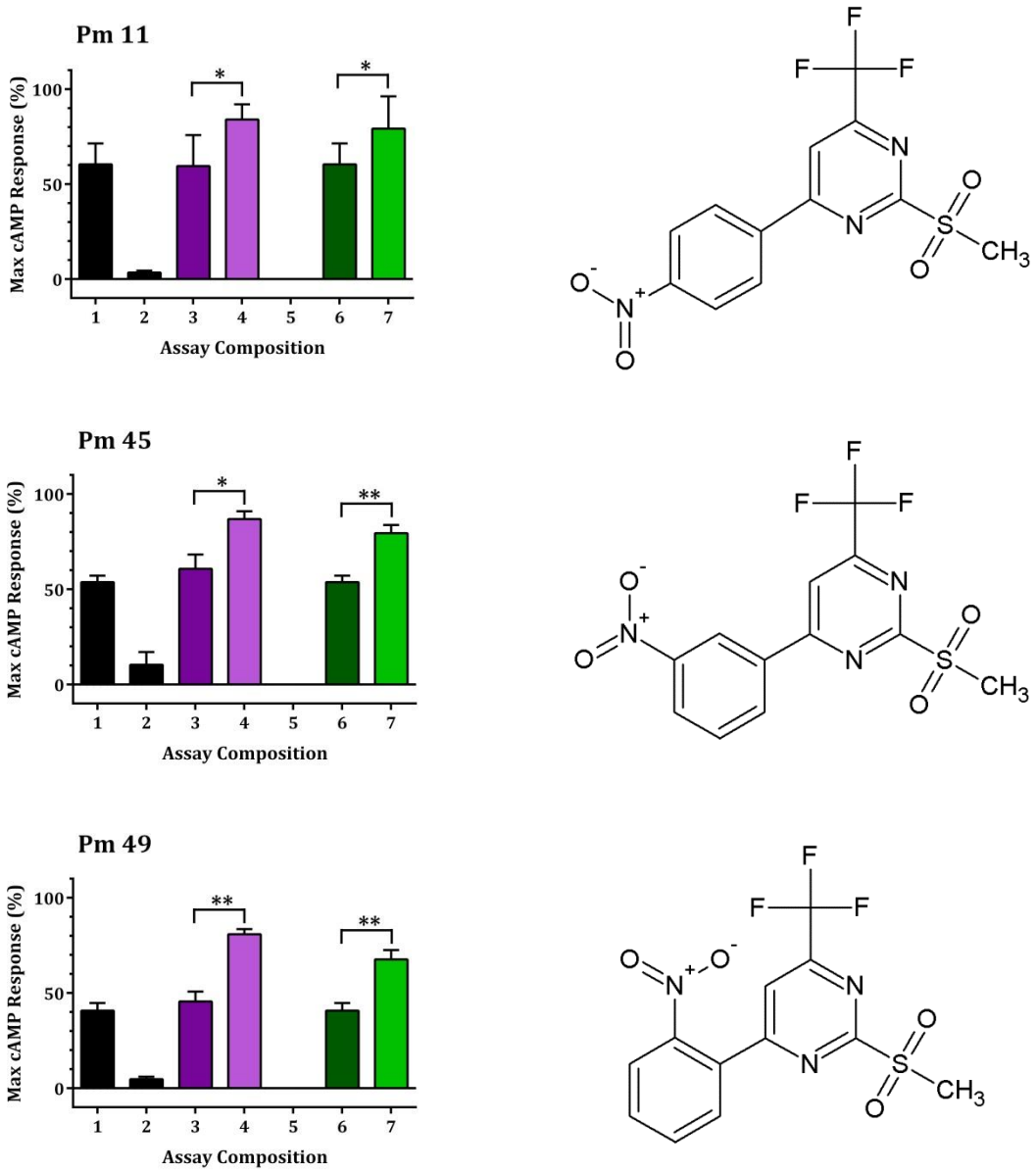

Figure 3.21 cAMP accumulation profiles of Pm compounds with a nitrogen dioxide-modified benzene ring.

Para-NO_2 modified Pm 11 achieved a mean cAMP response of around 60% but S.E.M > 10%, suggesting poor experimental repeats. *Ortho*-NO_2 modified Pm 49 was the least active (E_{MAX} ~ 40%, n=3). Pm 49 enhanced receptor activity to give a higher degree of modulation in the presence of GLP-1(9-36) than Pm 11 and 45 with and increased cAMP response of approximately 40% (**P<0.01) *versus* in increase of approximately 25% with Pm 11 and 45. Co-administered with Ex4(9-39) ~ 30% cAMP response increase is observed *versus* approximately 20-25% with Pm 11 and 45.

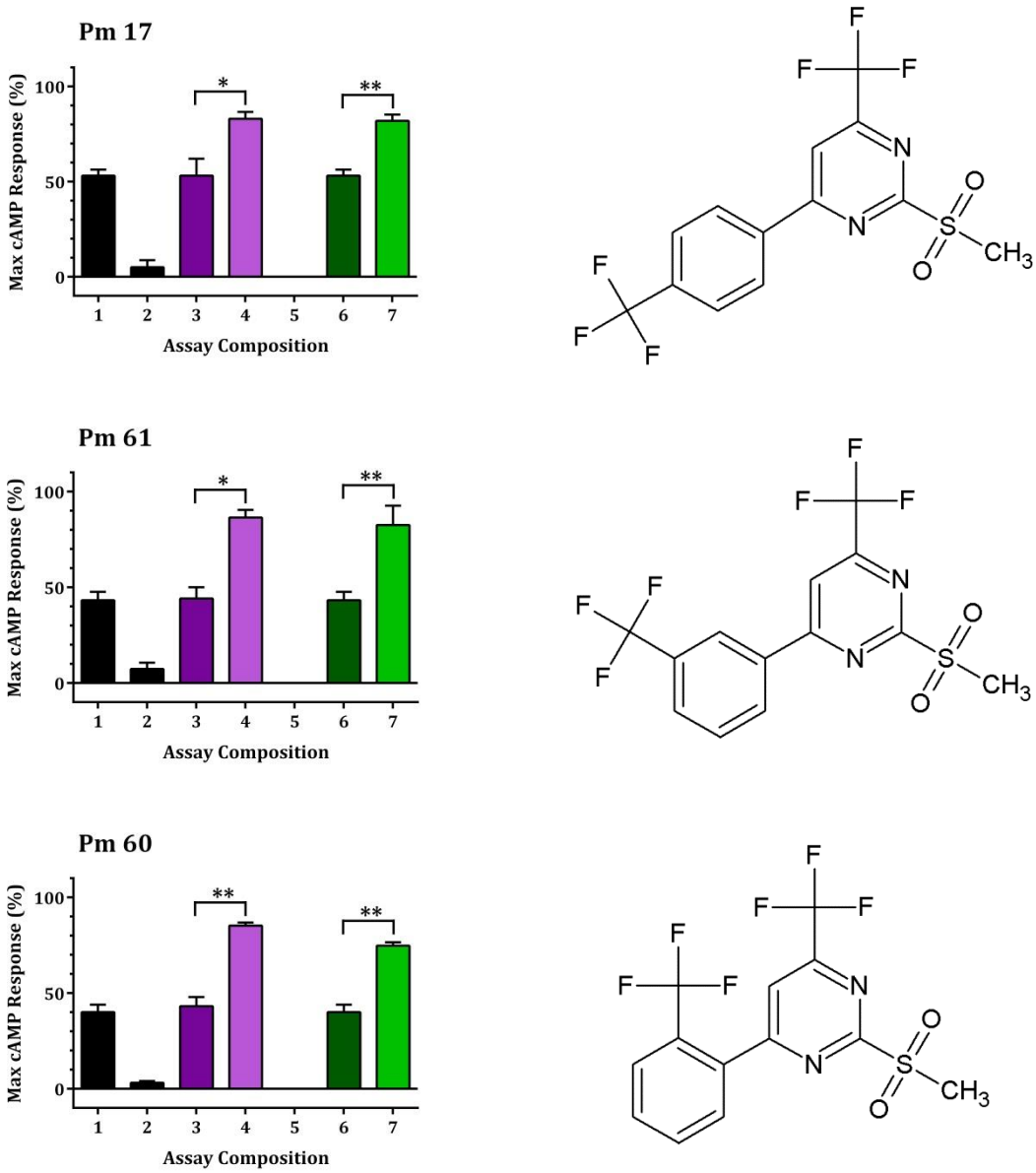

Figure 3.22 cAMP accumulation profiles of Pm compounds with a trifluoromethyl-modified benzene ring.

TFM modified Pm compounds 17, 61 and 60 all showed similar cAMP responses when administered alone, of between 40 and 55 % E_{MAX}. Pm 61 (*meta*-TFM modification) and Pm 60 (*ortho*-TFM modification) showed similar allosteric modulating properties at GLP-1R with both GLP-1(9-36) (*P<0.05, **P<0.01 respectively) and Ex4(9-39) (**P<0.01 for both, n=3) where the cAMP response in the presence of peptide was approximately doubled in comparison to stimulation with compound alone. *Para*-TFM modified Pm 17 was also capable of receptor modulation in the presence of truncated peptides and showed an enhancement of approximately 25% cAMP production.

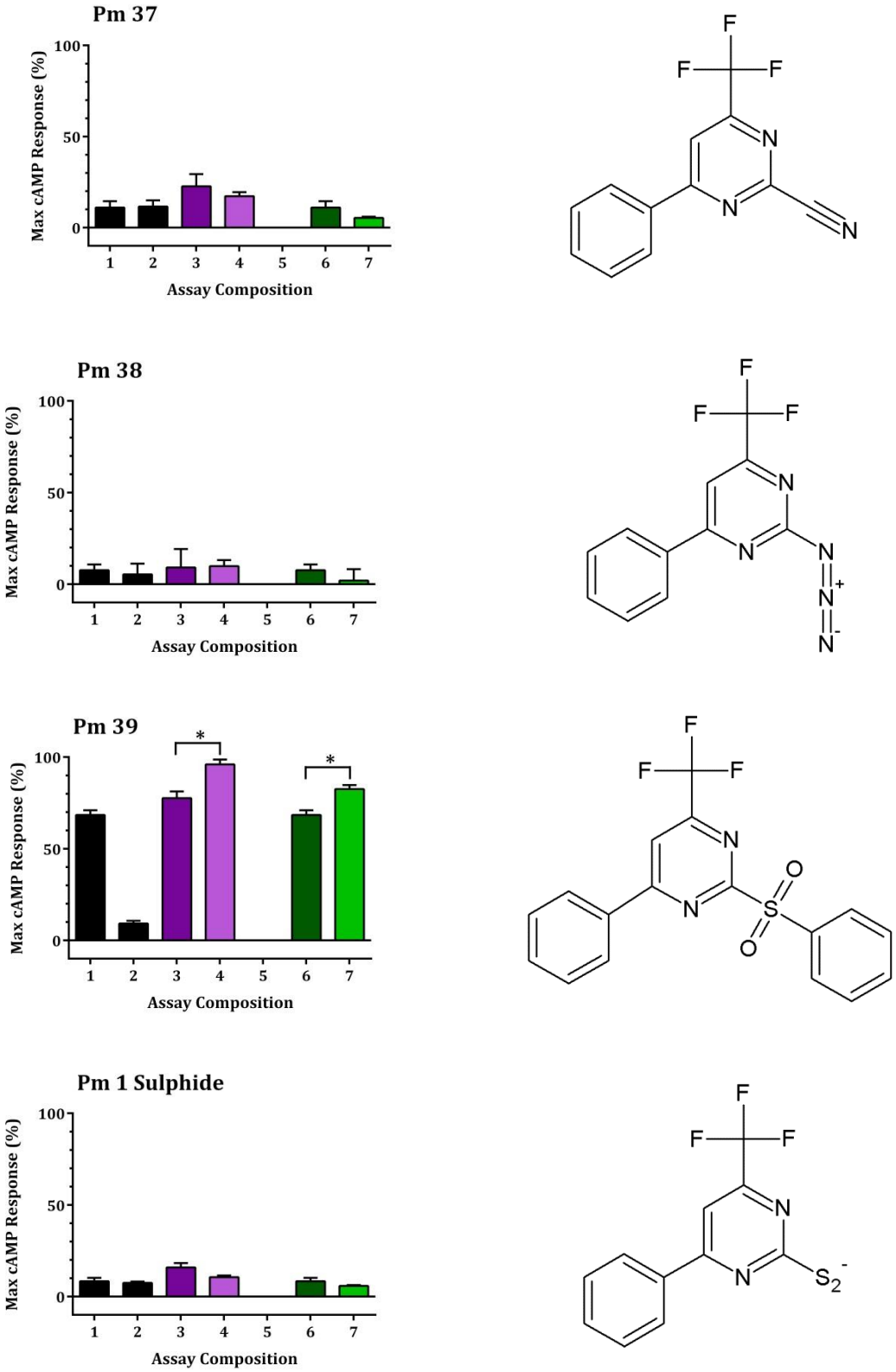

Figure 3.23 cAMP accumulation profiles of Pm compounds with replaced or extended sulphur dioxide groups.

Replacement of the sulphur-dioxide group removed the ability of the Pm compound to activate GLP-1R. Pm 37 (cyanide replacement), Pm 38 (azide replacement) and Pm 1 sulphide (S^{2-} replacement) did not activate GLP-1R with greater than 10% activity (n=3). Pm 37, Pm 38 and Pm 1 sulphide did not enhance receptor activity in the presence of 10nM GLP-1(9-36) nor Ex4(9-39) to any level of statistical significance.

Pm 39 had a benzene ring extension to the sulphur dioxide group and had high intrinsic activity of around 70% E_{MAX} when administered at 100 μM alone at GLP-1R. Pm 39 also retained receptor modulating properties such that co-stimulation with 10 nM GLP-1(9-36) resulted in almost full receptor activity ($P<0.05$). Indeed, Pm 39 was also capable of allosterically modulating Ex4(9-39)-mediated response to approximately 80% E_{MAX}.

The final group of Pm compounds to be observed using the miniscreen technique were those with a trifluoromethyl group replacement or removal; Figures 3.24 and 3.25. Pm 8, 27, 28, 34, 41 and Pm 55 were not agonists when administered alone, much like the compounds, Pm 37, 38 and Pm 1 sulphide which had a replacement of the SD functional group. Unlike Pm 37, 38 and Pm 1 sulphide, some Pm compounds with a SD group replacement retained allosteric-modulating characteristics when administered alongside GLP-1(9-36). Specifically, Pm 8 (t-butyl-amine replacement of TFM group) gave an approximate cAMP response of 5 % E_{MAX} at 100 μM, yet when administered with 10 nM GLP-1(9-36) gave approximately ~30 % E_{MAX} cAMP response (*$P<0.05$, n=3), yet Pm 8 did not enhance Ex4(9-39) activity when co-administered at GLP-1R expressing FlpIn-HEK cells. Pm 41 (cyanide replacement of TFM group) gave a cAMP response of 5 % E_{MAX} at 100 μM, yet co-administered with 10 nM GLP-1(9-36) gave a cAMP response of approximately ~45% E_{MAX}. Pm 62 (chlorine replacement of TFM group) retained agonist activity at GLP-1R and gave approximately 30% E_{MAX} cAMP response when administered alone, yet in the presence of 10 nM GLP-1(9-36) was increased to approximately 70%, (n=3, **$P<0.01$) and in the presence of 10 nM Ex4(9-39) was increased to approximately 50 % (n=3, *$P<0.05$). Pm 34 has a benzene ring replacement of the TFM group, this modification resulted in a negative cAMP response under basal level of cAMP production (%E_{MAX} ~ -25%, n=3). Pm 34 was incapable of positively modulating the cAMP responses of GLP-1(9-36) and Ex4(9-39) to statistically significant levels at GLP-1R expressing cells.

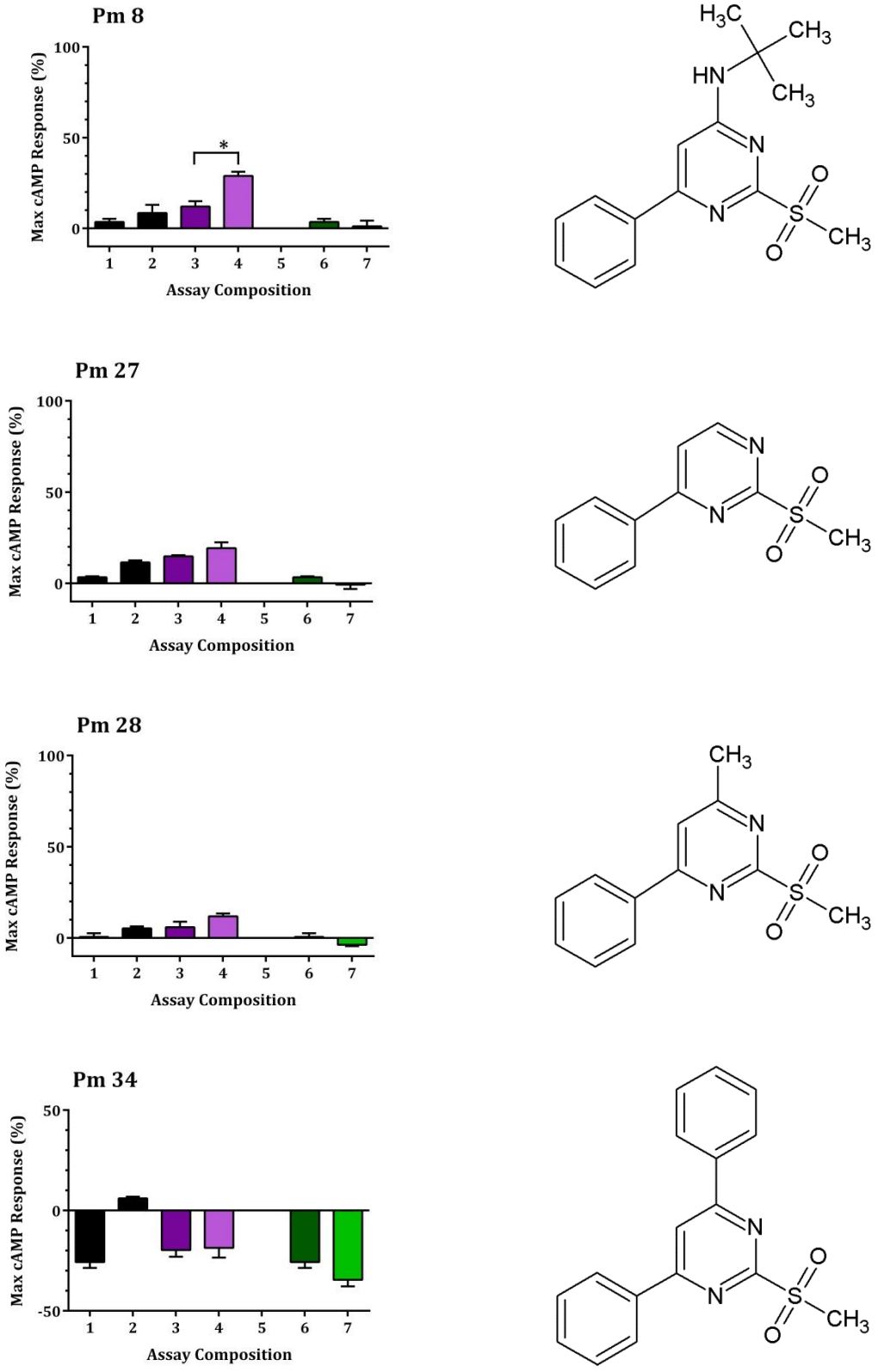

Figure 3.24 cAMP accumulation profiles of Pm compounds with removal of, or replacement of the trifluoromethyl group (C1 of the pyrimidine ring).

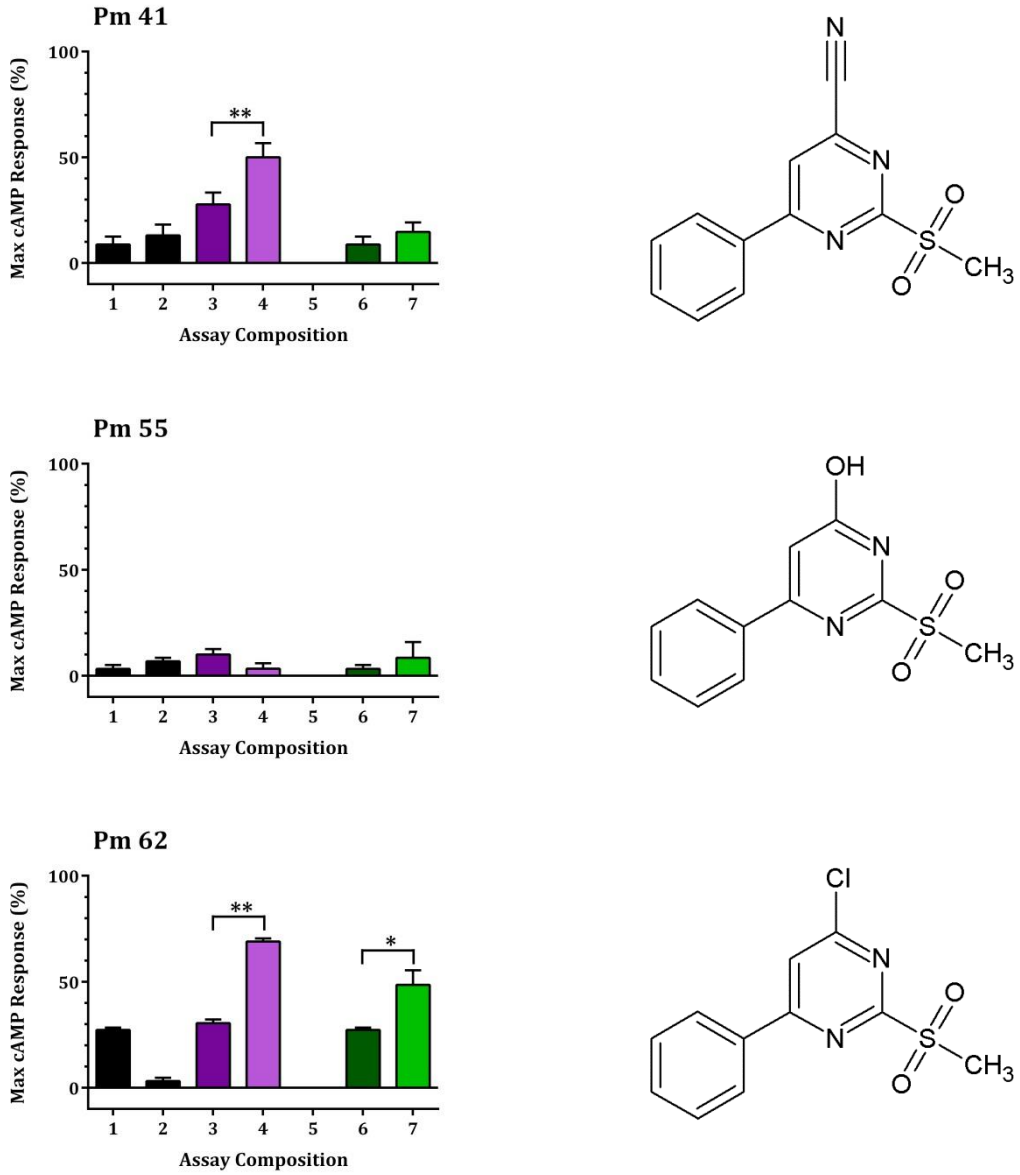

Figure 3.25 cAMP accumulation profiles of Pm compounds with a functional group replacement of the trifluoromethyl group (C1 of the pyrimidine ring).

3.4.11 Investigation of non-agonist GLP-1R modulators

The results from section 3.4.10 suggested that the benzene ring modifications in the *para*, *ortho* and *meta* positions mainly resulted in slightly different signalling profiles in the presence of truncated peptide ligands, however they were all ago-allosteric GLP-1R modulators (with the exception of Pm 13 and Pm 44). Replacement of the TFM group rendered the compounds inactive at GLP-1R alone, yet two compounds, Pm 8 and Pm 41, retained the ability

to modulate GLP-1R enhancement of cAMP production when 100 μM of the Pm compound was used alongside 10 nM GLP-1(9-36), suggesting allosteric modulating properties without intrinsic agonist characteristics. This was explored further by using full dose-response curves of GLP-1(9-36) in the presence of increasing Pm 41 concentrations (Figure 3.26.A) or increasing Pm 8 concentrations (Figure 3.26.B) in dual-activation assays at GLP-1R expressing FlpIn-HEK 293 cells.

Increasing concentrations of Pm 8 did not result in statistically significant increase in potency of GLP-1(9-36) amide according to a paired one tailed Student's t-test, however a four-fold increase in potency was observed using 100 μM Pm 8 (EC_{50} = 64.56 nM) when compared to GLP-1(9-36) alone (EC_{50} = 260 nM) (Figure 3.26.A). An increased potency using 100 μM Pm 8 was concomitant with an increased $\%E_{MAX}$ (GLP-1(9-36) alone: 71.82% cAMP response, GLP-1(9-36) + 100 μM Pm 8: 86.54% cAMP response) (Table 3.10). A dose-response curve for Pm 8 was performed simultaneously with the curves shown in Figure 3.26.A (data not shown for simplicity of Figure 3.26.A) and did not produce a dose-response curve; these data and the increased potency at 100 μM upon co-stimulation of GLP-1(9-36) suggest Pm 8 may be an allosteric modulator with no inherent agonist activity.

A paired, one-tailed Student's t-test was performed upon the pEC_{50} values for GLP-1(9-36) in the presence and absence of Pm 41, and demonstrated that Pm 41, like Pm 8, was unable to modulate the GLP-1(9-36) cAMP response to a statistically significant level. Despite this, Table 3.11 and Figure 3.26.B both show a left shift in GLP-1(9-36) potency in the presence of increased Pm 41 concentration. The %Span decreased as concentration of Pm 41 increased (Table 3.11), Figure 3.26.B demonstrated this visibly, as the base line cAMP response increased as Pm 41 dose increased at 100 pM GLP-1(9-36). A dose-response curve for Pm 41 was performed simultaneously with the curves shown in Figure 3.26.B (data not shown for simplicity of Figure 3.26.B) and *did* produce a dose-response curve. These data taken together suggest Pm 41 had intrinsic efficacy at GLP-1R, and therefore ago-allosteric, not an allosteric modulator without inherent agonist characteristics as was suggested from the results from section 3.4.10.

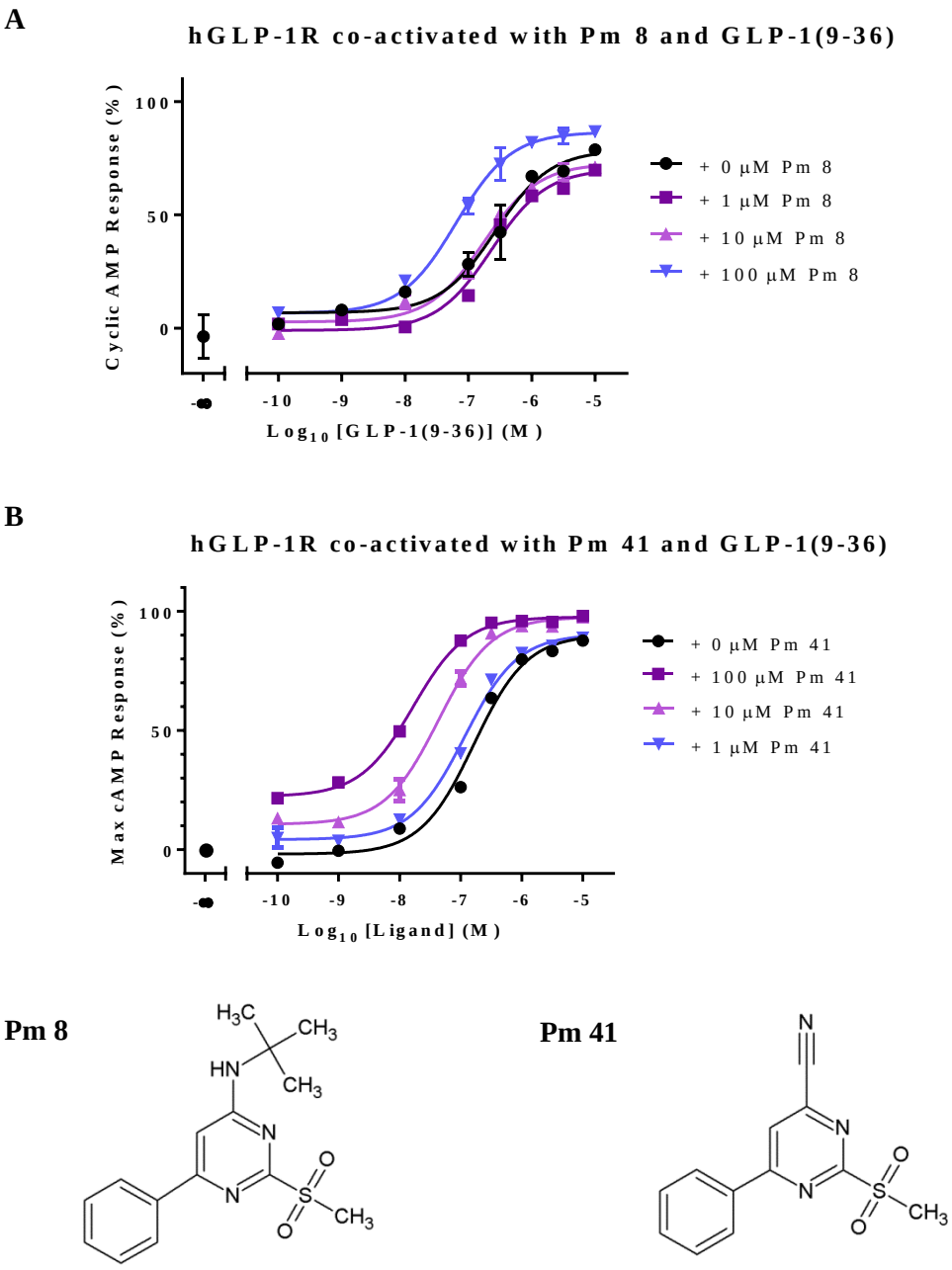

Figure 3.26. Allosteric modulation of GLP-1(9-36)amide at hGLP-1R expressing FLP-IN HEK 293 cells using non-agonist Pm compounds 8 and 41.

A. Co-activation of hGLP-1R using Pm 8 and GLP-1(9-36). Accompanying statistics are displayed in Table 3.10. **B**. Co-activation of hGLP-1R using Pm 41 and GLP-1(9-36). Accompanying statistics are displayed in Table 3.11 Structures of Pm 8 and Pm 41 are shown. Graphs shown are from one individual experiment, representative of n=3 separate experiments, and are normalised to the cAMP response of 1 µM GLP-1(7-36).

	+ 0 µM Pm 8	+ 1 µM Pm 8	+ 10 µM Pm 8	+ 100 µM Pm 8
***p*EC$_{50}$**	6.58 ± 0.01	6.64 ± 0.06	6.76 ± 0.10	7.19 ± 0.12
% E$_{MAX}$	71.82 ± 6.19	70.25 ± 2.79	72.7 ± 2.71	86.54 ± 5.41
% Span	71.82 ± 5.30	71.23 ± 2.80	69.96 ± 5.51	80.01 ± 4.19

Table 3.10 *p*EC$_{50}$, % E$_{MAX}$ and % Span corresponding to Figure 3.26.A.

	+ 0 µM Pm 41	+ 1 µM Pm 41	+ 10 µM Pm 41	+ 100 µM Pm 41
***p*EC$_{50}$**	6.74 ± 0.08	6.86 ± 0.11	7.35 ± 0.09	7.84 ± 0.05
% E$_{MAX}$	89.15 ± 6.18	93.18 ± 6.41	98.64 ± 3.64	97.95 ± 1.29
% Span	89.72 ± 5.31	91.40 ± 5.05	90.76 ± 2.09	76.00 ± 2.82

Table 3.11 *p*EC$_{50}$, % E$_{MAX}$ and % Span corresponding to Figure 3.26.B.

3.5 Discussion

3.5.1 Pm Compound Library Analysis

From the initial screening process 15 compounds were determined to have %E$_{MAX}$ at GLP-1R-expressing cells of 55 % cAMP response and above (Table 3.2, Table 3.3). These were then used in a cell-free cAMP accumulation assay to identify any quenching properties the ligands possessed at a wavelength of 665 nm which would give false positive signal data. Pm 31, 40 and 43 all showed a significant signal reduction at 665 nm in a dose-dependent manner (Figure 3.6). As there were no cells present in the assay there was no organism to produce cAMP, the dose-dependent reduction in emission at 665 nm from FRET can be attributed to either the disruption of the FRET signal from the excited europium molecule, or the absorbance of the emission signal from the Alexa Fluor® 647-anti cAMP antibody.

Pm 42 was identified as the most potent compound with partial agonist activity and µM potency. Pm42 gave reliable replicate values and was the only compound from the Pm compound library which fully plateaued when administered at 100 µM, therefore Pm 42was the only compound which gave a dose-response curve from which the activity and potency could be correctly calculated. The potency values from the other Pm compounds were based on the activity values from which GraphPad Prism had extrapolated from the gradient of the curve, therefore were not reliable (Figure 3.7.B, Table 3.3). Pm 42 was unable to compete with radiolabelled ^{125}I-GLP-1(7-36) binding at isolated membranes expressing hGLP-1R (Figure 3.8

B); therefore no IC_{50} value could be attained to gage Pm compound affinity for the GLP-1R. These data suggested Pm 42 may bind to an allosteric site.

The hypothesis that Pm 42 binds to a structurally distinct site at the GLP-1R was further explored by using an antagonist competition dose-response curve, whereby GLP-1R activation was attempted with a dose-response curve of Pm 42 in the presence of increasing concentrations of the orthosteric antagonist Ex4(9-39) (Figure 3.9.B). Rather than the dose-response curve shifting to the right, resulting from competition and displacement of Pm 42 from the orthosteric binding pocket (as shown by GLP-1(7-36) activity in increasing Ex4(9-39) concentrations (Figure 3.9.A)), the curve shifted to the left and upwards, indicating not only an increased potency in the presence of antagonist, but also increased E_{MAX}. These data suggested a positive allosteric interaction between the non-peptide and Ex4(9-39) binding at the orthosteric site. This potentiation of Pm 42 response by Ex4(9-39) was further explored by investigating the concentration range at which Ex4(9-39) elicited cooperativity with Pm 42. Ex4(9-39) concentrations were examined from a range of 1 μM to 0.1 nM in an antagonist dose-response curve in the presence of increasing concentrations of Pm 42; 1 μM, 10 μM and 100 μM, as Pm 42 had an EC_{50} of 6.5 μM, therefore concentrations below 1 μM would not give a reliable cAMP response. Interestingly, at these active Pm 42 concentrations, Ex4(9-39) enhanced the cAMP response further in a concentration-dependent manner (Figure 3.9.C and Table 3.7). The concentration at which Ex4(9-39) gave an enhanced cAMP response to non-peptide agonist Pm 42 was closely associated with its half-inhibitory concentration (pIC_{50} = 8.15 ± 0.01, n=3, Table 3.4) suggesting that the occupancy of the receptor by Ex4(9-39) is critical for the allosteric properties observed.

Ex4(9-39) is extensively described in the literature as an antagonist of the GLP-1R, yet the data described here suggest Ex4(9-39), despite having lost the activity-providing residues 1 through 8 from its N-terminus, still retains some ability to activate GLP-1R, but only when it is in the presence of the ago-allosteric modulator Pm 42. We hypothesise that this is due to an altered conformation of the receptor induced by Pm 42, and this correlates well with the data from the analogously truncated peptide in GLP-1: GLP-1(15-36), which is a partial agonist at the GLP-1R. GLP-1(15-36) is capable of receptor activation; therefore there must be residues further toward the C-terminus than the critical N-terminal 8 residues responsible for a maximum response that are capable of receptor interaction. Research has shown that Ex4(9-30) (loss of the C-terminal trp-cage and analogous to GLP-1(15-36)amide) is capable of receptor activation in rat GLP-1R expressing HEK cells (unpublished data, work performed by Dr. Nasr) when glutamic acid (E) residue at position 16 is replaced by the more flexible residue glycine (G), the analogous residue found in GLP-1(15-36) at position 22. The inherent rigidity of Ex4(9-39) throughout residues 9-30 may be responsible for the lack of activity of Ex4(9-39) at the GLP-1R

when in its native, non-allosterically modified state. This hypothesis is discussed further in Chapter 4.

One way to interpret the data presented here demonstrating an antagonist obtaining agonist properties at the GLP-1R, is that in the presence of concentrations near or exceeding the EC_{50} for Pm 42 (6.5 μM), Pm 42 alters receptor conformation so that Ex4(9-39) becomes an agonist with nM potency. The data presented here suggest that Pm 42 alters and stabilises a certain allosterically modified receptor conformation, that is structurally capable of allowing a second interaction around the orthosteric site, permitting the more central residues of Ex4(9-39) to access activating residues within the receptor that are exposed due to the presence of Pm42. The implications of these data are discussed further in Chapter 5.

3.5.2 Pharmacological properties of Pm 42 with GLP-1(9-36)

The observation that Pm 42 is capable of stabilising receptor conformation to permit an antagonist to act as an agonist provoked the hypothesis that it may be able to enhance the activity of other N-terminally truncated peptides, namely the truncated metabolite GLP-1(9-36). An orally available ligand with such properties could have particularly useful therapeutic effects as GLP-1(9-36) is present in the circulation at higher concentrations that the parent peptide GLP-1(7-36) (Egan *et al.*, 2002). Dual activation assays using Pm 42 in combination with the truncated peptides GLP-1(9-36) and GLP-1(15-36), and with the full length ligand were performed (Figure 3.10). These data demonstrated that Pm 42 was unable to enhance potency of GLP-1(7-36) and GLP-1(15-36), yet it positively affected the response of GLP-1(9-36). Both the potency and maximal activity of the GLP-1(9-36)-mediated cAMP response were increased in the presence of Pm 42, for example, the addition of 100 μM Pm 42 enhanced the potency of GLP-1(9-36) at the receptor more than 40-fold (Table 3.8). The E_{MAX} was also affected, whereby GLP-1(9-36) alone gave 83 % activity, yet in the presence of only 1 μM Pm 42 activity was increased to 98 %, and to 100 % active with 10 μM and 100 μM Pm 42. This shift into nM potency and full agonist activity of GLP-1(9-36), in the presence of Pm 42, suggests the cAMP response is akin to that given by the full length peptide and perhaps this could translate into a higher insulin secretory response when administered *in vitro*, and perhaps even *in vivo*.

3.5.3 Insulinotropic effects of GLP-1(9-36) co-administered with Pm 42

The hypothesis that Pm 42 is capable of stabilising receptor conformation to enhance the cAMP response elicited by truncated peptide ligands at GLP-1R-expressing HEK cells proved to be correct, but only for GLP-1(9-36). To further analyse the small molecule's potential for receptor modulation in insulin secretory terms, an insulin secretion test was performed using Pm 42 along with GLP-1(9-36) using the secretory cell line INS-1 832/13.

Whereas the FLP-IN HEK 293 cell line constitutively overexpresses the human GLP-1 receptor due to being under the control of two promoters (P_{SV40} and P_{CMV}), the INS-1 832/13 cell line originates from a rat insulinoma tumour, stably transfected with a plasmid containing the human proinsulin gene (Hohmeier *et al.*, 2000), therefore receptor levels are lower and correspond more to actual physiological expression levels. INS-1 cells were originally isolated by dispersion of a transplantable radiation-induced insulinoma tumor from NEDH rats into a tissue culture medium containing β-mercaptoethanol (Asfari *et al.*, 1992) and were stably transfected with a plasmid containing the human proinsulin gene; therefore secrete a heterogeneous mix of both rat and human insulin.

INS-1 832/13 cells were exposed to the secretagogue GLP-1(7-36) and the potential secretagogues Pm 42 and GLP-1(9-36) under high glucose conditions for 2 hours following a low glucose episode. As expected, 1 μM GLP-1(7-36) did have a statistically significant increase on insulin secretion versus high glucose alone. It was discovered that whilst administered alone, 10 μM Pm 42 had no statistically significant effect upon insulin secretion, and GLP-1(9-36) did not increase insulin secretion to a statistically significant level at any concentration used. Pm 42 only had a statistically significant effect on insulin secretion when administered along with GLP-1(9-36) (Figure 3.11, Table 3.9). When INS-1 832/13 were co-incubated with buffer containing 10 μM Pm 42 and 0.1, 1 or 5 μM of GLP-1(9-36) there was a statistically significant increase of insulin secretion. Surprisingly when INS-1 832/13 cells were co-stimulated with 5 μM GLP-1(9-36) and 10 μM Pm 42, the level of insulin secretion rose above the level given by the full-length peptide. A concentration of 5 μM GLP-1(9-36) is not physiologically relevant, yet it does show there is a correlation between the dose of peptide and non-peptide ligand combination with the titre of insulin secreted. The enhanced insulin secretory response is most likely due to the enhanced intracellular cAMP level, as GLP-1R is primarily coupled to the $G\alpha_s$ pathway, yet it may also be enhanced by non-peptide induced calcium influx. Increased intracellular cAMP levels lead to higher proportions of activated PKA and Epac2 within the beta cell (Baggio & Drucker, 2007); both proteins are mediators of insulin secretion.

These data are in agreement with similar findings in the field of allosteric modulators. An example of an allosteric modulator capable of potentiating insulin secretion *in vitro* is compound 2 (Figure 3.27). Knudsen and co-workers (Knudsen *et al*., 2007) found that compound 2 significantly enhanced cAMP production at plasma membranes from BHK cells expressing the GLP-1R, and also found that compound 2 enhanced GLP-1 specific binding to isolated membranes from BHK cells. Knudsen and co-workers found that compound 2 enhanced insulin secretion from isolated islets from CD1 wild-type mice, but not from GLP-1R K/O mice, and only enhanced insulin secretion under hyperglycaemic levels of 10 mM glucose, not at 3 mM glucose. Furthermore, Knudsen and co-workers found that compound 2 enhanced insulin release from perfused rat pancreas in *ex vivo* studies in a glucose-dependent manner. *In vitro* studies by Irwin *et al*. (Irwin *et al*., 2010) on BRIN-BD11 cells saw similar results for insulin secretion, and *in vivo* results using mice showed compound 2 significantly decreased the overall glucose excursion, but did not *significantly* enhance insulin secretion, although insulin secretion was enhanced in the presence of compound 2. Another group of compounds similar in structure to the Pm library were the ones assayed in a study by Sloop and co-workers (Sloop *et al.*, 2010), which were also found to possess glucose-dependent insulinotropic characteristics. Sloop and co-workers found that compound B (Figure 3.27) was capable of enhancing cAMP release from HEK293 cells expressing the GLP-1R using a CRE-luciferase assay, and found that its action was not blocked by Ex4(9-39). Sloop *et al*. then used static islet cultures from Sprague Dawley rats to assay compound B mediated effects on insulin release and found that compound B potentiates insulin release only in high glucose conditions (11.2 mM glucose) and not under low glucose conditions. Sloop and co-workers also found that compound B had statistically significant additive effects on GLP-1-mediated insulin release *in vivo* using the hyperglycemic clamp model in Sprague Dawley rats (Sloop *et al*., 2010). Interestingly all non-peptide GLP-1R agonists capable of potentiating glucose-dependent insulin release have a sulphur oxide moiety.

Allosteric non-peptide compounds capable of altering receptor conformation to permit usage of endogenous levels of GLP-1(9-36) through making it more potent at GLP-1R have great therapeutic potential. This would be especially useful in the case of T2D as the metabolite GLP-1(9-36) is at higher circulating levels in comparison to the full length peptide, therefore insulin secretion would be enhanced 2-3 fold (Egan *et al*., 2002). Pm 42 at 10 μM is unable to potentiate insulin secretion above the basal level, therefore if a compound like Pm 42 with allosteric properties made it to everyday treatment there would be no risk of hypoglycaemia from excessive insulin secretion; a problem associated with some anti-diabetic treatments. An ago-allosteric modulator with these properties would only be active (in the sense of insulin secretion) in the presence of GLP-1(9-36) as there is positive cooperative between the ligands,

both increasing endogenous cAMP levels and insulin secretion levels. GLP-1 is released post-prandially, therefore the peptide hormone metabolite would only be present after eating and would only take effect then and be cleared by the kidneys naturally, at physiological levels, thereby potentially alleviating the patient of nausea from excessive secretagogue levels in circulation. Allosteric modulators have promising scope as therapeutics for the more delicately-tuned hormonally-balanced bodily processes when their normal function is disturbed.

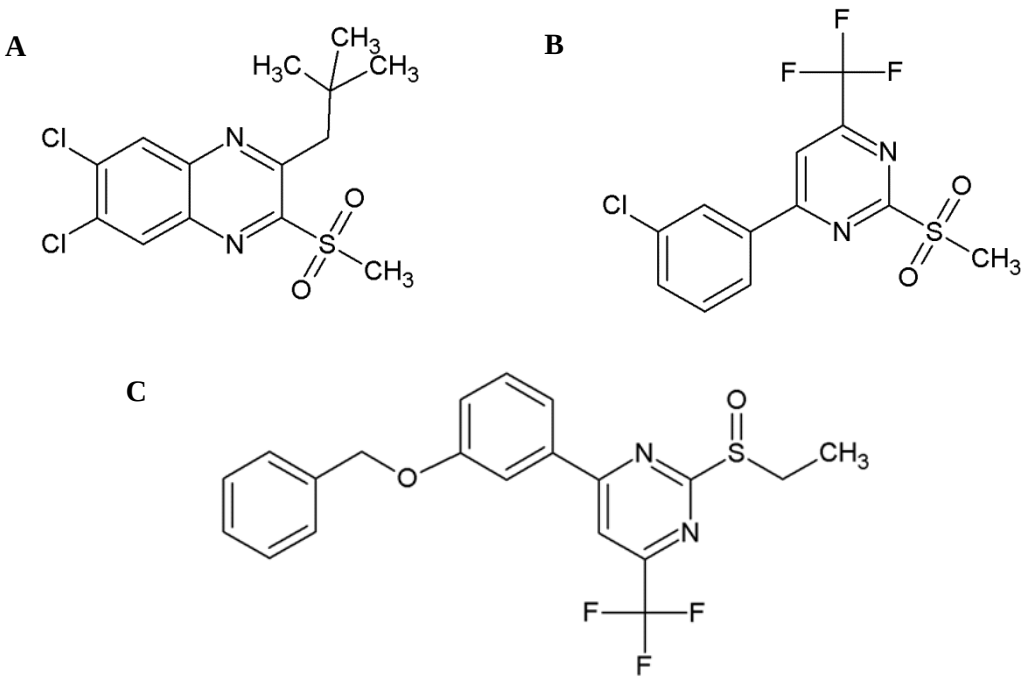

Figure 3.27 Non-peptide GLP-1R agonists capable of potentiating glucose-dependent insulin release. A. Compound 2 (Knudsen *et al*., 2007). **B**. Pm 42. **C**. Compound B or BETP (Sloop *et al*., 2010).

3.5.4 Allosteric properties of the Pm library

Pm 42 enhances insulin secretion in INS-1 832/13 cells when administered with GLP-1(9-36), most likely through activation of the $G\alpha_s$ pathway. Therefore the other Pm compounds may, by extension, also have insulinotropic activities if they too enhance the cAMP response at hGLP-1R expressing HEK cells in the presence of low concentrations of GLP-1(9-36). In order to detect this allosteric property that may also relate to insulinotropic properties in the remaining Pm compounds in the library, a screening protocol was devised using 100 µM of Pm compound with either 10 nM GLP-1(9-36)amide or 10 nM Ex4(9-39). This technique (miniscreen) was

applied to all the compounds in the Pm series to identify any traits or characteristics from the functional groups that relate to increased or decreased cooperativity between the Pm compound and truncated ligands. Concentrations of 10 nM were chosen for the truncated peptides in this screen as these concentrations lay just on the cusp of the dose-response curve, therefore cAMP produced by 10 nM GLP-1(9-36) lay just below levels of detection when alone, yet when co-administered with Pm 42 in GLP-1R expressing cells there is a marked observable increased cAMP response (Figures 3.9.C and 3.10.A), therefore a 10 nM concentration was ideal for identifying the allosteric nature the non-peptide has upon the truncated peptide.

There was no discernible pattern between the position (*ortho*, *meta* or *para*) of functional groups surrounding the benzene ring of the Pm compound and the cAMP response. Generally when the observed value (from *in vitro* experimentation) *was* statistically significantly greater than the expected value (addition of cAMP responses of 10 nM peptide and 100 μM Pm compound) when the non-peptide was administered with 10 nM GLP-1(9-36), it also gave a statistically significant increased response when co-stimulated with Ex4(9-39), suggesting the mechanism of allosteric modulation at the GLP-1R affects the truncated peptides in a similar fashion, despite one being documented as a partial agonist and the other an antagonist. This observation is understandable, as the mode of binding of Ex4 and GLP-1 are very similar, with them both binding at the orthosteric site (Runge *et al*., 2008; Underwood *et al*., 2010), therefore they will both presumably extend into the transmembrane bundle to interact with the activation cortex in a similar manner too. This would suggest the modulation of the receptor by an ago-allosteric compound would by implication have a similar effect upon the two peptide ligands, despite Ex4(9-39) being truncated by an additional 6 residues in comparison to the level of truncation of GLP-1(9-36), herein lies the key questions: how is the GLP-1 receptor activated? Are the mechanisms of activation of GLP-1R by Ex4 and GLP-1(7-36) different? These questions are addressed in chapters 4 and 5 of this thesis.

The large-scale miniscreen of the Pm compounds did uncover some interesting properties of the moieties of the compounds and their associated ability to activate the $G\alpha_s$ pathway. Figures 3.23, 3.24.A and 3.24.B show the cAMP accumulation results from those Pm compounds with a replaced or extended sulphur dioxide group and those with a removed or replaced trifluoromethyl group. The data demonstrated that certain modifications completely obliterated their activation and allosteric abilities at hGLP-1R expressing cells. For example, Pm 37, 38 and Pm 1 sulphide have various SD replacements and subsequently lost inherent activation and allosteric modulation ability, whereas Pm 39 which has a benzene ring addition to the end of the SD group retained intrinsic and allosteric activity at the GLP-1R. This suggests the SD moiety is essential for receptor interaction. There had been speculation that the reason behind this is the sulphur dioxide group could be capable of covalent interaction with a cysteine

residue at the GLP-1R as studies have shown that Pm compounds covalently bind with free cysteine residues in solution (unpublished data by Dr. Migliore). This is explored in the appendix of this thesis.

3.5.5 Allosteric modulators of the GLP-1 receptor

TFM group replacement or removal obliterates intrinsic agonist activity at GLP-1R, unless the replacement moiety is also electronegative (Pm 62, chlorine replacement). Despite this, two of the Pm compounds (Pm 8 and Pm 41) retained allosteric properties (in the presence of GLP-1(9-36), allowing them to modulate the GLP-1R to shift into a more active conformation without activating it itself, yet they were unable to enhance Ex4(9-39) activity at 10 nM, therefore they display peptide specificity There is another non-peptide ligand in the literature that has these properties, a small flavonoid named quercetin which is not itself an agonist yet alters receptor specificity for calcium signalling in FLP-IN CHO cells overexpressing the hGLP-1R when co-administered with either GLP-1(7-36) or Ex4(1-39) but not alone (Koole *et al*., 2010). The two compounds with these characteristics are Pm 8-an amine linked t-butane moiety replacement of TFM- and Pm 41- a cyanide replacement of the TFM group. Neither Pm 8 nor Pm 41 gave a cAMP response above 20% that of GLP-1(7-36) (Table 3.2), therefore were both classed as non-agonists at the GLP-1R.

Data from the miniscreen showed Pm 8 and Pm 41 were the best allosteric modulators, as characterised by those compounds whose $\%E_{MAX}$ result from measuring the cAMP response was enhanced by over 150 % when co-administered with 10 nM GLP-1(9-36) in comparison to alone. Only three Pm compounds fell within this category and they all had TFM moiety replacements. Pm 41 activity increased 11-fold in the presence of 10 nM GLP-1(9-36), Pm 8 activity increased over 8-fold in the presence of 10 nM GLP-1(9-36), and Pm 62 activity increased 2.5-fold in the presence of 10nM GLP-1(9-36).

The non-agonist allosteric compounds Pm 8 and Pm 41 were co-administered alongside a full dose-response curve of GLP-1(9-36) at 3 concentrations, 1 μM, 10 μM and 100 μM shown in Figure 3.26.A and B. There was a definite leftward shift of the GLP-1(9-36) dose-response curve when the assay was carried out under increasing Pm 41 concentrations, in a dosage dependent manner, as expected from an allosteric modulator. However, there is also a notable upward shift of the baseline of the GLP-1(9-36) curve, also in a concentration dependent manner, which is quantifiable as the % Span of the curve decreases as the $\%E_{MAX}$ increases under increasing Pm 41 concentrations, these data suggest that Pm 41 is not purely

allosteric and does indeed possess intrinsic agonist activity. Pm 8 may be an allosteric modulator, however data remain inconclusive as there is no statistically significant increase in potency or activity of GLP-1(9-36) dose response curve at the GLP-1R until concentrations of 100 μM Pm 8 are reached, and even then the increase in % E_{MAX} could be explained by the increase in % Span. The percentage increase in apparent activity (% E_{MAX}) is adjoined by an almost equivalent rise in baseline with the addition of 100 μM (as exemplified by the % Span), suggesting the resultant apparent increase in activity is a simple addition of the two ligand's effects at the receptor.

These data suggest the TFM moiety could be manipulated further to engineer a compound that is truly allosteric and capable of enhancing GLP-1(9-36) potency without intrinsic activity. This would help understand the mechanism of allosteric modulation at Family B GPCRs, clearly further work in this area is required. Ideally the crystal structure of the transmembrane region of GLP-1R bound by a non-peptide ligand would be solved. The advent of this is surely approaching, as the crystal structures of the transmembrane domain of two Family B GPCRs have recently been solved, both members of the Secretin Subfamily as is the GLP-1 receptor: the corticotropin-releasing factor receptor 1 (Hollenstein, 2013), and the glucagon receptor (Siu, 2013).

3.6 Summary

In summary, the Pm compounds are a group of ago-allosteric modulators of which most activate the GLP-1 receptor with μM potency. The Pm compounds are generally partial agonists that are capable of cooperating with the truncated peptide GLP-1(9-36) to enhance potency, and in some cases are capable of cooperating with Ex4(9-39) to switch the peptide from antagonist to partial agonist with nM potency akin to its affinity.

A miniature screening process was devised to identify those compounds which altered GLP-1R conformation in such a way that it would enhance the maximum activity of GLP-1(9-36) when administered together, using only 10 nM of GLP-1(9-36). This screening process could potentially be applied to the drug screening process in the discovery of non-peptide drugs for treatment of T2D in a large-scale industrial setting.

Pm 42 was discovered to be the most potent and is similar in structure to compound A and compound B in the literature. This work shows that Pm 42 is able to potentiate insulin secretion from INS-1 cells. These findings are consistent with the publication from Sloop and

co-workers, who showed that compound B potentiated insulin secretion from isolated pancreatic islets (Sloop *et al*., 2010).

Chapter 4

Peptide-Mediated Glucagon-Like Peptide-1 Receptor Activation

Extending the 'Two-Domain' Binding Model

4.1. Introduction

The chimeric domain swopping studies between the CT and PTH receptors with amino-terminal substitutions between the CT and PTH hormones showed the amino terminus of the peptide hormones were complementary to the TM domain of the receptor, and the carboxyl-terminus of the peptides were complementary to the NTD of the receptors (Bergwitz *et al*., 1996). This two-domain model has since been used to describe the interaction between Family B GPCRs and their cognate peptide ligands (Hoare, 2005). The activating amino-region of GLP-1 and Ex4 have been shown to reside within the first 8 residues, and the affinity-providing carboxyl region of GLP-1 and Ex4 have been hypothesised to reside from the 9th residue onward (Figure 4.1) (López de Maturana *et al*., 2003; Al-Sabah & Donnelly, 2003b). N-terminal truncation of the first 8 residues of GLP-1(7-36) to yield GLP-1(15-36) reduces affinity for the GLP-1R more so than the equivalent truncation in Ex4 (Montrose-Rafizadeh *et al*., 1997). N-terminal truncation of the first 8 residues of Ex4 and GLP-1 to yield Ex4(9-39) and GLP-1(15-36) reportedly removes activity at the GLP-1R without total loss of affinity (Göke *et al*., 1993; Thorens *et al*., 1993; Montrose-Rafizadeh *et al*., 1997; Serre *et al*., 1998). In contrast, recent data revealed that GLP-1(15-36) retains some agonist activity as shown by Patterson *et al*. (2011) in recombinant HEK-293 cells overexpressing the hGLP-1R.

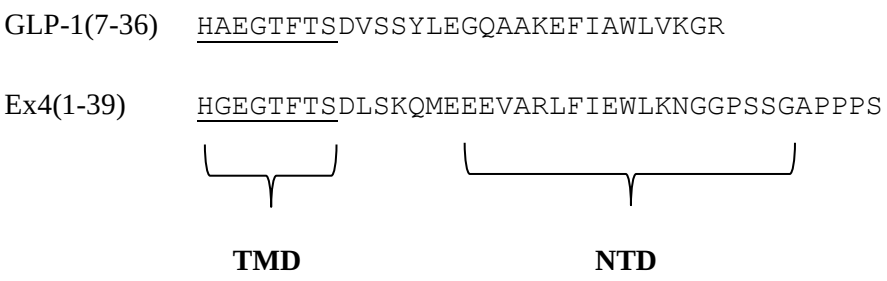

Figure 4.1 Interacting regions of GLP-1(7-36) and Ex4(1-39) with GLP-1R

Underlined peptide sequence denotes the amino region of the peptides postulated to activate GLP-1R by interaction with the TMD. Non-underlined peptide sequence denotes residues postulated to provide peptide affinity for GLP-1R by interaction with the NTD.

The discovery that GLP-1(15-36) (which lacks the first 8 amino terminal residues postulated to be involved in receptor activation) could activate GLP-1R directly opposes the hypothesis that the amino-terminal peptide residues are required for GLP-1R activation.

These data suggest there are residues within the ligand that are required for activity that reside to a more C-terminal locus than previously proposed. This implies the two-domain model may be too simplistic and may need re-evaluating or extending.

4.2 Aims and Strategy

The ability of GLP-1(15-36) to activate the receptor and the inability of Ex4(9-39) to activate the receptor suggests differential activation mechanisms between these ligands. The differences between binding mode of GLP-1 and Ex4 are explored in this chapter by using cAMP accumulation assays of truncated peptide analogues at FlpIn-HEK 293 cells constitutively overexpressing human GLP-1R. Truncated and mutated peptide analogues are used in cAMP accumulation assays and heterologous affinity binding assays to better understand the roles of individual residues within GLP-1 and Ex4 peptides in GLP-1R binding and activation. Specifically this chapter aims to:

- Use truncated variants of GLP-1 and exendin-4 to scrutinize the contribution to binding and activity that the amino and carboxyl termini of these ligands play.
- Use mutated variants of GLP-1 to examine the N-terminal residues of GLP-1(15-36) and their role in displaying efficacy at GLP-1R expressing cells.
- Use the data obtained to propose a third hypothesis of Class B G protein-coupled receptor activation via a "brace model".

4.3 Methods

The procedures used in this section are fully described in Chapter 2, methods and materials. The methods used in this section include: crude cell membrane preparation (section 2.2.1.7), BCA assay (section 2.2.1.8), radioligand specific binding assay (section 2.2.3.2.a), radioligand competition binding assay (section 2.2.3.2.b), cAMP accumulation (LANCE) assay (section 2.2.3.1) and data analysis (section 2.2.4).

4.4 Results

4.4.1 Crude membrane specific binding assay and receptor quantification

FlpIn-HEK 293 cells constitutively overexpressing the hGLP-1R were cultured and harvested as described in methods section 2.2.1.7. The resultant crude membrane preparation was used in a radioligand specific binding assay to assess the appropriate membrane dilution to use that would yield < 10% total counts added so the Cheng-Prussoff equation could be applied to calculate B_{MAX}.

The resultant data are displayed in Figure 4.2. Figure 4.2 shows a 1/100 dilution of crude membrane yielded an ^{125}I-GLP-1(7-36) total binding value of 8858 cpm, total counts added to each well was 60813 cpm, therefore this membrane dilution was too low. A 1/200 crude membrane dilution resulted in a total binding value of 4202 cpm which is below 10 % of 60813 cpm, with negligible non-specific binding. This value was acceptable and within limitations, therefore a crude membrane dilution of 1/200 was employed for the rest of the radioligand binding assays exemplified within this chapter.

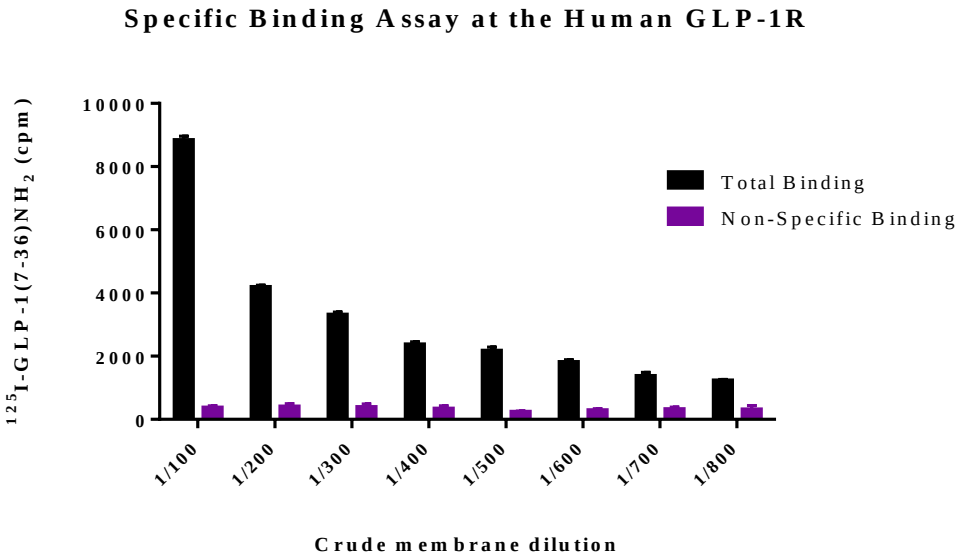

Figure 4.2. Specific binding of radiolabelled GLP-1(7-36) at the hGLP-1R obtained from crude membrane preparations of HEK-293 cells.

An average of 60813 cpm ^{125}I-GLP-1(7-36) were added to each well, the resulting cpm shown as bars represent the average of a membrane dilution performed in triplicate, the S.E.M for each value are shown as error bars. The 1/200 membrane dilution was selected as the optimal dilution as total binding cpm is < 10% total counts added to the assay (4202 cpm < 6081 cpm).

To quantify protein content within the crude membrane preparations in order that B_{MAX} could be calculated as an approximation of receptor numbers within the sample, a bicinchoninic acid (BCA) assay was performed. A standard curve was created with a known concentration of protein using bovine serum albumin as standard with the resultant absorbance at 562 nm, the raw data of which is shown in Table 4.1 and the graph shown in Figure 4.3. Simultaneously, a crude membrane preparation was subject to a number of dilutions and was quantified for absorbance at 562 nm, the raw data is shown in Table 4.2. The BCA standard assay was analysed using GraphPad Prism 6.0 and the linear equation from which was determined to be $y = 0.5624x + 0.01129$, where x and y represent the protein concentration and the absorbance (562 nm) respectively. The crude membrane dilution absorbance range were used to quantify the concentration of protein within each sample according to this equation, and the average protein content within the crude membrane preparation was determined to be 7.6 ± 0.3 mg/mL (Table 4.2). These values were used to quantify B_{MAX} following homologous competition binding assays as exemplified later in this chapter.

[BSA] (mg/mL)	Absorbance (562 nm)			Average Absorbance (562 nm)
0.0	0.000	0.000	0.000	0.000
0.2	0.128	0.125	0.123	0.125
0.4	0.248	0.255	0.243	0.249
0.6	0.360	0.351	0.363	0.358
0.8	0.462	0.452	0.453	0.456
1.0	0.577	0.573	0.552	0.567

Table 4.1. Absorbance (562 nm) from the standard BCA assay.

The raw data was collected in triplicate and used to construct Figure 4.3.

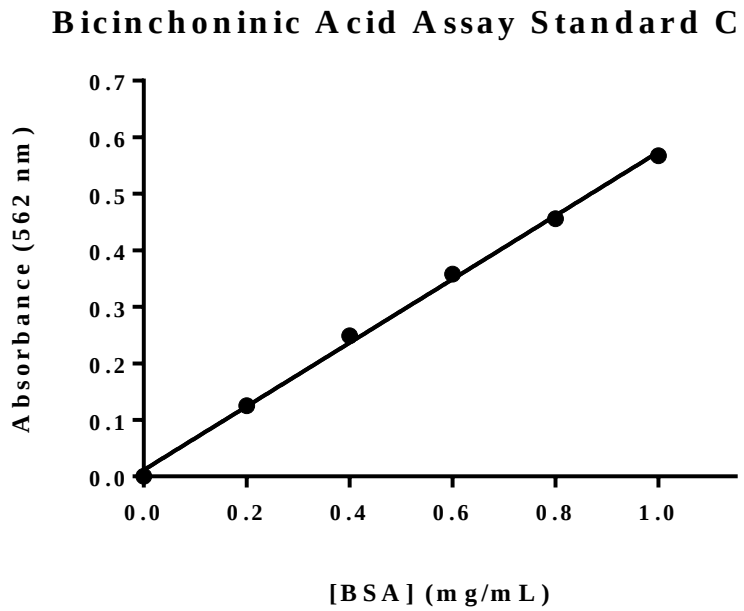

Figure 4.3. BCA assay standard curve.

Values were performed in triplicate and the average plotted on the graph with error bars portraying the S.E.M. Associated data are shown in Table 4.1. The equation of this standard curve is y = 0.5624x + 0.01129 and was used to quantify the protein content of the crude membrane preparations as shown in Table 4.2.

Membrane dilution	Absorbance (562 nm)			Average Absorbance (Y)	Protein in sample (mg/mL) (x)	Total Protein (mg/mL)
1 in 5	0.705	0.702	0.681	0.696	1.217	
1 in 10	0.384	0.378	0.390	0.384	0.663	6.627
1 in 20	0.241	0.241	0.245	0.242	0.411	8.216
1 in 30	0.157	0.159	0.157	0.158	0.260	7.808
1 in 40	0.115	0.122	0.123	0.120	0.193	7.732
1 in 50	0.127	0.106	0.105	0.113	0.180	
				Membrane preparation protein content (mg/mL) ± S.E.M		**7.6 ± 0.3**

Table 4.2. Absorbance (562 nm) readings of crude membrane dilutions, associated protein content in samples and total protein content in the crude membrane preparation.

Absorbance (562 nm) values displayed here and in Table 4.1 are blank corrected. The average absorbance (y) was used to solve the equation $y = 0.5624x + 0.01129$ where x represents the protein content in the sample. The dilution factor of the sample was then taken into consideration for those samples selected. The average total protein values were solved to give an average protein content value of 7.6 ± 0.3 mg/mL.

4.4.2. Cross-examination of GLP-1 ligands and their equivalents in Exendin-4

To analyse the relative roles that the various sections of peptide ligands play toward affinity and efficacy, the individual sections of the GLP-1 and Ex4 were analysed by using differently truncated analogues of the peptides to stimulate cAMP accumulation at hGLP-1R expressing cells. The sequences of the peptides used in this study are shown in Figure 4.4 below. The affinity of these peptides for the hGLP-1R was also analysed using competition binding analysis in order to decipher any differences in affinity between the truncated ligands.

Figure 4.4. Peptide sequence alignment of ligands used in Figure 4.5.

Purple numbering denotes residue positions of the Ex4 peptide and truncated variants thereof, and blue numbering denotes residue positions of the GLP-1 peptides. Those residues corresponding to the numerical positioning indicators have been underlined. Note the different numbering between the two peptides. The individual domains are highlighted as follows: the hypothesised amino region (N) as yellow; the helical (H) region as green; the Ex-region (Ex) as blue. All peptides used in this study were C-terminally amidated.

The truncated ligands of GLP-1 and exendin were custom synthesised to incorporate and omit specific sections of the peptide believed to be important for certain characteristics. The helical 'H-region' of GLP-1 as highlighted green in Figure 4.4 is known to adopt an α-helical conformation (Underwood *et al.*, 2010) as shown in structural analysis, and is thought to confer affinity to the two-domain binding model. The 'N-region' encompasses the first 8 amino-terminal residues as highlighted yellow in Figure 4.4, and are thought to provide efficacy in the two-domain binding model. The extended 'Ex-region' located C-terminally to the H-region, exclusively in Ex4 peptides, is highlighted blue in Figure 4.4, and is thought to confer extra affinity to the rat GLP-1R, but not the human GLP-1R (Mann

et al., 2010b). The peptides used in this study contain variations of the N-, H-, and Ex-regions so that the addition or omission of these regions can be analysed with regards to activity and affinity. In addition to observing the roles of the N-, H-, and Ex-regions, the effect of loss of the first two amino-terminal residues is studied using GLP-1(9-36) and Ex4(3-39) at the hGLP-1R.

The loss of the first two most N-terminally located residues in both ligands had a profound effect on potency, which was more pronounced in GLP-1. Potency was reduced over 1,800-fold in exendin; the EC_{50} of 7.2 x 10^{-13} for Ex4(1-39) was increased to 1.3 x 10^{-9} M in Ex4(3-39) (Figure 4.5.A), whereas potency was reduced over 21,700-fold in GLP-1 peptide ligands, where GLP-1(9-36) achieved an EC_{50} of 1.3 x 10^{-7} M in comparison to an EC_{50} of 6.2 x 10^{-12} M in GLP-1(7-36) (Figure 4.5.C).

The affinities of the ligands for crude membranes were affected in a similar manner, whereby the truncation of the first two residues from the amino-terminus had a more pronounced effect at GLP-1 peptides. Only a five-fold decrease in affinity was observed in Ex4; Ex4(1-39) IC_{50} was 1.4 x 10^{-9} M whereas Ex4(3-39) IC_{50} was 6.9 x 10^{-9} M (Figure 4.5.B), yet over a 110-fold decrease in affinity was observed in the GLP-1 peptides: GLP-1(7-36) IC_{50} was 1.8 x 10^{-9} M, yet the IC_{50} for GLP-1(9-36) was 2.0 x 10^{-7} M (Figure 4.5.D).

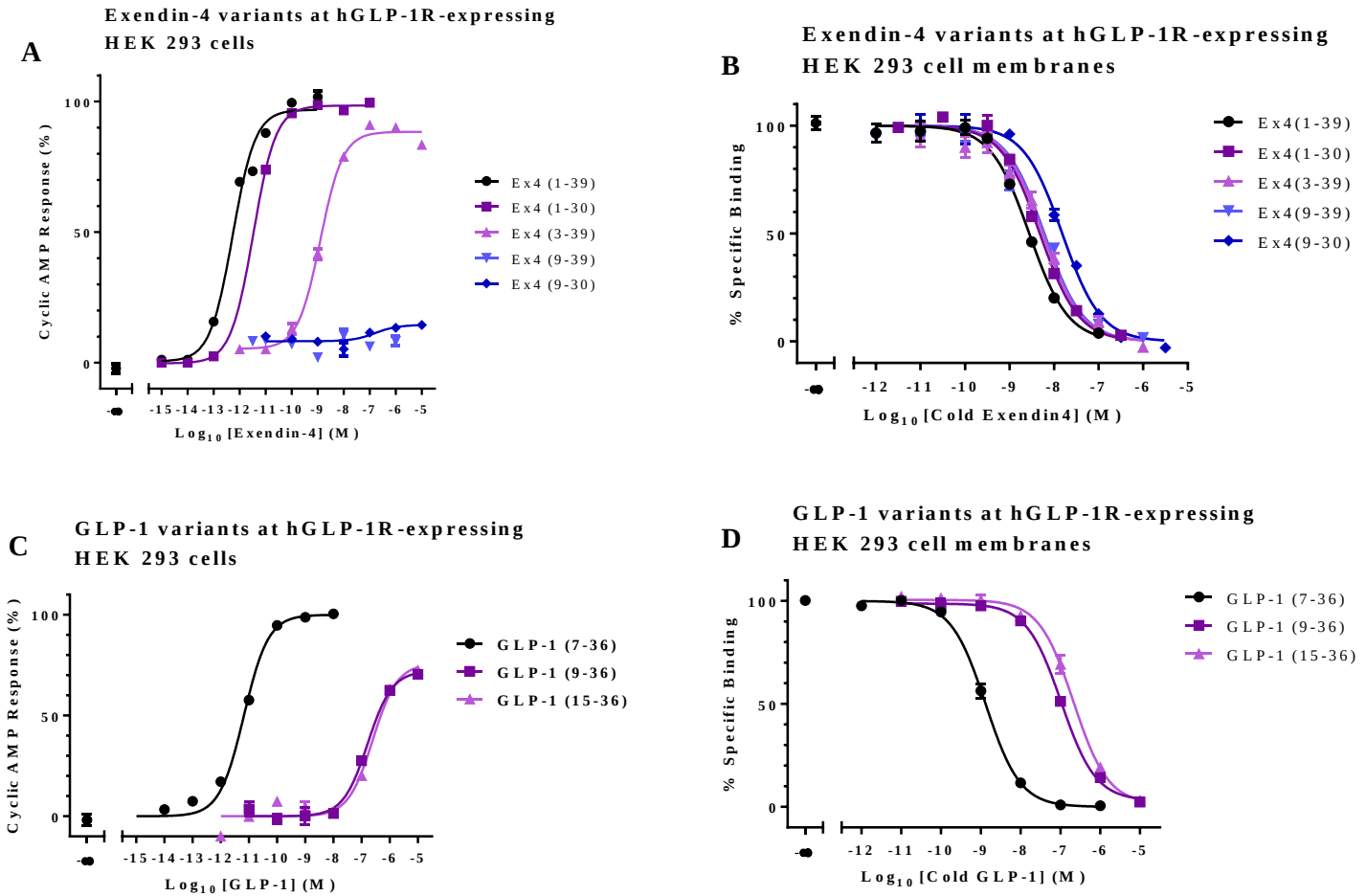

Figure 4.5 Cyclic AMP dose-response curves and competition binding profiles of GLP-1 and Ex4 and truncations thereof at GLP-1R.

Cyclic AMP dose-response curves are shown in parts **A.** and **C.** for Ex4 and GLP-1 ligands respectively. Peptide-induced cAMP response was normalised to the top and bottom of the full agonist curves. Affinity competition curves are shown in parts **B.** and **D.** for Ex4 and GLP-1 ligands respectively. Unlabelled ligands competed off 75 pM ^{125}I-GLP-1(7-36) and data expressed as % specific binding. All curves are representative of n=3 independent experiments. The sequences of the ligands used are shown in Figure 4.4 and the resultant statistical data in Table 4.3.

Removal of the amino-region from GLP-1(7-36) to yield GLP-1(15-36), leaving just the H-region, resulted in a large reduction in potency over the full length peptide. Over a 37,500-fold reduction in potency was observed alongside a 254-fold reduction in affinity at the hGLP-1R (Figures 4.5.C and D, Table 4.3). Interestingly, the % E_{MAX} and pEC_{50} of GLP-1(15-36) and GLP-1(9-36) were the same, yet the affinity of GLP-1(15-36) for the receptor was half that of GLP-1(9-36), suggesting there were residues between positions 10 and 14 which made an additional interaction with the receptor, crucial for affinity, but not for activity.

	Peptide characteristics at the hGLP-1R		
	***p*EC$_{50}$**	**% E$_{MAX}$**	***p*IC$_{50}$**
Ex4(1-39)	12.14 ± 0.03	100	8.84 ± 0.22
Ex4(1-30)	11.42 ± 0.02	100.20 ± 0.67	8.80 ± 0.40
Ex4(3-39)	8.87 ± 0.03	80.83 ± 2.29	8.16 ± 0.04
Ex4(9-39)	ND	ND	8.18 ± 0.05
Ex4(9-30)	8.56 ± 1.26	16.80 ± 4.7	7.63 ± 0.09
GLP-1(7-36)	11.21 ± 0.11	100	8.75 ± 0.07
GLP-1(9-36)	6.87 ± 0.11	75.99 ± 1.25	6.70 ± 0.14
GLP-1(15-36)	6.63 ± 0.10	76.77 ± 2.19	6.34 ± 0.19

Table 4.3. Binding and activation properties of various peptides at the human GLP-1 receptor.

Mean pEC_{50} and pIC_{50} values ± S.E.M. from at least three independent experiments (n=3) are shown. % E_{MAX} is relative to the maximal signal produced by full agonists GLP-1 or Exendin-4. ND means that no value could be determined.

The effects of N-region truncation of Ex4 peptides can be analysed by comparison of full-length and Ex-domain truncated exendin variants: Ex4(1-39)/Ex4(9-39), and Ex4(1-30)/Ex4(9-30) (Figure 4.5, Table 4.3). Removal of the first 8 residues of Ex4(1-30) to give Ex4(9-30) resulted in a 1,396-fold reduction in potency with an 83.2% reduction in activity, yet affinity readings for the Ex-domain-less Ex4 peptides were reduced only 15-fold. Comparison of full-length Ex4(1-39) with amino-region truncated Ex4(9-39) gave similar results to the Ex-region truncated Ex4 peptides. Loss of the first 8 residues of Ex4(1-39) resulted in total loss of activation with a modest reduction in affinity for the receptor. The IC_{50} value for the fully intact peptide versus Ex4(9-39) showed only a 5-fold reduction in affinity (Table 4.3). These data demonstrated the amino-region of Ex4 ligands were required for activation of GLP-1R, and most of their affinity-providing residues for the receptor resided within the H-region as affinity

remained very similar between the two peptide analogues. These results also suggest the N-region of the exendin peptides is more critical to providing activity to GLP-1R than the N-region of the GLP-1 peptides.

The next part of this study probes the N- and H-regions of GLP-1 individually by the use of N- and H-region truncated peptides to specifically determine which residues contribute toward efficacy, and the level of truncation that can be tolerated within the peptide.

4.4.3 Analysis of the amino and helical region of GLP-1

The ability of GLP-1(15-36) to activate the GLP-1R, despite having lost the activity-providing amino-region according to the two-domain model, prompted further investigation. Multiple peptides were custom synthesised to pin-point the minimal peptide sequence required for receptor activation.

Peptides were designed to incorporate fewer residues within the *amino*-region by truncating the peptide amino-terminally from GLP-1(15-36) to GLP-1(18-36) (Figure 4.6). These were analysed through cAMP accumulation and competition affinity binding studies by Dr. Nasr. GLP-1(15-36) did activate the receptor, yet further truncation resulted in total loss of activity without any significant loss of affinity for the receptor (Table 4.4).

	7 15 20 30 36
GLP-1(7-36)	**H**AEGTFTS**D**VSSY**L**EGQAAKEFI**A**WLVKG**R**
GLP-1(15-36)	**D**VSSY**L**EGQAAKEFI**A**WLVKG**R**
GLP-1(16-36)	VSSY**L**EGQAAKEFI**A**WLVKG**R**
GLP-1(17-36)	SSY**L**EGQAAKEFI**A**WLVKG**R**
GLP-1(18-36)	SY**L**EGQAAKEFI**A**WLVKG**R**
GLP-1(7-14)	**H**AEGTFTS
GLP-1(7-15)	**H**AEGTFTS**D**
GLP-1(7-16)	**H**AEGTFTS**D**V
GLP-1(7-17)	**H**AEGTFTS**D**VS
GLP-1(7-18)	**H**AEGTFTS**D**VSS
GLP-1(7-19)	**H**AEGTFTS**D**VSS**Y**
	7 15 19

Figure 4.6. Sequences of N- and C-terminally truncated GLP-1 peptides used by Dr. Nasr.

The purple numbering system denotes the position of residues highlighted bold in the sequence.

A seperate sequential set of peptides were then designed to incorporate fewer residues from the *helical*-region of GLP-1 as possible, starting with GLP-1(7-19) and truncating carboxyl-terminally until residue 14 (terminating at GLP-1(7-14)) to test the hypothesis that D15 is crucial for receptor activation (Figure 4.6). The results from cAMP accumulation and competition affinity analysis (also performed by Dr. Nasr, unpublished data) showed that GLP-1(7-19) was a full agonist with low potency (Table 4.4). Further C-terminal truncation to GLP-1(7-18) and (7-17) was followed by a slight reduction in potency, yet GLP-1(7-16) was incapable of receptor activation (Table 4.4). None of the C-terminally truncated peptides displayed any detectable level of binding at the GLP-1R. This is consistent with the two-domain theory, hypothesising the H-region contributes to affinity in the binding system.

Dr. Nasr's binding and efficacy table of truncated GLP-1 peptides at hGLP-1R			
	***p*EC$_{50}$**	***p*IC$_{50}$**	**% E$_{MAX}$**
GLP-1(7-36)	10.89 ± 0.29	9.24 ± 0.12	100
GLP-1(7-14)	ND	ND	ND
GLP-1(7-15)	ND	ND	ND
GLP-1(7-16)	ND	ND	ND
GLP-1(7-17)	4.48 ± 0.19	ND	96.8 ± 5
GLP-1(7-18)	4.57 ± 0.12	ND	89.2 ± 11
GLP-1(7-19)	4.76 ± 0.03	ND	102.5 ± 5
GLP-1(15-36)	6.81 ± 0.08	6.94 ± 0.14	93.7 ± 1
GLP-1(16-36)	ND	6.68 ± 0.18	ND
GLP-1(17-36)	ND	6.92 ± 0.09	ND
GLP-1(18-36)	ND	6.60 ± 0.04	ND

Table 4.4. Binding and activation data of N- and C-terminally truncated GLP-1 peptides at the human GLP-1 receptor.

Mean *p*EC$_{50}$ and *p*IC$_{50}$ values ± S.E.M. from at least three independent experiments (n=3) are shown. % E$_{MAX}$ is relative to the maximal signal produced by full agonist GLP-1(7-36). ND means that no value could be determined. Data obtained by Dr. Nasr, permission was granted to use these data in this thesis.

4.4.4 Analysis of D15 for GLP-1 peptide-mediated GLP-1R activation

The negatively charged side-chain of D15 was investigated as the critical activating moiety by designing D15A peptides in the full length GLP-1(7-36), N-terminally truncated GLP-1(15-36) and C-terminally truncated GLP-1(7-17) peptides (Figure 4.7).

```
                      7       15    20          30    36
GLP-1(7-36)           HAEGTFTSDVSSYLEGQAAKEFIAWLVKGR
GLP-1(7-36) D15A      HAEGTFTSAVSSYLEGQAAKEFIAWLVKGR
GLP-1(15-36)                DVSSYLEGQAAKEFIAWLVKGR
GLP-1(15-36) D15A           AVSSYLEGQAAKEFIAWLVKGR
GLP-1(7-17)           HAEGTFTSDVS
GLP-1(7-17) D15A      HAEGTFTSAVS
                      7       15
```

Figure 4.7. D15A-mutated GLP-1 peptide sequences used in Figure 4.8.

Purple numbering denotes the position of residues highlighted in bold. Residues mutated to alanine are highlighted purple.

The D15A mutation in the GLP-1(15-36) peptide resulted in substantial loss of activity at the GLP-1R, from a 94% response in wild type peptide to a 20% response using the mutant peptide. The S.E.M. of the % activity of GLP-1(15-36)D15A was considerable, over 25% of the total activity achieved, therefore it is debatable if GLP-1(15-36)D15A can be regarded as an agonist. Potency of GLP-1(15-36)D15A was reduced 2.5-fold in comparison to the wild type peptide, with a low S.E.M., suggesting the $p\mathrm{EC}_{50}$ is reproducible but $\mathrm{E}_{\mathrm{MAX}}$ is not, therefore it is perhaps best to regard it as a poor partial agonist. Interestingly, the D15A mutation at GLP-1(15-36) increased affinity of the peptide for the receptor 2.5-fold in comparison to the wild-type peptide.

The D15A mutation in the full-length GLP-1(7-36) peptide reduced potency and affinity of the ligand considerably at the GLP-1R, yet maximal activity was unchanged (Figure 4.8, Table 4.5). Introduction of alanine in place of aspartic acid in the GLP-1(7-36) ligand resulted in a 23-fold decrease in potency, concomitant with an 18-fold decrease in affinity of the peptide at the receptor, thus, the rightward-shift in potency may be attributed to the reduction in affinity.

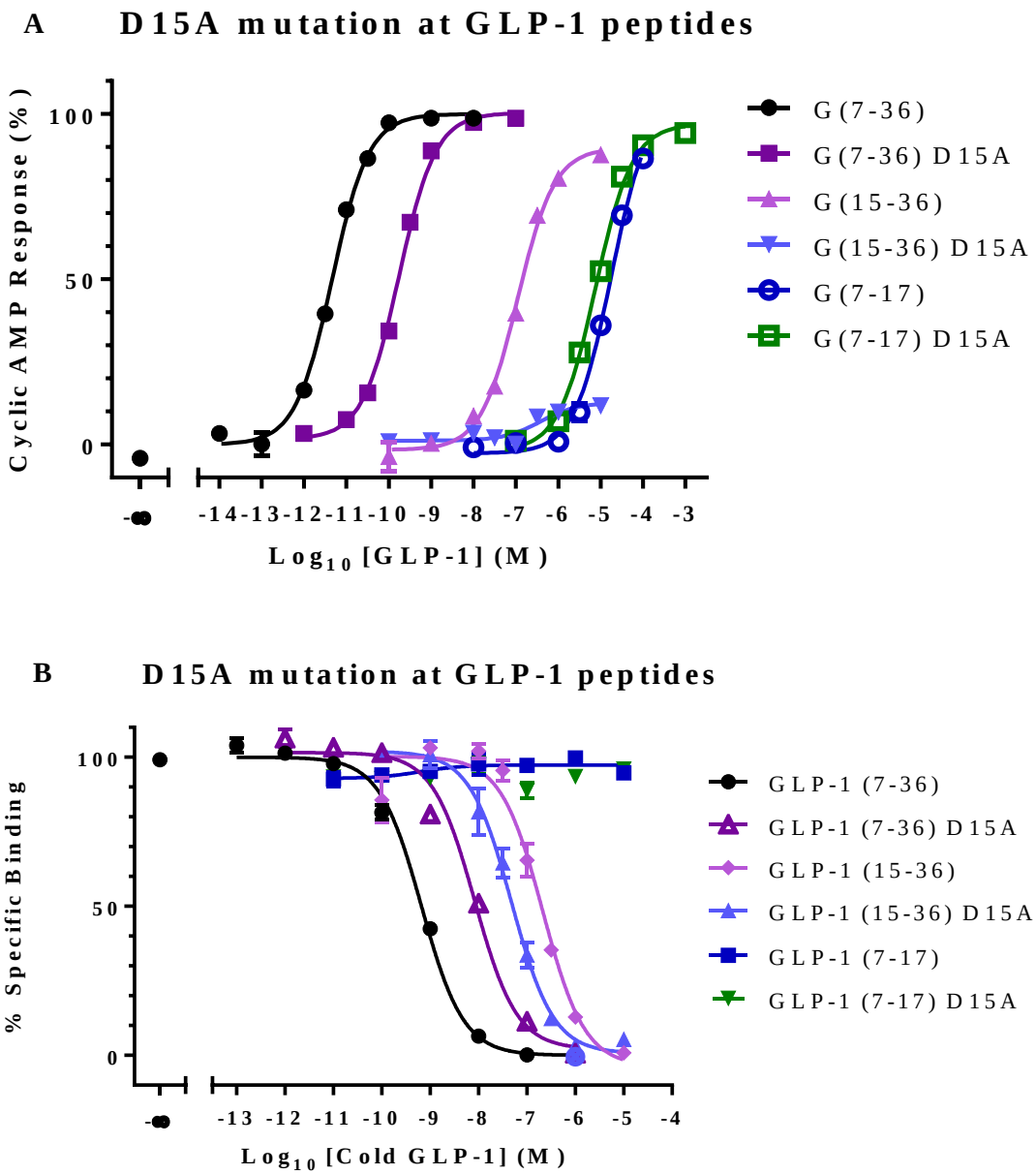

Figure 4.8. Activation and binding profiles of GLP-1 peptides and their D15A mutated counterparts.

Graphs show results from one individual experiment which are representative of n=3 separate cAMP dose-response curves **(A)** and competition affinity binding curves **(B)** for the GLP-1 peptides displayed in Figure 4.7. Associated statistical results are displayed in Table 4.5. Cyclic AMP response is quantified as a percentage of the maximal response as given by 10 nM of the full agonists. Unlabelled ligands competed against 75 pM ^{125}I-GLP-1(7-36)amide for binding at crude membrane preparations expressing human GLP-1R, and the data expressed as a percentage of specific binding.

The affinity of the C-terminally truncated peptide GLP-1(7-17) for the GLP-1R could not be quantified, suggesting it was unable to compete against ^{125}I-GLP-1(7-36) for receptor binding. The D15A mutation did not affect affinity of the GLP-1(7-17) peptide to a measurable level. Maximal activity and potency of the mutated GLP-1(7-17)D15A peptide at hGLP-1R remained unchanged (Table 4.5).

These data show that the D15A mutation is well tolerated in the poor agonist GLP-1(7-17). However the D15A mutation reduces both potency and affinity in the full-length peptide GLP-1(7-36) without affecting maximal activity, and considerably reduces activity in the N-terminally truncated GLP-1(15-36) peptide without significantly altering affinity.

	D15A GLP-1 mutant peptide response		
	***p*EC$_{50}$**	**% E$_{MAX}$**	***p*IC$_{50}$**
GLP-1(7-36)	11.26 ± 0.04	100.0 ± 0.0	9.26 ± 0.11
GLP-1(7-36)D15A	9.89 ± 0.07	100.06 ± 0.76	8.01 ± 0.04
GLP-1(15-36)	6.40 ± 0.19	93.74 ± 1.34	6.94 ± 0.14
GLP-1(15-36)D15A	6.81 ± 0.08	19.54 ± 5.94	7.37 ± 0.05
GLP-1(7-17)	4.84 ± 0.31	106.40 ± 4.75	ND
GLP-1(7-17)D15A	5.00 ± 0.06	98.01 ± 0.61	ND

Table 4.5. Binding and activation data of N- and C-terminally truncated GLP-1 peptides with D15A mutations at human GLP-1 receptor.

Table displays the mean *p*EC$_{50}$ and *p*IC$_{50}$ values ± S.E.M. from three independent experiments (n=3). % E$_{MAX}$ is relative to the maximal signal produced by the full agonist GLP-1(7-36). ND means that no value could be determined. All peptides used were C-terminally amidated.

4.4.5 Polarity at position 15 is required for maximal GLP-1(15-36) activity

Further investigation of the characteristics observed above was carried out by substituting aspartic acid at position 15 in GLP-1(15-36) peptides to other residues to test the hypothesis that it is the negatively charged side chain of D15 that makes the critical activating interaction. The peptides used are shown in Figure 4.9 and include the mutated residues: GLP-1(15-36)D15E, GLP-1(15-36)D15A and GLP-1(15-36)D15G, to investigate the effect of mutation at position 15 of GLP-1(15-36).

	7 15 20 30 36
GLP-1(7-36)	**H**AEGTFTS**D**VSSY**L**EGQAAKEFI**A**WLVKG**R**
GLP-1(15-36)	**D**VSSY**L**EGQAAKEFI**A**WLVKG**R**
GLP-1(15-36)D15A	**A**VSSY**L**EGQAAKEFI**A**WLVKG**R**
GLP-1(15-36)D15E	**E**VSSY**L**EGQAAKEFI**A**WLVKG**R**
GLP-1(15-36)D15G	**G**VSSY**L**EGQAAKEFI**A**WLVKG**R**
	7 15 20 30 36

Figure 4.9. The D15X-mutated GLP-1(15-36) peptide sequences used in Figure 4.10.

Peptides were modified at the D15 residues to residues with different properties to explore the nature of the interaction of the amino acid at position 15 of GLP-1(15-36). Purple numbering denotes the position of residues highlighted in bold. All peptides used in this study were C-terminally amidated.

Mutation of the side-chain of residue D15 at GLP-1(15-36) peptides result in different activation profiles depending on the nature of the side-chain (Figure 4.10.A, Table 4.6), yet affinity of the peptide for the receptor as seen through competition affinity binding studies remained unchanged (Figure 4.10.B, Table 4.6). The mutations of D15 of the GLP-1(15-36) all resulted in increased affinity for the GLP-1R; D15G resulted in a 2-fold increased affinity, D15E resulted in a 3.5-fold increase, and D15A resulted in a 4.5-fold increase.

The GLP-1(15-36) D15G mutation did not affect the potency of the peptide, yet the maximal response at the receptor was almost halved in comparison to the wild-type truncated ligand (Table 4.6, Figure 4.10.A). As previously demonstrated, the GLP-1(15-36)D15A mutation resulted in loss of efficacy at GLP-1R-expressing cells (Table 4.5, Table 4.6) to poor/non-agonist status. Interestingly, the D15E mutation did not result in reduction of maximal response in comparison to the wild-type GLP-1(15-36) peptide, suggesting that a negative charge is required at position 15 for maximal peptide efficacy. Indeed, the D15E mutation also resulted in increased potency for the receptor, from an EC_{50} of 3.16×10^{-7} M to 3.98×10^{-8} M; an 8-fold increase in potency.

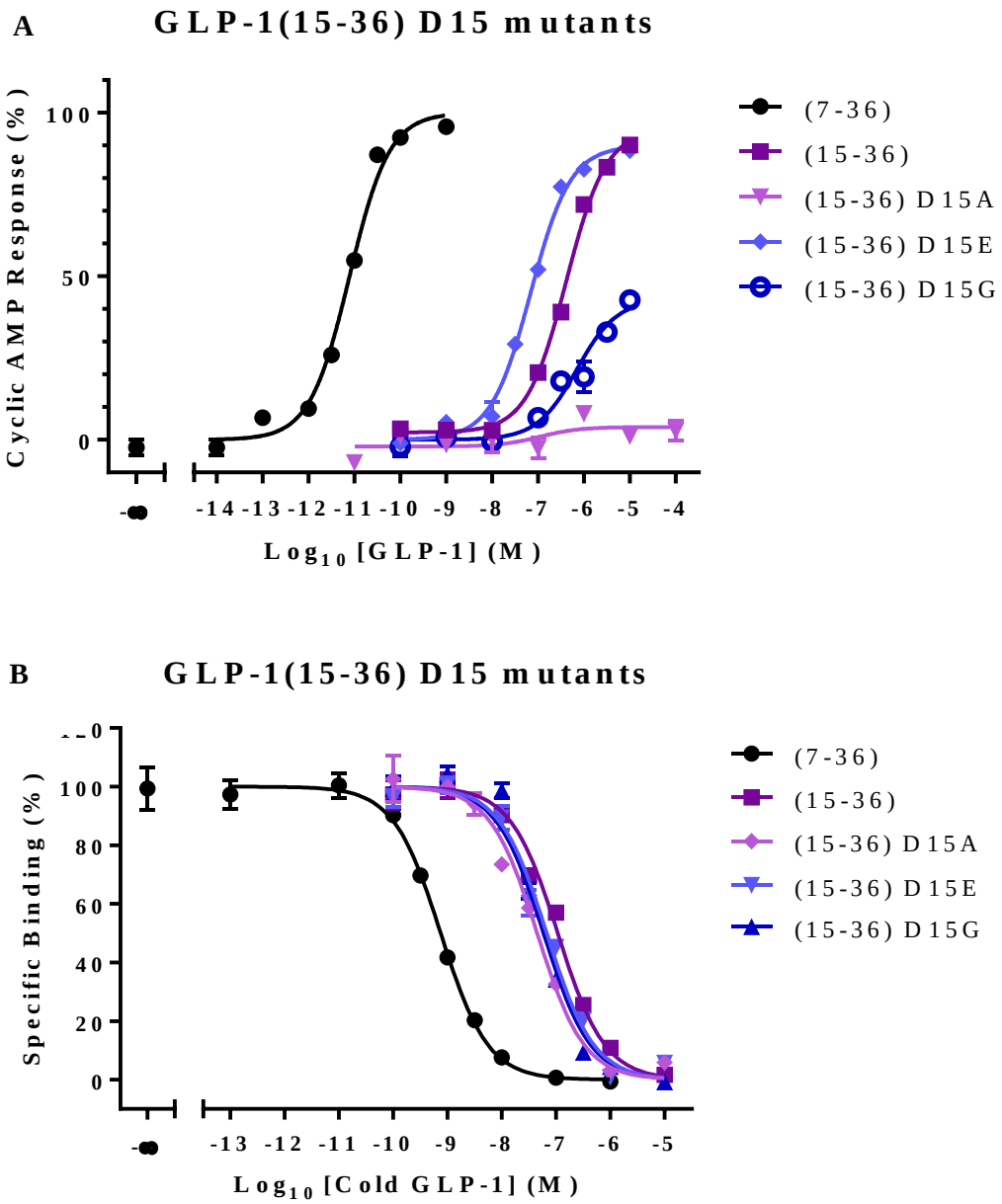

Figure 4.10. Binding and activation profiles of GLP-1(15-36) peptides and their D15X mutated counterparts.

Graphs shown are representative of n=3 cAMP dose-response curves **(A)** and competition affinity binding curves **(B)** for the GLP-1 peptides displayed in Figure 4.9. Cyclic AMP response is quantified as a percentage of the maximal response as given by 10 nM of the full agonist GLP-1(7-36). Unlabelled ligands competed against 75 pM ^{125}I-GLP-1(7-36) for hGLP-1R binding at crude membrane preparations, and the data expressed as a percentage of specific binding. Associated statistical results are shown in Table 4.6.

	GLP-1(15-36) D15 mutant response		
	***p*EC$_{50}$**	**% E$_{MAX}$**	***p*IC$_{50}$**
GLP-1(7-36)	11.21 ± 0.10	100 ± 0.0	9.21 ± 0.10
GLP-1(15-36)	6.50 ± 0.07	92.05 ± 2.04	7.02 ± 0.06
GLP-1(15-36)D15A	7.88 ± 0.47	11.45 ± 4.98	7.67 ± 0.32
GLP-1(15-36)D15E	7.40 ± 0.17	89.17 ± 4.85	7.57 ± 0.20
GLP-1(15-36)D15G	6.60 ± 0.25	48.63 ± 6.55	7.35 ± 0.12

Table 4.6. Binding and activation data of N-terminally truncated GLP-1(15-36) peptides with D15X mutations at the human GLP-1 receptor.

Table displays the mean *p*EC$_{50}$ and *p*IC$_{50}$ values ± S.E.M. from three independent experiments (n=3). % E$_{MAX}$ is relative to the maximal signal produced by the full agonist GLP-1(7-36). Corresponding peptide sequences and dose-response curves are shown in Figure 4.9 and 4.10 respectively.

4.4.6 Exploring the nature of D15, V16 and S17 at GLP-1(7-17) ligands

Data from section 4.4.3 showed that further C-terminal truncation of GLP-1(7-17) to GLP-1(7-16) and smaller peptides, resulted in loss of efficacy at the GLP-1R, suggesting that residue S17 is required for efficacy in this 11-mer. Section 4.4.3 also showed residue D15 was required for activity in the amino-terminally truncated GLP-1(15-36), these data together suggested the 15-DVS-17 region was required for truncated peptide activity, and perhaps full peptide activity.

Residues D15, V16 and S17 were mutated in GLP-1(7-17) peptides to glycine residues (Figure 4.11), as knocking out an activating residue in such a low potency peptide would most likely result in ablation of efficacy, allowing identification of the activating residue. A cAMP dose-response curve was performed at FLP-IN HEK 293 cells constitutively overexpressing the hGLP-1R, and competition affinity curves were performed on membranes harvested from these cells, the resultant graphs are shown in Figure 4.12 with accompanying data in Table 4.7.

	7 15 20 30 36
GLP-1(7-36)	HAEGTFTSDVSSYLEGQAAKEFIAWLVKGR
GLP-1(7-17)	HAEGTFTSDVS
GLP-1(7-17)D15G	HAEGTFTS**G**VS
GLP-1(7-17)V16G	HAEGTFTSD**G**S
GLP-1(7-17)S17G	HAEGTFTSDV**G**
GLP-1(7-17)D15A	HAEGTFTS**A**VS
	7 15

Figure 4.11. The D15X, V16G and S17G-mutated GLP-1(7-17) peptide sequences used in Figure 4.12

Residues mutated are highlighted purple. The numbering system used is standard GLP-1 peptide numbering starting at position 7 and is displayed both above and below the peptide sequences. All peptides used were C-terminally amidated.

No affinity binding data could be gleaned from any of the mutant peptides, demonstrating that glycine mutations in the 15-DVS-17 region of the GLP-1(7-17) peptide did not result in measurably enhanced affinity for the receptor (Figure 4.12.B). The cAMP dose-response curves in Figure 4.12.A showed that a glycine mutation in any of the positions between residue 15 and 17 resulted in an increased potency, yet a reduction in maximal activity. Both D15A and D15G mutations enhanced potency 15.5-fold over wild-type GLP-1(7-17), yet D15G had only 75% maximal efficacy of wild-type, whereas the D15A mutation maintains the efficacy of the wild-type peptide (Table 4.7). GLP-1(7-17)V16G resulted in a 5-fold increase in potency over wild-type, but reduced maximal activity, with 75% activity of wild-type GLP-1(7-17). GLP-1(7-17)S17G had the most pronounced increase in potency of 28.3-fold over wild-type, and retains 91% maximal activity of the wild-type peptide (Table 4.7).

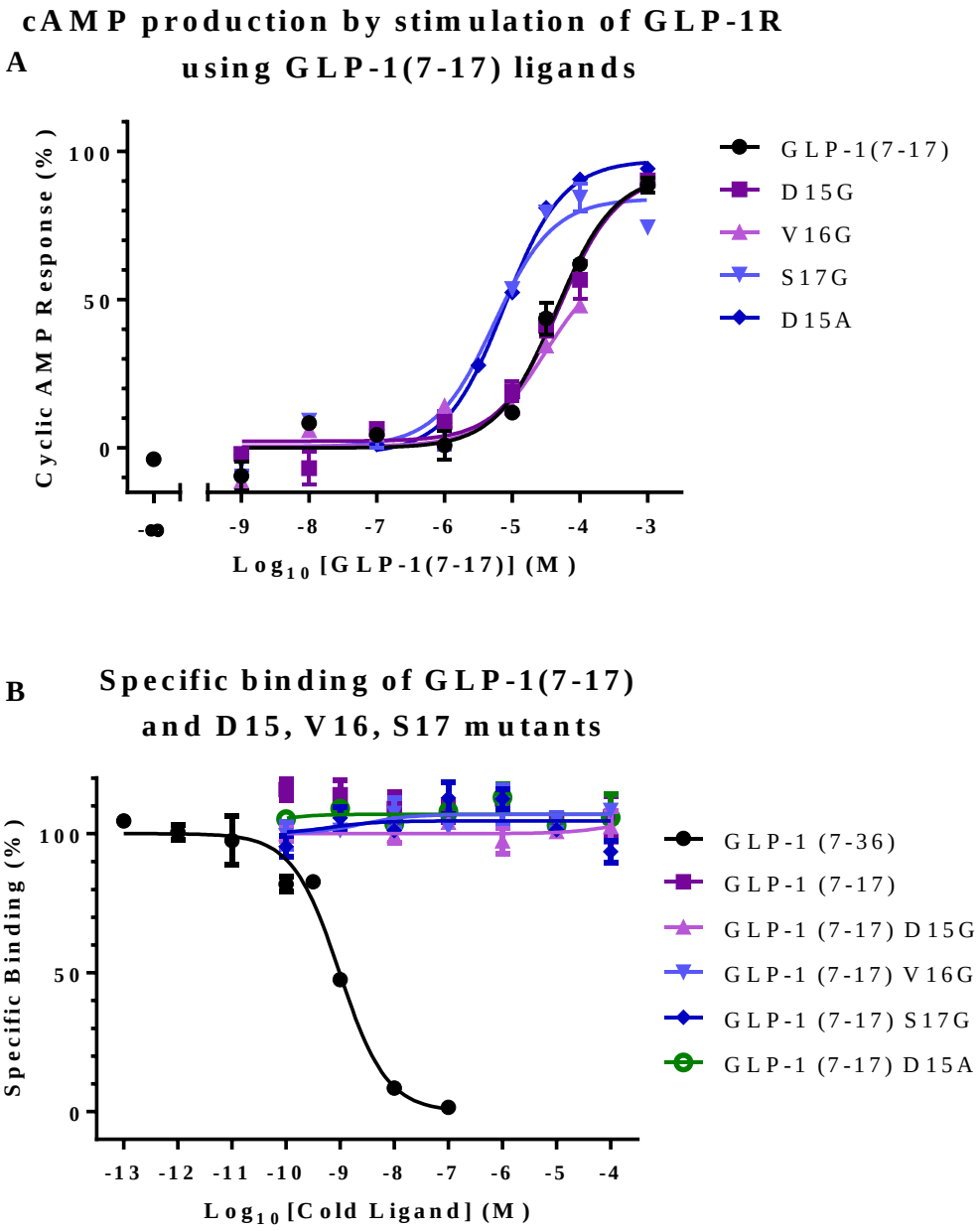

Figure 4.12. Binding and activation profiles of GLP-1(7-17) peptides and their D15, V16 and S17-mutated counterparts.

Graphs shown are representative of n=3 cAMP dose-response curves **(A)** and competition affinity binding curves **(B)** for the GLP-1 peptides displayed in Figure 4.11. Cyclic AMP response is quantified as a percentage of the maximal response as given by 10 nM of the full agonist GLP-1(7-36) (not shown on graph for clarity). Unlabelled 'cold' ligands competed against 75 pM ^{125}I-GLP-1(7-36) for hGLP-1R binding at crude membrane preparations and the data expressed as a percentage of specific binding. Associated statistical results are shown in Table 4.7.

	GLP-1(7-17) D15, V16, S17 mutant responses		
	pEC_{50}	% E_{MAX}	pIC_{50}
GLP-1(7-17)	3.81 ± 0.28	97.28 ± 5.67	ND
GLP-1(7-17)D15G	5.00 ± 0.39	74.72 ± 14.75	ND
GLP-1(7-17)V16G	4.51 ± 0.04	73.16 ± 6.04	ND
GLP-1(7-17)S17G	5.26 ± 0.05	88.86 ± 2.84	ND
GLP-1(7-17)D15A	5.00 ± 0.06	98.01 ± 0.61	ND

Table 4.7. Binding and activation data of C-terminally truncated GLP-1(7-17) peptides with D15, V16 and S17 mutations at the human GLP-1 receptor.

Table displays the mean pEC_{50} and pIC_{50} values ± S.E.M. from three independent experiments (n=3). % E_{MAX} is relative to the maximal signal produced by the full agonist GLP-1(7-36). Corresponding peptide sequences and dose-response curves are shown in Figure 4.11 and Figure 4.12 respectively.

4.4.7 Analysis of 15-DVS-17 in GLP-1 peptides as the activating region

C-terminal GLP-1(7-17) truncation to GLP-1(7-16) and smaller peptides resulted in loss of activity (Table 4.4). Furthermore, N-terminal truncation exceeding GLP-1(15-36) resulted in loss of activity (Table 4.4) without significant loss of peptide affinity. These data taken together suggest the activity-providing residues for GLP-1 peptides reside within the D15, V16 and S17 region. This hypothesis was tested by mutating these three residues to all-glycine residues simultaneously in the GLP-1(7-36), GLP-1(15-36) and GLP-1(7-17) peptides. The primary sequences of these peptides are shown in Figure 4.13, the cAMP responses in Figure 4.14.A, and the affinity competition curves in Figure 4.14.B.

```
                        7       15     20          30     36
GLP-1(7-36)             HAEGTFTSDVSSYLEGQAAKEFIAWLVKGR
GLP-1(7-36)GGG          HAEGTFTSGGGSYLEGQAAKEFIAWLVKGR
GLP-1(15-36)                    DVSSYLEGQAAKEFIAWLVKGR
GLP-1(15-36)GGG                 GGGSYLEGQAAKEFIAWLVKGR
GLP-1(7-17)             HAEGTFTSDVS
GLP-1(7-17)GGG          HAEGTFTSGGG
                        7       15
```

Figure 4.13. GLP-1 peptide sequences used in Figure 4.14.

Full-length GLP-1(7-36), C-terminally truncated GLP-1(7-17) and N-terminally truncated GLP-1(15-36) and their associated mutant peptides with a 15DVS17-15GGG17 mutation are termed GLP-1(x-x)GGG, with the mutated area coloured purple.

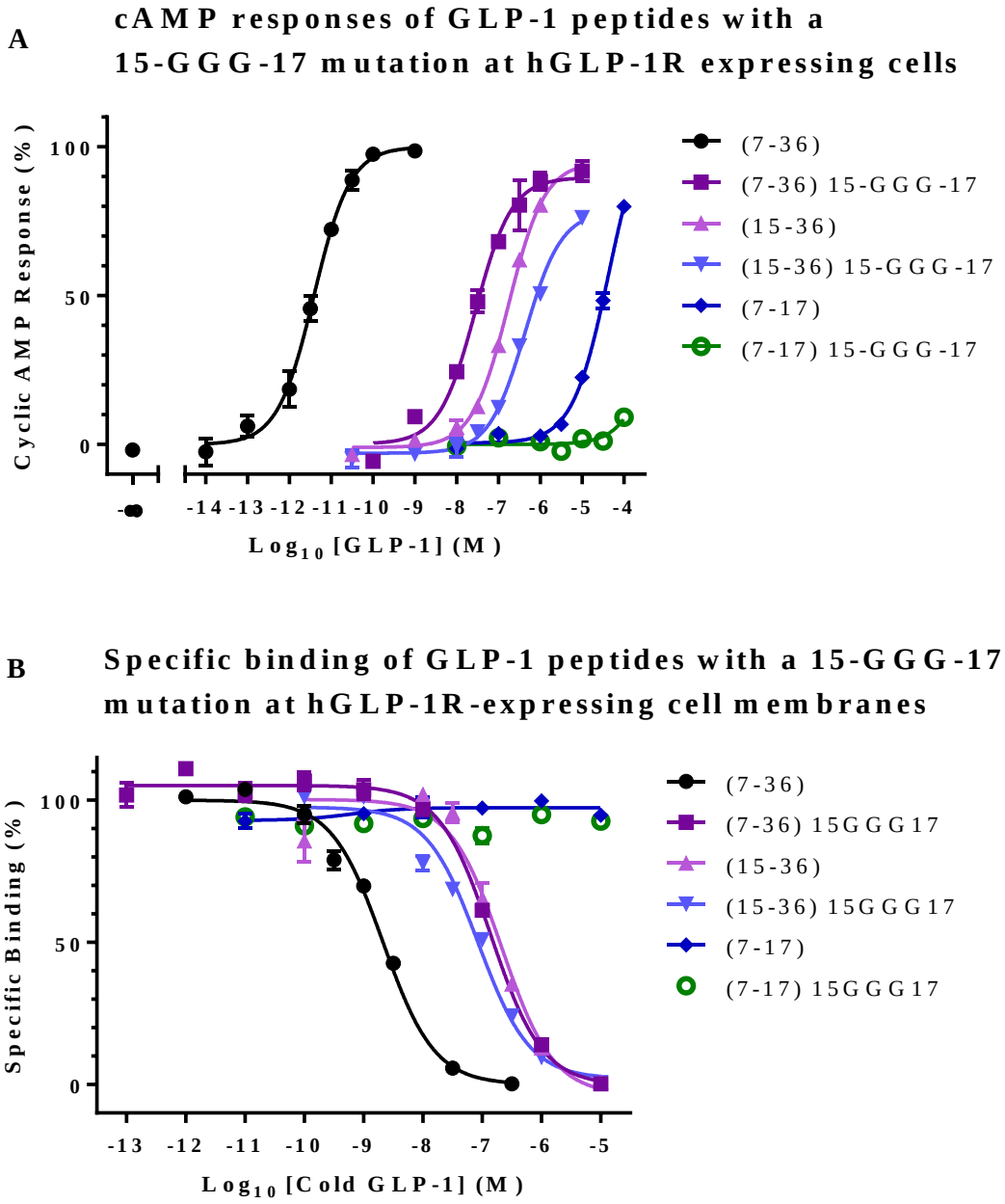

Figure 4.14. Binding and activation profiles of GLP-1(x-x) peptides and their 15DVS17-15GGG17-mutated counterparts.

Graphs shown are representative of n=3 cAMP dose-response curves **(A)** and competition affinity binding curves **(B)** for the GLP-1 peptides displayed in Figure 4.13. Cyclic AMP response is quantified as a percentage of the maximal response as given by 10 nM of the full agonist GLP-1(7-36). Unlabelled 'cold' GLP-1 ligands competed against 75 pM ^{125}I-GLP-1(7-36) for hGLP-1R binding at crude membrane preparations and the data expressed as a percentage of specific binding. Associated statistical results are shown in Table 4.8.

	GLP-1 15-GGG-17 mutant peptide responses		
	***p*EC$_{50}$**	**% E$_{MAX}$**	***p*IC$_{50}$**
GLP-1(7-36)	11.52 ± 0.13	100.0 ± 0.0	9.24 ± 0.12
GLP-1(7-36)GGG	7.43 ± 0.10	80.82 ± 6.66	6.76 ± 0.11
GLP-1(15-36)	6.72 ± 0.13	91.16 ± 1.66	6.94 ± 0.14
GLP-1(15-36)GGG	6.25 ± 0.16	79.59 ± 1.36	7.11 ± 0.07
GLP-1(7-17)	4.84 ± 0.31	106.40 ± 4.75	ND
GLP-1(7-17)GGG	ND	ND	ND

Table 4.8. Binding and activation data of GLP-1(7-36), GLP-1(15-36) and GLP-1(7-17) wild-type peptides and associated 15DVS17-15GGG17 mutated peptides at the human GLP-1 receptor.

Table displays the mean *p*EC$_{50}$ and *p*IC$_{50}$ values ± S.E.M. from three independent experiments (n=3). % E$_{MAX}$ is relative to the maximal signal produced by the full agonist GLP-1(7-36). Corresponding peptide sequences and dose-response curves are shown in Figure 4.13 and Figure 4.14 respectively.

Interestingly, the mutation of section 15-17 to glycine residues in GLP-1(7-17) resulted in obliteration of activity (Figure 4.14.A, Table 4.8) with no detectable binding affinities (Figure 4.14.B), whereas individual mutation of residues 15, 16 and 17 to glycine at GLP-1(7-17) did not result in loss of activity at the GLP-1R (Figure 4.12). In contrast, the same mutation of residues 15-17 in GLP-1(15-36) did not result in loss of activity at GLP-1R (Figure 4.14.A), but did result in a 3-fold reduction of potency in comparison to wild-type GLP-1(15-36), yet the mutant peptide had a 1.5-fold increase in affinity for GLP-1R (Figure 4.14.B). The maximal activity of GLP-1(15-36) was negatively affected by the tri-glycine mutation; achieving 87% of maximal activity achieved by the wild-type peptide (Table 4.8).

The most profound effect of the tri-glycine mutation at position 15-17 was observed in the full length peptide GLP-1(7-36). The tri-glycine mutation in GLP-1(7-36) resulted in a 12,302-fold reduction in potency, concomitant with a 302-fold reduction in peptide affinity for GLP-1R. Maximal activity of mutated GLP-1(7-36) was reduced to 81% in comparison to the wild-type peptide (Figure 4.14, Table 4.8).

4.5 Discussion

4.5.1 Discussion of results

Despite earlier studies suggesting that the first 8 residues of GLP-1 were critical for activity (Montrose-Rafizadeh *et al.* (1997)), the discovery that GLP-1(15-36), which completely lacks these residues, retains intrinsic activity at the GLP-1R requires extension of the two-domain theory. Figures 4.5, 4.8 and 4.10, and Tables 4.3 to 4.6 inclusive showed that GLP-1(15-36) had approximately the same level of potency and efficacy as GLP-1(9-36). These data are in agreement with the findings of Patterson *et al.* (2011) and Donnelly (2012) and are contradictory to the initial findings by Montrose-Rafizadeh *et al.* (1997).

GLP-1(9-36) showed higher affinity for the GLP-1R than GLP-1(15-36), suggesting there is a residue within the 9-15 region of the peptide ligand conferring affinity but not attributing significant efficacy. These findings are in agreement with the Lin and Wang model (Lin & Wang, 2008) which proposes that G10 and D15 of GLP-1 are responsible for the correct orientation and binding pose of the peptide ligand. Losing the region of peptide which contained G10, but not D15, would result in loss of native ligand structure within the N-region, which would thereby impede ligand binding, explaining the loss of affinity observed between GLP-1(9-36) and GLP-1(15-36).

Conversely, the Lin and Wang model of receptor activation proposes F12 of GLP-1 interacts with a hydrophobic cavity on the top on the receptor core domain by means of the hydrophobic effect, which in their model contributed toward amino-region mediated activity. If F12 interacted with a hydrophobic cavity within the core domain, GLP-1(9-36) would presumably be significantly more active than GLP-1(15-36) as GLP-1(15-36) does not possess F12, therefore the data presented within this chapter do not correlate with this proposition. However, F12 may contribute toward affinity rather than efficacy, as GLP-1(9-36) possessed higher affinity for the GLP-1R than GLP-1(15-36), this may be mediated by F12 interacting with the receptor, but not contributing toward efficacy in accordance with the Lin & Wang model.

The observation that GLP-1 ligands containing only 11 residues (GLP-1(7-17)) were capable of receptor activation suggested that *both* the N- and H-regions of GLP-1 are not required for receptor activity, only *one* region is required. Additionally the region (either the N- or H-region) *must* contain the residues 15-17, as further truncation from either the amino-

terminus of GLP-1(15-36), or the carboxyl terminus of GLP-1(7-17) yielded a ligand with no inherent activity, for example GLP-1(7-16) and GLP-1(16-36) were incapable of receptor activity (Table 4.4). These data lead to the conclusions that the critical residues for GLP-1R activation by truncated ligands were residues 15, 16 and 17, and that without these residues the truncated ligands are antagonists (Table 4.4) as GLP-1(16-36), (17-36) and (18-36) still retained receptor affinity but not efficacy. This further implies that this region is in fact the critical region required for receptor activity

Aspartate 15* is postulated to be responsible for maintaining correct ligand pose (Lin & Wang, 2008), Adelhorst *et al.* (1994) found that D15A mutation in full length GLP-1 resulted in no adenylyl cyclase activity and Siegel *et al.* (1999) found that D15 substitution resulted in both loss of efficacy and affinity at the GLP-1R, thus D15 was targeted as a focus point in this study.

D15A mutations were assayed for the effect of the mutation in both N- and H-region truncated peptides, and the full-length GLP-1(7-36) peptide, with interesting outcomes; the D15A mutation in GLP-1(15-36) obliterated peptide activity at the receptor without disrupting affinity, in fact, affinity of GLP-1(15-36)D15A was enhanced over w/t. This is comparable to the proposition that D15 is responsible for holding the ligand in correct orientation, as it is possible the D15A mutation disrupted some intra-helical bonding within the peptide, thereby destroying the tertiary structure of the ligand, making it no longer complementary to the binding pocket or able to interact with appropriate residues. Conversely, it is also feasible that the negative side chain of D15 makes an essential interaction with the receptor, and once this negative charge is removed and replaced with a hydrophobic residue the electrostatic interaction no longer occurred resulting in loss of activity. However, this may not be the case as the GLP-1(15-36)D15G mutated peptide was capable of eliciting a response, with a lower potency and half maximal activity than the wild-type GLP-1(15-36) ligand, yet it may well be the case, as glycine is renowned for its inherent flexibility when part of a peptide chain, therefore the positioning of glycine at the amino terminus may have allowed for enhanced rotamer movement, and the carboxyl backbone of G15 may well interact with a critical binding pocket within the receptor.

It would appear that the negative charge at position 15 in GLP-1(15-36) was required for optimal receptor interaction, as a D15E mutation rendered the peptide more potent in eliciting a cAMP response; however it is interesting that in C-terminally truncated GLP-1(7-17) no change was observed in ligand efficacy upon the D15A mutation. Upon alanine mutation of residue 15 in GLP-1(7-36), a 23-fold reduction in potency was coupled with an 18-fold reduction of affinity for the receptor; these data suggest that D15 played a critical binding function with the receptor. These data suggest that residue 15 is an important residue for the

functionality of the peptide; this may be due to assisting correct ligand orientation, or due to it forming a critical interaction at the receptor, aiding active receptor conformation.

Mapelli *et al.* (2009) demonstrated that in GLP-1(7-17), residues 16 and 17 could be modified by use of biphenylalanine derivitives to produce a peptide that had only 2 orders of magnitude lower potency in comparison to the full length peptide. By further modification of A8 and F12 of GLP-1(7-17) with aminoisobutyric acid and an α-methyl-phenylalanine derivative respectively, they generated a truncated peptide with potency only 2 to 3 fold lower than the full length ligand. This discovery showed that the activating residues invariably reside within the 7*-17* region, and demonstrated further that the helical region is not necessarily required for deliverance of the activating residues to the receptor by providing affinity to the system. Hence residues 15-17 were inspected closely in this chapter, focusing particularly on residues 16 and 17, as Mapelli *et al.* (2009) showed that these could be modified to produce a peptide capable of near w/t potency in a truncated peptide, suggesting these residues are of significant importance to receptor recognition.

Mutation of residues 15, 16 and 17 in GLP-1(7-17), all to glycine residues, knocked out the ability of this peptide to activate the receptor, yet the D15A individual mutation had no effect. When residues 15 to 17 were mutated to glycine residues in the longer GLP-1(15-36) ligand, the result was less catastrophic than in the GLP-1(7-17) peptide. Mutation of residues 15, 16 and 17 in GLP-1(15-36) influenced activity without affecting affinity, whereby the potency was reduced and maximal activity was reduced by 13%, yet the D15A single mutation in GLP-1(15-36) rendered it incapable of receptor activation without a loss in affinity. Indeed, there was a profound effect upon GLP-1(7-36) potency when D15, V16 and S17 were mutated to all-glycine residues, to such an extent that the EC_{50} was reduced four orders of magnitude, and the affinity was affected such that it mimicked the affinity of w/t GLP-1(15-36) for the receptor: a 302-fold reduction in affinity. This showed the all-glycine mutation within residues 15-17 of GLP-1 had a more profound effect upon GLP-1 ligands containing the amino region, from residues 7-15, where the glycine mutations affected both the affinity and potency of the ligand for the receptor, whereas the D15A mutation had more of an effect upon GLP-1(15-36) where activity was knocked out. These data suggest that the critical activity-providing region is veritably located within residues 15, 16 and 17.

The reduction of potency and affinity was not equally weighted between the two peptides GLP-1(9-36) and Ex4(3-39) in comparison to their full-length peptides, despite the same level of N-terminal truncation. Ex4(3-39) was 1,805-fold less potent, yet affinity was reduced only 5-fold in comparison to Ex4(1-39). GLP-1(9-36) was 21,878-fold less potent, and had a 112-fold reduction in affinity in comparison to GLP-1(7-36). The % E_{MAX} between these

two ligands were essentially the same (76 % and 81 %), yet originally both GLP-1(9-36) and Ex4(3-39) were thought to be antagonists or inverse agonists (Vahl *et al*., 2003; Montrose-Rafizadeh *et al*., 1997).

It is clear that the effect of amino-terminal truncation upon activity and affinity are more pronounced in GLP-1 ligands than Ex4 ligands, suggesting different modes of activation (Figure 4.5). The increased helicity of Ex4 ligands may result in an inability to bend and flex to make crucial activating interactions at the GLP-1R like GLP-1 peptides do (Figure 4.15); however data from Chapter 3 of this thesis suggest N-region-less Ex4 peptides still retain the propensity to become an agonist under the right receptor conformation in the presence of allosteric modulator. This is re-iterated in Table 4.3, where Ex4(9-30) is a poor partial agonist with nM activity, suggesting that the residues for activity are still present within the H-region, yet intrinsic activity is substantially reduced by loss of the first 8 residues, but could be rescued in the presence of a GLP-1R allosteric modulator. Nevertheless, GLP-1 ligands still retain ability to activate the GLP-1R after removal of the 'activity-providing' amino-region under the non-modulated receptor conformation, suggesting all is not what it seems with this ligand, and that the two-domain model may not be the entire story for this particular peptide.

4.5.2 The proposed tethered/ slingshot binding model (HAN acronym)

These data suggest that GLP-1 possesses three regions, all critical for maximal receptor activity, with the main activating motif located within the 15-DVS-17 region of the peptide. In a new model proposed here, these three regions are denoted '**N**' for the ami**n**o-terminally located residues which interact with the receptor TMD, approximately H7-S14, '**A**' for the **a**ctivity-providing residues which are D15*, V16* and S17*, and the '**H**' region for the α-**h**elical residues located C-terminally which interact with the receptor NTD. The data presented here suggest that two of the three regions must be retained for partial agonist activity, and activity is not observed in the absence of the **A** region. The implications for the binding model is that the **N** and **H** regions of the ligand bind to the TMD and the NTD of the receptor respectively, acting as a brace, positioning the activating **A** region precisely so it can interact with the receptor, thereby activating it. The main difference with this model and the two-domain model is in the two-domain model efficacy is given to the residues within the **N** domain, whereas in the model presented here, the **N** domain is postulated to account for only the affinity generated within the core domain. Research has shown that a D198A mutation of the ECL1/TM2 region of the GLP-1R resulted in reduced GLP-1(7-36) affinity without loss of activity, and this receptor mutation

affected only GLP-1(7-36) and not GLP-1(15-36) lacking the **N** domain, suggesting the activating **A** domain is separate from the **N** domain (López de Maturana & Donnelly, 2002).

The '**HAN**' model proposes a truncated peptide can retain the ability to activate GLP-1R so long as the '**A**' region is present (Figure 4.15.B i and ii), but for optimal activity and sub-nM potency, both the **H** and **N** regions are required for correct positioning of the activity providing region **A**. Loss of either brace region **N** or **H** would result in reduced affinity and sub-optimal positioning of **A**, thereby resulting in a partial agonist with μM potency (GLP-1(15-36)) or a full agonist with μM potency (GLP-1(7-17)).

In summary, the **HAN** model proposes that the main activity of GLP-1 is derived from the interaction between residues 15*-17* with the receptor TMD which is denoted the **A** interaction. These three residues are held in correct position by the interactions between the **N** domain with the TMD, and the **H** domain with the NTD, acting as a rigid brace structure. A lowered potency agonist is obtained with the combination of the **N** + **A** regions, and partial agonist activity with lowered potency is obtained with the combination of the **H** + **A** regions as exemplified by the data obtained in this chapter. Moreover, GLP-1(15-36)15-GGG-17 was capable of acting as an agonist despite the loss of the side chains on residues 15-17, demonstrating it is most likely the peptide backbone that is responsible for receptor activation within the **A** domain of the peptide ligand.

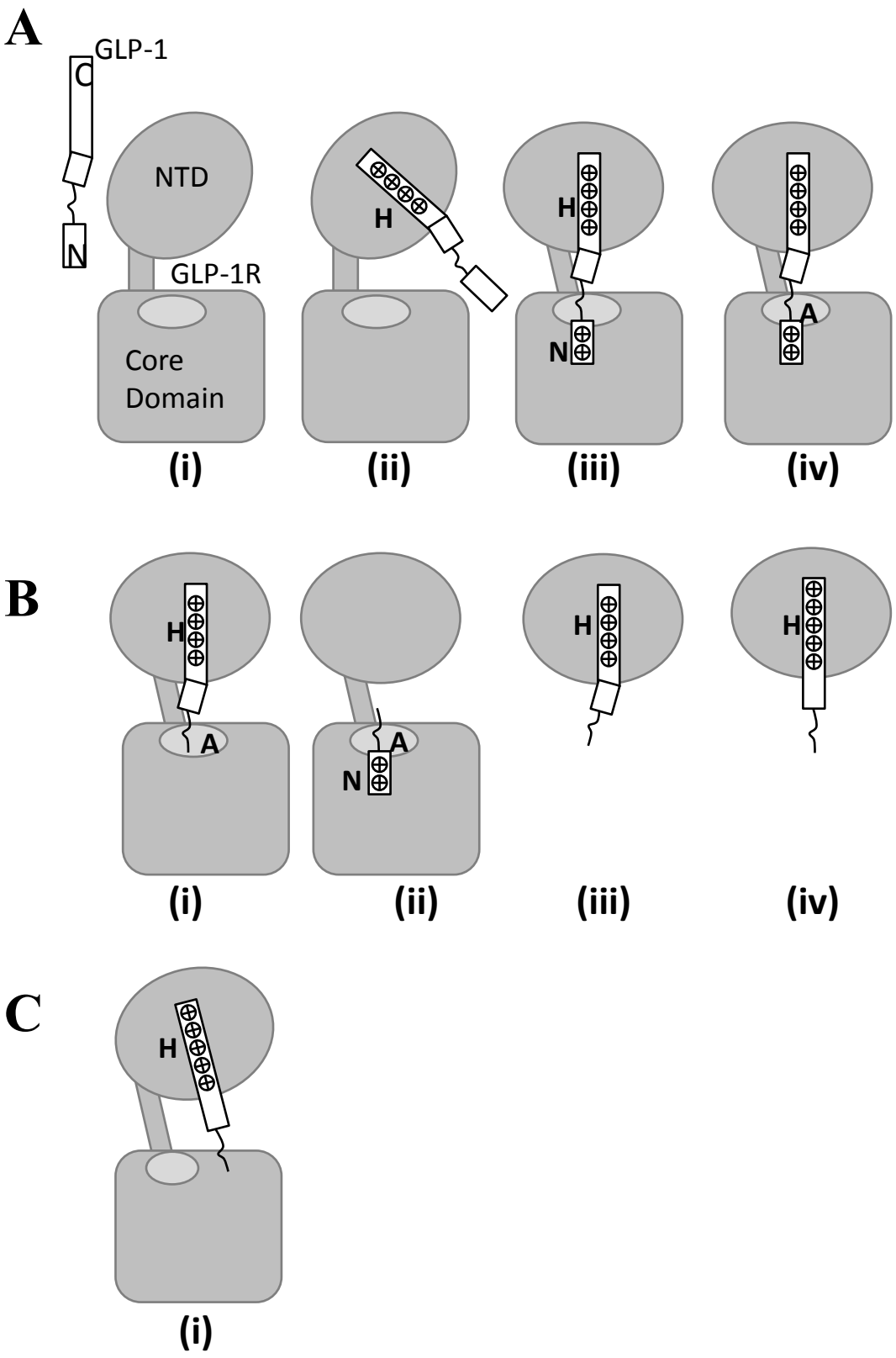

Figure 4.15. Cartoon representation of peptide-receptor interactions in the HAN model. Cartoon constructed by Dr. Donnelly.

(A) (i) The ligand and receptor in the unbound state. **(ii)** The helical C-terminal region of the ligand first binds to the NTD via the H interaction which provides the majority of the ligand-receptor affinity (affinity is depicted by the cross within a circle). **(iii)** The N-terminal region of the ligand forms a low-affinity interaction with the core domain, forming the second part of the brace. **(iv)** The brace interaction positions residues 15-17 at the activation site of the receptor such that the activating A interaction is formed via main chain interactions from the ligand. Note that there are likely to be interactions between the core domain (ECL2) and regions of the ligand on the C-terminal side of the residues 15-17 which are not depicted in this simplistic cartoon.

(B) The receptor can still be activated when one of the two brace interactions has been removed. For example, **(i)** residues 7-14 of GLP-1 can be deleted, breaking the N interaction. Peptide affinity is moderately reduced and the A interaction is more difficult to form. Alternatively, **(ii)** the H interaction can be removed by truncating residues 18-36. The peptide had drastically reduced affinity but occupied receptors can form the A interaction. The isolated NTDs bound to **(iii)** GLP-1(15-36) and **(iv)** Ex4(9-30) – the former has a kinked helix while the latter has a regular helix.

(C) (i) Ex4(9-30) cannot form the A interaction since the critical activating residues are not correctly placed at the receptor's activation site as there is no kink in the helix at position 16 (G22 equivalent in GLP-1).

Chapter 5

General Discussion

5.1 Pm Compounds Allosterically Modulate Cyclic AMP Production and Insulin Secretion at GLP-1R-Expressing Cells

The Pm compounds are a small library of 48 compounds based upon the pyrimidine compound Pm 1, with modifications to the benzyl ring, trifluoromethyl group and sulphur dioxide group. On the starting date of this work there were non-peptide, small molecule agonists documented for the GLP-1R, such as compound 2 (Koole *et al*., 2010), a quinoxaline (Knudsen *et al*., 2007) and Boc 5, a large cyclobutane derivative (Chen *et al*., 2007) but none possessed a pyrimidine based structure. In late December 2010 a publication by Eli Lilly was released, documenting 'compound A' and 'compound B', which both possessed a pyrimidine base, and compound A showed remarkable similarity to our Pm 3 (Sloop *et al*., 2010). The findings presented within this thesis correlate well with the documented research performed by Sloop and co-workers, as discussed within this section.

The primary focus of this study was the investigation of the structure-activity relationship of the Pm compounds with hGLP-1R. These aims were achieved by devising a small-scale, high throughput, miniature screening process. This screening process allowed the efficacy of the individual compounds at 100 μM, as pre-determined by the use of known small molecule agonists of the GLP-1R in the recombinant FlpIn-HEK293 cell line, overexpressing human GLP-1R.

The most potent of the active Pm compounds was Pm 42, which had a *meta* chlorine modification to the benzyl ring. Pm 42 was found to be a partial agonist with sub μM potency at hGLP-1R-expressing cells. Pm 42 was shown to be unable to compete for orthosteric binding *versus* radiolabelled ^{125}I-GLP-1(7-36) at crude FlpIn-HEK293 membrane preparations overexpressing hGLP-1R, which suggested allosteric binding. GLP-1(7-36) and antagonist Ex4(9-39) both bind to the orthosteric site (Runge *et al*., 2008; Underwood *et al*., 2010) therefore an antagonist competition curve demonstrated their competitive nature for binding at the orthosteric site, as the relative potency of GLP-1(7-36) was decreased under increasing concentrations of antagonist Ex4(9-39). An antagonist competition curve was performed using Pm 42 *versus* increasing concentrations of Ex4(9-39). Interestingly the antagonist competition curve with Pm 42 demonstrated that Ex4(9-39) did not antagonise the agonist activity of Pm 42, consistent with the findings that Pm 42 could not displace ^{125}I-GLP-1(7-36) from crude FlpIn-HEK293 membrane preparations. Furthermore, Ex4(9-39) enhanced Pm 42 activity, which showed that the two ligands were working cooperatively, and suggested that Pm 42 acts at GLP-1R via a different mechanism to GLP-1(7-36).

We hypothesised that Pm 42 may also have cooperative effects upon GLP-1 binding at GLP-1R, as cooperative effects were observed with Ex4(9-39), therefore co-stimulatory experiments were designed to simultaneously activate hGLP-1R with the peptides: GLP-1(7-36), GLP-1(9-36) and GLP-1(15-36), in the presence of 1 μM, 10 μM and 100 μM Pm 42. The co-stimulatory dose-response curves showed that Pm 42 only had a positive cooperative effect upon intracellular cAMP concentration at hGLP-1R expressing cells when co-stimulated with GLP-1(9-36). Potency of GLP-1(9-36) was increased 50-fold, and maximal activity was increased from partial activity to full activity in the presence of 10 μM Pm 42 (Table 3.8.ii).

The data that suggested Pm 42 did not potentiate the cAMP response by GLP-1(7-36) were contradictory to the data presented by Sloop *et al.* (2010) which showed that compound B, similar in structure and function to the Pm compounds, was capable of potentiating GLP-1(7-36) cAMP response in HEK293 cells expressing hGLP-1R. The concentrations of GLP-1(7-36) used in the cAMP accumulation study by Sloop *et al.* (2010) which responded to the presence of 10 μM compound B were: 1.5 pM, 2.7 pM and 3.7 pM. It is not clear why these concentrations were used, however they were not used to mimic postprandial circulating GLP-1(7-36) concentrations, as fasting levels of GLP-1(7-36) are between 5-10 pM which rise to 15-50 pM after nutrient ingestion, which are 10 to 30-fold higher than the concentration of GLP-1(7-36) used in that study. The results presented by Sloop *et al.* (2010) were contradictory to the findings that Pm 42 did not potentiate intracellular cAMP production in the presence of GLP-1(7-36). This may be due to the different protocol used for analysing cAMP production. Whereas Pm 42 and GLP-1(7-36) were co-stimulated with 10,000 cells per well in a 384-well format for 10 minutes, 37°C, over a range of GLP-1(7-36) concentrations, from 0.1 pM to 1 nM in the presence of 0, 1, 10 and 100 μM Pm 42 in this study, Sloop *et al.* (2010) stimulated an *unknown* quantity of HEK293 cells in 96 well format (suggesting there were more cells present as 96 well plate wells hold a higher volume, and have a larger surface area than 384 well plates) with the disclosed concentrations of agonists for 20 minutes. Both protocols used homogenous time resolved FRET to quantify cAMP.

The data shown for the cAMP production of HEK 293 cells stimulated with GLP-1(7-36) and compound B simultaneously in the findings of Sloop *et al.* (2010) are presented in a misleading format, as they do not account for the additive effects of independent cAMP production by these two agonists. Within the figure, the simple numerical addition of the two cAMP responses from the independent addition of the two agonists GLP-1(7-36) and compound B are not compared with the response from their co-administration. In fact it appears that compound B and GLP-1(7-36) have no cooperative effect on each other and the increase of cAMP response was misinterpreted, since10 μM compound B generated 12 nM cAMP, 1.2 pM

GLP-1(7-36) generated 15 ± 6 nM cAMP, and together they generated 31 ± 4 nM. However, in the absence of statistical analysis, it is not clear whether this represents a significant allosteric enhancement.

As insulin secretion is potentiated by PKA and Epac2-mediated effects, which are the secondary effector proteins activated by cAMP, it was hypothesised that the cooperative effects of GLP-1(9-36) and Pm 42 on cAMP production could mimic the insulinotropic effects of GLP-1(7-36) at insulin secretory cell lines. The insulin secretory cell line INS-1 832/13 was used to test this hypothesis. INS-1 832/13 cells were incubated with GLP-1(9-36) at 0.1, 1 and 5 μM in the presence and absence of 10 μM Pm 42 for 2 hours in the presence of 16.7 mM glucose, following a low glucose incubation for 3 hours in 3 mM glucose-containing media, and the results compared to incubation with 1 μM GLP-1(7-36). Administered alone, 10 μM Pm 42 and 0.1, 1 and 5 μM GLP-1(9-36) had no statistically significant effect upon insulin secretion from INS-1 832/13 cells, however when incubated simultaneously a statistically significant increase in insulin release was observed for all concentrations of GLP-1(9-36). Indeed, 1 μM GLP-1(9-36) in the presence of 10 μM Pm 42 achieved a similar insulin secretory response as 1 μM GLP-1(7-36), and 5 μM GLP-1(9-36) with 10 μM Pm 42 achieved a higher insulin secretory response than 1 μM GLP-1(7-36) (Figure 3.11, Table 3.9). Consistent with these data, data in the literature show that non-peptide molecule compound B, which has similar basic architecture as our Pm compounds with a benzyloxy substituent at the *meta* position of the benzyl ring, is capable of potentiating the secretory insulin response of static islet cultures from Sprague Dawley rats when administered with GLP-1(7-36) (Sloop *et al*., 2010).

These data have potentially considerable therapeutic interest, a molecule that targets the GLP-1R and works synergistically with endogenous circulating peptides could be used to treat not only the relative insulin deficiency seen in T2D, but also address the underlying issues associated with T2D such as β cell failure and loss of β cell mass, by targeting the GLP-1R. A non-peptidic compound which acts allosterically, that not only potentiates the cAMP response and insulin secretory effect of the intact fully potent agonist GLP-1(7-36) (potentially if the results from Sloop *et al.,* (2010) are taken into consideration), but also the responses of the truncated metabolite GLP-1(9-36) could have a major impact on the treatment of T2D. GLP-1(9-36) is present at 3 to 4 times higher concentration in the bloodstream than its full length counterpart, thereby if those circulatory levels of endogenous peptide can be exploited by use of an orally bioavailable non-peptidic molecule, it may circumvent the need for self-injection for administration of treatments such as exenatide or liraglutide, and may have similar beneficial physiological outcomes (Baggio & Drucker, 2007).

5.2 Application of Altered Conformational States to Drug Screening Processes

The second focus of this study was to devise a second rapid screening process to study the structure-activity relationship between the Pm compounds and the truncated peptides GLP-1(9-36) and Ex4(9-39). Data collected in sections 3.6 and 3.7 of this thesis showed that Pm 42 allosterically modulated the effects of Ex4(9-39) and GLP-1(9-36) respectively; we hypothesised there may be a correlation between structural characteristics of the Pm compound library and their ability to modulate the cAMP responses of these two peptides. Therefore a secondary screening process was devised from the dose-response curves shown in Figure 3.12, based on the hypothesis that data could be gleaned from using specific concentrations of peptide that resided just below the cusp of their dose-response curves, co-stimulated alongside Pm compounds, to study the level of cooperativity between peptide and small molecule. In the case of Ex4(9-39) which did not generate cAMP accumulation data alone to yield a dose-response curve, the concentration used within the secondary miniscreen was 10 nM, as this concentration of Ex4(9-39) clearly demonstrated the effects of 100 μM Pm 42 upon the cAMP signalling profile of Ex4(9-39) in Figure 3.9.C.

The secondary small scale miniature screening process revealed that the sulphur dioxide group is absolutely required for intrinsic agonism and allosteric modulating properties, consistent with the findings of Sloop *et al.* (2010). The *para*, *meta* and *ortho* positioning of functional group substituents upon the benzyl ring motif played no major part in modulation of the cAMP responses of neither GLP-1(9-36) nor that of Ex4(9-39). Interestingly however, the secondary miniature screen showed that the trifluoromethyl motif is required for intrinsic efficacy, but not for allosteric modulation, as Pm 41 and Pm 8 (which had a cyanide and a nitrogen-linked tertiary butyl group replacements of the trifluoromethyl motif respectively) possessed less than 20% intrinsic activity at GLP-1R, yet when administered concomitantly with GLP-1(9-36) gave a statistically significant increase in cAMP response over the two ligands administered separately (Figure 3.24, 3.25 and 3.26). Interestingly these effects were GLP-1 ligand specific, and did not result in an increased cAMP response from Ex4(9-39), suggesting the TFM group may be critical for intrinsic Pm compound activity at GLP-1R, and that the GLP-1R must occupy a partially active state for Ex4(9-39) to further enhance potency.

These data present a novel finding that Ex4(9-39) elicits a cAMP response within GLP-1R-expressing cells in the presence of pyrimidine-substituted non-peptidic compounds. These data could potentially be applied to the current process of drug screening. Traditionally drug

screening employs the use of a high throughput screening system to identify drugs which are capable of activating a particular pathway. There has been minimal success in identifying Family B GPCR small molecule agonists; this is most likely attributed to the two-domain activation mechanism that requires multiple contacts between ligand and receptor amongst the NTD, extracellular loops and core domain for maximum activity. As such, the non-peptide agonists identified for class B GPCRs only possess μM potency. However, as seen within Chapter 3 of this thesis, a non-peptide partial agonist with only μM potency can achieve nM potency and full activity in the presence of GLP-1(9-36). Indeed, those pyrimidine-substituted compounds which were identified as being inactive alone at GLP-1R demonstrated the ability to enhance the cAMP production of GLP-1(9-36), which would have otherwise been regarded as inactive molecules. This demonstrated that the traditional screening technique would miss those potential receptor ligands capable of modulating receptor conformation to alter and enhance the signalling profile of other peptide ligands.

These data suggest that a better screening technique for the discovery of novel non-peptide agonist of Family B GPCRs would be to not look for a molecule capable of mimicking the activation profile of the full-length 30 residues peptide hormone, an endeavour that is seemingly impossible, but to search for a ligand that can enhance the effects of endogenous circulatory peptide ligands. This could be achieved by applying a small concentration of peptide, whose stimulus is required to be enhanced, and to screen for small molecules which enhance the effects of those peptides. This simple addition to traditional screening procedures will no doubt result in the discovery of novel compounds capable of enhancing the effects of naturally occurring peptides, as many potential allosteric modulators will have been overlooked using traditional screening techniques.

5.3 Re-defining the Activating-Providing Residues within GLP-1 and Ex4

The final aim of this project was to better understand the nature of the activating interaction between peptide ligands GLP-1 and Ex4 at hGLP-1R expressing FlpIn-HEK293 cells by observing the different binding and activation profiles using competition binding assays and cAMP accumulation assays respectively. The activity-providing region of the peptides GLP-1 and Ex4 have been defined as the first 8 amino-terminal residues, hence Ex4(9-39) has been extensively denoted as an antagonist of the GLP-1R in the literature, and until recently

(Patterson *et al*., 2011b) GLP-1(15-36) was thought to be an antagonist too (Montrose-Rafizadeh *et al*., 1997), however GLP-1(15-36) is now thought to be a partial agonist with sub μM potency. The data gathered in section 4.4.2 of this thesis using GLP-1(15-36) and Ex4(9-39) at hGLP-1R expressing cells are consistent with the data in the literature, where GLP-1(15-36) activated hGLP-1R, whereas Ex4(9-39) failed to activate hGLP-1R.

Although GLP-1(7-36) and Ex4(1-39) are both agonists, truncation of the first 8 residues resulted in a different activity profile for these two peptide ligands. Truncation of the first 8 residues of GLP-1(7-36) to give GLP-1(15-36) resulted in a 257-fold reduction in affinity for GLP-1R, a 38,019-fold reduction in potency at GLP-1R and a 23.2% reduction in maximal activity. Conversely, truncation of the first 8 residues of Ex4(1-39) to give Ex4(9-39) resulted in only a 4.6-fold reduction in affinity for GLP-1R, yet activity was abolished at GLP-1R. These data are consistent with the data in the literature, whereby the Ex4 peptide was reported to confer a 95% of its total binding energy within the H-interaction and only 5% within the N-interaction, whereas GLP-1 was reported to confer 82% of its total binding energy within the N interaction and 18% within the N interaction (Al-Sabah & Donnelly, 2003b).This difference in binding energy between the two ligands has been attributed to the increased number of interactions between the Ex4 helical region and the GLP-R NTD in comparison to GLP-1(7-36) and the NTD (Runge *et al*., 2007; Runge *et al*., 2008; Underwood *et al*., 2010).

In addition to an increased number of contacts within the NTD of GLP-1R, Ex4 has multiple intra-helical interactions causing an increased α-helical propensity in comparison to GLP-1, which is held in a more rigid conformation. In addition to intrahelical interactions causing superior helicity and rigidity in comparison to GLP-1, Ex4 lacks the glycine residue at position 16 (GLP-1 equivalent residue position 22), which has been shown to cause a kink in GLP-1 by NMR analysis (Neidigh *et al*., 2001). The result of this kink in GLP-1 is postulated to enhance flexibility within this region, resulting in the N-terminal part of GLP-1 (from G22 to H7) to be orientated in a different angle to its C-terminal helical segment in comparison to Ex4 peptides. In terms of receptor binding, the kink would most likely confer a different interaction within the receptor core domain in comparison to that of Ex4, which may explain the differences of the nature of activity of these two ligands when the first 8 residues are truncated from the amino-terminus.

Since both GLP-1(7-36) and Ex4(1-39) are able to fully activate the receptor, the observed difference in peptide-receptor core domain interaction only results in different contributions to affinity. An increased number of receptor-ligand interactions do not translate into increased potency; this further suggests the core-domain interactions of the two ligands are different (lest they would have similar characteristics upon truncation of the first 8 residues,

which they do not). These data infer that the efficacy-generating component of the peptides' interaction with the core domain is independent from the affinity-generating component, and suggests the peptide efficacy-generating region is located more C-terminally than the first 8 residues. This hypothesis was explored by using GLP-1 peptides that were further truncated from the amino-terminus from GLP-1(15-36) to analyse the residues that confer efficacy to the receptor.

Truncated GLP-1 peptides were designed to serially remove residues N-terminally from GLP-1(15-36), to give GLP-1(16-36), (17-36) and (18-36) to locate which residue was critical for receptor activity. Cyclic AMP accumulation assays at FlpIn HEK293 cells overexpressing hGLP-1R showed that whilst GLP-1(16-36), (17-36) and (18-36) retained affinity for GLP-1R, they had no activity, suggesting the critical residue for activity was D15. This hypothesis was explored further using small C-terminally truncated peptides from GLP-1(7-19) to GLP-1(7-14), and site directed mutagenesis of D15 in full length and truncated GLP-1 peptides.

The shorter length, C-terminally truncated peptides lacking the affinity-providing region but retaining the hypothesised activity-providing N-region were assayed for activity and affinity at GLP-1R. None of the C-terminally truncated peptides were capable of competing for GLP-1R binding against ^{125}I-GLP-1(7-36), most likely because they lacked the helical region, which has been shown to bind the secretin fold within the GLP-1R NTD (Underwood *et al.*, 2010) and to confer the largest percentage of binding energy (Al-Sabah & Donnelly, 2003b). GLP-1(7-14) showed neither affinity, nor activity at GLP-1R. Interestingly, despite the presence of the hypothesised activity-providing amino-terminal 8 residues and D15, GLP-1(7-15) was unable to activate GLP-1R. However GLP-1(7-17) did activate GLP-1R with μM potency.

These data are consistent with the findings of Mapelli *et al.* (2009) who showed that GLP-1(7-17) (sequence 7*-HAEGTFTSDVS-17*), with V16 and S17 substituted with biphenylalanine derivatives, and replacing A2 with aminoisobutyric acid, and F6 with a-methyl-phenylalanine derivative, was capable of activating GLP-1R with nM potency only 2 to 3-fold lower than native GLP-1(7-36). These data, along with the discovery that GLP-1(15-36) retains activity at GLP-1R led to the conclusion that residues 15-17 are essential for peptide activity. Therefore we proposed an extension of the two-domain binding model which shows that the amino termini 'N' (residues 7-14) and the helical region 'H' provide affinity for GLP-1R to form a brace-like structure for precise positioning of the activating region (A), consisting of residues 15, 16 and 17, to interact with the receptor (Figure 4.15). Within this proposed model, it is possible to truncate the either the N or the H regions and for the peptide to remain active, as long as the A region remains intact to make the critical activating interaction with the receptor.

Residues 15, 16 and 17 were mutated to glycine residues within peptides GLP-1(7-36), GLP-1(15-36) and GLP-1(7-17) to analyse the effect of loss of side chains from the activating A region. Interestingly all the peptides except GLP-1(7-17) retained activity at GLP-1R upon mutation. The tri-glycine mutation at residues 15, 16 and 17 of GLP-1(7-36) resulted in a 12,303-fold reduction in potency, with a 19 % reduction in maximal activity and a 302-fold decrease in affinity, demonstrating the removal of side chains at the activating region primarily affected potency of the peptide, yet some activity was still retained. The tri-glycine mutation at residues 15, 16 and 17 of GLP-1(15-36) resulted in a 3-fold reduction in potency and maximal activity was reduced 11% with no change in affinity. The tri-glycine mutation at residues 15, 16 and 17 of GLP-1(7-17) resulted in total loss of activity at GLP-1R. These data taken together suggest the side chains of the activity-providing region (residues 15, 16 and 17) of GLP-1R within the new model are required for full activity, yet some activity is retained within the tri-glycine mutants, suggesting it may be the peptide backbone of this region that makes contact with GLP-1R, and activity is amplified in the presence of the side chains within this region.

The apparent inability of GLP-1(7-17)15-GGG-17 to activate GLP-1R within the concentration range used within the assay (100 μM to 10 nM) may represent a decrease in potency of the peptide which is not visible within the concentration range used in the assay. The potency of GLP-1(7-36) was decreased with the tri-glycine mutation; therefore the potency of GLP-1(7-17) may also be decreased with the tri-glycine mutation. However the wild-type version of GLP-1(7-17) achieved an EC_{50} of 1.4×10^{-5} M, therefore a 10-fold reduction of potency (1.4×10^{-4} M) would result in a dose-response curve from which an EC_{50} would not be quantifiable from the concentration range assayed. Further work in this region would be to stimulate GLP-1R expressing cells with a higher concentration of GLP-1(7-17)15-GGG-17.

D15* is an important residue for receptor activation as shown by the results in sections 5.4.3-5.4.7 of this thesis. A negative charge at residue 15 is conserved in some secretin peptides (Figure 5.1), such as CRF, GLP-2, secretin, GIP, Ex4, GLP-1 and glucagon. Conservation of negative charge at position 15 throughout some secretin peptides suggests a critical role for this residue.

According to the current two-domain model of GLP-1R activation, the activating N-interaction is defined as the interaction between the residues of the ligand that are situated within the first 8 residues of the peptide and the TMD of the receptor, which causes activation upon residue interaction (Hoare, 2005). However, numerous data in the results sections of this thesis clearly show that this is not the case for GLP-1 peptides, as truncation of the first 8 residues in GLP-1 (to give GLP-1(15-36)) results in an agonist with reduced affinity and severely reduced efficacy, but an agonist nonetheless. We propose the loss of activity and

affinity upon truncation of the first 8 residues of GLP-1 is due to loss of one of the affinity-providing regions, rather than loss of the activity-providing residues as previously thought. Indeed, truncation of the first 8 residues in Ex4 does result in a peptide with no inherent activity at the GLP-1R, unless co-administered with a non-peptidic ago-allosteric modulator (Chapter 3 of this thesis) suggesting that Ex4(9-39) still possesses the residues required for receptor activation, but the inherent unyielding nature of the α-helical segment holds residues D9*-M14* (those residues that do not interact with the NTD of GLP-1R but jut out into space in the crystal structure (Runge *et al*., 2008)) in a rigid conformation, disallowing interaction with the TMD, unless the TMD conformation is allosterically altered to envelop these residues.

Peptide	Sequence of first 9 residues
Corticotropin-releasing factor (CRF)	SEEPPISLD
Growth hormone releasing hormone (GHRH)	YADAIFTNS
Glucagon-like peptide-2 (GLP-2)	HADGSFSDE
Vasoactive intestinal polypeptide (VIP)	HSDAVFTDN
Pituitary adenylate cyclase-activating polypeptide (PACAP)	HSDGIFTDS
Secretin	HSDGTFTSE
Glucose-dependent insulinotropic peptide (GIP)	YAEGTFISD
Exendin-4 (Ex4)	HGEGTFTSD
Glucagon-like peptide-1 (GLP-1)	HAEGTFTSD
Glucagon (GCG)	HSQGTFTSD

Figure 5.1. Conservation of the 9 amino terminal residues of some secretin-like peptides.

Sequences were found using the UniProtKB database and aligned using Clustal Ω. Red, blue and green highlighting indicates hydrophobic, negatively charged and polar residues respectively.

When Ex4(9-39) was used in a dose-response curve alone, the peptide gave no cAMP response at FlpIn-HEK293 cells overexpressing hGLP-1R. However, under the same conditions, Ex4(9-39), an antagonist, gave a dose-response curve in the presence of 1 μM, 10 μM and 100 μM Pm 42. The EC_{50} of the dose-response curves were approximately equivalent to the IC_{50} of Ex4(9-39), and in the absence of Ex4(9-39) the three concentrations of Pm 42 gave a constant cAMP response, indicating that the dose-response curve was indeed the effects of

Ex4(9-39) activating GLP-1R. D15 and S17 are conserved between GLP-1 and Ex4, suggesting these residues are of importance. Within this thesis a new model is proposed whereby these residues are required for receptor activation, and these residues are capable of interacting with receptor residues through inherent flexibility in GLP-1(15-36), but not in Ex4(9-39), yet this can be overcome in the presence of allosteric modulator Pm 42, whereby Ex4(9-39) is capable of activating GLP-1R (Figure 5.2).

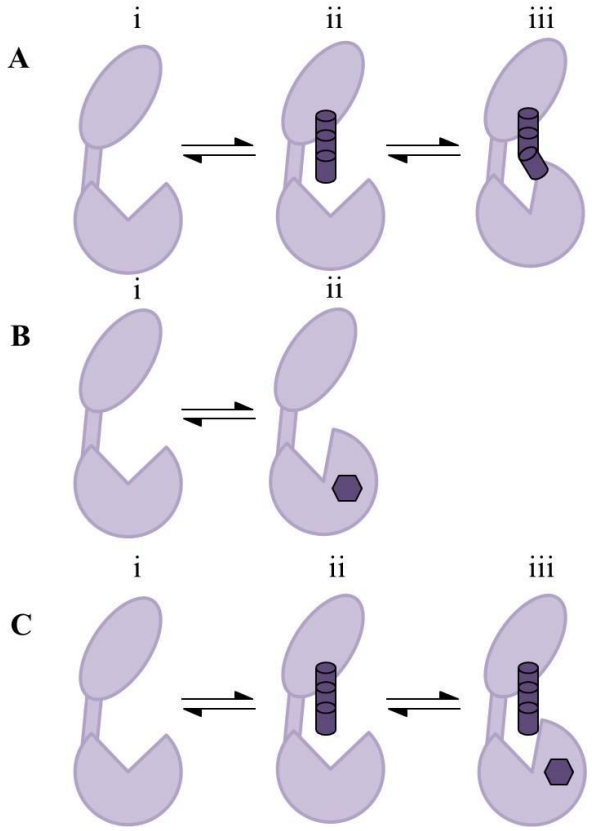

Figure 5.2 Cartoon diagram of the hypothesised receptor conformational change in the presence of non-peptide and the effect on antagonist Ex4(9-39).

A. GLP-1R (lilac structure) in inactive non-bound state **(i)** complexes with GLP-1(15-36) (purple helix) **(ii)** and is thereby activated **(iii)** due to the inherent flexibility at position 22 conferred by the glycine residue which permits contact of activating residues 15, 16 and 17 with GLP-1R.
B. GLP-1R in the active non-bound state **(i)** complexes with Pm 42 (purple hexagon) whereby there is a conformational shift in the TM helices **(ii)** thereby activating the receptor.
C. GLP-1R in active non-bound state **(i)** binds Ex4(9-39) (rigid purple helix) **(ii)** which does not activate the receptor as the helix is more rigid than the analogously truncated GLP-1(15-36) therefore cannot make the activating contacts with receptor residues. Upon Pm 42 binding **(iii)** there is a conformational shift within the TM bundle which allows the activity providing residues at the extreme N-terminus of Ex4(9-39) to interact with the receptor core domain, causing an additional enhancement to activity as seen in Figure 3.9.C which permits residues 9, 10 and 11 (equivalent of GLP-1 residues 15, 16 and 17) to make the activating contacts.

5.4 Further Work

Possible further work regarding the Pm compounds would ideally be to identify other signalling pathways which are activated, as recently it has been shown that ligands of GPCRs show signal bias, and are capable of activating more than one pathway. For example the observation of intracellular calcium release could be assayed within the cell, either via flex station technology or a high throughput screening assay such as the HTRF® IP-One Tb functional assay from cisbio which measures the accumulation of the downstream metabolite inositol phosphate 1 following $G\alpha_q$-coupled GPCR activation. Ideally observation of the Pm compound-induced effects on the β arrestin and pERK/MAPK signalling pathway would be studied too.

In the Eli Lilly publication (Sloop *et al*., 2010) an initial screening process was performed on 2,000 compounds for ability to activate GLP-1R, whereby compound A was initially found to be a partial agonist of GLP-1R capable of receptor activation with μM potency. However, more time was spent modifying and optimising the structure first before analysis was performed, to produce compound B, which was more potent than compound A, and more active. In a similar manner, ideally a larger, more diverse Pm compound library would have been made with more robust and varied modifications, rather than more delicate structural modifications, to identify a unique compound, which *then* could have been optimised by altering the positioning of functional groups. However, the TFM and SD groups seem essential for Pm compound-mediated cAMP production, so perhaps more compounds could be synthesised with more chemically diverse properties within these groups to potentially identify a compound with better activating properties. Furthermore an extension of the benzene ring with a larger group may produce a more active compound such as compound B.

Further work would also include creating a GIP-receptor/GLP-1R chimera. The Pm compounds do not activate the GIPR (appendix), and by swapping domains it may be possible to pinpoint the location of binding of the Pm compounds, and then to narrow this region down to performing an alanine scan of the area to locate residues involved in complexing the compounds. An alanine scan of ECL2 was performed and Pm compounds assayed at the mutant receptors, but no site of binding was located (Appendix). Also it would be ideal to co-stimulate INS-1 832/13 cells in the presence of Pm 42 and GLP-1(7-36), as research shows that non-peptide agonists of GLP-1R of the pyrimidine sub-class can indeed enhance the effect of GLP-1(7-36) within static pancreatic cultures of Sprawgue-Dawley rat islets at low concentrations of GLP-1(7-36) (Sloop *et al*., 2010). Additionally it would be beneficial to observe if the Pm

compounds are capable of inducing insulin secretion *in vitro* in the presence of GLP-1 peptides, using isolated pancreatic islets, or *ex vivo* using perfused pancreatic cultures to observe whole-organ responses to the Pm compounds in the presence of GLP-1 peptides.

A cell viability assay would ideally be performed on FlpIn-HEK 293 cells following incubation with Pm compounds, as other non-peptide agonists have been reported to be cytotoxic. Compound 2 had been documented to present a bell-shaped curve in cAMP accumulation studies when incubated with at HEK293 cells overexpressing GLP-1R for 10 minutes, which was thought to be concomitant with compound 2-associated cytotoxicity. This hypothesis was confirmed using trypan blue staining on HEK293 cells following a 90 minute incubation with 100 μM compound 2 (Coopman *et al*., 2010).

5.5 Summary

- A small library of pyrimidine substituted non-peptide compounds were analysed for efficacy at GLP-1R and it was found that the trifluoromethyl group and sulphur dioxide group are essential for GLP-1R activity.
- Active Pm compounds were capable of allosterically modulating the cAMP response of truncated peptide GLP-1(9-36) when co-stimulated with 1 μM Pm compound at GLP-1R expressing cells.
- The small scale screening procedure could be applied to drug screening processes on an industrial scale to identify allosteric modulators for the treatment of diseases associated with Family B GPCRs.
- The activity-providing region of GLP-1 peptides resides within residues 15-17 rather than being uniquely located to the first 8 residues.
- An extension to the two-domain model of GLP-1R activation was proposed, suggesting the helical and amino-most region of the peptide acts as a brace to position activating residues 15, 16 and 17 correctly.
- It is most likely the polypeptide backbone interacts with GLP-1R TMD activating it within the activating ‘A’ region of GLP-1.
- Negative charge at D15 in GLP-1(15-36) is required for activity.
- The Pm compounds allosterically alter GLP-1R conformation such that Ex4(9-39) can further activate the receptor, giving a dose-response curve with EC_{50} relative to Ex4(9-39) IC_{50}.

References

A

AbdAlla S., Lother H., El Massiery A. & Quitterer U. (2001) Increased AT(1) receptor heterodimers in preeclampsia mediate enhanced angiotensin II responsiveness, *Nat. Med*. **7:** 1003–1009.

Adelhorst K., Hedegaard B. B., Knudsen L. B.& Kirk O. (1994) Structure-activity studies of glucagon-like peptide-1. *J. Biol. Chem.* **269:** 6275–6278.

Adler E., Hoon M. A., Mueller K. L., Chandrashekar J., Ryba N. J. & Zuker C. S. (2000) A novel family of mammalian taste receptors. *Cell.* **100:** 693–702.

Al-Sabah S. & Donnelly D. (2003a) A model for receptor-peptide binding at the glucagon-like peptide-1 (GLP-1) receptor through the analysis of truncated ligands and receptors. *Br. J. Pharmacol.* **140:** 339-346.

Al-Sabah S. & Donnelly D. (2003b) The positive charge at Lys-288 of the glucagon-like peptide-1 (GLP-1) receptor is important for binding the N-terminus of peptide agonists. *FEBS Lett*. **553:** 342-346

Al-Sabah S. & Donnelly D. (2004). The primary ligand-binding interaction at the GLP-1 receptor is via the putative helix of the peptide agonists. *Protein Pept. Lett.* **11:** 9–14.

Angers S., Salahpour A., Joly E., Hilairet S., Chelsky D., Dennis M. & Bouvier M. (2000) Detection of beta 2-adrenergic receptor dimerization in living cells using bioluminescence resonance energy transfer (BRET). *Proc. Natl. Acad. Sci. U. S. A.* **97:** 3684-3689.

Araç D., Boucard A. A., Bolliger M. F., Nguyen J., Soltis S. M., Südhof T. C. & Brunger A. T. (2012) A novel evolutionarily conserved domain of cell-adhesion GPCRs mediates autoproteolysis. *EMBO J.* **31:** 1364–1378.

Archbold J. K., Flanagan J. U., Watkins H. A., Gingell J. J. & Hay D. L. (2011) Structural insights into RAMP modification of secretin family G protein-coupled receptors: implications for drug development. *Trends Pharmacol. Sci*. **32:** 591–600.

Asfari M., Janjic D., Meda P., Li G., Halban P. A. & Wollheim C. B. (1992) Establishment of 2-mercaptoethanol-dependent differentiated insulin-secreting cell lines. *Endocrinology*. **130:**167–178.

Astrup A. & Finer N. (2000) Redefining type 2 diabetes: 'diabesity' or 'obesity dependent diabetes mellitus'? *Obes. Rev.* **1:** 57-59.

Attwood, T. K. & Findlay, J. B. (1993) Design of a discriminating fingerprint for G‐protein‐coupled receptors. *Protein Eng.* **6:** 167–176.

B

Baggio L. L. & Drucker D. J. (2007) Biology of incretins: GLP-1 and GIP. *Gastroenterology.* **132:** 2131–2157.

Bazarsuren A., Grauschopf U., Wozny M., Reusch D., Hoffmann E., Schaefer W., Panzner S. & Rudolph R. (2002). In vitro folding, functional characterization, and disulfide pattern of the extracellular domain of human GLP-1 receptor. *Biophys. Chem*. **96:** 305–318.

Bell G. I, Sanchez-Pescador R., Laybourn P. J. & Najarian R. C. (1983) Exon duplication and divergence in the human preproglucagon gene. *Nature* **304:** 368–71.

Berg C., Neumeyer K. & Kirkpatrick P. (2003) Teriparatide. *Nature Rev. Drug Discov*. **2:** 257–258.

Bergwitz C., Gardella T. J., Flannery M. R., Potts J. T., Kronenberg H. M., Goldring S. R. & Jüppner H. (1996). Full activation of chimeric receptors by hybrids between parathyroid hormone and calcitonin. *J. Biol. Chem.* **271:** 26469–26472.

Bhanot P., Brink M., Samos C. H., Hsieh J. C., Wang Y., Macke J. P., Andrew D., Nathans J. & Nusse R. (1996) A new member of the frizzled family from Drosophila functions as a Wingless receptor. *Nature.* **382:** 225–230.

Bhavsar S., Mudaliar S. & Cherrington A. (2013) Evolution of Exenatide as a Diabetes Therapeutic. *Current Diabetes Reviews* **9:** 161-193.

Bjarnadóttir, T. K., Fredriksson, R. & Schiöth, H. B. (2005) The gene repertoire and the common evolutionary history of glutamate, pheromone (V2R), taste(1) and other related G protein-coupled receptors. *Gene* **362:** 70–84.

Black J. (1989) Drugs from emasculated hormones: the principle of syntopic antagonism. *Science* **245:** 486–493.

Bose A. K., Mocanu M. M., Carr R. D. & Yellon D. M. (2007) Myocardial ischaemia-reperfusion injury is attenuated by intact glucagon like peptide- 1 (GLP-1) in the in vitro rat heart and may involve the p70s6K pathway. *Cardiovasc. Drugs Ther.* **21:** 253–256.

C

Chen D., Liao J., Li N., Zhou C., Liu Q., Wang G., Zhanga R., Zhanga S., Lina L., Chena K., Xiea X., Nana F., Andrew A. Younga D. & Wang M-W. (2007) A non-peptidic agonist of glucagon-like peptide 1 receptors with efficacy in diabetic db/db mice. *Proc. Natl. Acad. Sci. U S A.* **104:** 943–948.

Chen Q., Pinon D. I., Miller L. J., & Dong M. (2009) Molecular Basis of Glucagon-like Peptide 1 Docking to Its Intact Receptor Studied with Carboxyl-terminal Photolabile Probes *J. Biol. Chem*. **284:** 34135-34144.

Chen Q., Pinon D. I., Miller L. J. & Dong M. (2010) Spatial approximations between residues 6 and 12 in the amino-terminal region of glucagon-like peptide 1 and its receptor: a region critical for biological activity. *J Biol Chem*. **285:** 24508–24518.

Christopoulos A. & Kenakin T. (2002) G Protein-Coupled Receptor Allosterism and Complexing. *Pharmacol. Rev.* **54:** 323–374.

Claing A., Laporte S. A., Caron M. G. & Lefkowitz R. J. (2002). Endocytosis of G protein-coupled receptors: roles of G protein-coupled receptor kinases and beta-arrestin proteins. *Progress in Neurobiology*. **66:** 61-79.

Clark A. J. (1937) General Pharmacology: Heffter's Handbuch d. exp. Pharmacology (Ergband 4), Springer.

Conigrave A. D., Quinn S. J. & Brown E. M. (2000) L-Amino acid sensing by the extracellular Ca^{2+}-sensing receptor. *Proc. Natl. Acad. Sci. U. S. A.* **97:** 4814–4819.

Conn P. J, Christopoulos A. & Lindsley C. W. (2009) Allosteric modulators of GPCRs: a novel approach for the treatment of CNS disorders. *Nature Reviews Drug Discovery* **8:** 41-54.

Conte C., Ebeling M., Marcuz A., Nef P. & Andres-Barquin P. J. (2002) Identification and characterization of human taste receptor genes belonging to the TAS2R family. Cytogenet. *Genome Res.* **98:** 45–53.

Coopman K., Huang Y., Johnston N., Bradley S. J., Wilkinson G. F. & Willars G. B. (2010) Comparative effects of the endogenous agonist GLP-1 7–36 amide and a small molecule ago-allosteric agent 'compound 2' at the GLP-1 receptor. *J. Pharmacol. Exp. Ther.* **334:** 795–808.

Cure P., Pileggi A. & Alejandro R. (2008) Exenatide and rare adverse events. *N. Engl. J. Med.* **358:** 1969–1970; discussion 1971–1962.

D

De Lean A., Stadel J. M. & Lefkowitz R. J. (1980). A ternary complex model explains the agonist-specific binding properties of the adenylate cyclase-coupled beta-adrenergic receptor. *J Biol Chem.* **255:** 7108-7117.

De Wire S. M., Ahn S., Lefkowitz R. J. & Shenoy S. K. (2007) β-Arrestins and Cell Signaling. *Annu. Rev. Physiol.* **69:** 483–510.

Deacon C. F., Plamboeck A., Moller S. & Holst J. J. (2002) GLP-1-(9–36) amide reduces blood glucose in anesthetized pigs by a mechanism that does not involve insulin secretion. The adipoinsular axis: effects of leptin on pancreatic β-cells. *Am. J. Physiol. Endocrinol. Metab.* **282:** E873–E879.

Dixon R. A. F., Kobilka B. K., Strader D. J., Benovic J. L., Dohlman H. G., Frielle T., Bolanowski M. A., Bennett C. D., Rands E., Diehl R. E., Mumford R. A., Slater E. E., Sigal I. S., Caron M. G., Lefkowitz R. J. & Strader C. D. (1986) Cloning of the gene and cDNA for mammalian B -adrenergic receptor and homology with rhodopsin. *Nature* **321:** 75–79.

Dong M., Li Z., Pinon D. I., Lybrand T. P. & Miller L. J. (2004) Spatial approximation between the amino terminus of a peptide agonist and the top of the sixth transmembrane segment of the secretin receptor. *J. Biol. Chem.* **279:** 2894–2903.

Dong M., Pinon D. I., Asmann Y. W. & Miller L. J. (2006). Possible endogenous agonist mechanism for the activation of secretin family G protein-coupled receptors. *Mol. Pharm.* **70:** 206–213.

Donnelly D. (1997) The arrangement of the transmembrane helices in the secretin receptor family of G-protein-coupled receptors. *FEBS Lett.* **409:** 431–436.

Donnelly D. (2012) The structure and function of the glucagon-like peptide-1 receptor and its ligands. *Br. J. Pharmacol.* **166:** 27–41.

Doyle M. E. & Egan J. M. (2007) Mechanisms of action of glucagon-like peptide 1 in the pancreas. *Pharmacol. Ther.* **113:** 546–593.

Duarte A. I., Moreira P. I. & Oliveira C. R. (2012) Insulin in central nervous system: more than just a peripheral hormone. *J. Aging. Res*. 384017–384038.

Duarte A. I., Candeias E., Correia S. C., Santos R. X., Carvalho C., Cardoso S., Plácido A., Santos M. S., Oliveira C. R. & Moreira P. I. (2013) Crosstalk between diabetes and brain: Glucagon-like peptide-1 mimetics as a promising therapy against neurodegeneration. *Biochimica et Biophysica Acta* **1832:** 527–541.

During, M. J., Cao, L., Zuzga, D. S., Francis, J. S., Fitzsimons, H. L., Jiao, X., Bland, R. J., Klugmann, M., Banks, W. A., Drucker, D. J. & Haile, C. N. (2003) Glucagon-like peptide-1 receptor is involved in learning and neuroprotection. *Nat. Med.* **9:** 1173–1179.

E

Egan J. M., Meneilly G. S., Habener J. F. & Elahi D. (2002) Glucagon-Like Peptide-1 Augments Insulin-Mediated Glucose Uptake in the Obese State *J. Clinical. Endocrinol. Metab.* **87:** 3768-3773.

El-Moustaine D., Granier S., Doumazane E., Scholler P., Rahmeh R., Bron P. Mouillac B., Banères J. L., Rondard P. & and Pin J-P. (2012) Distinct roles of metabotropic glutamate receptor dimerization in agonist activation and G-protein coupling. *Proc. Natl. Acad. Sci. U. S. A.* **109:** 16342–16347.

Elahi D., Egan J. M., Shannon R. P., Meneilly G. S., Khatri A., Habener J. F. & Andersen D. K. (2008) GLP-1 (9-36) amide, cleavage product of GLP-1 (7-36) amide, is a glucoregulatory peptide. *Obesity.* **16:** 1501–1509.

Eliasson L., Ma X., Renström E. Barg S., Berggren P. O., Galvanovskis J., Gromada J., Jing X., Lundquist I., Salehi A., Sewing S. & Rorsman P. (2003) SUR1 regulates PKA-independent cAMP-induced granule priming in mouse pancreatic B-cells. *J. Gen. Physiol*. **121:** 181–197.

Eng J., Kleinman W. A., Singh L., Singh G. & Raufman J-P. (1992) Isolation and characterization of exendin-4, an exendin-3 analogue, from Heloderma suspectum venom. *J. Biol. Chem.* **267:** 7402–7405.

F

Fan T., Varghese G., Nguyen T., Tse R., O'Dowd B. F. & George S. R. (2005) A role for the distal carboxyl tails in generating the novel pharmacology and G protein activation profile of mu and delta opioid receptor heterooligomers. *J. Biol. Chem.* **280:** 38478–38488.

Flower D. R. (1999). Modelling G protein-coupled receptors for drug design. *Biochimica et Biophysica Acta* **1422:** 207-234.

Fredriksson, R., Lagerstrom, M. C., Lundin, L. G. & Schioth, H. B. (2003) The G-protein-coupled receptors in the human genome form five main families. Phylogenetic analysis, paralogon groups, and fingerprints. *Molecular Pharmacology.* **63:** 1256-1272.

G

Gallwitz B., Witt M., Paetzold G., Morays-Wortmann C., Zimmermann B., Eckart K., Fölsch U. R. &Schmidt W. E. (1994). Structure/activity characterization of glucagon-like peptide-1. Eur. J. Biochem. 225: 1151–1156.

Galvez T., Duthey B., Kniazeff J., Blahos J., Rovelli G., Bettler B., Prezeau L. & Pin J. P. (2001) Allosteric interactions between GB1 and GB2 subunits are required for optimal $GABA_B$ receptor function. *Embo. J.* **20:** 2152–2159.

Gautier J. F., Fetita S., Sobngwi E. & Salaün-Martin C. (2005) Biological actions of the incretins GIP and GLP-1 and therapeutic perspectives in patients with type 2 diabetes. *Diabetes Metab*. **31:** 233-242.

Gether, U. (2000) Uncovering molecular mechanisms involved in activation of G protein-coupled receptors. *Endocrine Reviews*. **21:** 90-113.

Gloerich M. & Bos J. L. (2010) Epac: defining a new mechanism for cAMP action. *Annu. Rev. Pharmacol. Toxicol.* **50:** 355-375.

Goddard A. D. & Watts A. (2012) Regulation of G protein-coupled receptors by palmitoylation and cholesterol. *BMC Biology* **10:** article 27.

Göke R., Fehmann H.-C., Linn T., Schmidt H., Krause M., Eng J. & Göke B. (1993). Exendin-4 is a high potency agonist and truncated exendin-(9-39)-amide an antagonist at the glucagon-like peptide 1-(7-36)-amide receptor of insulin-secreting β-cells. *J. Biol. Chem.* **268:** 19650–19655.

Göke R., Just R., Lankat-Buttgereit B. & Göke B. (1994). Glycosylation of the GLP-1 receptor is a prerequisite for regular receptor function. *Peptides.* **15:** 675–681.

Gromada J., Brock B., Schmitz O. & Rorsman P. (2004) Glucagon-like peptide-1: regulation of insulin secretion and therapeutic potential. *Basic Clin. Pharmacol. Toxicol.* **95:** 252–262.

Gros R., You X., Baggio L. L., Kabir M. G., Sadi A. M., Mungrue I. N., Parker T. G., Huang Q., Drucker D. J. & Husain M. (2003) Cardiac function in mice lacking the glucagon-like peptide-1 receptor. *Endocrinology.* **144:** 2242–2252.

Gutzwiller J. P., Hruz P., Huber A. R., Hamel C., Zehnder C., Drewe J., Gutmann H., Stanga Z., Vogel D. & Beglinger C. (2006) Glucagon-like peptide-1 is involved in sodium and water homeostasis in humans. *Digestion.* **73:** 142–150.

H

Hanson, M. A. & Stevens, R. C. (2009) Discovery of new GPCR biology: one receptor at a time. *Structure.* **17:** 8-14.

Hansotia T. & Drucker D. J. (2005) GIP and GLP-1 as incretin hormones: lessons from single and double incretin receptor knockout mice. *Regul. Pept.* **128:** 125-134.

Harikumar K. G., Wootten D., Pinon D. I., Koole C., Ball A. M., Furness S. G., Graham B., Dong M., Christopoulos A., Miller L. J. & Sexton P. M. (2012) Glucagon-like peptide-1

receptor dimerization differentially regulates agonist signaling but does not affect small molecule allostery. *Proc. Natl. Acad. Sci. U. S. A.* **109:** 18607-18612.

Hausdorff W. P., Caron M. G. & Lefkowitz, R. J. (1990) Turning off the signal: desensitization of beta-adrenergic receptor function. *FASEB J.* **4:** 2881–2889.

Hebert T. E., Moffett S., Morello J. P., Loisel T. P., Bichet D. G., Barret C. & Bouvier M. (1996) A peptide derived from a beta2-adrenergic receptor transmembrane domain inhibits both receptor dimerization and activation. *J. Biol. Chem.* **271:** 16384-16392.

Herrmann C., Goke R., Richter G., Fehmann H. C., Arnold R. & Goke B. (1995) Glucagon-like peptide-1 and glucose-dependent insulin-releasing polypeptide plasma levels in response to nutrients. *Digestion.* **56:** 117–126.

Hilairet S., Bouaboula M., Carriere D., Le Fur G. & Casellas P. (2003) Hyper-sensitization of the Orexin 1 receptor by the CB1 receptor: evidence for cross-talk blocked by the specific CB1 antagonist, SR141716. *J. Biol. Chem*. **278:** 23731–23737.

Hill S. J. (2006) G-protein-coupled receptors: past, present and future. *British Journal of Pharmacology* **147:** S27–S37.

Hoare S. R. J. (2005) Mechanisms of peptide and nonpeptide ligand binding to Class B G-protein-coupled receptors. *Drug Discov Today* **10:** 417–427.

Hoare S. R. J. (2007) Allosteric Modulators of Class B G-Protein-Coupled Receptors. *Current Neuropharmacology* **5:**168-179.

Hoare S. R. J., de Vries G. & Usdin T. B. (1999) Measurement of agonist and antagonist ligand-binding parameters at the human parathyroid hormone type 1 receptor: evaluation of receptor states and modulation by guanine nucleotide. *J. Pharmacol. Exp. Ther.* **289:** 1323-33.

Hollenstein K., Kean J., Bortolato A., Cheng R. K. Y., Doré A. S., Jazayeri A., Cooke R. M., Weir M. & Marshall F. H. (2013) Structure of class B GPCR corticotropin-releasing factor receptor 1. *Nature.* **499:** 438–443.

Holz G. G., Kang G., Harbeck M., Roe M. W. & Chepurny O. G. (2006) Cell physiology of cAMP sensor Epac. *J. Physiol.* **577:** 5-15.

Hu, J., Hauache, O. & Spiegel, A. M. (2000) Coupling of agonist binding to effector domain activation in metabotropic glutamate-like receptors *J. Biol. Chem.* **275:** 16382-16389.

Hupe-Sodmann K., McGregor G. P., Bridenbaugh R., Göke R., Göke B., Thole H., Zimmermann B. & Voigt K. (1995) Characterisation of the processing by human neutral endopeptidase 24.11 of GLP-1(7-36) amide and comparison of the substrate specificity of the enzyme for other glucagon-like peptides. *Regul. Pept*. **58:** 149-156.

I

Ishihara, T., Nakamura S., Kaziro Y., Takahashi T., Takahashi K. & Nagata S. (1991) Molecular cloning and expression of a cDNA encoding the secretin receptor. *Embo J.* **10:** 1635–1641.

K

Kahout T. A. & Lefkowitz R. J. (2003). Regulation of G-protein coupled receptor kinases and arrestins during receptor desensitization. *Mol. Pharmacol*. **63:** 9–18.

Kaihara K. A., Dickson L. M., Jacobson D. A., Tamarina N., Roe M. W., Philipson L. H. & Wicksteed B. (2013) β-Cell–specific protein kinase A activation enhances the efficiency of glucose control by increasing acute-phase insulin secretion. *Diabetes* **62:** 1527–1536.

Kang G., Chepurny O. G., Rindler M. J., Collis L., Chepurny Z., Li W. H., Harbeck M., Roe M. W. & Holz G. G. (2005) A cAMP and Ca^{2+} coincidence detector in support of Ca^{2+}-induced Ca^{2+} release in mouse pancreatic beta cells. *J. Physiol*. **566:** 173-88.

Kashima Y., Miki T., Shibasaki T., Ozaki N., Miyazaki M., Yano H. & Seino S. (2001) Critical role of cAMP-GEFII-Rim2 complex in incretin-potentiated insulin secretion. *J. Biol. Chem.* **276:** 46046-46053.

Kastin A. J., Akerstrom V. & Pan W. (2002) Interactions of glucagon-like peptide-1 (GLP-1) with the blood–brain barrier. *J. Mol. Neurosci.* **18:** 7–14.

Katz B. & Thesleff S. (1957) A study of the desensitisation produced by acetylcholine at the motor end-plate. *Journal of Physiology-London* **138:** 63-80.

Kazakos K. (2011) Incretin effect: GLP-1, GIP, DPP4. *Diabetes Research And Clinical Practice.* **93S:** S32–S36.

Kellett G. L. & Brot-Laroche E. (2005) Apical GLUT2: a major pathway of intestinal sugar absorption. *Diabetes.* **54:** 3056-3062.

Kenakin T. (2004) Principles: Receptor theory in pharmacology *Trends Pharmacol. Sci.* **25:** 186-192.

Kieffer T. J., McIntosh C. H. & Pederson R. A. (1995) Degradation of glucose-dependent insulinotropic polypeptide and truncated glucagon-like peptide 1 in vitro and in vivo by dipeptidyl peptidase-IV. *Endocrinology.* **136:** 3585–3596.

Knudsen L. B., Kiel D., Teng M., Behrens C., Bhumralkar D., Kodra J. T., Holst J. J., Jeppesen C. B., Johnson M. D., de Jong J. C., Jorgensen A. S., Kercher T., Kostrowicki J., Madsen P., Olesen P. H., Petersen J. S., Poulsen F., Sidelmann U. G., Sturis J., Truesdale L., May J. & Lau J. (2007). Small-molecule agonists for the glucagon-like peptide 1 receptor. *Proc. Natl. Acad. Sci. U S A* **104:** 937–942.

Kolakowski, L. F. Jr. (1994) GCRDb: a G protein-coupled receptor database. *Receptors Channels.* **2:** 1-7.

Koole C., Wootten D., Simms J., Valant C., Sridhar R., Woodman O. L., Miller L. J., Summers R. J., Christopoulos A. & Sexton P. M. (2010) Allosteric ligands of the glucagon-like peptide-1 receptor (GLP-1R) differentially modulate endogenous and exogenous peptide responses in a pathway-selective manner: Implications for drug screening. *Mol Pharmacol.* **78:** 456–465.

Koole C., Savage E. E., Christopoulos A., Miller L. J., Sexton P. M. & Wootten D. (2013) Minireview: Signal Bias, Allosterism, and Polymorphic Variation at the GLP-1R: Implications for Drug Discovery. *Molecular Endocrinology* **27:** 1234–1244.

Kothare P. A., Linnebjerg H., Isaka Y., Uenaka K., Yamamura A., Yeo K. P., de la Peña A., Teng C. H., Mace K., Fineman M., Shigeta H., Sakata Y. & Irie S. (2008) Pharmacokinetics,

pharmaco-dynamics, tolerability, and safety of exenatide in Japanese patients with type 2 diabetes mellitus. *J. Clin. Pharmacol.* **48:** 1389-99.

Kristiansen K. (1994) Molecular mechanisms of ligand binding, signaling, and regulation within the superfamily of G-protein-coupled receptors: molecular modeling and mutagenesis approaches to receptor structure and function. *Pharmacology & Therapeutics* **103:** 21– 80.

Kubo, Y., Miyashita, T. & Murata, Y. (1998) Structural basis for a Ca^{2+}-sensing function of the metabotropic glutamate receptors. *Science* **279:** 1722–1725.

L

Lagerström, M. C. & Schiöth, H. B. (2008) Structural diversity of G protein-coupled receptors and significance for drug discovery. *Nature Reviews Drug Discovery* **7:** 339-357.

Larsen P. J., Tang-Christensen M. & Jessop D. S. (1997) Central administration of glucagon-like peptide-1 activates hypothalamic neuroendocrine neurons in the rat. *Endocrinology.* **138:** 4445–4455.

Lee S. C. & Pervaiz S. (2007) Apoptosis in the pathophysiology of diabetes mellitus. *Int. J. Biochem. Cell. Biol.* **39:** 497-504.

Leech C. A., Dzhura I., Chepurny O. G., Schwede F., Genieser H. G. & Holz G. G. (2010) Facilitation of β-cell K_{ATP} channel sulfonylurea sensitivity by a cAMP analog selective for the cAMP-regulated guanine nucleotide exchange factor Epac. *Islets.* **2:** 72-81.

Li Y., Hansotia T., Yusta B., Ris F., Halban P. A. & Drucker D. J. (2003) Glucagon-like peptide-1 receptor signaling modulates cell apoptosis. *J. Biol. Chem.* **278:** 471–478.

Li J., Edwards P. C., Burghammer M., Villa C. & Schertler G. F. (2004) Structure of bovine rhodopsin in a trigonal crystal form. *J. Mol. Biol.* **343:**1409-1438.

Li N., Lu J. & Willars G. B. (2012) Allosteric Modulation of the Activity of the Glucagon-like Peptide-1 (GLP-1) Metabolite GLP-1 9–36 Amide at the GLP-1 Receptor. *PLoS ONE* **7:** e47936.

Lin F. & Wang R. X. (2009) Molecular modeling of the three-dimensional structure of GLP-1R and its interactions with several agonists *J. Mol. Model* **15:** 53–65.

Light P. E., Manning Fox J. E., Riedel M. J. & Wheeler M. B. (2002) Glucagon-like peptide-1 inhibits pancreatic ATP-sensitive potassium channels via a protein kinase A- and ADP-dependent mechanism. *Mol. Endocrinol.* **16:** 2135–2144.

Liu X., He Q., Studholme D. J., Wu Q., Liang S. & Yu L. (2004) NCD3G: a novel nine-cysteine domain in family 3 GPCRs. *Trends Biochem. Sci.* **29:** 458–461.

López de Maturana R. & Donnelly D. (2002) The glucagon-like peptide-1 receptor binding site for the N-terminus of GLP-1 requires polarity at Asp198 rather than negative charge. *FEBS Lett*. **530:** 244-248.

López de Maturana R., Willshaw A., Kuntzsch A., Rudolph R. & Donnelly D. (2003). The isolated N-terminal domain of the Glucagon-like Peptide-1 (GLP-1) receptor binds exendin peptides with much higher affinity than GLP-1. *J Biol Chem* **278:** 10195–10200.

López de Maturana R., Treece-Birch J., Abidi F., Findlay J.B. & Donnelly D. (2004) Met-204 and Tyr-205 are together important for binding GLP-1 receptor agonists but not their N-terminally truncated analogues. *Protein Pept. Lett*. **11:** 15-22.

López-Ilasaca M. (1998) Signaling from G-protein-coupled receptors to mitogen-activated protein (MAP)-kinase cascades. *Biochem Pharmacol*. **56:** 269-77.

Luttrell L. M. & Lefkowitz R. J. (2002) The role of β-arrestins in the termination and transduction of G-protein-coupled receptor signals. *J. Cell Sci*. **115:** 455–465.

M

Ma P. & Zemmel R. (2002). Value of novelty? *Nature Reviews Drug Discovery* **1:** 571-572.

MacDonald P. E., Wang X., Xia F., El-kholy W., Targonsky E. D., Tsushima R. G. & Wheeler M. B. (2003) Antagonism of rat beta-cell voltage-dependent K^+ currents by exendin 4 requires dual activation of the cAMP/protein kinase A and phosphatidylinositol 3-kinase signaling pathways. *J. Biol. Chem.* **278:** 52446-52453.

Mann R.J., Al-Sabah S., López de Maturana R., Sinfield J.K. & Donnelly D. (2010a) Functional coupling of Cys-226 and Cys-296 in the glucagon-like peptide-1 (GLP-1) receptor indicates a disulfide bond that is close to the activation pocket *Peptides* **31:** 2289-2293

Mann R. J., Nasr N. E., Sinfield J. K., Paci E. & Donnelly D. (2010b). The major determinant of exendin-4/glucagon-like peptide 1 differential affinity at the rat glucagon-like peptide 1 receptor N-terminal domain is a hydrogen bond from SER-32 of exendin-4. *Br. J. Pharmacol.* **160:** 1973–1984.

Mapelli C., Natarajan S. I., Meyer J. P., Bastos M. M., Bernatowicz M. S., Lee V. G., Pluscec J., Riexinger D. J., Sieber-McMaster E. S., Constantine K. L., Smith-Monroy C. A., Golla R., Ma Z., Longhi D. A., Shi D., Xin L., Taylor J. R., Koplowitz B., Chi C. L., Khanna A., Robinson G. W., Seethala R., Antal-Zimanyi I. A., Stoffel R. H., Han S., Whaley J. M., Huang C. S., Krupinski J. & Ewing W. R. (2009) Eleven Amino Acid Glucagon-like Peptide-1 Receptor Agonists with Antidiabetic Activity *J. Med. Chem*. **52:** 7788-7799

McIntyre N., Holsworth D. C. & Turner D. S. (1964) New interpretation of oral glucose tolerance. *Lancet* **2:** 20-21.

McLatchie L. M., Fraser N. J, Main M. J., Wise A., Brown J., Thompson N., Solari R., Lee M. G. & Foord S. M. (1998) RAMPs regulate the transport and ligand specificity of the calcitonin-receptor-like receptor. *Nature* **393:** 333–339.

Meier J. J., Gallwitz B., Schmidt W. E. & Nauck M. A. (2002) Glucagon-like peptide 1 as a regulator of food intake and body weight: therapeutic perspectives. *Eur. J. Pharmacol*. **440:** 269-79.

Miller L. J., Dong M., Harikumar K. G. & Gao F. (2007) Structural basis of natural ligand binding and activation of the Class II G-protein-coupled secretin receptor. *Biochem Soc Trans.***35:** 709–712.

Miller L. J., Chen Q., Lam P.C-H., Pinon D. I., Sexton P. M., Abagyan R. & and Dong M. (2011) Refinement of Glucagon-like Peptide 1 Docking to Its Intact Receptor Using Mid-region Photolabile Probes and Molecular Modeling *J. Biol. Chem*. **286:** 15895-15907

Min J. & DeFea K. (2011) β-Arrestin-Dependent Actin Reorganization: Bringing the Right Players Together at the Leading Edge. *Molecular Pharmacology* **80:** 760-768.

Montrose-Rafizadeh C., Yang H., Rodgers B. D., Beday A., Pritchette L. A. & Eng J. (1997). High potency antagonists of the pancreatic glucagon-like peptide-1 receptor. *J. Biol. Chem.* **272:** 21201–21206.

Montrose-Rafizadeh C., Avdonin P., Garant M. J., Rodgers B. D., Kole S., Yang H., Levine M. A., Schwindinger W. & Bernier M. (1999) Pancreatic glucagon-like peptide-1 receptor couples to multiple G proteins and activates mitogen-activated protein kinase pathways in Chinese hamster ovary cells. *Endocrinology* **140:** 1132–1140.

Moon M. J., Kim H. Y., Park S., Kim D. K, Cho E. B., Park C. R., You D. J., Hwang J. I., Kim K., Choe H. & Seong J. Y. (2012) Evolutionarily Conserved Residues at Glucagon-like Peptide-1 (GLP-1) Receptor Core Confer Ligand-induced Receptor Activation. *J. Biol. Chem*. **287:** 3873-3884.

Murone M., Rosenthal A. & de Sauvage F. J. (1999) Sonic hedgehog signalling by the patched-smoothened receptor complex. *Curr. Biol*. **9:** 76–84.

N

Nagell C. F., Pedersen J. F. & Holst J. J. (2007) The antagonistic metabolite of GLP-1, GLP-1 (9-36)amide, does not influence gastric emptying and hunger sensations in man. *Scand. J. Gastroenterol.* **42:** 28-33.

Nathans J. & Hogness D. S. (1984) Isolation and nucleotide sequence of the gene encoding human rhodopsin. *Proc. Natl. Acad. Sci. U.S.A.* **81:** 4851–4855.

Nauck M., Frid A., Hermansen K., Shah N. S., Tankova T., Mitha I. H., Zdravkovic M., Düring M. & Matthews D. R. (2009) Efficacy and safety comparison of liraglutide, glimepiride, and placebo, all in combination with metformin, in type 2 diabetes: the LEAD (liraglutide effect and action in diabetes)-2 study. *Diabetes Care.* **32:** 84–90.

Neidigh J. W., Fesinmeyer R. M., Prickett K. S. & Andersen N. H. (2001). Exendin-4 and glucagon-like-peptide-1: NMR structural comparisons in the solution and micelle-associated states. *Biochemistry* **40:** 13188–13200.

Nelson G., Hoon M. A., Chandrashekar J., Zhang Y., Ryba N. J. & Zuker C. S. (2001) Mammalian sweet taste receptors. *Cell.* **106:** 381–390.

Neumiller J. J. & Campbell R. K. (2009). Liraglutide: a once-daily incretin mimetic for the treatment of type 2 diabetes mellitus. *Ann. Pharmacother.* **43:** 1433–1444.

Nyström T. (2008) The potential beneficial role of glucagon-like peptide-1 in endothelial dysfunction and heart failure associated with insulin resistance. *Horm. Metab. Res.* **40:** 593–606.

O

Orskov C., Holst J. J. & Nielsen O. V. (1988) Effect of truncated glucagon-like peptide-1 [proglucagon-(78–107) amide] on endocrine secretion from pig pancreas, antrum, and nonantral stomach. *Endocrinology.* **123:** 2009–2013.

P

Pal K., Melcher K. & Xu H. E. (2012) Structure and mechanism for recognition of peptide hormones by Class B G-protein-coupled receptors. *Acta Pharmacol. Sin*. **33:** 300–311.

Palczewski K., Kumasaka T., Hori T., Behnke C. A., Motoshima H., Fox B. A., Trong L. I., Teller D. C., Okada T., Stenkamp R. E., Yamamoto M. & Miyano M. (2000). Crystal structure of rhodopsin: A G protein-coupled receptor. *Science.* **289:** 739-745.

Parthier C., Reedtz-Runge S., Rudolph R. & Stubbs M. T. (2009). Passing the baton in class B GPCRs: peptide hormone activation via helix induction? *Trends. Biochem. Sci.* **34:** 303–310.

Patterson J. T., Day J. W., Gelfanov V. M. & DiMarchi R. D. (2011a). Functional association of the N-terminal residues with the central region in glucagon-related peptides. *J. Pept. Sci.* **17:** 659–666.

Patterson J. T., Ottaway N., Gelfanov V. M., Smiley D. L., Perez-Tilve D., Pfluger P. T., Tschöp M. H.& DiMarchi R. D. (2011b) A Novel Human-Based Receptor Antagonist of Sustained Action Reveals Body Weight Control by Endogenous GLP-1 *ACS Chem. Biol.* **6:** 135-145.

Perry T., Haughey N. J., Mattson M. P., Egan J. M. & Greig N. H. (2002) Protection and reversal of excitotoxic neuronal damage by glucagon-like peptide-1 and exendin-4. *J. Pharmacol. Exp. Ther.* **302:** 881-888.

Perry T. & Greig N. H. (2003) The glucagon-like peptides: a double-edged therapeutic sword? *Trends Pharmacol. Sci.* **24:** 377-383.

Pin J. P., Kniazeff J., Liu J., Binet V., Goudet C., Rondard P. & Prézeau L. (2005) Allosteric functioning of dimeric class C G-protein-coupled receptors. *FEBS Journal.* **272:** 2947–2955.

Pitcher J. A., Inglese J., Higgins J. B., Arriza J. L., Casey P. J., Kim C., Benovic J. L., Kwatra M. M., Caron M. G. & Lefkowitz R. J. (1992) Role of βγ subunits of G proteins in targeting the β-adrenergic receptor kinase to membrane-bound receptors. *Science.* **257:** 1264–1267.

Pronin A. N., Tang H., Connor J. & Keung W. (2004) Identification of ligands for two human bitter T2R receptors. *Chem. Senses.* **29:** 583–593.

R

Rasmussen S. G., Jensen A. D., Liapakis G., Ghanouni P., Javitch J. A. & Gether U. (1999) Mutation of a highly conserved aspartic acid in the beta2 adrenergic receptor: constitutive

activation, structural instability, and conformational rearrangement of transmembrane segment 6. *Mol. Pharmacol.* **56:** 175–184.

Rasmussen S. G.F., Choi H. J., Rosenbaum D. M., Kobilka T. S., Thian F. S., Edwards P. C., Burghammer M., Ratnala V. R. P., Sanishvili R., Fischetti R. F., Schertler G. F. X., Weis W. I. & Kobilka B. K. (2007) Crystal structure of the human β2 adrenergic G-protein-coupled receptor. *Nature* **450:** 383-387.

Rasmussen S. G. F, DeVree B. T., Zou Y., Kruse A. C., Chung K.Y., Kobilka T. S., Thian F. S., Chae P. S., Pardon E., Calinski D., Mathiesen J. M., Shah S. T., Lyons J. A., Caffrey M., Gellman S. H., Steyaert J., Skiniotis G., Weis W. I., Sunahara R. K. & Kobilka B. K. (2011) Crystal structure of the beta2 adrenergic receptor-Gs protein complex. *Nature* **477:** 549–555.

Raufman J.-P., Singh L., Singh G. & Eng J. (1992). Truncated glucagon-like peptide-1 interacts with exendin receptors on dispersed acini from guinea pig pancreas. *J. Biol. Chem.* **267:** 21432–21437.

Richter G., Feddersen O., Wagner U., Barth P., Goke R. & Goke B. (1993) GLP-1 stimulates secretion of macromolecules from airways and relaxes pulmonary artery. *Am. J. Physiol.* **265:** 374–381.

Rosenbaum, D. M., Rasmussen, S. G. F. & Kobilka, B. K. (2009) The structure and function of G-protein-coupled receptors. *Nature.* **459:** 356-363.

Runge S., Wulff B. S., Madsen K., Bräuner-Osborne H. & Knudsen L. B. (2003). Different domains of the glucagon and glucagon-like peptide-1 receptors provide the critical determinants of ligand selectivity. *Br. J. Pharmacol.* **138:** 787–794.

Runge A., Schimmer S., Oschmann J., Schiødt C. B., Knudsen S. M., Jeppesen C. B., Madsen K., Lau J., Thøgersen H. & Rudolph R. (2007). Differential structural properties of GLP-1 and exendin-4 determine their relative affinity for the GLP-1 receptor N-terminal extracellular domain. *Biochemistry* **46:** 5830–5840.

Runge S., Thøgersen H., Madsen K., Lau J. & Rudolph R. (2008). Crystal structure of the ligand-bound glucagon-like peptide-1 receptor extracellular domain. *J. Biol. Chem.* **283:** 11340–11347.

S

Salahpour A., Angers S., Mercier J. F., Lagace M., Marullo S. & Bouvier M. (2004) Homodimerization of the beta2-adrenergic receptor as a prerequisite for cell surface targeting. *J. Biol. Chem.* **279:** 33390–33397.

Samama P., Cotecchia S., Costa T. & Lefkowitz R. J. (1993) A mutation-induced activated state of the beta2-adrenergic receptor. Extending the ternary complex model. *J. Biol. Chem*. **268:** 4625–4636.

Schulte G. & Bryja V. (2007) The Frizzled family of unconventional G protein-coupled receptors. *Trends Pharmacol. Sci*. **28:** 518–525.

Serre V., Dolci W., Schaerer E., Scrocchi L., Drucker D., Efrat S. & Thorens B. (1998). Exendin-(9-39) is an inverse agonist of the murine glucagon-like peptide-1 receptor: implications for basal intracellular cyclic adenosine 3′, 5′- monophosphate levels and b-cell glucose competence. *Endocrinology* **139:** 4448–4454.

Sexton P. M., Morfis M., Tilakaratne N., Hay D. L., Udawela M., Christopoulos G. & Christopoulos A. (2006) Complexing receptor pharmacology: modulation of family B G protein-coupled receptor function by RAMPs. *Ann. N. Y. Acad. Sci.* **1070:** 90–104.

Shenoy S. K., Mcdonald P. H., Kahout T. A. & Lefkowitz R. J. (2001) Regulation of receptor fate by ubiquitination of activated beta-2 adrenergic receptor and beta-arrestin. *Science.* **294:** 1307–1313.

Sicree R., Shaw J. & Zimmet P. (2006) in: D. Gan (Ed.), *Diabetes Atlas. International Diabetes Federation, Brussels,* **3:** 15–103.

Siegel E. G., Gallwitz B., Scharf G., Mentlein R., Morys-Wortmann C., Fölsch U. R., Schrezenmeir J., Drescher K. & Schmidt W. E. (1999). Biological activity of GLP-1-analogues with N-terminal modifications. *Regul Pept* **79:** 93–102.

Singh S., Chang H. Y., Richards T. M., Weiner J. P., Clark J. M. & Segal J. B. (2013) Glucagon like peptide 1-based therapies and risk of hospitalization for acute pancreatitis in type 2 diabetes mellitus: a population based matched case-control study. *JAMA. Intern. Med.* **173:** 534–539.

Siu F. Y., He M., de Graaf C., Han G. W., Yang D., Zhang Z., Zhou C., Xu Q., Wacker D., Joseph J. S., Liu W., Lau J., Cherezov V., Katritch V., Wang M. W. & Stevens R. C. (2013) Structure of the human glucagon class B G-protein-coupled receptor. *Nature.* **499:** 444–449.

Sloop K. W., Willard F. S., Brenner M. B., Ficorilli J., Valasek K., Showalter A. D., Farb T. B., Cao J. X., Cox A. L., Michael M. D., Gutierrez Sanfeliciano S. M., Tebbe M. J. & Coghlan M. J. (2010). Novel small molecule glucagon-like peptide-1 agonist stimulates insulin secretion in rodents and from human islets. *Diabetes* **59:** 3099–3107.

Song W. J, Seshadri M., Ashraf U., Mdluli T., Mondal P., Keil M., Azevedo M., Kirschner L. S., Stratakis C. A. & Hussain M. A. (2011) Snapin mediates incretin action and augments glucose-dependent insulin secretion. *Cell Metab.* **13:** 308–319.

Stacey M., Lin H. H., Gordon S., & McKnight A. J. (2000) LNB-TM7, a group of seven-transmembrane proteins related to family-B G-protein-coupled receptors. *Trends Biochem. Sci.* **25:** 284–289.

Sternweis P. C., Northup J. K., Smigel M. D. & Gilman A. G. (1981) The regulatory component of adenylate cyclase. Purification and properties. *J. Biol. Chem.* **256:** 11517-11526.

T

Taniguchi H., Yazaki N., Endo T. & Nagasaki M. (1996) Pharmacological profile of T-0632, a novel potent and selective CCKA receptor antagonist, in vitro. *Eur. J. Pharmacol.* **304:** 147-154.

Teng M., Truesdale L. K. & Bhumralkar D. WO2000/42026 Non-Peptide GLP-1 Agonists. 2000.

Terrillon S. & Bouvier M. (2004) Roles of G-protein-coupled receptor dimerization: From ontogeny to signalling regulation. *EMBO Rep.* **5:** 30-34.

Tesmer J. J. G. (2012) A GAIN in understanding autoproteolytic G protein-coupled receptors and polycystic kidney disease proteins. *EMBO J.* **31:** 1334–1335.

Thorens B. (1992). Expression cloning of the pancreatic β cell receptor for the gluco-incretin hormone glucagon-like peptide 1. *Proc Natl Acad Sci U S A* **89:** 8641–8645.

Thorens B., Porett A., Bühler L., Deng S. P., Morel P. & Widmann C. (1993). Cloning and functional expression of the human islet GLP-1 receptor. Demonstration that exendin-4 is an agonist and exendin-(9-39) an antagonist of the receptor. *Diabetes.* **42:** 1678–1682.

Tibaduiza E. C., Chen C. & Beinborn M. (2001). A small molecule ligand of the glucagon-like peptide 1 receptor targets its amino-terminal hormone binding domain. *J. Biol. Chem*. **276:** 37787–37793.

Tillil H., Shapiro E. T., Miller M. A., Karrison T., Frank B. H., Galloway J. A., Rubenstein A. H. & Polonsky K. S. (1988) Dose-dependent effects of oral and intravenous glucose on insulin secretion and clearance in normal humans. *Am. J. Physiol.* **254:** E349-57.

Tobin A. B. (2008) G-protein-coupled receptor phosphorylation: where, when and by whom. *Br. J. Pharmacol.* **153:** S167–S176.

Toft-Nielsen M. B., Damholt M. B., Madsbad S., Hilsted L. M., Hughes T. E., Michelsen B. K. & Holst J. J. (2001) Determinants of the impaired secretion of glucagon-like peptide-1 in type 2 diabetic patients. *J. Clin. Endocrinol.* **86:** 3717–3723.

Tyndall J. D. & Sandilya R. (2005) GPCR agonists and antagonists in the clinic. *Med. Chem.* **1:** 405–421.

U

Underwood C. R., Garibay P., Knudsen L. B., Hastrup S., Peters G. H., Rudolph R. & Reedtz-Runge S. (2010) Crystal structure of glucagon-like peptide-1 in complex with the extracellular domain of the glucagon-like peptide-1 receptor. *J. Biol. Chem.* **285:** 723–730.

Underwood C. R., Knudsen S. M., Wulff B. S., Bräuner-Osborne H, Lau J. Knudsen L. B., Peters G. H. & Reedtz-Runge S. (2011) Transmembrane α-Helix 2 and 7 Are Important for Small Molecule-Mediated Activation of the GLP-1 Receptor. *Pharmacology*. **88:** 340–348.

V

Vahl T. P., Paty B. W., Fuller B. D., Prigeon R. L. & D'Alessio D. A. (2003). Effects of GLP-1-(7-36) amide, GLP-1-(7-37), and GLP-1-(9-36) amide on intravenous glucose tolerance and glucose-induced insulin secretion in healthy humans. *J. Clin. Endocrinol. Metab*. **88:** 1772–1779.

Van Dijk G. & Thiele T. E. (1999) Glucagon-like peptide-1 (7-36) amide: a central regulator of satiety and interoceptive stress. *Neuropeptides.* **33:** 406-414.

Verspohl E. J. (2009) Novel therapeutics for type 2 diabetes: incretin hormone mimetics (glucagon-like peptide-1 receptor agonists) and dipeptidyl peptidase-4 inhibitors. *Pharmacol Ther.* **124:** 113-138.

Vinson, C. R., Conover, S. & Adler, P. N. (1989) A Drosophila tissue polarity locus encodes a protein containing seven potential transmembrane domains. *Nature* **338:** 263–264.

W

Wang, Y., Macke J. P., Abella B. S., Andreasson K., Worley P., Gilbert D. J., Copeland N. G., Jenkins N. A. & Nathans J. (1996) A large family of putative transmembrane receptors homologous to the product of the Drosophila tissue polarity gene frizzled. *J. Biol. Chem.* **271:** 4468–4476.

Watkins H. A., Au M. & Hay D. L. (2012) The structure of secretin family GPCR peptide ligands: implications for receptor pharmacology and drug development. *Drug Discov. Today* **17:** 1006–1014.

Weiss J. M., Morgan P. H., Lutz M. W. & Kenakin T. P. (1996). The cubic ternary complex receptor-occupancy model I. Model description. *Journal of Theoretical Biology* **178:** 151-167.

Westh P. (2004) Preferential Interaction of Dimethyl Sulfoxide and Phosphatidyl Choline Membranes. *Biochimica et Biophysica Acta*. **1664:** 217-223.

Wheatley M., Wootten D., Conner M. T., Simms J., Kendrick R., Logan R. T., Poyner D. R. & J Barwell J. (2011) Lifting the lid on GPCRs: the role of extracellular loops. *Br. J. Pharmacol.* **165:** 1688–1703.

Willard F. S., Bueno A. B. & Sloop K. W. (2012) Small Molecule Drug Discovery at the Glucagon-Like Peptide-1 Receptor. *Experimental Diabetes Research.* Art. I. D: 709893-709901.

Wootten D., Lindmark H., Kadmiel M., Willcockson H., Caron K. M., Barwell J., Drmota T. & Poyner D. R. (2013) Receptor activity modifying proteins (RAMPs) interact with the VPAC 2 receptor and CRF 1 receptors and modulate their function. *Br. J. Pharmacol.* **168:** 822–834.

X

Xiao Q., Giguere J., Parisen M., Jeng W. S., Pierre P. L., Brubaker P. L. & Wheeler M. B. (2001). Biological activities of glucagon-like peptide-1 analogues in vitro and in vivo. *Biochemistry* **40:** 2860–2869.

Y

Young A. A., Gedulin B. R., Bhavsar S., Bodkin N., Jodka C., Hansen B. & Denaro M. (1999) Glucose-lowering and insulin-sensitizing actions of exendin-4: studies in obese diabetic (ob/ob, db/db) mice, diabetic fatty Zucker rats, and diabetic rhesus monkeys (Macaca mulatta). *Diabetes.* **48:** 1026–1034.

Z

Zhou J., Wang X., Pineyro M. A. & Egan J. M. (1999) Glucagon-like peptide 1 and exendin-4 convert pancreatic AR42J cells into glucagon- and insulin-producing cells. *Diabetes* **48:** 2358-2366.

References

Zimmet P., Alberti K. G. & Shaw J. (2001) Global and societal implications of the diabetes epidemic. *Nature.* **414:** 782-787.

Appendices

Locating the Allosteric Binding Site of Pyrimidine Partial Agonist Pm 42 at Human GLP-1R-Expressing Cells

Appendix

A.1 Introduction

The data presented here are in an appendix as the work was incomplete, or inconclusive, or did not follow the trend of the work presented within the results sections.

The Pm compounds were hypothesised to bind within the transmembrane region into an activation pocket, as a similar study was performed by Underwood *et al*. (2011) by using a chimeric receptor with sections taken from the glucagon and the GLP-1 receptors, which showed that the critical binding region lie between TM2 and TM5 as a portion of GLP-1R TMD containing TM2 to TM5 was sufficient to activate GCGR containing GLP-1R TMD TM2-TM5 subsegments. Following from this, and previous studies showing the importance of mobility of the extracellular loops for receptor activation (Wheatley *et al*., 2011), site-directed modifications of the GLP-1R were made in the vicinity of hGLP-1R extracellular loop 2, using a double alanine-scanning technique.

Previous experimentation performed by Dr. Migliore suggested that the Pm compounds covalently bind to cysteine residues (data not shown). Site directed mutagenesis was performed on GLP-1R at cysteine residues which have not been shown to be involved in maintaining the structural integrity of GLP-1R, therefore Cys 46, 62, 71, 85, 104, 126, 226 and 296 (Mann *et al*., 2010a) were not mutated.

A.2 Aims and Strategy

As ECL2 lies between TM2 and TM5 and has been implicated in ligand selectivity and binding across many GPCRs, a double alanine scan was performed on residues 286-312 which encompass ECL2 residues. The vector containing hGLP-1R was pcDNA5/FRT, and mutations were introduced using QuikChange mutagenesis. The mutant hGLP-1R was sequenced by Beckman Coulter genomics. The resulted mutant GLP-1R DNA was stably transfected into FlpIn-HEK293 cells and cAMP accumulation assays were performed using GLP-1(7-36) and Pm 42 to analyse any change in signalling exclusive to Pm 42.

The experiments by Dr. Migliore prompted the investigation of Pm compound-mediated GLP-1R stimulation via covalent attachment to a cysteine residue. An alanine scan of cysteine residues within GLP-1R was performed. Resultant mutant DNA was transiently transfected into FlpIn-HEK293 cells and cAMP accumulation analysis was performed on the cells 48 hours following transfection. cAMP accumulation assays were performed using 1 μM GLP-1(7-36)

and 100 μM Pm 42 to analyse any change in signalling exclusive to Pm 42 which could potentially identify a single cysteine residue responsible for Pm 42-mediated GLP-1R activation.

A.3 Methods

A.3.1 QuikChange® Site-Directed Mutagenesis

Cysteine to alanine site-directed mutations within the human GLP-1R DNA expressed in the pcDNA5/FRT vector were engineered by performing QuikChange® mutagenesis, using the primers as specified in section 2.1.11. Into a thin-walled PCR tube, the following reagents were added in order as follows: 38 μL MQ, 5 μL of 10 x concentrated Pfu reaction buffer, 200 μM dNTP mix, 400 nM forward primer, 400 nM reverse primer, 5 ng template plasmid DNA and 2.5 U of PfuUltra DNA polymerase (1 μL), these were mixed thoroughly and placed in a PCR Sprint thermocycler. According to the QuikChange® manual, the thermocycler was set to an initial DNA denature phase of 95°C for 1 minute, followed by 16 cycles of 95°C for 30 seconds, 55°C for 1 minute and 68°C for 7 minutes, completed by a final extension phase of 68°C for 10 minutes. Parental methylated and hemimethylated template DNA was then digested using 10 U DpnI (1 μL) for 16 hours at 37°C. The resulting DNA was then transformed into Supercompetent E.coli (2.2.2.3) and plated out on LB agar plates supplemented with ampicillin.

Site-directed mutagenesis was performed by Rachel Dods (BSc (hons)) and Vincent Knight-Schrijver (BSc (hons)) under my supervision and guidance. DNA sequences were checked by myself following sanger sequencing by Beckman Coulter Genomics sequencing services.

A.4 Results

cAMP accumulation assays were performed on mutant GLP-1R which were stably transfected into FlpIn-HEK-293 cells. Cells were stimulated with 100 μM Pm 42 and response normalised to the response given by 1 μM GLP-1(7-36). The cAMP responses given by the following mutant GLP-1R were statistically significant following comparison to the cAMP response of Pm 42 at wild-type hGLP-1R expressing cells using the Student's t-test: KY288/289AA, ED292/293AA, WT297/298AA, I398A and LP311/312AA (Figure A.1). The

mutant receptors which gave a statistically significant cAMP response in comparison to wild-type hGLP-1R were cross checked against GLP-1(7-36) induced dose-response data and correspondent expression levels and it was found that lower Pm 42 cAMP response correlated with a lowered receptor expression level in FlpIn-HEK293 cells (data not shown but is available in the Master's Thesis by Rachel Dods.)

cAMP accumulation assays were performed on mutated cysteine hGLP-1R using concentrations of agonists as follows: 1. 10 μM GLP-1(9-36); 2. 10 nM GLP-1(9-36); 3. 100 μM Pm 42; 4. 10 nM GLP-1(9-36) and 100 μM Pm 42 together; 5. 2% *v*/*v* DMSO. cAMP response were normalised to the response given by 1 μM GLP-1(7-36) which was performed simultaneously. A paired, two-tailed Student's t-test was used to analyse any significant deviation of cAMP response from the wild-type hGLP-1R response. C174A and C341A mutations gave statistically significant responses from 100 μM Pm 42 mediated stimulation in comparison to wild-type GLP-1R (Figure A.2). Mutant hGLP-1R C174A gave a reduced cAMP response from Pm 42-mediated stimulation, but also displayed a reduced cAMP response from 10 μM GLP-1(9-36) and a reduced cAMP response from costimulation using 10 nM GLP-1(9-36) and 100 μM Pm 42. Mutant hGLP-1R C341A showed a significantly increased cAMP response from 100 μM Pm 42 in comparison to wild-type hGLP-1R response. No other mutant showed significant deviation from the wild-type hGLP-1R cAMP response.

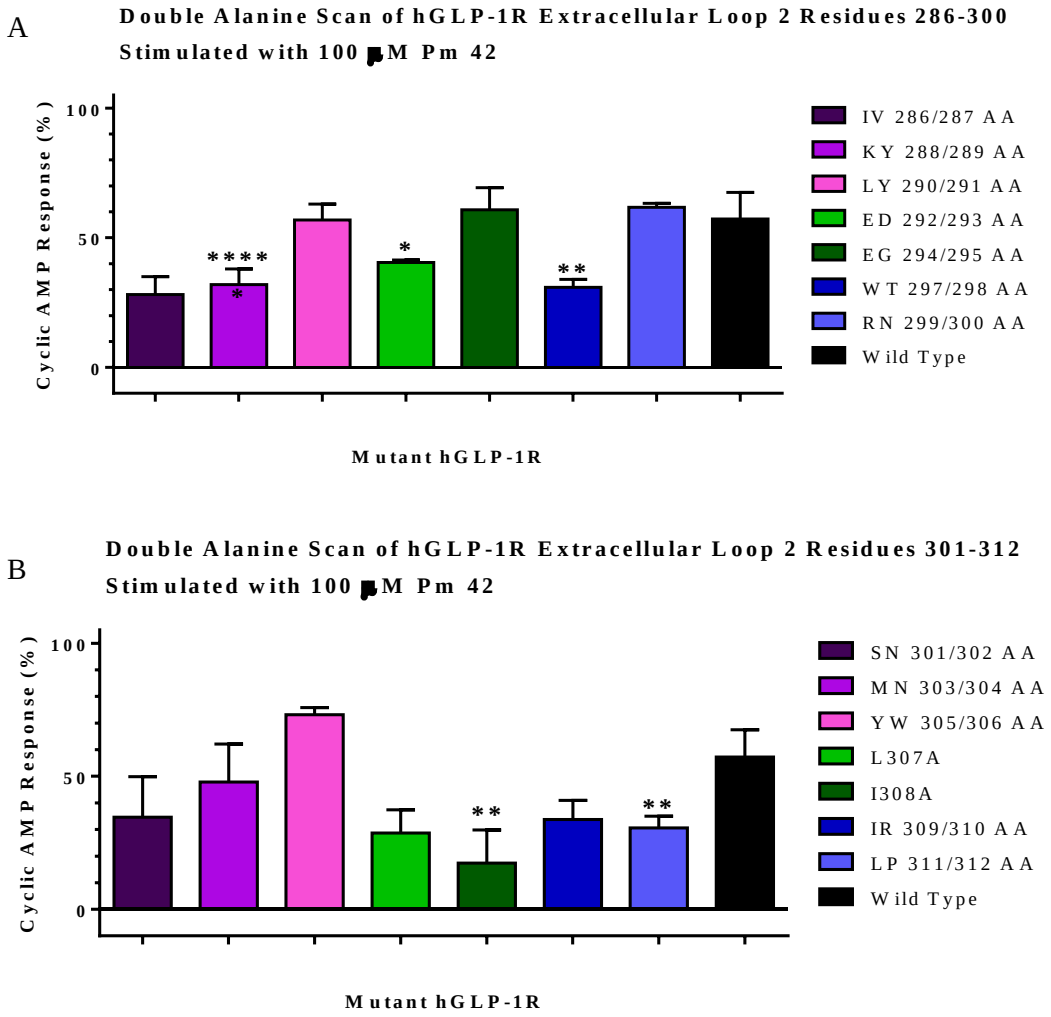

Figure A.1. FLP-IN HEK 293 cells expressing extracellular loop 2 mutant hGLP-1R, stimulated with 100 µM Pm 42.

Mutant hGLP-1R expressing cells were stimulated alongside the wild-type hGLP-1R as a control. A.1.A depicts double alanine mutations of ECL2 residues 286-300 (not including Cys 296) and A.1.B shows alanine mutated residues 301-312. Values shown correspond to the average +/- S.E.M of n=3 independent experiments. Each mutant data set was normalised individually using the cAMP response from 1 µM GLP-1 (7-36) as 100 % active, and the cAMP response given by stimulation buffer alone as 0 % active at said mutant (data not shown). A paired, two-tailed student's T-test was performed to compare % cAMP response of 100 µM Pm 42 at the mutant hGLP-1R versus the response elicited at the wild-type hGLP-1R (n=3) * P<0.05, ** P<0.01, *** P<0.001, **** P<0.0005, ***** P<0.0001.

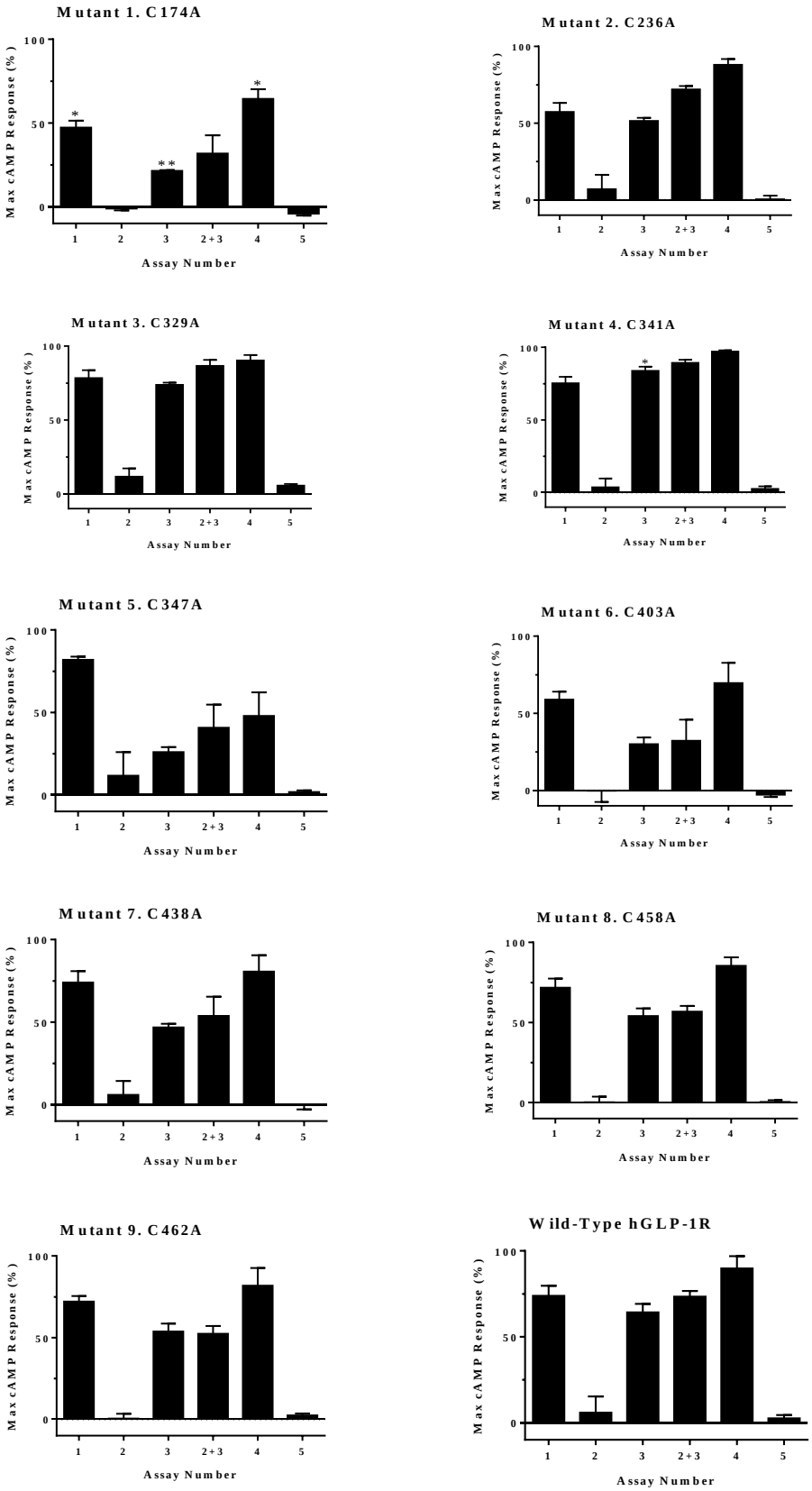

Figure A.2. cAMP responses of GLP-1R containing site-directed mutated cysteine residues.

FlpIn-HEK293 cells transiently transfected with mutant cysteine GLP-1R were stimulated for 10 minutes with the following concentrations of ligands: 1. 10 μM GLP-1(9-36); 2. 10 nM GLP-1(9-36); 3. 100 μM Pm 42; 4. 10 nM GLP-1(9-36) and 100 μM Pm 42 together; 5. 2% *v/v* DMSO, where 2 + 3 represents the numerical addition of the independent cAMP responses given by 10 nM GLP-1(9-36) and 100 μM Pm 42, whereas 4 shows the observed experimental outcome of co-stimulation. cAMP responses were normalised to the response given by 1 μM GLP-1(7-36). Data show the amalgamation of n=3 independent experiments. A Student's t-test was performed to analyse significant deviation from wild-type GLP-1R responses, where * denotes P<0.05 and ** denotes P<0.01.

Pm 42 and compound 2 were analysed for efficacy at HEK-293 cells constitutively expressing the human gastric inhibitory polypeptide receptor using cAMP accumulation assays. Whilst GIP(1-42) showed sub nM potency, neither Pm 42 nor compound 2 gave a cAMP response.

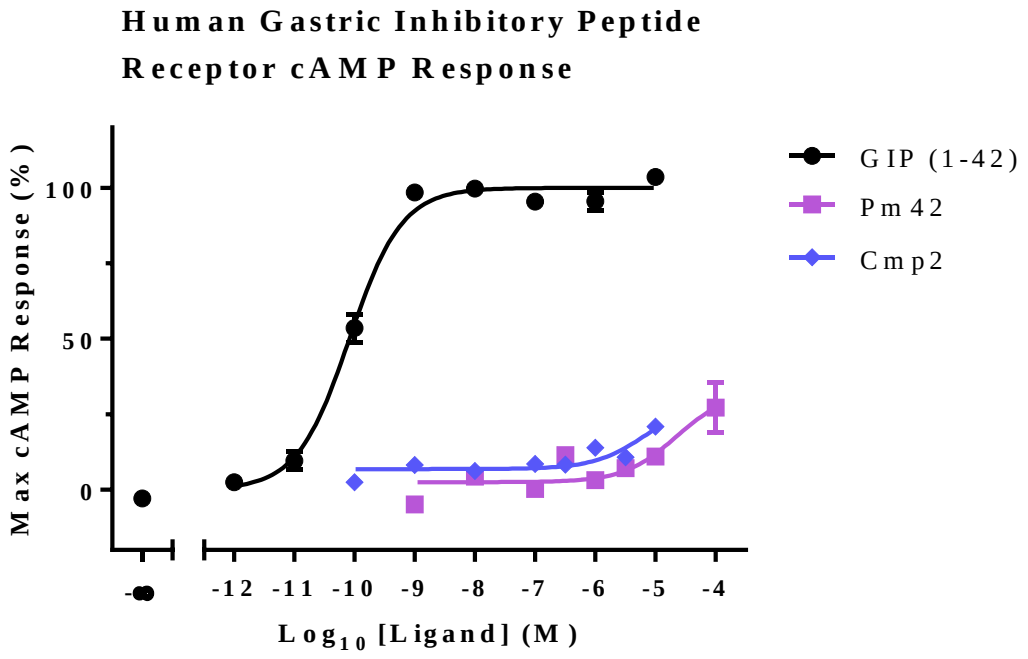

Figure A.3. cAMP response of human GIPR expressing HEK-293 cells stimulated by agonist GIP(1-42) and GLP-1R non-peptide agonists Pm 42 and compound 2.

Cells were sown at a density of 10,000 cells per well and were stimulated for 30 minutes with ligands. Data was normalised to the response given by 10 μM GIP(1-42).Data is representative of n=3 independent experiments.

A.5 Discussion

Whilst ECL2 mutants KY288/289AA, ED292/293AA, WT297/298AA, I398A and LP311/312AA showed significantly different cAMP responses to 100 μM Pm 42 in comparison to wild-type hGLP-1R, a full dose-response curve using GLP-1(7-36) was subsequently performed on these mutants which showed a reduced potency, suggesting either the mutation had affected both Pm compound and GLP-1 peptide mediated signalling, or expression levels had fallen. Homologous competition binding analysis (shown in the Master's Thesis of Rachel Dods) and subsequent B_{MAX} calculations revealed that GLP-1R expression levels were decreased, suggesting the reduced Pm 42 cAMP response was an artefact of lowered levels of receptor expression. These data suggested ECL2 mutation had no effect upon Pm 42 cAMP response, suggesting Pm 42 does not bind using ECL2 residues.

Alanine scanning of cysteine residues within hGLP-1R showed C174A and C341A mutations gave statistically significant responses (Figure A.2). cAMP responses given by 10 μM GLP-1(9-36) and by co-stimulation of 10 nM GLP-1(9-36) with 100 μM Pm were also reduced at the C174A mutant hGLP-1R in comparison to wild-type GLP-1R responses. These data suggest that as more than one agonist-induced response is affected it was a reduced level of expression of the transiently transfected receptor that caused the reduced cAMP response. In contrast to the C174A mutant receptor, the C341A receptor showed significantly increased Pm 42 cAMP response in comparison to wild-type hGLP-1R. An increased cAMP response at C341A hGLP-1R suggests that Pm 42 does not bind to Cys 341. No other mutant receptor cAMP responses showed significant deviation from the wild-type hGLP-1R response. These data suggest that Pm 42 does not bind any cysteine residues which are not involved in maintaining the structural integrity of the tertiary structure of GLP-1R. They may bind conserved cysteines involved in maintaining the secretin fold at the NTD or the disulphide bind between ECL1 and 2, however an alanine scanning technique of these residues to analyse Pm 42 mediated activity may result in lowered expression level of misfolded GLP-1R through the breakage of disulphide bonds, therefore is not suitable for Pm 42 mediated GLP-1R activation analysis.